

***INNOVATIVE GEOTHERMAL ENERGY SOURCE FOR
CLEAN ENERGY GENERATION:
THE NEED OF NIGERIAN TELECOMMUNICATIONS
INDUSTRY FOR EFFICIENT COMMUNICATION DELIVERY***

FINAL REPORT

Submitted to

THE NIGERIAN COMMUNICATIONS COMMISSION (NCC)

BY

Aigbedion Isaac (Professor of Geophysics, SRF, FIMC, NAPE, SEG, AGU, AAPG, MNGS),

Ambrose Alli University, Ekpoma

(Lead Researcher)

Salufu Samuel Obomheile (COMEG, MNMGS, MSPE)

Ambrose Alli University, Ekpoma

Aikhuele Daniel Osezua (COREN, MIAENG, MNIME)

OFFSHORE TECHNOLOGY INSTITUTE, University of Port Harcourt, River State)

MARCH, 2023.

TABLE OF CONTENTS

TITLE	PAGE
TABLE OF CONTENTS.....	ii-iv
LIST OF FIGURES	v
LIST OF TABLES	xiii
EXECUTIVE SUMMARY	xvii-xxi
CHAPTER ONE	1
1.0 Introduction.....	1
1.1 Statement of the Problem.....	9
1.2 Justification of the Research	9
1.3 Literature Review (Previous Works)	9
1.4 Objective of the Research	12
1.3 Scope of the Research Work	12
CHAPTER TWO	183
2.0 Materials and Methods.....	13
2.1 Estimation of Formation Temperature from Well Log Data.....	15
CHAPTER THREE	189
3.0 Geothermal Energy Assessment of Nigeria: Geological and Hydrogeological Studies	199
3.1 Southwest Nigeria Geology and Hydrogeology	199
3.1.1 Geology of Ikogosi	199
3.1.2 Hydrogeology of Ikogosi	21
3.1.3 Geology of Olumirin Erin	23
3.1.4 Hydrogeology of Olumirin Erin	25
3.2 North Central Nigeria Geology and Hydrogeology.....	25
3.2.1 Geology of Azara, Akiri, Awe, Kanje, Keana and Ribi	25
3.2.2 Hydrogeology of Azara, Akiri, Awe, Kanje, Keana and Ribi	27
3.2.3 Geology of Farin Ruwa Warm Spring	32
3.2.4 Hydrogeology of Farin Ruwa	34
3.2.5 Geology of Abaji	34
3.2.6 Geology of Igbonla and Egeneja Warm Springs	36
3.2.7 Hydrogeology of Igbonla and Egeneja Warm Spring.....	38
3.3 North Eastern Nigeria Geology and Hydrogeology	40
3.3.1 Geology of Ruwan Zafi Springs	40
3.3.2 Hydrogeology of Ruwan Zafi.....	41
3.3.3 Geology of Yankari Park and Wikki warm spring.....	42
3.3.4 Hydrogeology of Yankari and Wikki.....	44
3.4 South South Nigeria Geology and Hydrogeology	45

3.4.1	Geology of Azukala	45
3.4.2	Hydrogeology of Azukala	46
3.4.3	Geology of Ishiagu.....	47
3.4.4	Hydrogeology of Ishiagu.....	48
3.4.5	Geology of Ugep Warm and Cold Springs.....	48
3.4.6	Hydrogeology of Ugep Warm and Cold Springs.....	50
3.4.7	Geology of the Niger Delta and the Geothermal Potentials	51
3.5	South Eastern Nigeria Geology and Hydrogeology	56
3.5.1	Geology of Okigwe and Afikpo.....	56
3.5.2	Hydrogeology of Okigwe.....	58
3.5.3	Geology of Nsukka	58
3.5.4	Hydrogeology of Nsukka	60
CHAPTER FOUR.....		61
4.0	Analyses and interpretation of airborne gravity data of some locations in Nigeria for Geothermal Exploration	61
4.1	Materials and Methods.....	61
4.2	Akiri - Sheet 232	64
4.3	Ado Ekiti- Sheet 244	65
4.4	Ijebu-Ode - (Sheet 280)	67
4.5	Lokoja – (Sheet 247)	69
4.6	Auchi – (Sheet 266).....	71
4.7	Nsukka – (Sheet 287).....	73
4.8	Onitsha – (Sheet 300)	75
4.9	Geothermal potential of Abakaliki (Sheet 303).....	79
4.10	Toro-(Sheet 147)	80
4.11	Kaltungo – (Sheet 173).....	82
4.12	Numal – (Sheet 196).....	85
4.13	Kotonkarfi – (Sheet 227).....	86
4.14	Pennigton Rivers_Bayelsa – (Sheet 326).....	88
4.15	Okigwe – (Sheet 312)	90
4.16	Geothermal potential of Chad Basin Northern Nigeria (Sheet 24).....	92
CHAPTER FIVE		94
5.0	Material and Methods (Aeromagnetic method).....	94
5.1	Theory of Methods	94
5.2	Aeromagnetic Results and Discussion across Nigeria: Stages 3 and 4 Deliverables	96
5.3	Geothermal Potential of Lere_Farin Ruwa_(Sheet 147).....	96
5.4	Geothermal potential of Kaltungo_ (Sheet 173).....	99
5.5	Geothermal potential of Numal_ (Sheet 196)	102

5.6	Geothermal potential of Kotonkarfi_ (Sheet 227)	104
5.7	Geothermal Potential of Akiri_ (Sheet 232).....	107
5.8	Geothermal Potential of Ado-Ekiti (Sheet 244)	109
5.9	Geothermal Potential of Lokoja _ (Sheet 247).....	112
5.10	Geothermal Potential of Auchi _ (Sheet 266)	114
5.11	Geothermal Potential of Nsukka _ (Sheet 287).....	117
5.12	Geothermal Potential of Onitsha_ (Sheet 300).....	119
5.13	Geothermal potential of Okigwe_(Sheet312).....	122
5.14	Geothermal potential of Bauchi _ (Sheet 148).....	125
5.15	Geothermal potential of Jalingo_(Sheet215).....	127
5.16	Geothermal Potential of Ilesha (Sheet 243)	130
5.17	Geothermal Potentials of Ijebu-Ode_280.....	132
5.18	Geothermal Potentials of Ijebu-Ife_281.....	135
5.19	Geothermal Potentials of Abo_311	137
5.20	Geothermal Potentials of Ugep_314.....	140
5.21	Geothermal Assessment of some selected BHT logs in Niger Delta.....	142
5.22	Proposed Cost of Drilling Geothermal Well, 2-5KM.....	144
CHAPTER SIX		146
6.0	Conclusion	146
6.1	Further Recommendations	152
ACKNOWLEDGMENTS		153
APPENDIX I		154
EXAMPLES OF ENERGY SPECTRUM AGAINST WAVE NUMBER COMPONENTS USING MATLAB SOFTWARE FROM THE AEROMAGNETIC DATA		154
APPENDIX 2:		184
Geological and Hydrogeological images across Nigeria.....		184
ARTICLE PUBLISHED AND WORKSHOPS/ CONFERENCES		207
REFERENCES		245

LIST OF FIGURES

FIGURES	TITLE	PAGE
Fig. 2.1:	Temperature gradient where temperature over a burial depth of 3km is about 75°C.	17
Fig. 3.1:	Regional Geology of Ekiti showing Ikogosi	19
Fig. 3. 2	(a) Quartz Schist exposure at Ikogosi, Ekiti (b) The lead researcher with one of the team member taking the attitude of the foliated Quartz Muscovite Schist at Ikogosi warm Spring, Ekiti (c) Weathered quartzite exposure at the topmost part of Ikogosi outcrop where restriction is placed (d) quartz mica schist foliation trend at Ikogosi in Ekiti, Nigeria	20
Fig. 3.3:	Rose diagram for foliation strike of quartz schist and quartz muscovite schist outcrop exposed at Ikogosi warm spring in Ekiti, Nigeria.	21
Fig. 3.4:	(a) The lead researcher of the research team taking water temperature at the apex of the outcrop (b) The lead researcher of the research team taking water temperature at the restricted limits (c) The lead researcher and one of the team member of the research team taking water temperature at the cold and warm water meeting point (d) The lead researcher of the research team feeling the warmness of the spring water with his palm.	22
Fig.3.5	Regional Geological map of part of Osun Sate showing Olumirin fall in Erin Ijesa where the study area falls	24
Fig 3.5:	(a) Quartz Schist exposure showing high pressure flow of water fall at Olumirin in Erin Ijesa, Osun State (b)The lead researcher with one of the team member standing on the quartzite boulder to measure water temperature at Olumirin fall at Erin Ijesa in Osun State (c) Weathered quartzite exposure at the topmost part of Ikogosi outcrop where restriction is placed (d) Quartz Schist exposure showing low pressure flow of water fall at Olumirin in Erin Ijesa, Osun State	24
Fig. 3.6:	Regional Geological map of southern part of Nasarawa showing part of Middle Benue Trough where the study areas fall	26
Fig. 3.6:	(a) Keana Formation in Nasarawa showing black shale, siltstone and sandstone lithology units (b) Awe Formation in Nasarawa showing outcrop exposure of black shale	27
Fig. 3.7:	(a) The lead researcher taking the temperature of Akiri Spring with thermometer with the assistant of the member	28

	of the team (b) The lead researcher taking the temperature of Awe Spring with thermometer at Awe 1thermal spring in Awe, Nasarawa State, Nigeria (c) The lead researcher taking the temperature of Azara Spring with thermometer	
Fig 3.8:	(a) The water fall at FarinRuwa(a) The lead researcher taking the temperature of FarinRuwa water fall with thermometer sitting on the migmatite rock in FarinRuwa, Nasarawa State, Nigeria.	33
Fig. 3.8:	(b) Regional Geological map of Farin Ruwa showing the area of study in Nasarawa State	33
Fig. 3.9	Regional Geological map of part of Abuja showing Abaji where the study area falls	35
Fig 3.9	(a) in Kwara State, Nigeria (b) Picture of Igbonla wrm spring in Kwara State, Nigeria (c) Member of the research team taking temperature of water at Egeneja in Basa Local Government of Kogi State, Nigeria (d) Outcrop section of rock units underlying Ebeneja in Kogi State, Nigeria	36
Fig. 3.10	Regional Geological map of part of Kwara State and Kogi State showing Igbonla and Egeneja where the study area falls	37
Fig.3.10:	(a) The lead researcher taking the temperature of the Spring with thermometer at Igbonla warm spring in Kwara State, Nigeria (b) Picture of Igbonla wrm spring in Kwara State, Nigeria (c) Member of the research team taking temperature of water at Egeneja in Basa Local Government of Kogi State, Nigeria (d) Outcrop section of rock units underlying Ebeneja in Kogi State, Nigeria	38
Fig. 3.11	Regional Geological map of Adamawa showing Ruwan Zafi area falls	40
Fig.3.11	(a) One of the member with the lead researcher of the research team taking water temperature along the river channel in Ruwan Zafi, Adamawa State, Nigeria (b) Exposure of the well cemented sandstone unit at the source of Ruwan Zafi spring, Adamawa State, Nigeria (c) Exposure of the well cemented sandstone unit alon part of Ruwan Zafi spring (d) Exposure of the well cemented sandstone unit about 20m away from the source of Ruwan Zafi spring, Adamawa State, Nigeria	41
Fig.3.12	Regional Geological map of Bauchi showing Wikki, Gwana, Mawulgo and Dimil springs in Yankari Park, Bauchi State, Nigeria.	43
Fig.3.12	(a) Some of the members with the lead researcher of the	43

	research team taking water temperature along the of- set river in Wikk, Bauchi State (b) Exposure of the well cemented sandstone unit by Wikki Spring water at Yankari Park, Bauchi State, Nigeria.	
Fig.3.13:	Regional Geological map of Edo North in Auchu showing Azukala area where the study was done.	46
Fig.3.14:	Regional Geological map of Delta North showing Ishiagu where the study was done.	48
Fig.3.15:	Regional Geological map of part of Cross River showing Ugep where the study area falls.	49
Fig.3.15	(a) Picture of Eze-aku Formation outcrop exposure at Ugep in Cross Rivers State, Nigeria (b) Amasiri Sandstone outcrop exposes at Ugep, in Cross River State, Nigeria (c) The lead researcher taking the temperature of the Spring with thermometer at Ugep Warm Spring at Ugep in Cross River State, Nigeria (d) Cold water spring at Ugep in Cross River State, Nigeria	50
Fig.3.16	Geological Map showing the Basins in Nigeria	52
Fig. 3.17	Formation Pressure vs temperature F	54
Fig. 3.18	Some BHT logs interpreted	54
Fig. 3.19 :	Regional Geological map of part of Imo State showing Okigwe where the study area falls	57
Fig.3.19 :	(a) Outcrop exposure of Ajali Sandstone in Uturu-Okigwe Roadshowing herring-bone cross beds (b) Outcrop exposure of Ajali Sandstone in Uturu-Okigwe Roadshowing Ophiomorpha burrows	57
Fig. 3.20a:	Regional Geological map of part of Enugu State showing Nsukka and environs where the study area falls	59
Fig.3.21:	(a) Outcrop exposure of black shale in Nsukka (b) Section of Nsukka Formation showing the shale unit and the sandstone unit in Nsukka	59
Fig.4.1:	Plots of spectrum energy against wave number (a) spectral block A1 (b) spectral block B1 (c) Spectral block C1 (d) spectral block D1 (e) spectral block E1 (f) spectral block F1 (g) spectral block G1 (h) spectral block H1 (i) spectral I1 (j) spectral block J1 (k) spectral block K1 and (L) spectral block L1	63
Fig.4. 2	Heat flow contour map of sheet 232 corresponding to Akiri	65
Fig.4. 3	Heat flow contour map of sheet 244 corresponding to Ado	67
Fig. 4.3a:	Heat flow contour map of sheet 280 corresponding to Ijebu – Ode (Ogun State)	69
Fig. 4.4	Heat flow contour map of sheet 247 corresponding to Lokoja	71
Fig.4. 5	Heat flow contour map of sheet 266 corresponding to Auchu	73
Fig.4.6	Heat flow contour map of sheet 287 corresponding to Nsukka	75

Fig.4.7a	Heat flow contour map of sheet 300 corresponding to Onitsha	77
Fig. 4.7b:	Anomaly map of Eastern Nigeria showing the anomalies in the central and southwestern regions of Afikpo and Umuahia. Geothermal Gradient map, CNM map and heat flow map.	78
Fig.4.7c:	Heat flow contour map of sheet 303 corresponding to Abakaliki (Ebonyi State)	80
Fig. 4.8	Heat flow contour map of sheet 147 corresponding to Toro	82
Fig.4.9	Heat flow contour map of sheet 173 corresponding to Kaltungo	84
Fig. 4.9.1	Heat flow contour map of sheet 196 corresponding to Numal	86
Fig. 4.9.2	Heat flow contour map of sheet 227 corresponding to Kotonkarfi	88
Fig. 4.9.3	Heat flow contour map of sheet 326 corresponding to Pennington Rivers	90
Fig. 4.9.4	Heat flow contour map of sheet 312 corresponding to Okigwe	92
Fig. 4.9.5:	Heat flow contour map of chad basin NE, Nigeria (Karriwa sheet 24)	93
Fig 5.1a :	Curie Point Depth Geological Map of (Sheet 147) corresponding to Lere_ Farin Ruwa	98
Fig 5.1b:	Geothermal Gradient Geological Map of (Sheet 147) corresponding to Lere_ Farin Ruwa	98
Fig 5.1c:	Heat flow Geological Map of (Sheet 147) corresponding to Lere_ Farin Ruwa	99
Fig 5.2a:	Curie Point Depth (CPD) Geological Map of (Sheet 173) corresponding to Kaltungo	100
Fig 5.2b:	Geothermal Gradient map of (Sheet 173) corresponding to Kaltungo	101
Fig 5.2c:	Heat flow map of (Sheet 173) corresponding to Kaltungo	101
Fig 5.3a.	CPD contour map of Sheet 196 corresponding to Numal	103
Fig.5.3b	Geothermal Gradient contour map of Sheet 196 corresponding to Numal	103
Fig 5.3c.	Heat flow contour map of Sheet 196 corresponding to Numal	104
Fig 5.4a.	CPD contour map of Sheet 227 corresponding to Kotonkarfi	105
Fig. 5.4b	Geothermal Gradient contour map of Sheet 227 corresponding to Kotonkarfi	106
Fig. 5.4c	Heat flow contour map of Sheet 227 corresponding to Kotonkarfi	106
Fig. 5.5a	CPD contour map of Sheet 232 corresponding to Akiri	108
Fig. 5.5b	Geothermal Gradient contour map of Sheet 232 corresponding to Akiri	108
Fig. 5.5c	Heat flow contour map of Sheet 232 corresponding to	109

	Akiri	
Fig.5.6a	CPD contour map of Sheet 244 corresponding to Ado-Ekiti	110
Fig. 5.6b	Geothermal gradient contour map of Sheet 244 corresponding to Ado-Ekiti	111
Fig 5.6c.	Heat flow contour map of Sheet 244 corresponding to Ado- Ekiti	111
Fig.5.7a	CPD contour map of Sheet 247 corresponding to Lokoja	113
Fig. 5.7b	Geothermal Gradient contour map of Sheet 247 corresponding to Lokoja	113
Fig. 5.7c	Heat flow map contour map of Sheet 247 corresponding to Lokoja	114
Fig 5.8a.	CPD contour map of Sheet 266 corresponding to Auchi	115
Fig.5.8b	Geothermal Gradient contour map of Sheet 266 corresponding to Auchi	116
Fig.5.8c	Heat flow contour map of Sheet 266 corresponding to Auchi	116
Fig. 5.9a	CPD contour map of Sheet 287 corresponding to Nsukka	118
Fig.5.9b	Geothermal Gradient contour map of Sheet 287 corresponding to Nsukka	118
Fig.5.9c	Heat flow contour map of Sheet 287 corresponding to Nsukka	119
Fig. 6.1a	CPD contour map of Sheet 300 corresponding to Onitsha	121
Fig.6.1b	Geothermal Gradient contour map of Sheet 300 corresponding to Onitsha	121
Fig.6.1c	Heat flow contour map of Sheet 300 corresponding to Onitsha	122
Fig.6.2a	CPD contour map of Sheet 312 corresponding to Okigwe	123
Fig.6.2b	Geothermal Gradient contour map of Sheet 312 corresponding to Okigwe	124
Fig. 6.2c	Heat flow contour map of Sheet 312 corresponding to Okigwe	124
Fig. 6.3a	CPD contour map of Sheet 418 corresponding to Bauchi	126
Fig. 6.3b	Geothermal gradient contour map of Sheet 418 corresponding to Bauchi	126
Fig.6.3c	Heat flow contour map of Sheet 418 corresponding to Bauchi	127
Fig. 6.4a	CPD contour map of Sheet 215 corresponding to Jalingo	128
Fig. 6.4b	Geothermal Gradient contour map of Sheet 215 corresponding to Jalingo	129
Fig. 6.4c	Heat flow contour map of Sheet 215 corresponding to Jalingo	129
Fig.6.5a	CPD contour map of Sheet 243 corresponding to Ilesha	131
Fig. 6.5b	Geothermal gradient contour map of Sheet 243 corresponding to Ilesha	131

Fig. 6.5c	Heat flow contour map of Sheet 243 corresponding to Ilesha	132
Fig. 6.6a:	CPD contour map of Sheet 280 corresponding to Ijebu-Ode	133
Fig 6.6b :	Geothermal Gradient contour map of Sheet 280 corresponding to Ijebu-Ode	134
Fig.6.6 c:	Heat flow contour map of Sheet 280 corresponding to Ijebu-Ode	134
Fig.6.7 a:	CPD contour map of Sheet 281 corresponding to Ijebu-Ife	136
Fig. 6.7b :	Geothermal Gradient contour map of Sheet 281 corresponding to Ijebu-Ife	136
Fig.6.7 c:	Heat flow contour map of Sheet 281 corresponding to Ijebu-Ife	137
Fig.6.8a :	CPD contour map of sheet 311 corresponding to Abo	138
Fig. 6.8b:	Geothermal gradient contour map of sheet 311 corresponding to Abo	139
Fig.6.8c:	Heat flow contour map of sheet 311 corresponding to Abo	139
Fig.6.9 a:	CPD contour map of sheet 314 corresponding to Ugep	141
Fig. 6.9b:	Geothermal gradient contour map of sheet 314 corresponding to Ugep	141
Fig.6.9c:	Heat flow contour map of sheet 314 corresponding to Ugep	142
Fig 7.1a:	Plots of spectrum energy against wave number (spectral block A Sheet 300) Spectra plots utilized to compute depths to the centroid of magnetic sources in the region.	154
Fig 7.1b	Plots of spectrum energy against wave number (spectral block B Sheet 300)	155
Fig 7.1c	Plots of spectrum energy against wave number (spectral block C Sheet 300)	156
Fig 7.1d	Plots of spectrum energy against wave number (spectral block D Sheet 300)	157
Fig 7.1e	Plots of spectrum energy against wave number (spectral block E Sheet 300)	158
Fig 7.1f	Plots of spectrum energy against wave number (spectral block F Sheet 300)	159
Fig 7.1g	Plots of spectrum energy against wave number (spectral block G Sheet 300)	160
Fig 7.1h	Plots of spectrum energy against wave number (spectral block G Sheet 300)	161
Fig 8.1a	Plots of spectrum energy against wave number (spectral block A Sheet 312)	162
Fig 8.1b	Plots of spectrum energy against wave number (spectral block B Sheet 312)	163
Fig 8.1c	Plots of spectrum energy against wave number (spectral block C Sheet 312)	164
Fig 8.1d	Plots of spectrum energy against wave number (spectral block D Sheet 312)	165
Fig 8.1e	Plots of spectrum energy against wave number (spectral block E Sheet 312)	166

Fig 8.1f	Plots of spectrum energy against wave number (spectral block F Sheet 312)	166
Fig 8.1g	Plots of spectrum energy against wave number (spectral block G Sheet 312)	167
Fig 8.1h	Plots of spectrum energy against wave number (spectral block H Sheet 312)	167
Fig 9.1a	Plots of spectrum energy against wave number (spectral block H Sheet 147A)	168
Fig 9.1b	Plots of spectrum energy against wave number (spectral block H Sheet 147B)	168
Fig 9.1c	Plots of spectrum energy against wave number (spectral block H Sheet 148A)	169
Fig 9.1d	Plots of spectrum energy against wave number (spectral block H Sheet 148B)	169
Fig 9.1e	Plots of spectrum energy against wave number (spectral block H Sheet 173A)	170
Fig 9.1f	Plots of spectrum energy against wave number (spectral block H Sheet 173B)	170
Fig 9.1g	Plots of spectrum energy against wave number (spectral block H Sheet 196A)	171
Fig 9.1h	Plots of spectrum energy against wave number (spectral block H Sheet 196B)	171
Fig 9.1i	Plots of spectrum energy against wave number (spectral block H Sheet 215A)	172
Fig 9.1j	Plots of spectrum energy against wave number (spectral block H Sheet 215B)	172
Fig 9.1k	Plots of spectrum energy against wave number (spectral block H Sheet 227A)	173
Fig 9.1l	Plots of spectrum energy against wave number (spectral block H Sheet 227B)	173
Fig 9.1m	Plots of spectrum energy against wave number (spectral block H Sheet 232A)	174
Fig 9.1n	Plots of spectrum energy against wave number (spectral block H Sheet 232B)	174
Fig 9.1o	Plots of spectrum energy against wave number (spectral block H Sheet 243A)	175
Fig 9.1p	Plots of spectrum energy against wave number (spectral block H Sheet 243B)	175
Fig 9.1q	Plots of spectrum energy against wave number (spectral block H Sheet 244A)	176
Fig 9.1r	Plots of spectrum energy against wave number (spectral block H Sheet 244B)	176
Fig 9.1s	Plots of spectrum energy against wave number (spectral block H Sheet 247A)	177
Fig 9.1t	Plots of spectrum energy against wave number (spectral block H Sheet 247B)	177
Fig 9.1u	Plots of spectrum energy against wave number (spectral block H Sheet 266A)	178
Fig 9.1v	Plots of spectrum energy against wave number (spectral block H Sheet 266B)	178

Fig 9.1w	Plots of spectrum energy against wave number (spectral block H Sheet 280A)	179
Fig 9.1x	Plots of spectrum energy against wave number (spectral block H Sheet 280B)	179
Fig 9.1y	Plots of spectrum energy against wave number (spectral block H Sheet 281A)	180
Fig 9.1z	Plots of spectrum energy against wave number (spectral block H Sheet 281B)	180
Fig 9.1Za	Plots of spectrum energy against wave number (spectral block H Sheet 287A)	181
Fig 9.1Zb	Plots of spectrum energy against wave number (spectral block H Sheet 287B)	181
Fig 9.1Zc	Plots of spectrum energy against wave number (spectral block H Sheet 300A)	182
Fig 9.1Zd	Plots of spectrum energy against wave number (spectral block H Sheet 300B)	182
Fig 9.1Ze	Plots of spectrum energy against wave number (spectral block H Sheet 311A)	183
Fig 9.1Zf	Plots of spectrum energy against wave number (spectral block H Sheet 311B)	183

LIST OF TABLES

TABLES	TITLE	PAGES
Table 3.1:	Attitude of the foliation of schist underlying Ikogosi, Ekiti	20
Table 3.2:	Point of water collection, conditions, rock unit and water temperature along the spring flow in Ikogosi, Ekiti State, Nigeria	23
Table 3.2a:	Point of water collection, conditions, rock unit and water temperature along the springs flow at Olumirin water fall in Erin IjesaOsun State, Nigeria. The temperature of the spring at the time of the measurement was found to range from 24- 28°C.	25
Table 4:	Point of water collection, conditions, rock unit and water temperature along the thermal springs flow in Nasarawa State, Nigeria	28
Table 5:	Point of water collection, conditions, rock unit and water temperature along Farin Ruwa warm spring in Nasarawa State, Nigeria.	34
Table 6:	Point of water collection, conditions, rock unit and water temperature along Igbonla warm spring in Kwara State and Egeneja Warm Spring in Kogi State, Nigeria	39
Table 7:	Point of water collection, conditions, rock unit and water temperature along Ruwan Zafi spring in Adamawa, State, Nigeria.	42
Table 8:	Point of water collection, conditions, rock unit and water temperature along the springs flow in Yankari Park, Bauchi State, Nigeria	44
Table 9:	Point of water collection, conditions, rock unit and water temperature along the springs flow in Azukala, Edo North, Nigeria	47
Table 10:	Point of water collection, conditions, rock unit and water temperature along the springs flow in Ugep, Cross Rivers State, Nigeria.	57
Table 11:	Reservoir fluid property (temperature and initial pressure) of some wells in the Niger Delta Basin	53
Table 12:	Calculation Of Formation Temperature From Abura Field Onshore Niger Delta:	56
Table 13:	Point of water collection, conditions, rock unit and water temperature along the springs flow in Uturu-Okigwe, Imo, Nigeria	58
Table 14:	Point of water collection, conditions, rock unit and water temperature along the springs flow in River Akpalla, Nsukka, Nigeria	60
Table 15:	summary of the results of the centroid depth, depth to basement, curie depth, geothermal gradient and the heat flow _Akiri	64

Table 16:	summary of the results of the centroid depth, depth to basement, curie depth, geothermal gradient and the heat flow _Ado	66
Table 16a:	summary of the results of the centroid depth, depth to basement, curie depth, geothermal gradient and the heat flow _Ijebu Ode	68
Table 17:	summary of the results of the centroid depth, depth to basement, curie depth, geothermal gradient and the heat flow _Lokoja	70
Table 18:	summary of the results of the centroid depth, depth to basement, curie depth, geothermal gradient and the heat flow _Auchi	72
Table 20:	summary of the results of the centroid depth, depth to basement, curie depth, geothermal gradient and the heat flow _Nsukka	74
Table 21:	summary of the results of the centroid depth, depth to basement, curie depth, geothermal gradient and the heat flow _Onitsha	76
Table 21a:	summary of the results of the centroid depth, depth to basement, curie depth, geothermal gradient and the heat flow _Abakaliki	79
Table 22:	summary of the results of the centroid depth, depth to basement, curie depth, geothermal gradient and the heat flow _Toro	81
Table 23:	summary of the results of the centroid depth, depth to basement, curie depth, geothermal gradient and the heat flow _Kaltungo	83
Table 24:	summary of the results of the centroid depth, depth to basement, curie depth, geothermal gradient and the heat flow _Numal	85
Table 25:	summary of the results of the centroid depth, depth to basement, curie depth, geothermal gradient and the heat flow _Kotonkarfi	87
Table 26:	summary of the results of the centroid depth, depth to basement, curie depth, geothermal gradient and the heat flow _Pennigton Rivers	89
Table 27:	summary of the results of the centroid depth, depth to basement, curie depth, geothermal gradient and the heat flow _Okigwe	91
Table 28:	summary of the results of the centroid depth, depth to basement, curie depth, geothermal gradient and the heat flow _Abakaliki	93
Table 29:	Summary of the results of the centroid depth, depth to basement, curie depth, geothermal gradient and the heat flow _Aeromagnetic_Lere_Farin Ruwa	97
Table 30	Summary of the results of the centroid depth, depth to basement, curie depth, geothermal gradient and the heat flow __Aeromagnetic_Kaltungo	100

Table 31	Summary of the results of the centroid depth, depth to basement, curie depth, geothermal gradient and the heat flow __Aeromagnetic_Numal	102
Table 32	Summary of the results of the centroid depth, depth to basement, curie depth, geothermal gradient and the heat flow __Aeromagnetic_Kotonkarfi	105
Table 33	Summary of the results of the centroid depth, depth to basement, curie depth, geothermal gradient and the heat flow __Aeromagnetic_Akiri	107
Table 34	Summary of the results of the centroid depth, depth to basement, curie depth, geothermal gradient and the heat flow __Aeromagnetic_Ado	110
Table 35	Summary of the results of the centroid depth, depth to basement, curie depth, geothermal gradient and the heat flow __Aeromagnetic_Lokoja	112
Table 36	Summary of the results of the centroid depth, depth to basement, curie depth, geothermal gradient and the heat flow __Aeromagnetic_Auchi	115
Table 37	Summary of the results of the centroid depth, depth to basement, curie depth, geothermal gradient and the heat flow __Aeromagnetic_Nsukka	117
Table 38	Summary of the results of the centroid depth, depth to basement, curie depth, geothermal gradient and the heat flow __Aeromagnetic_Onitsha	120
Table 39	Summary of the results of the centroid depth, depth to basement, curie depth, geothermal gradient and the heat flow __Aeromagnetic_Okigwe	123
Table 40	Summary of the results of the centroid depth, depth to basement, curie depth, geothermal gradient and the heat flow __Aeromagnetic_Bauchi	125
Table 41	Summary of the results of the centroid depth, depth to basement, curie depth, geothermal gradient and the heat flow __Aeromagnetic_Jalingo	128

Table 42	Summary of the results of the centroid depth, depth to basement, curie depth, geothermal gradient and the heat flow __Aeromagnetic- _Ilesha	130
Table 43	Summary of the results of the centroid depth, depth to basement, curie depth, geothermal gradient and the heat flow _ _Aeromagnetic_Ijebu Ode	133
Table 44	Summary of the results of the centroid depth, depth to basement, curie depth, geothermal gradient and the heat flow __Aeromagnetic- _Ijebu Ife	135
Table 45	Summary of the results of the centroid depth, depth to basement, curie depth, geothermal gradient and the heat flow __Aeromagnetic_Abo	138
Table 46	Summary of the results of the centroid depth, depth to basement, curie depth, geothermal gradient and the heat flow__Aeromagnetic_Ugeb	140
Table 46a :	Calculation Of The Geothermal Gradient And Formation Temperature From Abura Field Onshore Niger Delta: Tms = 80°f (27°C)	143
Table d :	Calculation Of The Geothermal Gradient And Formation Temperature From Northern field Offshore Delta: Tms = 80°F (27°C)	144

EXECUTIVE SUMMARY

Innovative Geothermal Energy Source for Clean Energy Generation: The need of Nigerian Telecommunications Industry for Efficient Communication delivery study focused on investigating the geothermal resource potential across Nigeria using geological and hydrological studies, high resolution aeromagnetic and airborne gravity data. A total of thirty (30) sheets of aeromagnetic data with a block dimension of 55 km x 55 km were processed and airborne gravity, with each bouguer map were divided into eight overlapping sub-sheets of 27.5 X 27.5 km sizes. Within the Niger Delta axis bottom hole temperature logs (BHT) for evidence of geothermal gradient were acquired and analysed. Six (6) selected fields from the Niger Delta Basin were analysed for geothermal viability.

The Geological and Hydrogeological work was done through the help of some field assistants mainly undergraduate and postgraduate students. Air temperatures at borehole sites and temperature of water at the bottom of borehole, were measured in situ with mercury maximum-minimum thermometer. Topographic maps, geologic compass and satellite navigator, were used as guide in locating thermal springs points, borehole sites and their features.

Geological and hydrological studies across Nigeria were done to identify potential areas with viable thermal resources and also investigate the geothermal surface manifestations which give an idea about geothermal conditions of Nigeria. The results of the study reveals that the warm springs in Ikogosi from the South-Western Nigeria have temperatures around (71°C) from the source and (41 °C) **1 km away** from the source ., Akiri (54 °C), Awe1-3 (41.5-32.7)°C , Farin Ruwa (43°C), and , Wikki warm springs (32 °C) Gwana (30.5°C), Malwulgo(30.5°C) , Ruwan Zafi (54 °C) Ruwan Dimil (26°C), Keana warm saline spring (34°C), Ribi warm saline spring (33.9 °C), Azara warm fresh water(32.7°C) and Kanje warm fresh water (34 °C) ,Numan, Rafin Ruwa (, Igbonla springs (54 °C) , Egeneja (43°C) from the North central; Ugep in Niger Delta area (45 °C) and *Azukala (37°C)in Edo State* have their thermal resources as hyper thermal, while other areas have either thermal or hypothermal (Olumirin water fall temperature (28°C) measurement was found to be hypothermal with no surface manifestation for geothermal, but with extended schist belt from the Ikogosi axis), River Akpalla (30°C) and Uturu-Okigwe (29 °C). Only warm springs with hyper thermal and thermal resources are viable for the electricity generation (Tables 3.2 – 14 and Figs: 3.1.3.21ab). **Hot springs waters may be classified as cold (<20°C), hypothermal (20–30°C), thermal (>30– 40°C) or hyperthermal (>40°C). Based on this classification, we were able to classify the springs studied across Nigeria in this research work.** Results from temperature measurements of springs, using thermometer, BHT data from Niger Delta oil wells and spectral analysis performed on the aeromagnetic and airborne gravity data suggest the occurrence of geothermal anomalies in most areas studied (Tables 3.2 – 46). On the premise of the BHT

information from oil wells in the Niger Delta and Anambra Basin it has been observed that the lowest values of geothermal gradient were found in the center of Niger Delta within the thick Tertiary sediments as 1.1-2.1 °C/100 m or 2.4-2.5 °C/100 m in Edo- Ologbo -Warri-Port Harcourt areas.

Thus, the spectral centroid method which result from low wave number part of the wave number-scaled (depth to the centroid) and high-wave-number portion of the power spectrum (depth to the top) were evaluated. The Curie point depth (CPD), geothermal gradient and heat flow were determined using appropriate parameters.

The heat flow threshold values delineated (80-100) mW/m² within the study areas across Nigeria implies high potential of the occurrences of geothermal energy exploration (Tables 15- 46). Heat flow values above the stated threshold of (80-100) mW/m² in the various regions can be said to be in abundance or anomalous for geothermal plant installations (Figs. 4.2- 6.9a-c) and (Tables 15-46).

The gravity data sets of the following locations: Toro (Sheet 147), Kaltungo _ (Sheet 173), Numal_ (Sheet 196), Kotonkarfi _ (Sheet 227), Akiri_ (Sheet 232), Ado _ (Sheet 244), Lokoja _ (Sheet 247), Auchi _ (Sheet 266), Nsukka _ (Sheet 287), Onitsha _ (Sheet 300), Okigwe_ (Sheet 312) and Pennigton Rivers_ (Sheet 326) were analysed using Geosoft Oasis montaj software across Nigeria for geothermal evidence.

The Nigerian Geological Survey Agency provided the aeromagnetic data (Sheets) used for this research. The data was obtained as part of the NGSAsponsored nationwide aeromagnetic survey in 2009 and the data were collected along a series of 200-meter-spaced NE SW flight lines with an average flight elevation of about 80 meters, with tie lines every 500 meters. Using the International Geomagnetic Reference Field (IGRF), 2005, the geomagnetic gradient was removed from the data. Also, the data was made available in the form of grids with a scale of 1:100,000. The total area covered in this study is approximately 55 by 55 km², extending from Latitude 7⁰ N to 7⁰ 30¹ N and Longitude 6⁰ E to 6⁰ 30¹ N.

This study's procedures include creating a Total Magnetic Intensity (TMI) map with Oasis Montaj software, separating regional and residual anomalies, dividing the residual map into eight overlapping blocks, performing spectral analysis on each block, evaluating the depth to the magnetic source with spectral analysis, and estimating the geothermal gradient and heat flow. The aeromagnetic data sets of the following locations Lere_ Farin Ruwa, (Sheet 147) , Kaltungo_ (Sheet 173), Numal_ (Sheet 196) , Kotonkarfi_ (Sheet 227), Akiri_ (Sheet 232), , Bauchi _Sheet (148), Jalingo_Sheet (215), Ado-Ekiti (Sheet 244),Lokoja (Sheet 247) , Auchi _ (Sheet 266) , Nsukka (Sheet 287) . Onitsha (Sheet 300) , Okigwe_ (Sheet 312) ,Ilesha (Sheet 243), Ijebu-Ode_(Sheet 280), Ijebu-Ife_ (Sheet 281), Abo_ (Sheet 311), and Ugep_ (Sheet 314) were analysed using Geosoft Oasis montaj Version 8.3, Matlab and Surfer Version 15 software's. The results from the Geological, hydrogeological, BHT measurements

,Aeromagnetic and airborne gravity interpretations correlated well and showed good manifestations of geothermal evidence for electricity generation (Tables 3.2- 14 abcd ; Figs 3.1-3.21ab) and (Tables 15-46 ; Figs 4.2-6.9 a-c).

Geothermal physical evidences, anomalous high heat flow values (ie 80-100 mW/m²and above) have been observed in some parts of Nigeria. These areas have geothermal reservoirs and thereby having the capacity to contribute to national energy requirements through the Nigeria telecommunication Commission. Geothermal resources exploration and development is a panacea to energy crises and global warming in Nigeria. Therefore, policy makes are encouraged to support this concerted effort to diversify energy solutions in Nigeria and also take a quantum leap in holistic renewable energy development and setting concrete carbon emission reduction goals.

It's therefore strongly recommended from the geological and hydrogeological assessment that areas:

- (i) with hot springs water thermal temperatures of (>30– 40°C) or hyperthermal (>40°C) be developed for geothermal power generation across Nigeria (tables 3.2- 14 and Figs 3.1-3.21ab) respectively. Such heat flow values are suggestive of anomalous geothermal conditions and are recommended for geothermal development in the areas of study.
- (ii) exploitation and geothermal power installations be carried out in areas where the heat flow values estimated falls within or above the threshold values (80-100) mW/m² across Nigeria, (high potential or anomaly of the occurrences of geothermal energy) , (Tables 15-46 and Figs 4.2-6.9 a-c) respectively. However, the published article, conference/ workshops acceptance are also attached in this report.
- (iii) A typical drilled borehole of 2-5 km deep to be drilled across Nigeria of temperatures between 40°C and over 300° is estimated to costs \$1-2 million, however the cost can vary depending on the drilling conditions. The estimated cost for 2-5km geothermal power plant installation is 3,991 USD per kilowatt.
- (iv) In Kenya, 2.5km well is drilled for about 2 million USD. This model is recommended for the Nigeria government since most wells fall within this range . For deeper kms as at this year, 2023 the estimated cost today: \$50-100 million USD, Barker and Huges • Need to reduce deep hard rock drilling costs by a factor of ~10.

This research results on geothermal parameters for power generation reveals that our Ikogosi results heat flow range from (97.64 – 207.97) w/m² and geothermal gradient of 38.90 – 82.86⁰C/km agrees with the similar research of Fawale and Nwankwo, 2019 where the heat flow was estimated to be 93.79 – 209.54 10 Wm⁻² and geothermal of 37.52-83.82⁰C/km. Most researches on Ikogosi reported that the surface temperature manifestations to be 41⁰C or 38⁰C. Our results indicated with more information, that at the restricted point by the community that the temperature is 71⁰C and 41⁰C at the accessible point 1 km away from the source and 38⁰C (Warm and cool water meeting point), in line with the study of Olurunfemi *etal*, 2011 that temperature is 38⁰C. The 38⁰C is the temperature at meeting point of the warm and cold water and not the entire warm spring average temperature.

Our research study on Ruwa Zafi area and environs using Aeromagnetic and Airborne gravity integration showed that the temperature from at the source of the warm spring is 54 °C (3.3.2) with high heat flow results for geothermal prospect, the heat flow values ranges from 66.65 to 122.13mW/m² (Section 4.12). This study further agrees with the works of Onyejiuwaka, & Iduma, (2020) on Assessment of Geothermal Energy Potential of Ruwan Zafi, Adamawa State and Environs, Northeastern Nigeria, using High Resolution Airborne Magnetic Data with temperature as 54°C and the associated mantle heat flow varies from about 84.48 to 172.53 mW/m² (Section3.3.2).

Eko *etal*, 2022 on geothermal assessment around Akiri reveals moderate geothermal and heat flow results around Akiri and Awe as (31.9-79.7)mW/m² which is below our research work on four integrated methods with heat flow of (71.33-197) mW/m² .There is the need for Eko *et al.*, (2022) to probe deeper into the earth's mantle using the appropriate method like the aeromagnetic, airborne data and BHT logs rather than the ground gravimeter due to the resolution and limitation of the equipment used by them.

Anyadiegwu and Aigbogun (2021) estimated the Curie Point Depth, Heat Flow and Geothermal Gradient Determined from Analysis of Aeromagnetic Data over parts of the Lower Benue Trough and Anambra Basin, Nigeria. The results revealed that the average Curie point Depth of the Study area is 8.07594 km, the Geothermal gradient obtained has an average value of 73 °C /km, The study area has an average heat flow of 170 mW/m². Results of airborne gravity spectral analysis for Akiri (middle Benue trough) study area revealed the occurrence of geothermal parameters: Curie point depth varied between 7.39 to 20.71km, geothermal gradient varied between 28.01 to 78.48 °C/km and heat flow values varied between 70.29 to 197.99 mW/m². Table 33 of our study showed that the Curie point depth values ranges from (7.44- 20.81) km, the geothermal gradient values ranges from (27.87– 77.95) °C/km and the heat flow values ranges from (69.68- 194.87) mW/m². The NE edge covering Jangwa, Azara, Akiri, and Ribi hosts the anomalous heat flow and geothermal gradient with corresponding shallowest values of curie point depth (Fig 5.5 a-c).Other regions like Kumar, Jutu, Kanje, Adawa, Atatakoro, and Kaza also show good geothermal manifestations, except few areas in SW covering Tunga with low heat flow below the recommended threshold value of (80 - 100)mW/m². In general the results for the area/ regions studied agrees with the works of Anyadiegwu and Aigbogun (2021). However, this research work surveys and recommend the current status of the geothermal, exploration, exploitation for electricity generation in Nigeria.

CHAPTER ONE

1.0

Introduction

Geothermal energy is heat derived within the sub-surface of the earth. Water and/or steam carry the geothermal energy to the Earth's surface. Depending on its characteristics, geothermal energy can be used for heating and cooling purposes or be harnessed to generate clean electricity. However, for electricity, generation high or medium temperature resources are needed, which are usually located close to tectonically active regions through geophysical study. Geothermal energy is known as a renewable, immense, and practically inexhaustible source with a technological maturity that is solid, clean, versatile, and useful to generate electricity, among other applications. Geothermal studies cover the variations in temperature in the Earth's crust and the phenomenon that influences the distribution of internal heat in our planet. Geothermal study is made through exploration, evaluation, and exploitation of this type of energy. This type of energy manifests on the surface in the form of volcanoes, geysers, fumaroles, hot springs, etc. Geothermal power plants have very low gaseous emissions to the air when compared with all other power generation technologies that emit carbondioxide (CO₂) as a normal part of the operation (DiPippo, 2012).

The Nations in the World have a common goal of making the World a global village, and the world a clean and safe place. The major sector that is needed to make the dream come true is the telecommunications industry. However, epileptic supply of energy to run every day to day activities in the telecommunications industry to have wider network coverage, regular and adequate availability of network for data services, voice communication and text messages in Nigeria has caused serious setback in the country, to meet up with the goal of the nations of the world .As a result, the telecommunications industry in Nigeria had to adopt alternative source of energy to meet up by self-generation of power, using diesel generators. This method of generating energy is inefficient, costly, and inadequate to support regular and wide network coverage because of huge limitations that are associated with it. Worst still, there is emission of carbon dioxide (CO₂) and greenhouse gases being associated with this alternative source of energy generation. These emissions constitutes serious environmental challenges thus, makes heat to be trapped in the atmosphere and the Carbon dioxide (CO₂) depleting ozone layer. This causes draught and ice at the polar region to melt. Hence causes desertification and coastal erosion, respectively.

In order to overcome these challenges of inefficiency in power supply in the telecommunications industry and environmental issues, then we need a better source of energy that will guarantee regular and efficient supply of power that will be cleaner and safer than the existing ones. The answer to this is geothermal energy. Geothermal (GT) energy has been known to be the safest and the cleanest source of energy. It occurs within the earth. Locating it is a major problem. However, in this research details of

combining suitable geophysical methods with geological information obtained from the geological mapping across Nigeria to track geothermal field and geothermal reservoir across Nigeria for onward utilization as source of power generation to run the mask and other activities in the telecommunications industry will help to detect the Geothermal reservoirs and recommend the appropriate plants for installations. Findings from previous research works have shown that countries like USA, China, Italy, Israel and many other countries of the world are using geothermal energy for power generation due to its clean technology. They are exploiting these geothermal reservoirs from their discovered geothermal fields as a source of clean energy. From this research work data gathering and interpretations the Nigerian telecommunication industry will be able to have regular and efficient power supply, and cleaner energy. The fact is that, geothermal energy does not deplete, there is no epileptic associated with it. It is steady and regular. This will eliminate the challenges in irregular availability of power and boost wider network coverage. As a result majorities that rely on data from the internet and some other services by the telecommunication industry will be able to run their daily work regularly without any interference.

Therefore this paper focuses on finding the possible geothermal reservoirs existing in Nigeria in order to help in solving the Nigeria's energy crisis.

Nigeria, with a population of over 200 million people, has been a slave to the energy conundrum. The need for alternative and cleaner energy sources as championed by the Nigerian Telecommunication through Geothermal sources is imperative to ensure Nigeria's energy growth and energy mix (fossil fuel and renewables). The Nigerian sector of the Chad Basin has been the location of intense petroleum exploration in the 1980s and early 1990s with 23 oil wells drilled and oil and gas found in some of them. These wells can also shed light on the presence of exploitable geothermal resources in the basin (Jitong, 2019). The increasing demand and cost of electricity in the past three decades have accelerated the search all over the world for and the development of renewable energy sources; namely solar, biomass, wind, hydro, geothermal, among others. The energy sector is of strategic importance to the economy of any nation, and a major driver for growth. The sector has a major role to play in reducing poverty, improving productivity and enhancing the general quality of life (Brimmo , etal, 2017 ; Sambo, 2015). However, Nigeria is currently facing an energy crisis, with less than 47% of the population having access to electricity. At the moment, Nigeria is only able to generate about 4,000 MW of power (out of an estimated) potential of 12,524MW).

Nigeria is endowed with large oil, gas, hydro and solar resources, and it has the potential to generate 12,524 MW of electric power from existing plants. On most days, however, it is only able to dispatch around 4,000 MW, which is insufficient for a country of over 200 million people. However, recent

evaluation indicates that Nigeria has generation capability of 4,000 MW, 85% of this capability is from gas-fired thermal power stations. The remaining 15% is from the three Large Hydroelectric power stations in the country (Abraham and Nkitnam, 2017). Nigeria is still far behind in tapping the abundance of geothermal energy resources. Many warm spring in Nigeria is a good geological evidence of potential geothermal energy. Hydrothermal reservoirs can serve as a sustainable potential source of energy because it is renewable. Globally, there is a serious energy concern as a result of the combustion of fossil fuels which causes climate change. The exhaustibility of fossil fuels, their unreliability and environmental implications have resulted in the search for alternative sources of energy. Geothermal (GT) energy, which is the energy of the 'Earths Heat', offers a renewable and reliable source of energy. However, as with most renewable energies, it is inherently regional and site specific, mostly associated with areas of magmatic episodes and crustal plate movements as evidence in our preliminary study.

Electricity generation is based on three major categories of energy, namely nuclear energy, fossil fuels and renewable energy sources (non fossil fuel). Most electricity is generated with steam turbines using fossil fuels, nuclear, biomass, geothermal and solar thermal energy. Other major electricity generation technologies include gas, hydro and wind turbines and solar photovoltaics. In Nigeria the primary sources of energy for the production of electricity are water, oil, gas and coal, hence, the types of power plants in the country are the hydro-electric and the thermal/fossil fuel power plants. Hydroelectric power systems and gas-fired systems are the two main power generating systems used presently. With these sources of electric power generation, Nigeria has grossly not met her citizens' demand for electricity hence the need for geothermal clean energy resources. About 60% of the country's population has no access to electricity services (Akuru and Okoro, 2014). Fossil fuel resources are not renewable and their usages contribute greenhouse gases significantly to the atmosphere. The world is transiting from generation of electric energy with fossil fuel to renewable energy sources that are environmentally friendly. Newsom (2012) observed that Nigeria is richly endowed with renewable energy resources and if effectively utilised for the generation of electricity, could ameliorate its supply, especially, in the rural communities. In 2016 the international energy agency reported that in transiting away from fossil fuel, renewable energy sources constitute about nine-tenths of new power which Europe added to the continent's electricity grids in 2015. America is known to be the world leader in electricity generation through geothermal sources and according to the 2018 state energy data, about 16 terawatt-hours of the total electricity energy supplied and consumed in the country is generated from geothermal sources. Owing to increasing quest for energy, (boasting electricity generation) in Nigeria and the Nigeria Telecommunication, estimation of renewable (GT) as alternative energy sources has become a necessity. It is imperative to utilize Nigerian's huge natural endowments to achieve this goal. One of the natural endowments that has not been utilized for large scale generation of electricity in

Nigeria is geothermal resources. Early research on geothermal gradient studies using spectral analysis of geomagnetic data covered Japan (Okubo and Matsunaga, 1994), United States of America (Mayhew, 1985; Blakely, 1988) and Greece (Tsokas et al., 1998; Stampolidis and Tsokas, 2002); they all made successes in deriving the depth to geologic structures under investigation, such as magnetic basement. Tselentis (1991) had emphatically affirmed that the study of the changes in Curie isotherm depth of an area has afforded worthwhile facts about the regional temperature distribution at depth and the concentration of subsurface geothermal energy; the region with considerable geothermal energy is signalled by an anomalous high temperature gradient and heat flow.

The deeper Cretaceous and Tertiary sequences of the Niger delta are geopressed geothermal horizons as seen in this study. In the Benue fold belt, extending from the Abakaliki anticlinorium to the Keana anticline and the Zambuk ridge, several magmatic intrusions emplaced during the Late Cretaceous line the axis of the Benue trough. Positive Bouguer gravity anomalies also parallel this trough and are being acquired and interpreted to indicate shallow mantle. Parts of this belt and the Ikom, the Jos plateau, Bauchi plateau, and the Adamawa areas, is being evaluated if it can experienced Cenozoic volcanism and magma-tism in stage 3.

Geological occurrence of hot springs and hydrothermal fluids in wells and boreholes are often considered as geothermal manifestations. Many hot springs in Nigeria were identified and surveyed for geothermal manifestations geologically. Many serve as a source of water supply to the nearby inhabitants, while others are being researched for their energy potential and a few have been developed into leisure and tourism sites. Many of these springs are low enthalpy geothermal springs, low enthalpy meaning having a temperature less than 60 degrees Celsius. Hot springs are formed by the interaction of water with heated porous rocks. **Hot springs waters may be classified as cold (<20°C), hypothermal (20–30°C), thermal (>30– 40°C) or hyperthermal (>40°C). Based on this classification, we were able to classify the few springs we study across Nigeria in this research work. A recommended threshold values of heat flow for a good source of Geothermal energy is set at (80-100) mW/m².**

Thermal Springs and Hyper thermal investigated are:

Ikogosi warm springs, Wikki , Gwana ,Malwugo,Dimil warm springs, Erin Olumirin waterfalls, Ruwan Zafi, Ruwan Dumi, Taganrahu, Keana warm saline spring, Ribí warm saline spring, Azara warm fresh water spring and Kanje warm fresh water spring. Akiri Warm springs,Ribí,, Numan, Fafin Ruwa, Igbonla springs and Awe warm saline springs 1. Others include Enemabia warm springs (Orokam,Ogbadigbo, Benue), Kerang springs (Plateau), Azukala, Edo state), Ugeb. The geothermal energy has a good underground storage potential and no greenhouse effect, Environmental impact

advantage and improved cost advantage with enormous resources of lava flows, volcanic sources and hot springs can be made viable to alleviating the state of Nigeria telecommunication power industry into a happy surviving nation and industry. The term “**warm water**” relates to all kinds of groundwater that are heated by the normal terrestrial heat gradient. The geological structure of Nigeria influences geothermal exploration extent within each geological province. Geothermal Heat Recovery from matured oil/gas fields in Nigeria is possible as done in other parts of the world. Within the Niger Delta axis we acquired and analyze bottom hole temperature logs (BHT) for evidence of geothermal gradient and further installation of geothermal power plant for electricity generation. This research discusses the potentials of generating additional energy through the conversion of depleting oil and gas wells to a geothermal energy plant in order to meet the energy demand of Nigerian Telecommunication Commission/ populace, and analysis of possible well integrity issues that these fields could encounter which might result to lost production or induce significant maintenance costs.

The concept of harnessing energy from a low-temperature mature oil & gas field in Nigeria has several underlining advantages. The modern universal quest for green and sustainable energy is a key factor considered when researching on this project having in mind that Nigeria’s electricity generation and distribution is less than 5000 MW for an astonishing population of over 200 million people. The need for ingenious ways of generating electricity for the host communities where over 90% of Nigeria earnings comes from cannot be overemphasized.

This concept of low-temperature energy recovery has thus been practiced in several regions of the world where there is considerably high surface temperature and pressure of the reservoir fluid, the water cut is over 60% and proximity of communities in the near that can utilize this energy. This candidature made the Western, Northern, Eastern and the Niger-Delta Nigeria, a very good environment to develop this type of exciting technology. A good number of oil wells and fields in the Niger Delta have been producing for a long time and have achieved water cut of well over 60%.

Temperature logs from selected wells were acquired from the Department of Petroleum Resources, Lagos an arm of Nigerian National Petroleum Corporation. (NNPC) for geothermal evidence in the Niger Delta for integration. The data were received in form of pdf file. In addition Nigerian block map containing the names and location of all the wells has been acquired form Department of Petroleum Resources, Lagos. This concept has been adopted in various region of the world like the hot water spring in Alaska where a two 200 kW ORC power plant was installed to generate a staggering 400 kW of electricity from an initially waste heat of with surface temperature of less than 75 °C spring. In a project between Ormat Nevada, Inc. and the Department of Energy (DOE) between the year 2007 to 2010 in Wyoming, a 250 kW ORC was installed and was designed to use about 40000 bpd 77 °C produced water using isopentane as the working fluid. This system generated about 180 kW of

electricity (Johnson et al., 2010). In Huabei oilfield in China, a 400 kW of power generator was installed with a binary screw expander system. Within the first nine month of usage, this system has generated around 31×10^4 kWh of electricity (Zhu et al. 2015). In 2014, Alimonti et al. presented a preliminary assessment on the possibility of generating power from the Villafortuna-Trecate Oil field. The project was also based on a single well system and through an Organic Rankine Cycle (ORC) plant. The result suggested that approximately 25 GWh of electric power can be generated over a 10 years period. The technological improvement has thus made it a lot more efficient to generate electricity from a low-temperature heat source via a binary power plant. The procedure of generating this electrical power is quite similar to the traditional power generation mechanism employed in the Clausius-Rankine Cycle. The knowledge of the geothermal gradient of a place helps in determining the suitability of such places for sitting geothermal plants for the generation of electricity that can be utilize for the NCC, industrial, domestic and recreational activities.

In this Project Geological and Geophysical information about a geothermal site was obtained by our researchers using different geophysical investigation techniques such as the aeromagnetic, gravity, Bottom Hole Temperature logs, resistivity data acquired over Nigeria were interpreted to examine the structures underlying the areas, geared toward assessing their geothermal viability. Using these techniques, faults and fissures, reservoir characteristics, altered and mineralized zones, the properties of geothermal fluids, the magma chamber locations and entire tectonic structures could be determined. The geothermal information across Nigeria will be derived as in this research from Bottom Hole Temperature (BHT) measurements (Niger Delta), analysis of aeromagnetic data, gravity data, electrical and heat flow studies.

All current literatures stated that Curie- point depths and heat flows greatly depends on geological conditions. In Geothermal exploration Heat flow is the primary observable parameter. Generally high values of heat flow corresponds to volcanic and metamorphic regions since the two units have high heat conductivities. Generally, airborne surveys as carried in this research are preferred because they allow faster and usually cheaper coverage of large and inaccessible areas. The data obtained from such surveys were presented in form of maps which allows, in addition to quantitative interpretation, a visualization of the geological structures of the subsurface of the Earth. This research aims to apply an efficient method to evaluate the factors influencing the geothermal energy prospects, identify and map prospective geothermal regions.

1.1 Statement of the Problem

Geothermal technology is heat mining from rocks which has been successfully used around the world but is ignored in Nigeria despite our energy needs. Consequently, this has led to undervaluing the long-term potential of geothermal energy available from large volumes of accessible sedimentary rock and basement rocks in Nigeria. Geothermal power is sometimes misconstrued to be an expensive source of electricity. While it is true geothermal power plants require a significant amount of start-up capital and some government assistance in the earliest phases of exploration, the overall capital costs and operating costs of geothermal power are significantly lower than many other technologies. To ascertain its competitiveness and viability among other renewable energy sources, its reservoirs (magma chamber), depth, heat flow and geologic features that gives indication of geothermal resources existence and geothermal maps indicating its volume will be determined. The possible cost of drilling a geothermal well per kilometer and cost of plant installation will be recommended.

1.2 Justification of the Research

The geological structure of Nigeria influences geothermal exploration extent within each geological province. Sedimentary basins in Nigeria have been explored for hydrocarbons for several decades, thus the oil companies collected large subsurface temperature data basis. But not much is known about geothermal conditions within Nigerian Precambrian crystalline province.

Nigeria is a country of insufficient production of electricity and poor energy distribution and transmission system. Electricity generation is based on thermal and hydro power plants, making up 66.7% and 33.3% of total power production respectively. Installed capacity is about 6 GB but only the small percentage out of it is in use. From among 149 million of Nigerian population (official data for 2009) only about 40% has an access to electricity (according to EIA, 2007), which is usually relatively easier within urban, developed areas than in rural peripheries. As Nigeria is one of the biggest producers of oil and gas in the world.

Geothermal energy can be described as the heat generated within the earth which could be exploited for human use. Geothermal resources are generally associated with tectonically active region which are generated as a result of temperature difference between the different parts of the asthenosphere (below the lithosphere) where convection movement are formed. This slow convection movement is said to be maintained by the radioactive elements and heat from the deepest part of the earth (Ojoawo, and Sedara 2016). Nigeria reveals a significant geothermal potential for high and low temperature geothermal system. The geological structure of Nigeria influences geothermal exploration extent within each geological province. Sedimentary basins in Nigeria have been explored for hydrocarbons for several decades, thus the oil companies collected large subsurface temperature data basis. But not much

has been done on geothermal conditions within Nigerian Precambrian crystalline province as stated earlier, hence this present study. Interest in studying geological structure by the integration of geophysical methods has been proven to have the capability of accurately characterizing geothermal reservoirs and exploration.

Several studies have been conducted to map the variation of the Curie depths, heat flow and Geothermal gradients across few areas in Nigeria (Abraham *et al*,2014, Odumodu and Mode, 2016, Oyedepo,2012, Olorunfemi *et al*. 2011, Fawale and Nwankwo, 2019, Tanaka, 1999) using one method in most cases by the researchers .Most geothermal studies are reviewed and compared with this research of integrated study.

So far, geothermal issues have not been widely known in Nigeria, although investigation of subsurface temperature of rock mass was carried out in some wells due to exploration for oil and gas within sedimentary basins. There were several projects being aimed at exploration of subsurface temperature distribution, carried out with a use of data from oil and gas boreholes as well as shallow water wells. The results of those studies as well as investigation of geothermal surface manifestations give an idea about geothermal conditions of some areas in Nigeria.

Considering the geological and structural conditions in Nigeria, three major areas have been identified for geothermal resource development namely; The Ikogosi warm spring located in Ekiti State, the Wikki spring in Bauchi and the Rafin Ruwa spring located in Plateau according to Ojearo and Sedra, 2016; Fawale and Nwankwo, 2019 and Olorunfemi *et al*. 2011. Besides these major areas, minor geothermal resources may exist in other parts of the country where fault related proofs may occur as surface expression. In order to completely validate the results and the conditions for geothermal manifestations, there is a need to carry out geological, geophysical, hydrogeological and BHT surveys and data interpretation using Oasis montaj, Arc Gis and surfur 8 softwares; because the integration of geophysical with geological data has been proven to have the capability of accurately characterizing geothermal reservoirs and exploring for new ones as long as more than one method is being considered for evaluation.

The different data set acquired and interpreted will provides different levels of accuracy, from heat anomalies, structural systems. By correlating different data sets, it is possible to deduce which ones are showing geothermal anomaly. This research applied four relevant integrated geological, hydrogeological and geophysical methods to asses' geothermal anomalies for possible electricity generation across Nigeria and provides the geological maps for exploitation/development. In order to overcome these challenges of inefficiency in power supply in the country/telecommunications industry

and environmental issues, then we need a better source of energy that will guarantee regular and efficient supply of power that will be cleaner and safer than the existing ones. The answer to this is geothermal energy, hence this research. Owing to increasing quest for energy, (boasting electricity generation) in Nigeria and the Nigeria Telecommunication, estimation of renewable (GT) as alternative energy sources has become a necessity.

1.3 Literature Review

Previous Works

Consumption of Electricity per capita in Nigeria is about 100 kWh. This is far below the consumption in South Africa, Brazil and China, which are 4,500, 1934 and 1379 kWh respectively (ECN, 2013; Akuru and Okoro, 2014; Olaoye, 2016). This is the cause of poor industrial growth and high unemployment rate in Nigeria (Oyedepo, 2012; Abraham and Nkitnam, 2017). Fossil fuel resources which Nigerians are solely dependent on are not renewable and their usages contribute greenhouse gases and subsequently affect the environment negatively (Ikechukwu *et al.*, 2015). The world is moving from generation of electric energy with fossil fuel to renewable energy sources that are environmentally friendly (Jassop, *et al.*, 1976). Nigeria is abundantly endowed with renewable energy resources, if it is utilized effectively for the generation of electricity; it will ameliorate the negative impacts that are associated with dependence on fossil fuel resources.

Several studies have been conducted to map the variation of the Curie depths, heat flow and Geothermal gradients across Nigeria (Abraham *et al.*, 2014, Odumodu and Mode, 2016, Oyedepo, 2012, Olorunfemi *et al.* 2011, Fawale and Nwankwo, 2019, Tanaka, 1999) using different methods. Shallow CPD and high heat flow were observed in most areas delineated.

Geophysical studies carried out at Ikogosi in Southwestern Nigeria showed that the curie depths (CPD) have been estimated as 16 km (Olorunfemi *et al.* 2011; Abraham *et al.* 2014), with shallow depths obtained around the Ikogosi Warm Spring (IWS) source (Abraham *et al.* 2014; Fawale and Nwankwo, 2019;). The result reveals that the Curie point depth varies 8.34 – 15.46 km with an average of 11.52 km, the geothermal gradient varies between 37.52 – 83.82 °C km⁻¹ with an average of 53.93 °C km⁻¹, while the heat flow varies between 93.79 – 209.54 mWm⁻² with an average of 134.82 mWm⁻². The low CPD observed in the area is to magmatic intrusion of granite and quartzite rock at the depth with the unit at the center attributed. The shallow CPD in Ikogosi has been attributed to magmatic intrusions at those depths Abraham *et al.* (2014).

However, Obande *et al.* (2014) and Abraham *et al.* (2015) carried out a study on the estimation of depth to the bottom of magnetic sources (DBMS) at Wikki Warm Spring in northeastern Nigeria, using

fractal distribution of sources approach. The result showed that average DBMS was estimated as 0.54 km with average thermal gradient of $54.11\text{ }^{\circ}\text{C km}^{-1}$ and heat flow value of 135.28 mW/m^2 . The generally shallow DBMS obtained in the study area was attributed to magmatic intrusion or diapirism in the subsurface and emphasized the effects of large-scale tectonic events during the evolution of the basin, as major influences on the thermal history.

Onyejiuwaka and Iduma (2020) had presented and published a paper on the assessment of Geothermal Energy Potential of Ruwan Zafi in Adamawa State and Environs, Northeastern Nigeria. They use High Resolution Airborne Magnetic Data in order to map out places with the potentials for application of geothermal energy for electricity generation and geothermal direct heating. They were able to delineate the range of the sediment thickness as 4273.58 and 8693.32 m and top boundary to magnetic bodies was estimated at depths ranging from 89.62 to 235.38 m. The range of the estimated basal depth was between 8.40 and 17.16 km; the geothermal gradient range was between 33.79 and 69.01°C/km and the associated mantle heat flow varies from about 84.48 to 172.53 mW/m^2 . They find out that the geothermal prospect area in this study are areas where thin layer of thermally insulated sediments cover the basement rocks and volcanic activities or the places with the shallowest depth to magnetic sources (Kasidi and Nur, 2012; Obande *et al.*, 2014), as observed in Lamurde, Ruwan Zafi, Lafia, Kiri, Banjiran and Shellen. The observed geothermal gradient greater than 48.11°C/km and heat flow greater than 120.26 mW/m^2 in these areas. They concluded that this observation reflects high potentials of geothermal resources occurrences in those places.

Alliu and Mazian (2018) concluded in their work that geothermal anomaly existed around Central Bauchi using image enhancement techniques on Landsat 8 satellite data.

Odumodu and Mode (2016) also found promising results in their study on Geothermal gradients and present day heat flow on seventy one wells in parts of the eastern Niger delta, using reservoir and corrected bottom-hole temperatures data and other data collected from the wells. The results showed that the geothermal gradients in the shallow/continental sections in the Niger delta vary between $10 - 18^{\circ}\text{ C/km}$ onshore, increasing to about 24° C/km seawards, southwards and eastwards. In the deeper (marine/paralic) section, geothermal gradients vary between $18 - 45^{\circ}\text{ C/km}$. Heat flow values computed using Petromod 1-D modeling software and calibrated against corrected BHT and reservoir temperatures suggests that heat flow variations in this part of the Niger delta range from $29-55\text{ mW/m}^2$ ($0.69-1.31\text{ HFU}$) with an average value of 42.5 mW/m^2 (1.00 HFU).

Akinnubi and Adetona, (2018) Investigated the Geothermal Potential within Benue State, Central Nigeria, From Radiometric and High-Resolution Aeromagnetic Data. The study area covers a total area

of 18,150 km², six aeromagnetic sheets cover the area, major towns are Markudi, Gboko, Otukpo, Akena, Akwana and Katsina-Ala. The geothermal gradient was estimated to range from a value of 62°C/km and 30°C/km respectively with an average value of 41.59 °C/km, anomalous high heat flow of 153.35, and 135.62 Wm⁻² was obtained within around Katsina- Ala and Oturkpo respectively that can be utilized for power generation.

Ayuba and Lawal (2019) Investigated the Geothermal Energy Resource Potential In Parts Of South Western Nigeria Using Aeromagnetic Data. Results indicates that the average Curie point depth (CPD) within the study area is 8.5 km followed by the average geothermal gradient of 42.5°Ckm⁻¹ and an average heat flow 55 mWm⁻².

Nwankwo and Ekine, A (2009) in their work on Geothermal Gradient in the Chad Basin, Nigeria, from Bottom Hole Temperature Logs indicated geothermal gradient range of 2.81 °C/100 m to 5.88 °C/100 m with an average of 3.71 °C/100 m. The thermal conductivity values from the different representative samples range from 0.58 W/m*K to 4.207 W/m*K with an average of 1.626 W/m*K. The work presented a heat flow value ranging from 45 mW/m² to about 90 mW/m² in the Nigerian sector of the Chad Basin.

Anyadiegwu and Aigbogun (2021) estimated the Curie Point Depth, Heat Flow and Geothermal Gradient Determined from Analysis of Aeromagnetic Data over parts of the Lower Benue Trough and Anambra Basin, Nigeria.

This paper evaluates the aeromagnetic data over parts of the Lower Benue Trough and Anambra Basin of North central and Southeastern Nigeria obtained from the Nigerian geological Survey Agency, Abuja to quantitatively determine the Curie Point Depth, Geothermal gradient, and Heat flow using Oasis montaj software, Fourpot software, and Surfer software. The results revealed that the average Curie point Depth of the Study area is 8.07594 km, the Geothermal gradient obtained has an average value of 73 °C/km, The study area has an average heat flow of 170 mW/m².

Abraham, and Nkitnam, (2017): Reviewed the Geothermal Energy in Nigeria corrected Bottom by using the Temperature (BHT) data measured in oil exploration wells drilled in Niger Delta and Anambra basin. They concluded that the lowest values of geothermal gradient were found in the centre of Niger Delta within the thick Tertiary sediments as 1.3-1.8 °C/100 m (Nwachukwu) or 2.2-2.6 °C/100 m in Warri-Port Harcourt area.

Mohammed, 2019 applied the BHT logs and gravity data to study Geothermal exploration in Nigeria. Temperature data obtained from oil drilling activities in some deep basins give a geothermal gradient of

up to 50°C/100 m. Temperatures of 100°C to 175°C were obtained at 1,200 to 2,600 m below the ground level in some part of the Nigerian sector of the Chad Basin. The Chad basin is reported as a rift-related basin, with recognized faults system. Interpreted gravity data from the Nigeria's Chad Basin shows that large geothermal anomalies in a fault-bounded graben-horst system are caused by uplifted mantle (thinned crust) to the depth range of 23–26 km in the Basin. There also exist some known and unknown thermal springs within Nigerian crystalline province. Water of warm springs in Akiri and Ruwan Zafi in Nigeria has the temperature of about 54°C, suggesting occurrence of some geothermal anomalies.

1.4 Objective of the Research

The main aim of this research work is to carry out “Innovative geothermal energy source for clean energy generation: The need of Nigerian telecommunication Industry for efficient communication delivery” The cost of geothermal power is, obviously, dependent upon the technology employed in bringing geothermal energy to the surface and converting it to electricity. Consequently, the specific objectives of this research work are to determine:

- i. area/zones (geothermal reservoirs/fields) across Nigeria using the integration of geological and geophysical exploration methods.
- ii. geological features like geothermal temperature (heat flow) etc that gives an indication of geothermal resources existence.
- iii. the depth of geothermal reservoir beneath the earth surface.
- iv. hydrothermal reservoir volume through the generation of geological map of the indications.
- v. the reservoir temperature.

1.5 Scope of Research Work

The scope of the research work are as follows:

- i. Integrate geological and geophysical exploration to delineate area/zones (geothermal reservoirs/fields) across Nigeria.
- ii. Identify geological features like geothermal temperature (heat flow) and magnetic intrusions that gives an indication of geothermal resources existence.
- iii. Identify the depth of geothermal reservoir beneath the earth surface.
- iv. Generate geological map of the indications (Hydrothermal reservoir volume).

CHAPTER TWO

2.0 Materials and Methods

The resources (materials) used for this research include; The global positioning system (GPS), Thermometer, clinometer, Geosoft oasis montaj, surfur, Arc Gis and mat lab software's ,the high resolution aeromagnetic and airborne gravity data , Bottom Hole temperature measurements logs and geological maps.

The geothermal potential of the study area from geological and hydrogeological point of view was determined as the first principle objective of the research using the clinometer, GPS, magnetometer and resistivity meter. Aeromagnetic data was also applied to generate the geological maps using Oasis Montaj, Malab program, surfur and Arc GIS software's for the geology and Hydrogeology of the various areas of the study. However in the Niger Delta Basin, well logs data were used to determine the geothermal potential in the areas. The Lithology along the borehole section of each locations, the nature of the aquifer, thermal gradient anomalous and temperature were determined from sub-surface geological point of view using Well logs data acquired from the oil industry.

Areas where there were outcrops and springs apart from the Niger Delta, the thermal springs were located using geographical coordinates during the field work and from existing literatures, Primary sources of information, secondary sources of information, and laboratory sources of information. This work was done through the help of some field assistants mainly undergraduate and postgraduate students. Air temperatures at borehole sites and temperature of water at the bottom of borehole, were measured in situ with mercury maximum-minimum thermometer. Topographic maps, geologic compass and satellite navigator, were used as guide in locating thermal springs points, borehole sites and their features while buckets were used for measurements of yields. In other to determine the geothermal energy potential through the rate of changes in temperature with depth (that is geothermal gradient). The temperature data collected on the study area are of two types; ground surface temperature (air temperature) at every thermal spring and borehole site, and groundwater temperatures measured at the bottom (depth) of each borehole and thermal spring location.. The thermometer was submerged into the thermal springs and bottom of boreholes. In case of boreholes, the thermometer was inserted into a PVC tube of 1¼ inch diameter and tied to a string (marine rope) of about 350 meters length. The string/marine rope was then lowered down the bottom of the borehole and allowed to remain there for at least 15 minutes to stabilize the temperature. In boreholes the temperatures were read after removing the thermometer from the PVC tube this was made possible because the thermometer has the ability to retain the last (highest) temperature reading until the mercury in the thermometer is drag down with the use of a magnet or thorough shaking. In thermal springs, the

Thermometer was not inserted into PVC tube but submerged directly into the spring and left there for 15 minutes after which the reading was taken.

The bottom hole temperatures (BHTs) were recorded at various depths during logging of some selected petroleum exploration wells across the Niger Delta. Several corrections were effected on the aeromagnetic, and aero-gravity data before the analysis; these include the international geomagnetic reference field (IGRF) correction using the year 2010 theoretical model. Other corrections, such as temporal and diurnal correction, were also affected. Other corrections applied on the magnetic data in the present study included the reduction to equator correction, which has to do with the realignment of the data on its causative source. The correction was performed to remove the impact of the bipolar effect of the earth that tends to displace the magnetic signal away from its source. Other processing applied to both magnetic and gravity data includes the horizontal derivative filtration and analytic signal computations to establish both the structural and lithologic information resulting from density and magnetic susceptibility contrast.

The spectral analysis was carried out on the bouguer of the gravity anomaly data of the study areas. The gravity data sets of the following locations: Toro (Sheet 147), Kaltungo (Sheet 173), Numal (Sheet 196), Kotonkarfi (Sheet 227), Akiri (Sheet 232), Ado (Sheet 244), Lokoja (Sheet 247), Auchi (Sheet 266), Nsukka (Sheet 287), Onitsha (Sheet 300), Okigwe (Sheet 312) and Pennigton Rivers (Sheet 326) were analysed using Geosoft Oasis montaj software. Each bouguer map was divided into eight overlapping sub-sheets of 27.5 X 27.5 km sizes. The spectral analysis by FFT was performed on each overlapping blocks and the plots of the logarithm of spectral energy $\ln(E)$ against the wave number (cycle/km) was produced using a Matlab program specifically designed to obtain the gradients for deepest depth (centroid depth) and depth to top of magnetic source. Each sub-sheet was further subjected to Fast Fourier Transform, a process that decomposes the gravity data into its energy spectrum and wave number components. The locations were labelled A-L (Sheet 232; A, Sheet 244; B, sheet 247; C, sheet 266; D, sheet 287; E, sheet 300; F, sheet 147; G, sheet 173; H, sheet 196; I; sheet 227; J, sheet 326; K and sheet 312; L). The energy spectrum was plotted against wave number components using MatLab software. This process deduced gradients in the form of depth to the top (Z_T) and centroid (Z_0) of sources. The depth to top of basement and centroid were used to evaluate Curie point depth (Z_b) and thereafter estimate the geothermal gradient and heat flow of study area. Curie point depths varies with geological situations (Ross *et al.*, 2006). Tanaka *et al.* (1999) established that CPD ranging below 10 km are attributable to volcanic and geothermal regions, 10 km to 15 km are attributable to Island arch and ridges, 20 km and above are attributable to Plateaus and 30 km and above are attributable to trenches. The heat flow value between 80mWm^{-2} and 100mWm^{-2} has been established to indicate geothermal anomalous conditions in an area for geothermal prospecting (Jessop

et al., 1976). It can therefore be deduced from this study that regions that fall within the range of 80 to 100 mWm⁻² are good spots for geothermal energy resources.

The aeromagnetic data was obtained as part of the NGSAsponsored nationwide aeromagnetic survey in 2009 and the data were collected along a series of 200-meter-spaced NE SW flight lines with an average flight elevation of about 80 meters, with tie lines every 500 meters. Using the International Geomagnetic Reference Field (IGRF), 2005, the geomagnetic gradient was removed from the data. Also, the data was made available in the form of grids with a scale of 1:100,000. The total area covered in this study is approximately 55 by 55 km², extending from Latitude 7° N to 7° 30' N and Longitude 6° E to 6° 30' N.

The aeromagnetic data sets of the following locations (Lere_ Farin Ruwa, Sheet 147) , Kaltungo_ (Sheet 173), Numal Sheet 196, , Kotonkarfi_ (Sheet 227), Akiri_ (Sheet 232), , Bauchi _Sheet 148, Jalingo_Sheet215, Ado-Ekiti (Sheet 244),Lokoja (Sheet 247) , Auchil_ (Sheet 266) , Nsukka (Sheet 287) . Onitsha (Sheet 300) , Okigwe_ (Sheet 312)Ilesha Sheet 243, Ijebu-Ode_280, Ijebu-Ife_281, Abo_311, Ugep_314 were analysed using Geosoft Oasis montaj Version 8.3, Matlab and Surfer Version 15 software's.

This study's procedures include creating a Total Magnetic Intensity (TMI) map with OASIS MONTAJ software, separating regional and residual anomalies, dividing the residual map into eight overlapping blocks as done in the Airborne gravity data interpretations, performing spectral analysis on each block, evaluating the depth to the magnetic source with spectral analysis, and estimating the geothermal gradient and heat flow. The geological, hydrogeological, airborne gravity and high resolution aeromagnetic data were integrated for the **Innovative Geothermal Energy Source of Clean Energy for electricity generation across Nigeria: The Need of Nigerian Telecommunications Industry for Efficient Communication Delivery.**

2.1 Estimation of Formation Temperature from Well Log Data

Knowing the original borehole temperature is important for establishing a geothermal gradient and for mitigating drilling challenges. The challenges with high-temperature and high-pressure wells, known as HT/HP wells, are currently of major concerns to the industry. At certain depths, rocks behave differently, likewise the fluid they contain and the functioning of the drilling equipment down-hole.

Temperature tool are attached to drilling stems and the temperature they measure are affected by the drilling processes. While measured Bottom Hole Temperature (BHT) is unreliable due to disturbed

formation before measurement, extrapolating the temperature to the initial time before circulation can be achieved by a correction method.

However, each measurement (LWD or Wireline) will give a trend highlighting the geothermal gradient. Geothermal gradient from the bases of prediction of temperature and for understanding evolution of the petroleum system in a basin. Uses of down hole temperatures include:

- Establishing a regional geothermal gradient
- Basin modeling and assessment of petroleum system maturation
- Estimation of resistivity and water saturation

Since basin temperature typically increases with depth, the important thing is to know the rate of increase. Different basins have different rates at which temperature changes with depth, and this rate of change is usually constant during steady sedimentation for a given basin. The rate of change of temperature with depth is known as temperature gradient or geothermal gradient. Temperature gradient is important because it determines the maturity of a source rock (remember that temperatures of at least 65°C will generate oil) and whether or not a petroleum prospect (available source, reservoir, seal rocks together with traps) should be drilled.

According to Nwachukwu (1976), the temperature at any depth can be specified by the relation:

$$T_z = a_0 + a_1 z \quad (1)$$

where T_z = wellbore temperature in °F.

a_0 = means surface temperature in °F

And a_1 = geothermal gradient in °F/ft

Also, equation (1) can be written as

$$T_f = T_{ms} + g_G D \quad (2)$$

where T_f = formation temperature at depth D ft,

T_{ms} = mean surface temperature in °F

And g_G = geothermal gradient in °F/100ft;

(Atlas Wirelineservices, 1985).

The mean surface temperature within the Niger Delta is normally assumed to be 80 °F (27°C) while the geothermal gradient is calculated using the following equation:

$$g_G = \frac{BHT-TMS}{TWD} \times 100^\circ\text{F}/100\text{ft} \quad (3)$$

where BHT = Bottom Hole Temperature ($^\circ\text{F}$)

And TWD = Total Well Depth (Ft).

From the Geophysical well log data used in this research work, the well depth was measured in meters and hence a conversion is made from meter to feet where in equals 3.281 ft.

With the knowledge of the geothermal gradient and the mean surface temperature, the formation temperature at a particular depth can be found from calculation (Equation 2) or by chart (Schlumberger, 1989b; Atlas Wireline services, 1985).

For each of the intervals that were interpreted, an average formation temperature was calculated using an average depth value for that interval (Equations 2 and 3)

Temperature gradient (G_T) is the change in temperature (dT) over a given change in depth (dZ), given as:

$$G_T = \frac{dT}{dZ} \quad (4)$$

An increase in temperature with increasing depth is illustrated in Fig. 2.1. The rate of change of temperature with depth in this case is about 0.0023 degree Celsius for every one metre (Temperature gradient = $0.025^\circ\text{C}/\text{m}$). This can be higher in oil fields due to abnormal pressures resulting from rapid burial or tectonics, chemical reactions and changes in fluid property

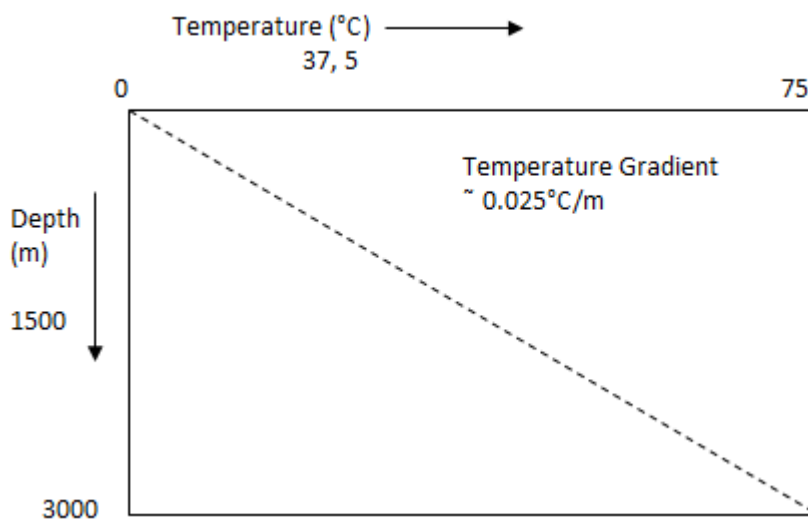


Fig. 2.1: Temperature gradient where temperature over a burial depth of 3km is about 75°C .

Temperatures in the subsurface can be measured using Wireline (a tool that measures temperature) where there is a well as carried out in the Eastern Nigeria by Odumodu and Mode (2016).

Although the most accurate temperature are usually obtained by BHT measurements as done in this study (Niger Delta), however, because of the prohibitive cost of drilling appraisal and developing wells, tested statistically spectral based methods also provide means of estimating the temperature through the data obtained from non-invasive geophysical methods called Magnetic/Airborne gravity.

CHAPTER THREE

3.0 Geothermal Energy Assessment of Nigeria: Geological and Hydrogeological Studies

3.1 Southwest Nigeria Geology and Hydrogeology

3.1.1 Geology of Ikogosi

Ikogosi falls within the South western Nigerian Basement Complex. It is bounded toward the South East and South region by migmatite and toward the extreme north is porphyritic schist and the North East is mixture of schist and phyllites (Fig.3.1) It is underlain by three rock units; quartz schist (Fig. 3.2a), quartz mica schist (Fig.3.2b), and quartzite (Fig. 3.2c). At the basal part of the spring where the cold and hot springs meet, the quart mica schist covers the area. The grains of the mica and quartz are very fine. Moving upward the outcrop of Ikogosi warm spring, the quartz grains become coarse and coarser grains until it eventually become quartz mineral 100% with schistose foliation with general trend of NNW-SSE (Fig. 3d), dip direction of ENE, and their dip varies from 42° to 76° as shown in Table 3.1. The minor trend of the foliation occurs along NNE-SSW direction with dominant trend running NNW-SSE (Fig. 3.3). Moving farther upward the outcrop, the rock unit transits to quartz schist. At the climax of the outcrop, the rock quartz schist mixed with quartzite. There is a fault that cut across the three rock units into the aquiferous layer in Ikogosi to form spring. The spring has its origin from afar off about almost 1km where people are not allowed to access. It is covered with thick forest and giant bush. The topographic elevation varies from 470m in the valleys to 550m on the hills.

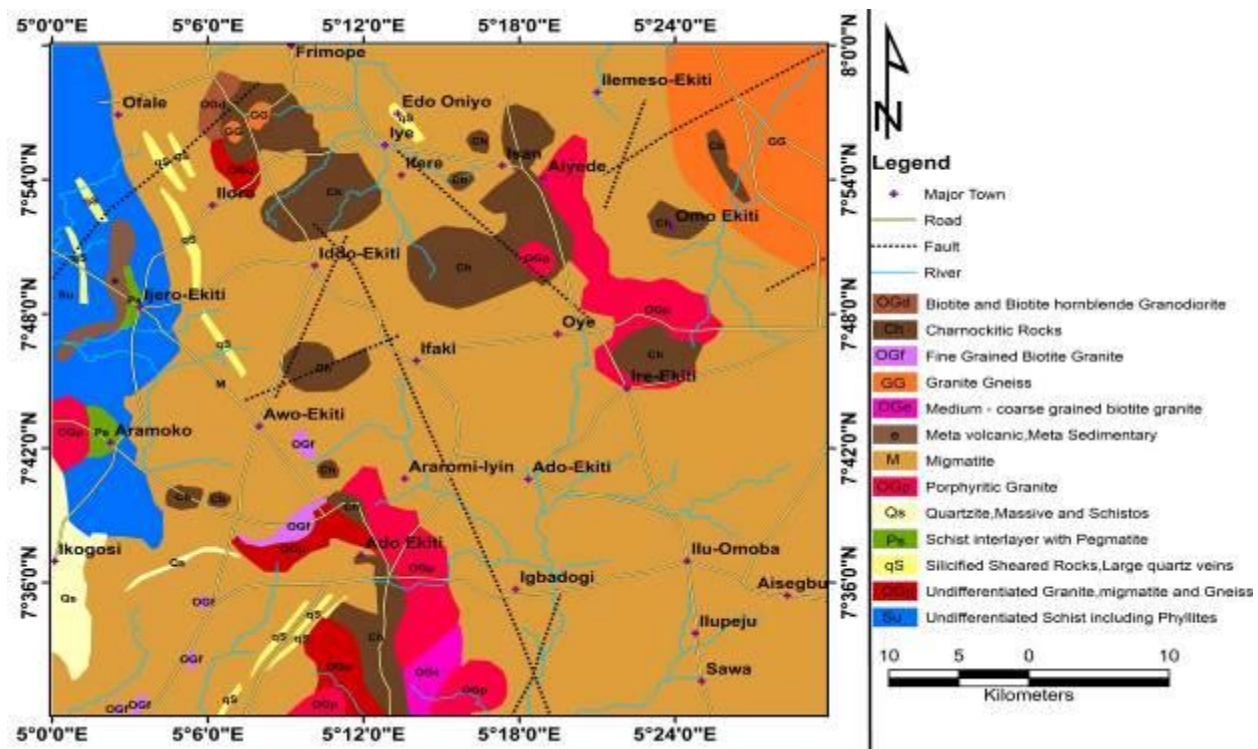


Fig. 3.1: Regional Geology of Ekiti showing Ikogosi



Fig. 3. 2: (a) Quartz Schist exposure at Ikogosi, Ekiti (b) The lead researcher with one of the team member taking the attitude of the foliated Quartz Muscovite Schist at Ikogosi warm Spring, Ekiti (c) Weathered quartzite exposure at the topmost part of Ikogosi outcrop where restriction is placed (d) quartz mica schist foliation trend at Ikogosi in Ekiti, Nigeria

Table 3.1: Attitude of the foliation of schist underlying Ikogosi, Ekiti

S/N	Strike of foliation	Dip direction	Dip
1	330°NNW-150°SSE	73°ENE	43°
2	321°NNW-143°SSE	73°ENE	44°
3	320°NNW-142°SSE	72°ENE	43°
4	340°NN-160°SS	74°ENE	42 °
5	360°NN-180°SS	89°ENE	54 °
6	340°NN-160°SS	70°ENE	42 °
7	345°NN-165°SS	75°ENE	40 °
8	10°NNE-143°SSW	53°ENE	76°
9	20°NNE-200°SSW	110°SSE	62°

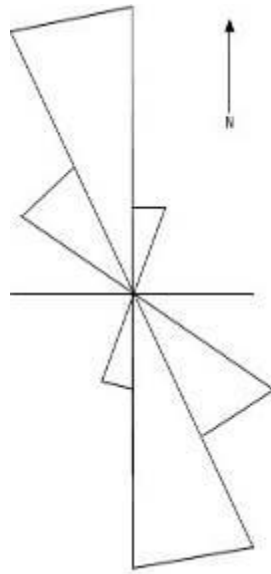


Fig. 3.3: Rose diagram for foliation strike of quartz schist and quartz muscovite schist outcrop exposed at Ikogosi warm spring in Ekiti, Nigeria.

3.1.2 Hydrogeology of Ikogosi

The hydrogeology of Ikogosi was studied with special attention on the origin of the flow, direction, temperature along the flow direction and rock units along the flow direction. The spring occurs in the area as a result of the fault that cut across the rock units underlying the area deep into the aquiferous layer. Through the fault, the groundwater flows to the surface at the almost 1 km apex of the outcrop (Fig.3.4a) away from the restriction limit (Fig. 3.4b and 3.4d). The slope becomes gentle down to the point where both the warm and the cold spring meet (Fig. 3.3c). The temperature of the spring varied along the direction of spring flow from the apex to downstream. The temperature was observed to be 71°C which is the maximum temperature at the apex where quartzite and quartz schist occur. As the spring flows down, the temperature drops gradually to 40°C till it reaches the restricted limits (Table 2).

Few meters away from this point is the point where both the cold and warm water meet, the temperature drops to 38°C. Away from this point, the temperature drops further to 34°C (Table 3.2)



Fig. 3.4: (a) The lead researcher of the research team taking water temperature at the apex of the outcrop (b) The lead researcher of the research team taking water temperature at the restricted limits (c) The lead researcher and one of the team member of the research team taking water temperature at the cold and warm water meeting point (d) The lead researcher of the research team feeling the warmth of the spring water with his palm.

Table 3.2: Point of water collection, conditions, rock unit and water temperature along the spring flow in Ikogosi, Ekiti State, Nigeria

S/N	Point along the spring	Condition	Rock unit	Temperature (°C)	Thermal Resource
1	The top most outcrop	Bushy and restricted	Quartzite	71	Hyper thermal
2	About 1km (1000m) away from source, fenced with bricks	Open and accessible	Quartz schist	41	Hyper thermal
3	10 meters from no. 2	Open and accessible	Quartz mica schist	40	Thermal
4	30 meters from no 3.	Open and accessible	Quartz mica schist	40	Thermal
5	50 meters, warm and cool water meeting point	Open and accessible	Quartz mica schist	38	Thermal(mostly reported by some researcher)
6	70m away from warm and cool water meeting point.	Open and accessible	Quartz mica schist	34	Thermal

**The geology of this warm spring is associated with magnetic volcanism and faulting. This implies that the temperature and geothermal resource i.e. hyper thermal and thermal energy generation information has been achieved.*

3.1.3 Geology of Olumirin Erin :Erin Ijesha

Olumirin fall is located in Erin Ijesa, Osun State. Erin water fall lies within the South West region Precambrian Basement Rock of Nigeria. Erin Ijesa underlain by Quartzite, quartzite Schist, and migmatite. The schist belt forms a ridge that trends from Osun to Ekiti State (Fig 3.5). However, Erin fall is underlain by quartzite schist (Fig.3.5 a) that is mixed up rarely with quartzite (Fig.3.5 b) in some few places. The water fall occurs in seven different altitudes. The pressure of the water fall is very high at these seven places as it can be seen in Fig.3.5 a while is very low in the bed or rock that the water fall flow horizontally across as shown in Fig.3.5 c. The quartzite schist foliation (Fig.3.5 d) has a general strike 14°N-194°S with dip of 34° and dip direction 94°E.

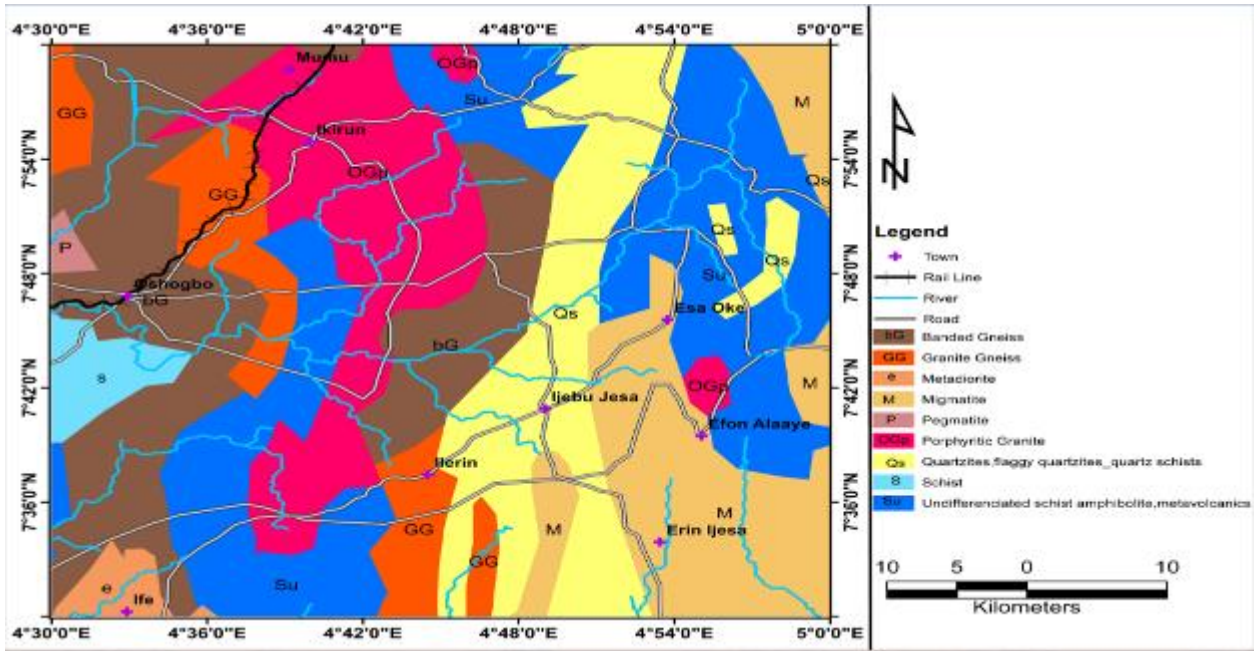


Fig.3.5: Regional Geological map of part of Osun State showing Olumirin fall in Erin Ijesa where the study area falls

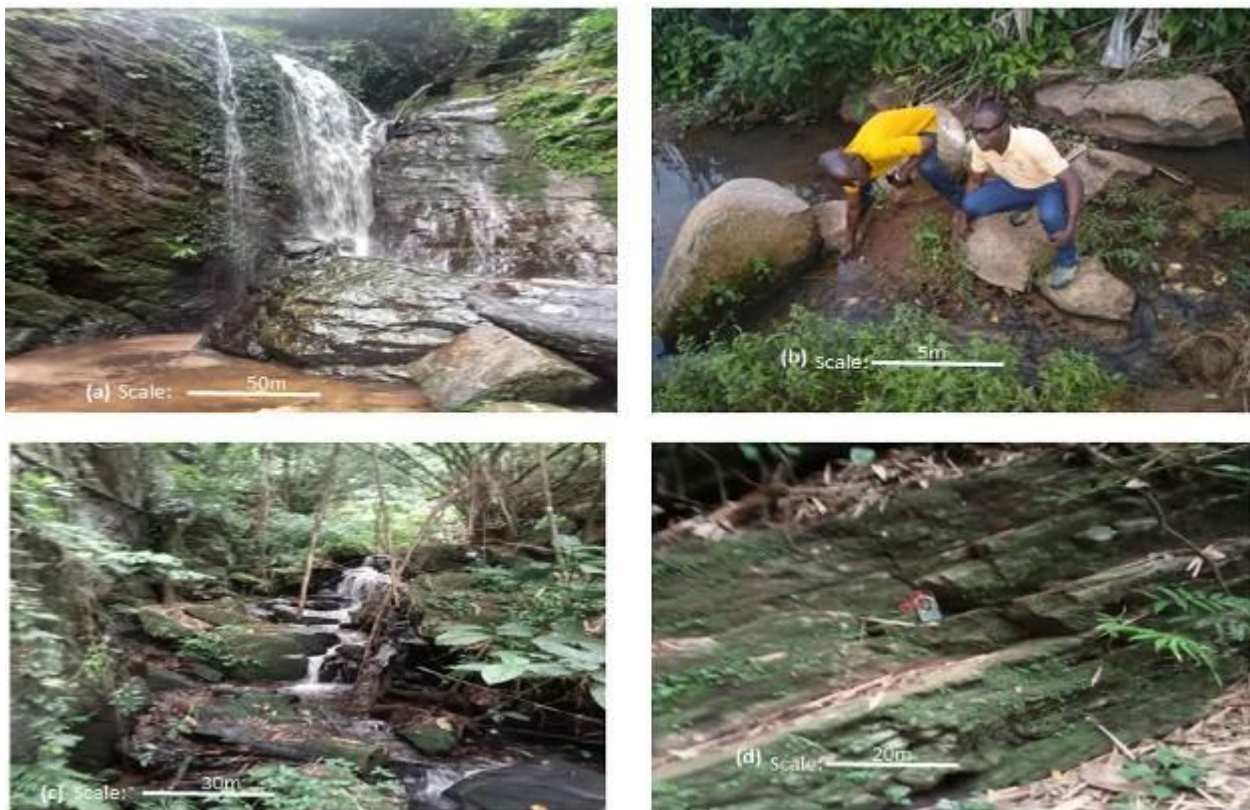


Fig 3.5: (a) Quartz Schist exposure showing high pressure flow of water fall at Olumirin in Erin Ijesa, Osun State (b)The lead researcher with one of the team member standing on the quartzite boulder to measure water temperature at Olumirin fall at Erin Ijesa in Osun State (c) Weathered quartzite exposure at the topmost part of Ikogosi outcrop where restriction is placed (d) Quartz Schist exposure showing low pressure flow of water fall at Olumirin in Erin Ijesa, Osun State.

3.1.4 Hydrogeology of Olumirin Erin

Table 3.2a: Point of water collection, conditions, rock unit and water temperature along the springs flow at Olumirin water fall in Erin Ijesa Osun State, Nigeria. The temperature of the spring at the time of the measurement was found to range from 24- 29°C.

S/N	Geothermal Site	Point along the spring	Rock units	Temperature (c)	Thermal Resources
1	Olumirin	About 1km (1000m) away from source closest to the source of the fall	Quartz schist	24	Hypothermal
2	Olumirin	10m away from the source of the fall	Quartz schist	25	Hypothermal
3	Olumirin	30m away from the source of the fall	Quartz schist	26	Hypothermal
4	Olumirin	50m away from the source of the fall	Quartz schist	28	Hypothermal
		70m away from the source of the fall	Quartz schist	29	hypothermal

** The hypo thermal temperature range results from the surface might not be prospective for geothermal energy utilization due to the threshold value., but the aeromagnetic showed prospectivity of geothermal energy generation in Erin Ijesha (Olumirin at shallow depth (Fig. 6.5c: Heat flow contour map of Sheet 243 corresponding to Ilesha.*

3.2 North Central Nigeria Geology and Hydrogeology

3.2.1 Geology of Azara, Akiri, Awe, Kanje, Keana and Ribí

Azara, Akiri, Awe, Keana and Ribí are located in the southern parts of Nasarawa State, Nigeria. The southern part of Nasarawa is covered by sedimentary rocks. The sedimentary rocks belong to Middle Benue Trough which is the part of the sedimentary basin that extends from the Gulf of Guinea and stretches to the part of northeast of Nigeria. The regional geology of the area is being controlled structurally by two troughs; Middle and Lower Benue Troughs. Keana, Awe and Kanje are bounded from the north to the east by alluvia deposits, at the southwest of the area, they are bounded by Basalt intrusions while the southwest is shale and limestone (Fig. 3.6). Azara, Akiri and Ribí are covered towards the southwest by alluvia deposits, at the southeast is shale and limestone boundary them and at

the north is feldspathic sandstone, poorly sorted medium-coarse grained sandstone except for Ribi that is only bounded from the north to the southeast by a migmatites. The formations in these areas are Eze-Aku Formation, Keana, Awe, and Asu River. The stratigraphic order of the areas is in the order of the Latest Cenomanian-Turonian succession in the central and southern Benue Trough.

The local Geology of Keana Awe and Kanje is siltstone that graded upward to fissile black shale. The black shale (Fig. 3.6a) transits upward into a micaceousarkosic, poorly sorted sandstone bed (Fig. 3.6b), with occasionally interbedded mudrock, planar cross-bedded, characterizes this formation. The partial anticlinelike feature around Awe town indicated that the formation has relatively high dips of 17–32° towards the north and south parts, while towards the northeast, the dip becomes lower in the range of 3–9° in that direction. Longitudinal strike-slip faults parallel to the major fold axis, dominate the area. This observation shows that the area has experienced series of crustal plate movement and the structure is an anticline that has been faulted. Azara, Akiri and Ribi are underlain micacious, poorly sorted cemented sandstone. The sandstone unit is cut across by close conjugate fractures (Joint) with infill of silica material.

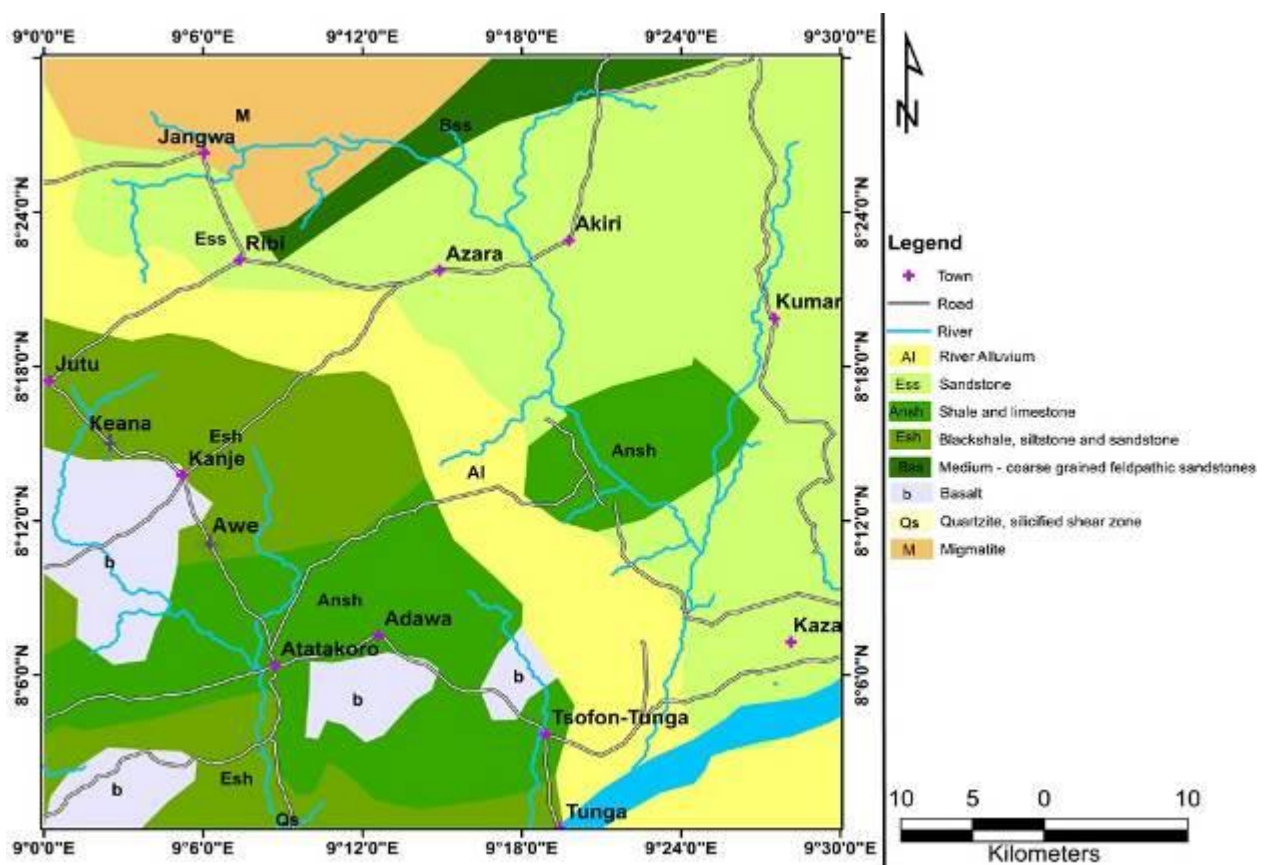


Fig. 3.6a: Regional Geological map of southern part of Nasarawa showing part of Middle Benue Trough where the study areas fall



Fig. 3.6: (a) Keana Formation in Nasarawa showing black shale, siltstone and sandstone lithology units (b) Awe Formation in Nasarawa showing outcrop exposure of black shale

3.2.2 Hydrogeology of Azara, Akiri, Awe, Kanje, Keana and Ribí

Akiri Thermal Spring is located in Akiri, about 4 kilometers north of Azara and less than 3 kilometers west of River Ankwe. It is covered by alluvial deposits of sand. The spring discharges from these sediments (Fig. 3.7a). Pool of the spring serves as a source of water for bathing and livestock and local source for salt. The temperature of the spring at the time of measurement was 54° C. The area is famous for barite mining and traditional salt production based on salty sediments. Awe Thermal Springs is located in Awe. It drains Awe Formation. It comprises three thermal springs (Table 4). Awe spring 1 is the most visible among the three springs. It is 67 km away from Lafia town. The area of the spring Awe 1 is about 500m in diameter. It is a low circular depression of seeps warm spring with temperature of 41.5°C. Awe spring 2 has temperature of 39.2°C. Awe spring 3 releases water with temperature 32.7°C, etc.



Fig. 3.7: (a) The lead researcher taking the temperature of Akiri Spring with thermometer with the assistant of the member of the team (b) The lead researcher taking the temperature of Awe Spring with thermometer at Awe 1thermal spring in Awe, Nasarawa State, Nigeria (c) The lead researcher taking the temperature of Azara Spring with thermometer.

Table 4: Point of water collection, conditions, rock unit, and water temperature along the thermal springs flow in Nasarawa State, Nigeria

S/N	Geothermal Site	Point along the spring	Rock units	Temperature (°C)	Thermal Resources
1	Akiri	1km closest to the source	Sandstone	54	hyperthermal
2	Akiri	10m away from source	Sandstone	54	hyperthermal
3	Akiri	30m away from source		52	hyperthermal
4	Akiri	50m away from source		52	hyperthermal
5	Akiri	70m away from Source		50.6	hyperthermal

Table 4 Continuation: Point of water collection, conditions, rock unit, and water temperature along the thermal springs flow in Nasarawa State, Nigeria

S/N	Geothermal Site	Point along the spring	Rock units	Temperature (°C)	Thermal Resources
1	Awe 1	Closest to the source	Sandstone/shale	41.5	Hyperthermal
2	Awe 1	10m away from source	Sandstone/shale	40.0	Hyperthermal
3	Awe 1	30m away from source	Sandstone/shale	39.3	Hyperthermal
4	Awe 1	50m away from source	Sandstone/shale	39.2	Hyperthermal
5	Awe 1	70m away from source	Sandstone/shale	38.7	Hyperthermal

Table 4 Continuation: Point of water collection, conditions, rock unit, and water temperature along the thermal springs flow in Nasarawa State, Nigeria.

S/N	Geothermal Site	Point along the spring	Rock units	Temperature (°C)	Thermal Resources
1	Awe 2	Closest to the source	Sandstone/shale	39.2	Thermal
2	Awe 2	10m away from source	Sandstone/shale	39.0	Thermal
3	Awe 2	30m away from source	Sandstone/shale	38.8	Thermal
4	Awe 2	50m away from source	Sandstone/shale	37.5	Thermal
5	Awe 2	70m away from source	Sandstone/shale	36.8	Thermal

Table 4 Continuation: Point of water collection, conditions, rock unit, and water temperature along the thermal springs flow in Nasarawa State, Nigeria.

S/N	Geothermal Site	Point along the spring	Rock units	Temperature (°C)	Thermal Resources
1	Awe 3	Closest to the source	Sandstone/shale	32.7	Thermal
2	Awe 3	10m away from source	Sandstone/shale	32.0	Thermal
3	Awe 3	30m away from source	Sandstone/shale	32.0	Thermal
4	Awe 3	50m away from source	Sandstone/shale	31.8	Thermal
5	Awe 3	70m away from source	Sandstone/shale	30.9	Thermal

Table 4 Continuation: Point of water collection, conditions, rock unit, and water temperature along the thermal springs flow in Nasarawa State, Nigeria.

S/N	Geothermal Site	Point along the spring	Rock units	Temperature (°C)	Thermal Resources
1	Ribi	Closest to the source.	Sandstone	33.9	Thermal
2	Ribi	10m away from source	Sandstone	32.5	Thermal
3	Ribi	10m away from source	Sandstone	32.0	Thermal
4	Ribi	10m away from source	Sandstone	31.9	Thermal
5	Ribi	10m away from source	Sandstone	31.3	Thermal

Table 4 Continuation: Point of water collection, conditions, rock unit, and water temperature along the thermal springs flow in Nasarawa State, Nigeria.

S/N	Geothermal Site	Point along the spring	Rock units	Temperature (°C)	Thermal Resources
1	Kanje	10m away from the source	Sandstone/Silt	34	Thermal
2	Kanje	30m away from the source	Sandstone/Silt	33	Thermal
3	Kanje	50m away from the source	Sandstone/Silt	32	Thermal
4	Kanje	70m away from the source	Sandstone/Silt	32	Thermal

Table 4 Continuation: Point of water collection, conditions, rock unit, and water temperature along the thermal springs flow in Nasarawa State, Nigeria.

S/N	Geothermal Site	Point along the spring	Rock units	Temperature (°C)	Thermal Resources
1	Keana	Closest to the source	Sandstone/Silt	34	Thermal
2	Keana	10m away from the source	Sandstone/Silt	34	Thermal
3	Keana	30m away from the source	Sandstone/Silt	33	Thermal
4	Keana	50m away from the source	Sandstone/Silt	32	Thermal
5	Keana	70m away from the source	Sandstone/Silt	32	Thermal

Table 4 Continuation: Point of water collection, conditions, rock unit, and water temperature along the thermal springs flow in Nasarawa State, Nigeria.

S/N	Geothermal Site	Point along the spring	Rock units	Temperature (°C)	Thermal Resources
1	Azara	Closest to the source	Sandstone	32.7	Thermal
2	Azara	10m away from the source	Sandstone	32.4	Thermal
3	Azara	30m away from the source	Sandstone	32.0	Thermal
4	Azara	50m away from the source	Sandstone	31.8	Thermal
5	Azara	70m away from the source	Sandstone	31.5	Thermal

**The geothermal site here (Akiri - Azara), hyper thermal/thermal might be prospective for geothermal energy utilization. The geothermal and hydro geological conditions here are favourable for geothermal exploration and development.*

3.2.3 Geology of Farin Ruwa Warm Spring

Farin Ruwa (*white water*) falls (Fig 3.8 a) is located along the boundary of Plateau State and Nasarawa State at Farin Ruwa, in Wamba Local Government Area of Nasarawa State. It is about 10 kilometres from Lafia, the Nasarawa state capital, and 30 kilometres from Wamba town. It falls within the Precambrian Basement Rock of Nigeria. Unusual rock of acid to intermediate composition, containing, in addition to fayalite, extremely iron rich pyroxenes, The topography of the area is more or less flat laying with the migmatites (Fig 3.8 b)occurring as low lying exposures, while the granitic rocks stands out conspicuously thus dotting the landscape. The water draws a total height of 152m from our measurement.

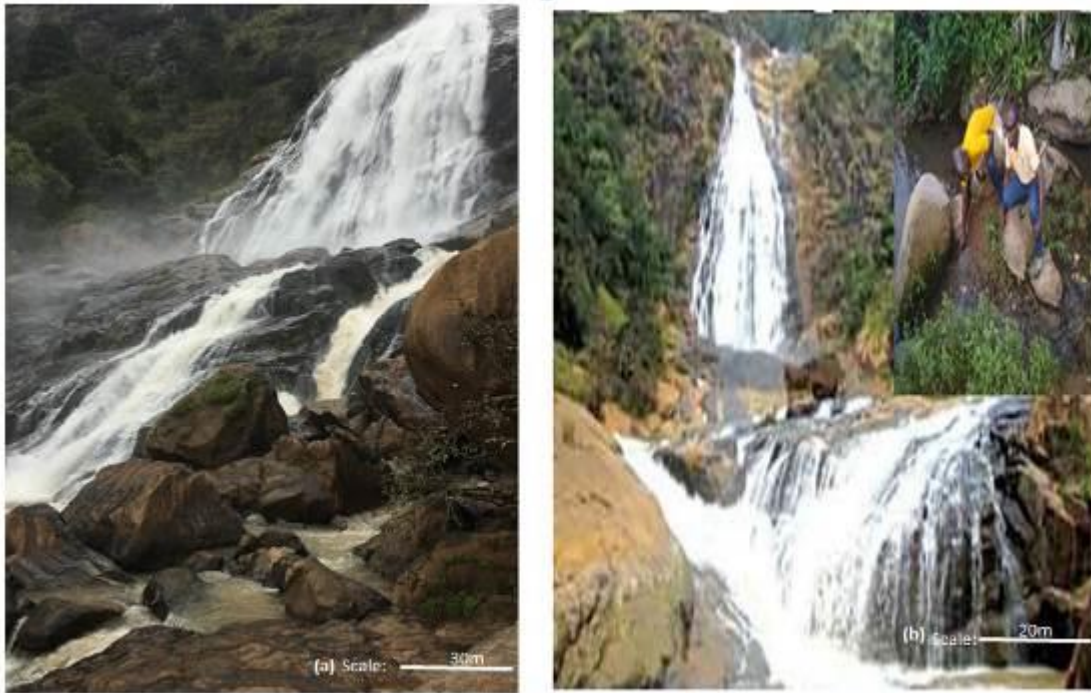


Fig 3.8: (a) The water fall at Farin Ruwa (a) The lead researcher taking the temperature of Farin Ruwa water fall with thermometer sitting on the migmatite rock in Farin Ruwa, Nasarawa State, Nigeria.

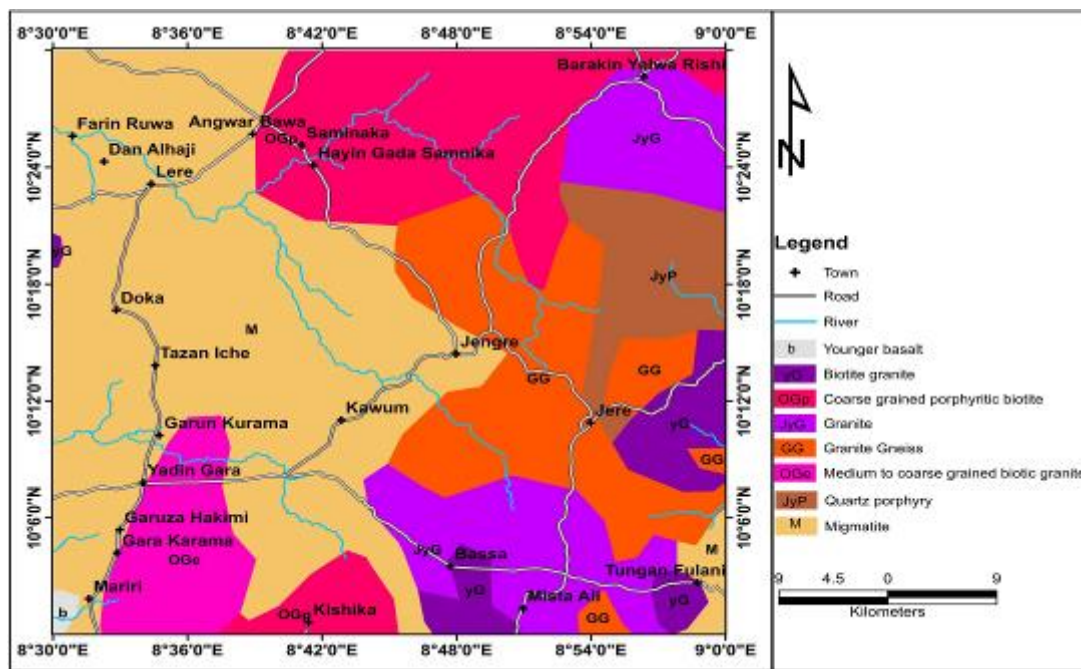


Fig. 3.8 (b): Regional Geological map of **Farin Ruwa** showing the area of study in Nasarawa State

3.2.4 Hydrogeology of Farin Ruwa

Farin Ruwa is located in Wamba Local Government Area of Nasarawa. A total of eight flowing streams of different sizes drain the area. Farin Ruwa Waterfall has its source from Sisimbaki Community in Wamba Local Government Area. Three out of these streams are studded with slippery rocks. The temperature of the spring as at the time of measurement was 43°C. The temperature varies along the river channel (see Table5). The thermal resources according to the temperature is hypothermal (Table 5). The thermal spring which also flows from Precambrian rocks (migmatite – gneiss) is a clear manifestation of volcanic activity.

Table 5: Point of water collection, conditions, rock unit, and water temperature along Farin Ruwa warm spring in Nasarawa State, Nigeria.

S/N	Geothermal Site	Point along the spring	Rock units	Temperature (°C)	Thermal Resources
1	Farin Ruwa	Closest to the source	Fayalit/migmatite	43	Hyperthermal
2	Farin Ruwa	10m away from the source	Fayalit/migmatite	43	Hyperthermal
3	Farin Ruwa	30m away from the source	Migmatite	42	Hyperthermal
4	Farin Ruwa	50m away from the source	Migmatite	42	Hyperthermal
5	Farin Ruwa	70m away from the source	Fayalit/Migmatite	41	Hyperthermal

**The temperature and hydro geological conditions are favourable for geothermal energy utilization and tourist center.*

3.2.5 Geology of Abaji

Abaji falls is located in Abuja. It lies within the Bida Basin. The basin runs in NW-SE trending, extending from Kotangorato Lokoja. The basin was formed by crustal movements that occurred in the Santonian tectonicera. The tectonic event affected the Benue Basin. After the Santonian event there was shallow cratonic sag and pull-apart that lead to the evolution of the basin. Sedimentary sequences in the basin include Nupe Group which divided the sedimentary successions into northern Bida and southern Bida Basins. The southern Bida Basin is made up of three formations includes; Lokoja Formation (Campanian to Maastrichtian), Patti Formation and Agbaja Ironstone. The formations have lateral equivalents in the northern Bida Basin. They are Bida Formation, Sakpe Ironstone, Enagi Siltstone and

Batati Ironstone, respectively. However, Abaji is underlain by Patti Formation which is mainly feldspathic sandstone and siltstone (Fig 3.9a). Along Abuja Lokoja Road, there is a section of Patti Formation. It comprises white to milky basal clay bed that graded upward to white laminated siltstone (Fig 3.9a) that becomes rich at the top with flaser beds which later on transmits into heterolith bed. The Heterolith graded into a well sorted sandstone bed that fills up ancient river channel (Fig. 3.9). The outcrop section was terminated by a very fine grained sandstone. Along Abuja-Lokoja Road, there are other outcrops that expose sandstone unit (Fig.3.9 b) while in other place, there lateral change in facies from sandstone or siltstone (Fig.3.9 c) to shale

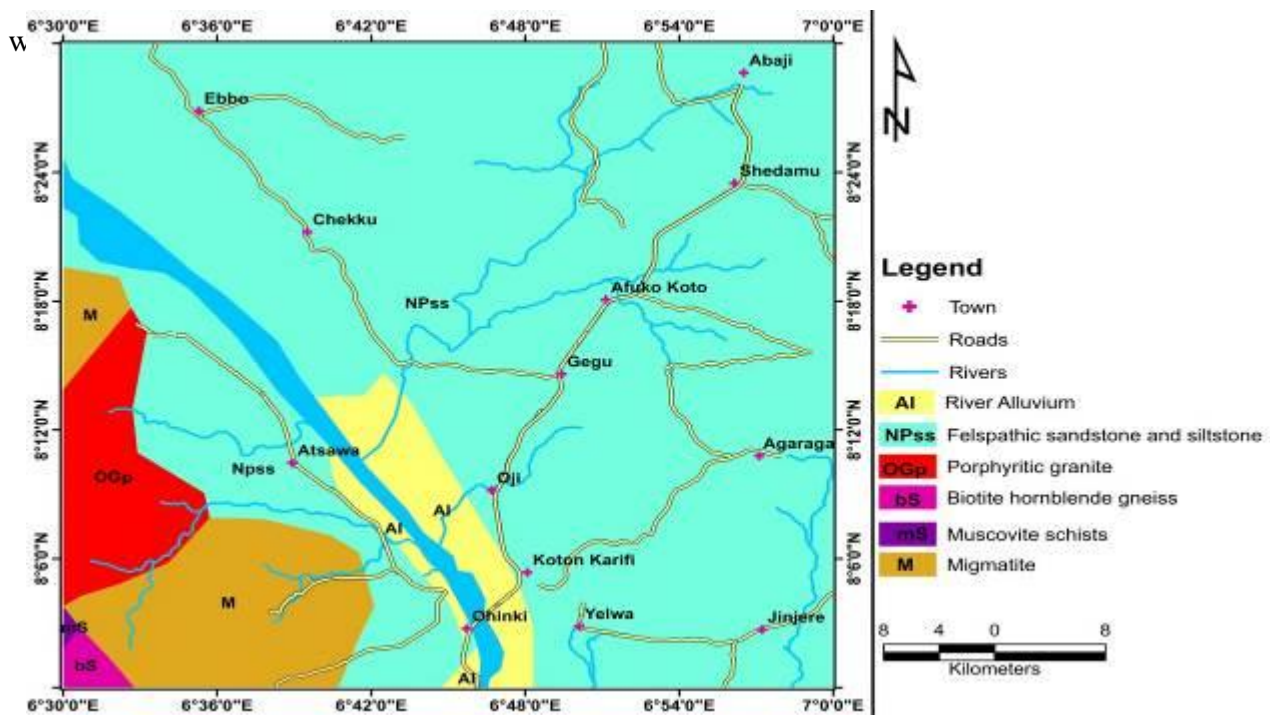


Fig. 3.9 Regional Geological map of part of Abuja showing Abaji where the study area falls

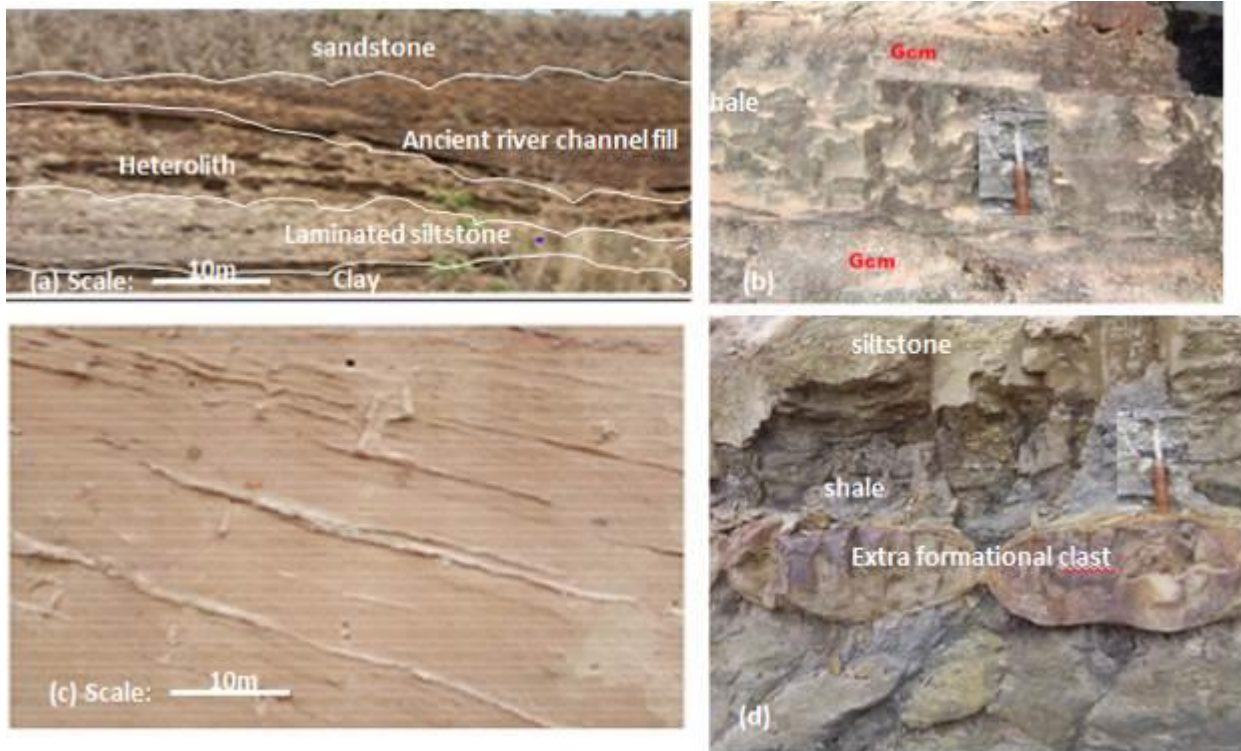


Fig 3.9:(a) in Kwara State, Nigeria (b) Picture of Igbonla warm spring in Kwara State, Nigeria (c) Member of the research team taking temperature of water at Egeneja in Basa Local Government of Kogi State, Nigeria (d) Outcrop section of rock units underlying Ebeneja in Kogi State, Nigeria

3.2.6 Geology of Igbonla and Egeneja Warm Springs

Igbonla warm spring is located at Igbonla in Irepodun LGA of Kwara State, Nigeria, while Egeneja warm spring is located at Egeneja in Basa LGA of Kogi State, Nigeria (Fig. 3.10). Igbonla has two different geologic settings; the Precambrian basement rock which underlies the northwest to the southwest of the area (Fig 3.10) and the sedimentary terrain which underlies the northeast to the southeast. The Precambrian basement rock encroaches into the central part of the area. The warm spring is located at the sedimentary portion of Igbonla (Fig.3.10 a & b). Geological mapping of the area showed that the area where the warm spring occurs is underlain by sandstones, siltstones, mudstone and conglomerates of sub-rounded cobbles, pebbles and granule sized quartz grains which are distributed in a clay matrix. Close to Agbaja plateau, Pegmatitic gneiss of basic content is outcropping mixed with mica schist series which has been folded. The fold has a general trend of NNW-SSE and NNE-SSW and is paralleled by the elongation of the main granitic bodies. It has a general steep dips with well-formed sets of joints with a common strike NE-SW direction and NW-SE direction in some of the place.

Egeneja spring (Fig. 3.10c) is underlain by mudstone and shale (Fig 3.10). It makes boundary with schist towards the west and Benue River at the northern part of the area (Fig.3.10). The outcrop

exposure in the area shows sequence of mudstone grading upward. The silt stone into silty clay. Silt clay transits upward unto shale. The shale is overlain by laminated very fine grained sandstone and passes upward unto a clayey sandstone bed (Fig 3.10d)

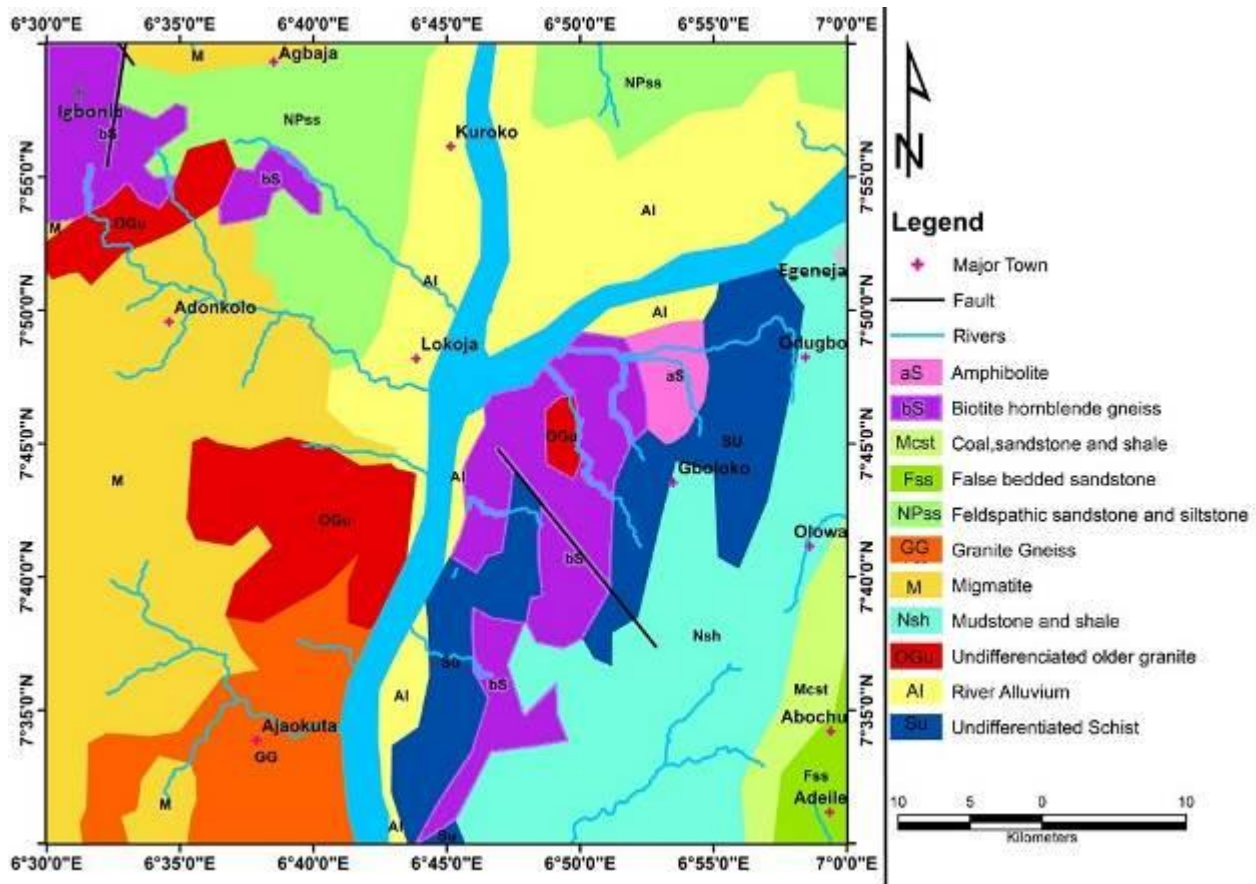


Fig. 3.10 Regional Geological map of part of Kwara State and Kogi State showing Igbonla and Egeneja where the study area falls



Fig.3.10: (a) The lead researcher taking the temperature of the Spring with thermometer at Igbonla warm spring in Kwara State, Nigeria (b) Picture of Igbonla wrm spring in Kwara State, Nigeria (c) Member of the research team taking temperature of water at Egeneja in Basa Local Government of Kogi State, Nigeria (d) Outcrop section of rock units underlying Ebeneja in Kogi State, Nigeria.

3.2.7 Hydrogeology of Igbonla and Egeneja Warm Spring

The area is poorly accessible with high topography ranging from 1150ft to 1245ft. Igbonla is covered by guinea savanna with thick bushes along the offset streams and sparse woods (Fig 3.10 b). Igbonla spring water temperature was measured as 54°C (Table 6) close to the source of the spring as at the time of measurement. The temperature decreases gradually as the spring flows away from its source. Egeneja warm spring has 43 ° C temperatures close to it source (Table 6) and gradually decreases away from the source.

Table 6: Point of water collection, conditions, rock unit and water temperature along Igbonla warm spring in Kwara State and Egeneja Warm Spring in Kogi State, Nigeria

S/N	Geothermal Site	Point along the spring	Rock units	Temperature (°C)	Thermal Resources
1	Igbonla	Closest to the source	Sandstone/siltstone	54	Hyperthermal
2	Igbonla	10m away from the source	Sandstone/siltstone	53	Hyperthermal
3	Igbonla	30m away from the source	Sandstone/siltstone	53	Hyperthermal
4	Igbonla	50m away from the source	Sandstone/siltstone	52	Hyperthermal
5	Igbonla	70m away from the source	Sandstone/siltstone	49	Hyperthermal

Table 6 continuation: Point of water collection, conditions, rock unit and water temperature along Igbonla warm spring in Kwara State and Egeneja Warm Spring in Kogi State, Nigeria

S/N	Geothermal Site	Point along the spring	Rock units	Temperature (°C)	Thermal Resources
1	Egeneja	Closest to the source	Sandstone/siltstone	43	Hyperthermal
2	Egeneja	10m away from the source	Sandstone/siltstone	42	Hyperthermal
3	Egeneja	30m away from the source	Sandstone/siltstone	42	Hyperthermal
4	Egeneja	50m away from the source	Sandstone/siltstone	41	Hyperthermal
5	Egeneja	70m away from the source	Sandstone/siltstone	40	Hyperthermal

**The temperature and hydro geological conditions within Igbonla and Egeneja springs implies high potential of the occurrences of geothermal resources as seen in table 6 above.*

3.3 North Eastern Nigeria Geology and Hydrogeology

3.3.1 Geology of Ruwan Zafi Springs

Ruwan Zafi is located in Adamawa State, Nigeria. It falls in between the Northern Benue Trough and North Eastern Basement Massif within the Gongola Basin. The Gongola Basin comprises Late Aptian - Early Abian sediments. Ruwan Zafi makes boundary with porphyritic granite in the southwest, migmatitic gneiss in the southeast, alluvium deposit in the east and shale and limestone in the north (Fig.3.11). Very fine grained sandstone, siltstone, and mudstone underlain Ruwan Zafi. The sandstone are well cemented with gentle dip that has been exposed by the river (Fig.3.11.a, b, c, d).

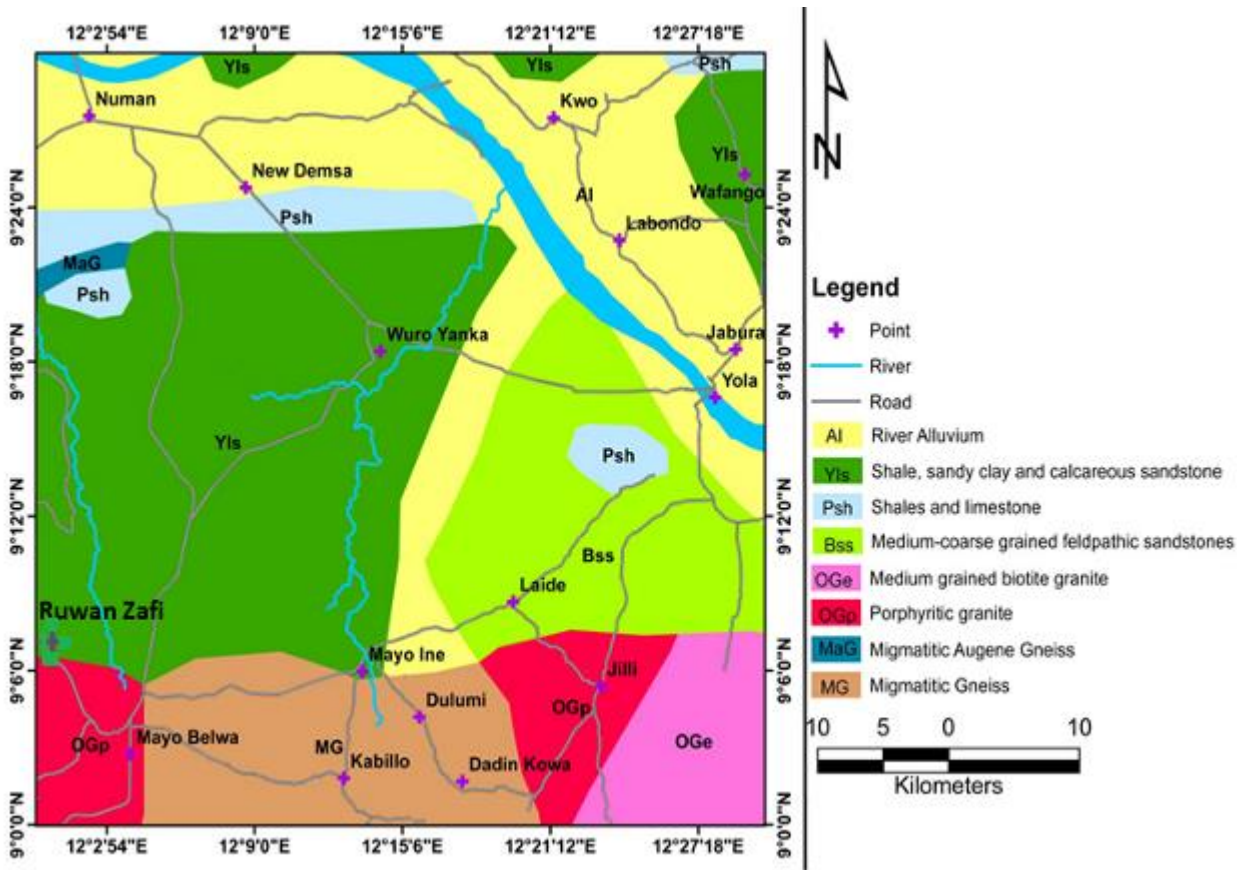


Fig. 3.11: Regional Geological map of Adamawa showing Ruwan Zafi area falls



Fig.3.11 (a) One of the member with the lead researcher of the research team taking water temperature along the river channel in Ruwan Zafi, Adamawa State, Nigeria (b) Exposure of the well cemented sandstone unit at the source of Ruwan Zafi spring, Adamawa State, Nigeria (c) Exposure of the well cemented sandstone unit along part of Ruwan Zafi spring (d) Exposure of the well cemented sandstone unit about 20m away from the source of Ruwan Zafi spring, Adamawa State, Nigeria.

3.3.2 Hydrogeology of Ruwan Zafi

The water flows as a river (Fig.3.11 a) from the source (spring) and drains the area under gravity influence which is controlled by the topography of the area. The spring was formed as a result of fault that cuts across the rock sequence that underlay Lamurde area. The surface temperature of Ruwan Zafi spring as at the time of measurement was from the source 54°C (Table 7). The surface temperature of the spring decreases gradually along the river as we move away from the source of the spring (Table 7).

Table 7: Point of water collection, conditions, rock unit and water temperature along Ruwan Zafi spring in Adamawa, State, Nigeria.

S/N	Geothermal Site	Point along the spring	Rock units	Temperature (°C)	Thermal Resources
1	Ruwan Zafi	Closest to the source	Sandstone/siltstone	54	Hyperthermal
3	Ruwan Zafi	10m away from the source	Sandstone/siltstone	53	Hyperthermal
4	Ruwan Zafi	30m away from the source	Sandstone/siltstone	48	Hyperthermal
5	Ruwan Zafi	50m away from the source	Sandstone/siltstone	47.8	Hyperthermal
6	Ruwan Zafi	70m away from the source	Sandstone/siltstone	47	Hyperthermal

**The geothermal site Ruwan Zafi thermal resources is hyper thermal, this means that the geothermal energy can be explored after integration of other geological and geophysical data in stages 2 and 3*

3.3.3 Geology of Yankari Park and Wikki warm spring

Yankari Game Reserve and Wikki lie within the Upper Benue Trough that extends into Bauchi State, Nigeria. The regional structure that was form in the Early Cretaceous rifting of the central West African basement uplift resulted to the evolution of the basin. The basin extends from the northern part of the Niger Delta and runs northeastwards and links up beneath Lake Chad. The stratigraphy of the area includes Kerri-Kerri Formation, Gombe Formation, Pindiga Formation, Yolde Formation, and Bima Formation. These formation forms nonconformity with the underlying basement rocks. However, The entire Yankari park which includes four springs; Gwana, Dimmi, Mawulgois and Wikki which is the most famous of all is located on the Kerri-Kerri Formation of Tertiary age. Kerr-Kerri Formation is underlain by Gombe Formation. The area is underlain by, Shale, limestone siltstones, sandstone (Fig.3.12 and Fig.3.12b), kaolinites and grits?

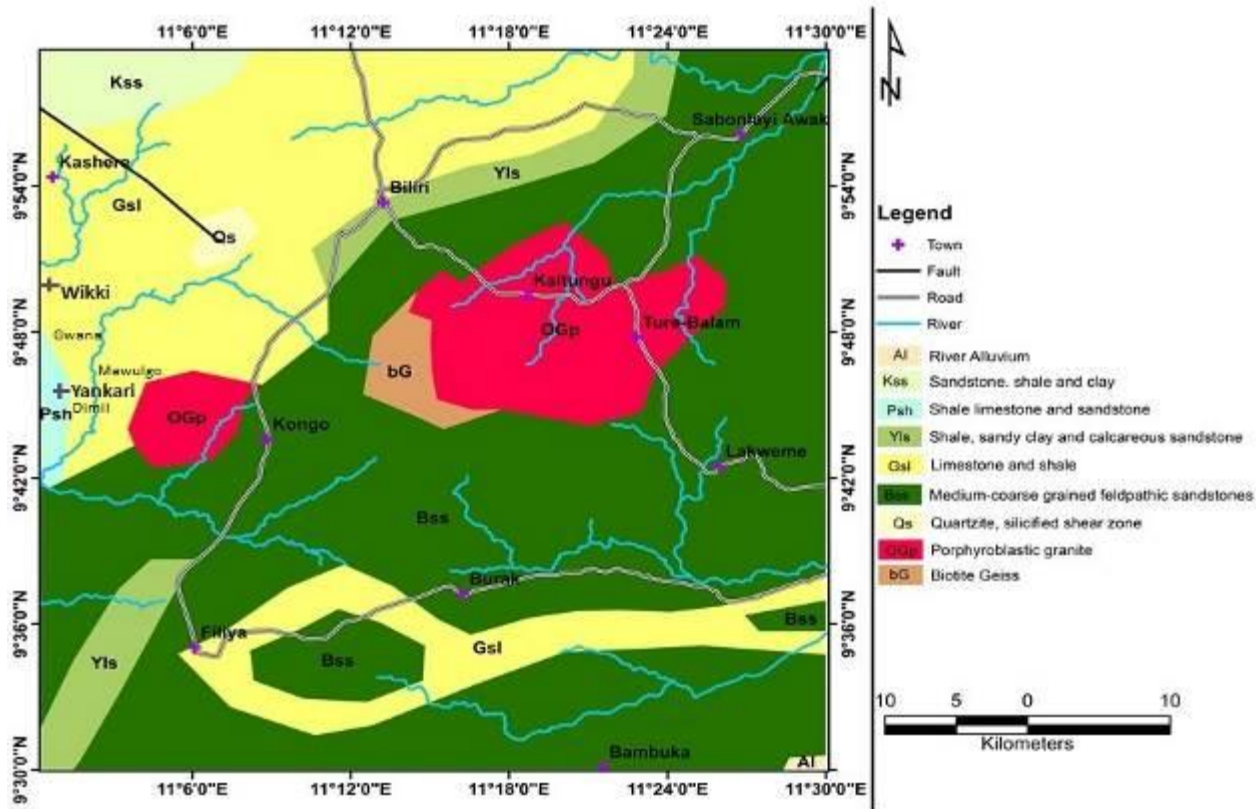


Fig.3.12: Regional Geological map of Bauchi showing Wikki, Gwana, Mawulgo and Dimil springs in Yankari Park, Bauchi State, Nigeria.



Fig.3.12 (a) Some of the members with the lead researcher of the research team taking water temperature along the of- set river in Wikk, Bauchi State (b) Exposure of the well cemented sandstone unit by Wikki Spring water at Yankari Park, Bauchi State, Nigeria.

3.3.4 Hydrogeology of Yankari and Wikki

Yankari Park has four major springs. Out of the four springs, three are warm (Table 8) and only Wikki is the major warm spring that is very large and covers largest extent with the highest surface temperature of 32°C as at the time the temperature was taken. Gwana and Mawulgo have 30.5°C (Table 8). The valleys of the Yashi, Yuli and Gaji Rivers flow with Alluvium sediments which are of more recent age. Towards the valley of Gaji, Yuli and Yashi Rivers, sandy loams and clayey soils of riverine alluvium are found. These rivers drain the Kerri-Kerri Formation exposing the sandstone and siltstone portion that is well cemented and indurated.

Table 8: Point of water collection, conditions, rock unit and water temperature along the springs flow in Yankari Park, Bauchi State, Nigeria

S/N	Geothermal Site	Point along the spring	Rock units	Temperature (°C)	Thermal Resources
1	Wikki	Closest to the source	Sandstone/siltstone	32.0	Thermal
2	Wikki	10m away from the source	Sandstone/siltstone	31.8	Thermal
3	Wikki	30m away from the source	Sandstone/siltstone	31.2	Thermal
4	Wikki	50m away from the source	Sandstone/siltstone	31.0	Thermal
5	Wikki	70m away from the source	Sandstone/siltstone	31.9	Thermal

Table 8 continuation: Point of water collection, conditions, rock unit and water temperature along the springs flow in Yankari Park, Bauchi State, Nigeria

S/N	Geothermal Site	Point along the spring	Rock units	Temperature (°C)	Thermal Resources
1	Gwana	Closest to the source	Sandstone	30.5	Thermal
2	Gwana	10m away from the source	Sandstone	30.0	Thermal
3	Gwana	30m away from the source	Sandstone	29.8	Thermal
4	Gwana	50m away from the source	Sandstone	29.3	Thermal
5	Gwana	70m away from the source	Sandstone	28.7	Thermal

Table 8 continuation: Point of water collection, conditions, rock unit and water temperature along the springs flow in Yankari Park, Bauchi State, Nigeria

S/N	Geothermal Site	Point along the spring	Rock units	Temperature (°C)	Thermal Resources
1	Mawulgo	Closest to the source	Sandstone/siltstone	30.5	Thermal
2	Mawulgo	10m away from the source	Sandstone/siltstone	30.9	Thermal
3	Mawulgo	30m away from the source	Sandstone/siltstone	29.6	Thermal
4	Mawulgo	50m away from the source	Sandstone/siltstone	29.1	Thermal
5	Mawulgo	70m away from the source	Sandstone/siltstone	28.9	Thermal

Table 8 continuation: Point of water collection, conditions, rock unit and water temperature along the springs flow in Yankari Park, Bauchi State, Nigeria

S/N	Geothermal Site	Point along the spring	Rock units	Temperature (°C)	Thermal Resources
1	Dimil	Closest to the source	Sandstone/shale	26.0	Hypothermal
2	Dimil	10m away from the source	Sandstone/shale	25.8	Hypothermal
3	Dimil	30m away from the source	Sandstone/shale	25.3	Hypothermal
4	Dimil	50m away from the source	Sandstone/shale	24.9	Hypothermal
5	Dimil	70m away from the source	Sandstone/shale	24.5	Hypothermal

**From Geological and hydro geological study results, Wikki, Gwana, Mawulgo, Dimil shows geothermal manifestations with only Dimil temperature (hypo thermal) below the recommended threshold.*

3.4 South-South Nigeria Geology and Hydrogeology

3.4.1 Geology of Azukala

Azukala is located in Etsako Central Local Government Area of Edo State, Nigeria. It falls within the arm of Anambra Basin in Edo State. It is underlain by Imo Formation. The Imo Formation around Azukala comprises sandstone, thick shale deposits and lignite (Fig.3.13). It is bounded at the north part by Nsukka Formation which comprises shale, sandstone and coal beds. Imo Formation's outcrop in Azukala axis of Etsako Central in Edo State is exposed by rivers that drain the area. The basal bed is

dark fissile shale. The shale is overlain by laminated dirty white siltstone, the siltstone bed graded upward to medium light yellowish sandstone.

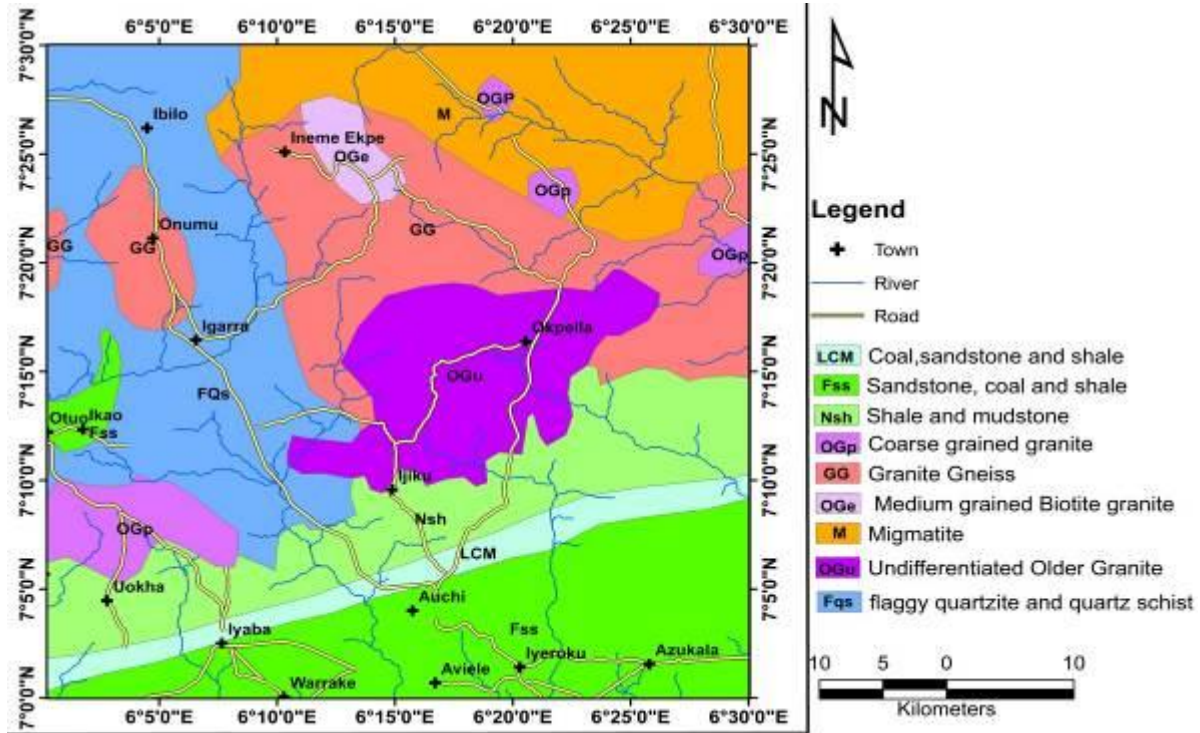


Fig.3.13: Regional Geological map of Edo North in Auchi showing Azukala area where the study was done.

3.4.2 Hydrogeology of Azukala

The area is known as Igueda meaning the way of rivers. The rivers are the off-set springs that flow from the aquiferous layer beneath the region and flow out to the surface as spring. The temperature of the river was about 37°C (Table 9) at the time of measurement. The river runs in the direction of south.

Table 9: Point of water collection, conditions, rock unit and water temperature along the springs flow in Azukala, Edo North, Nigeria

S/N	Geothermal Site	Point along the spring	Rock units	Temperature (°C)	Thermal Resources
1	Azukala	Along the stream	Sandstone/siltstone	37	Thermal
2	Azukala	10m away from stream	Sandstone	36	Thermal
3	Azukala	30m away from stream	Mudstone/shale	35	Thermal
4	Azukala	50m away from stream	Sandstone	35	Thermal
5	Azukala	70m away from stream	Mudstone/shale	34	Thermal

* From Geological, (temperature) and hydro geological study results, Azukala shows geothermal manifestations within the recommended threshold.

3.4.3 Geology of Ishiagu

Ishiaguis located in Delta State about 10km away from Ogwashi Olor. It falls within Anambra Basin. It is underlain by Ogwashi-Asaba Formation which comprises friable sandstone and mudstone. It is bounded by sequence of lignite, shale sandstone, clay, and mudstone at the northwest of the area.

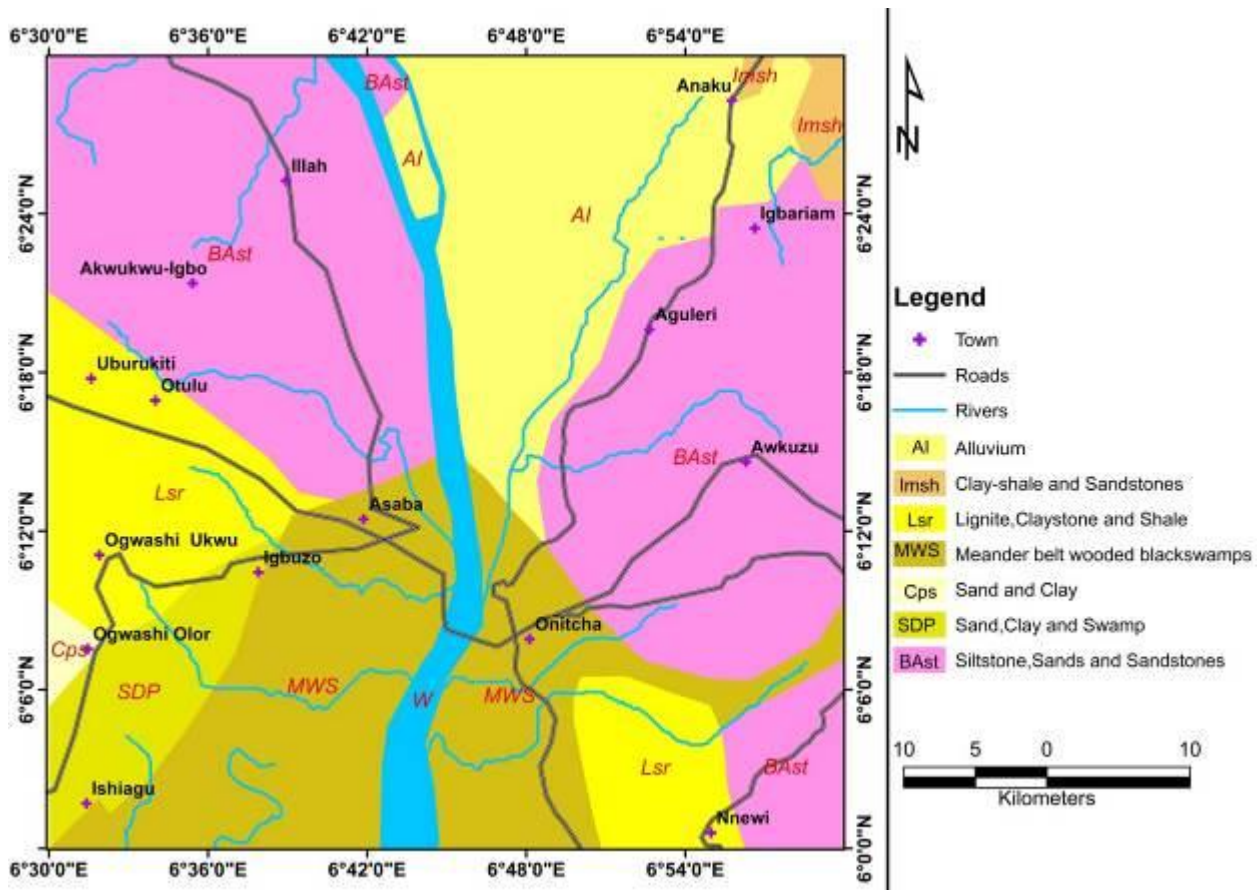


Fig.3.14: Regional Geological map of Delta North showing Ishiagu where the study was done

3.4.4 Hydrogeology of Ishiagu

Ishiagu where the spring as turn to wetlands thus makes the area a swamp. Streams cut across the area and river meanders the area. The swamp happier blackish to light blackish in the area (Fig.3.14). Toward the eastern part of Ishaigu is River Niger trending from the north down to the south while some other smaller rivers on the area empty their clastics in River Niger. It was difficult to take temperature of the water because of the swamp interfering with the river.

3.4.5 Geology of Ugep Warm and Cold Springs

Ugep warm and cold springs are located at Ugep in Cross River State, Nigeria. The area lies within the Ourthern Benue Trough. It is underlain by intercalation of shale, limestone, siltstone and sandstone (Fig map). Ugep warm and cold spring is underlain by Eze-aku Formation (Fig.3.15 a) The sandstone unit (Fig.3.15 b) is fine to coarse grained sandstone which coarsening upward. It occurs in linear and parallel northeast pattern trending ridges. The sandstone is alternated by shale sequence, slightly bioturbated, stratified and rippled bedded

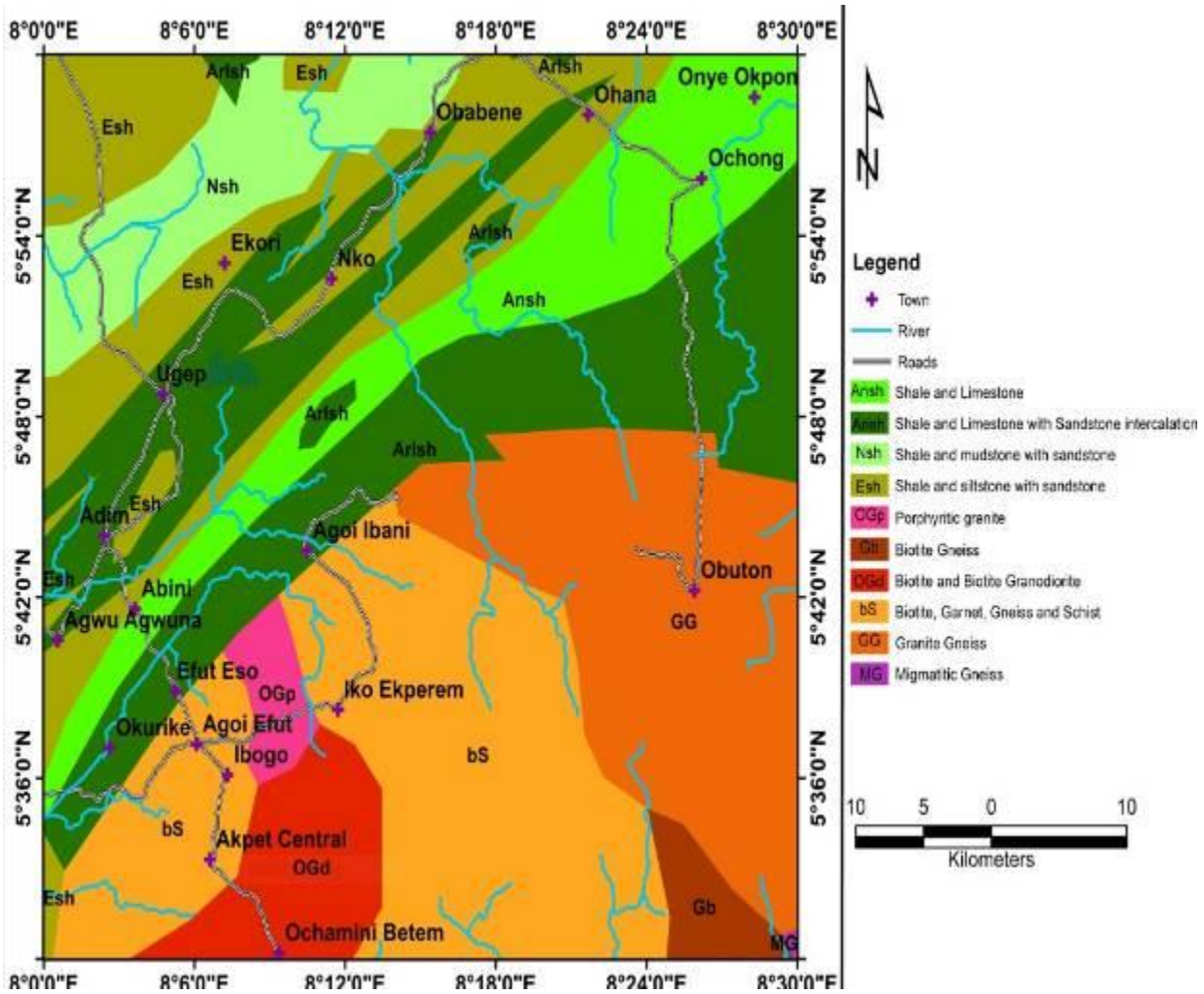


Fig.3.15: Regional Geological map of part of Cross River showing Ugep where the study area falls

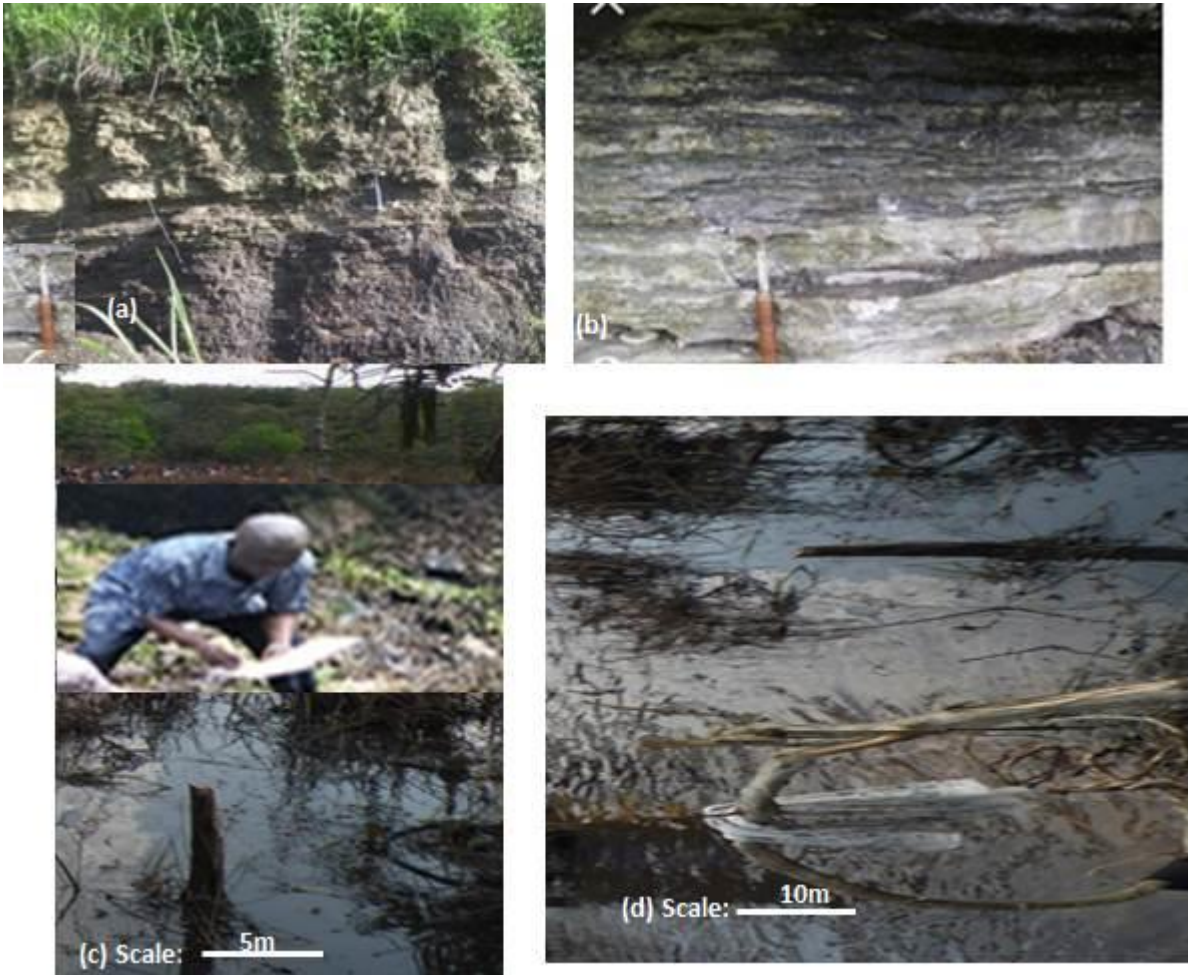


Fig.3.15 (a) Picture of Eze-aku Formation outcrop exposure at Ugep in Cross Rivers State, Nigeria (b) Amasiri Sandstone outcrop exposes at Ugep, in Cross River State, Nigeria (c) The lead researcher taking the temperature of the Spring with thermometer at Ugep Warm Spring at Ugep in Cross River State, Nigeria (d) Cold water spring at Ugep in Cross River State, Nigeria

3.4.6 Hydrogeology of Ugep Warm and Cold Springs

The warm and cold springs are that flow from two different faults that cut across the Eze-aku Formation underlying the area. The two springs form offset streams (Fig. 3.15 c and d) that have turned to slow to moderate flowing rivers that later join at several meters away from the two sources. The two springs follow the gradient of the topography of the area gently according to the nature of the topography of the area. The temperature of the warm spring as at the time of measurement was 45°C close to the source and decrease gradually to 27.6°C at the point where both the warm and cold springs intersect (Table 10). The cold spring was 27°C as at the time of measurement and maintained same temperature until the point where the two springs intersected each other and the temperature gradually rose to 31°C.

Table 10: Point of water collection, conditions, rock unit and water temperature along the springs flow in Ugep, Cross Rivers State, Nigeria.

S/N	Geothermal Site	Point along the spring	Rock units	Temperature (°C)	Thermal Resources
1	Ugep	Closest to the source of warm spring	Sandstone/siltstone	45	Hyperthermal
2	Ugep	10m away from the source of warm spring	Sandstone	40.5	Hyperthermal
3	Ugep	30m away from the source of warm spring	Sandstone/siltstone	31	Hypothermal
4	Ugep	50m away from the source of cold spring	Sandstone/shale	28	Hypothermal
5	Ugep	70m away from the source of warm spring	Sandstone/silt	27.6	Hypothermal

**The Geothermal resources of Ugep hyper thermal, might be prospective for geothermal energy utilization.*

3.4.7 Geology of the Niger Delta and the Geothermal Potentials

Niger Delta Basin is the youngest basins in Nigeria that sedimentation is still on-going. It makes boundary with Anambra Basin. The basin is filled with shallow marine and deltaic sediments that occur in diachronous manner. There are three major lithostratigraphic units within the Niger Delta Basin namely; Akata Formation which is the basal unit. It graded up to Agbada Formation which is more of shale and sandstone and the Benin Formation is the last unit which is the youngest among all. It is mainly sandstone with a thickness of 3000 m and covers over 9000 m out of the Bonny beach. Akata Formation is a marine prodelta shale deposit compacted and characterized by abnormal high-pressure siltstone formation. This formation is the main source rock for the Delta (Emujakporue and Ekine, 2014; Akpabio et al., 2013).

Recovery from Low-Temperature Co-Produced Water from Hydrocarbon reservoir. The concept adopted in this research work is heat annexation using an ORC. The Petroleum Expert simulation will indicate the wellhead temperature for the year in consideration and the multiphase flow situation. In most cases, Oil flows out of the well simultaneously with water and Gas. Thus, the thermal energy for all three phases needs to be calculated. The mass flow of the oil phase is known; hence the specific capacity is needed to obtain the heat flow. Since the specific heat capacity of crude depends on the oil temperature and grade of API, the equation below was used to calculate the specific heat capacity of crude oil dynamically (equation 5).

$$cp = (-1.39 * 10^{-6} * T + 1.847 * 10^{-3}) * API + (6.312 * 10^{-4}) * T + 0.352 \quad (5)$$

Heat capacity of crude oil [btu/lbm/°F] depending on temperature and °API. With correct data, the heat flow would be estimated considering the multiphase nature of the fluid.

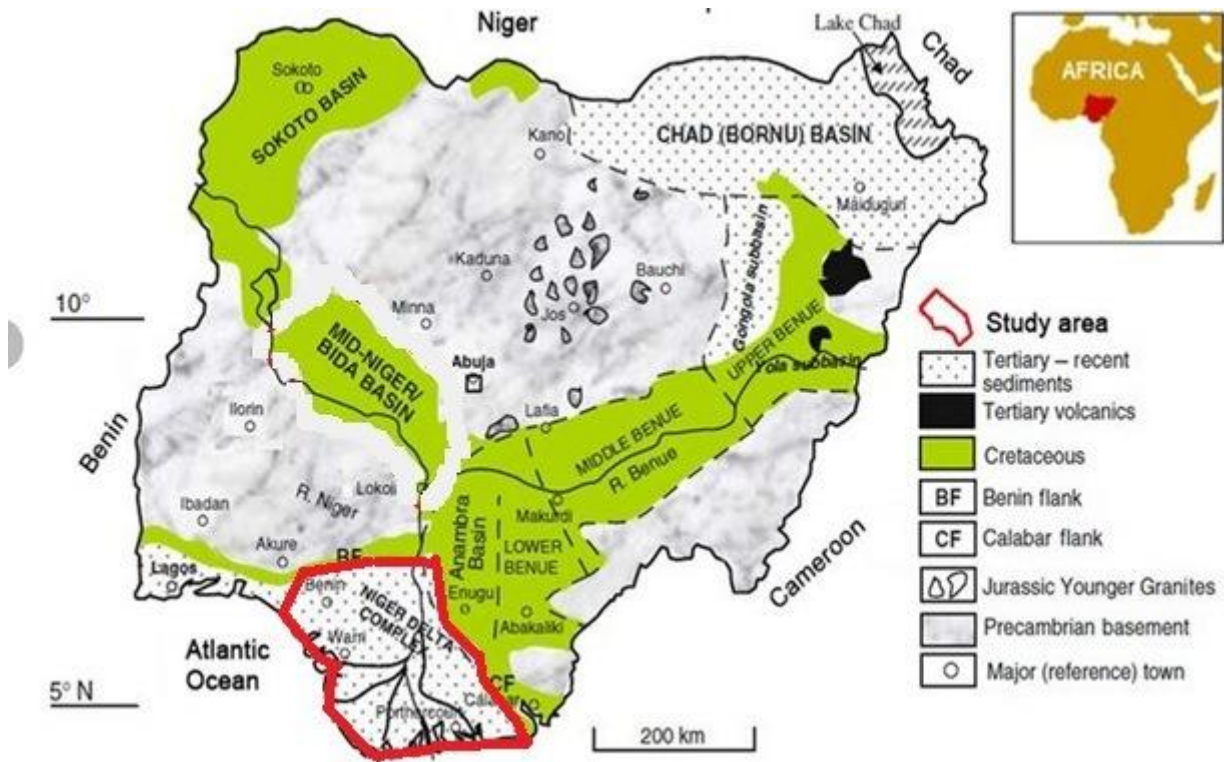


Fig.3.16 Geological Map showing the Basins in Nigeria

Table 11: Reservoir fluid property (temperature and initial pressure) of some wells in the Niger Delta Basin

Reservoirs	Initial Pressure	Temp	Boi	Oil Gravity	Initial GOR	Gas Gravity
	Psia	°F(°C)	rbbl/stb	degAPI	scf/stb	
1AB6	3502	139(59)	1.099	18.70	170	0.56
2AB6	3512	139(59)	1.099	18.03		0.53
3AB6	3748	146(63)	1.074	20.10	115	0.67
4AB6	3768	148(64)	1.170	22.08		0.61
5AB6	3899	150(66)	1.185	24.45	362	0.60
6AB6	3923	153(67)	1.131	27.13		0.66
1AB4(U)	4219	123(51)	1.185	38.92		0.66
1AB4(L)	4266	131(55)	1.185	39.95		0.67
2AB4	4358	159(71)	1.218	42.40	343	0.73
3AB4	4806	156(69)	1.269	44.10	616	0.68
4AB4	4470	165(74)	1.269	44.46		0.70
5AB4	4590	179(82)	1.860	47.50	2013	0.75
6AB4	4609	186(86)	1.659	47.10	1180	0.74
1AB1	5364	188(87)	1.678	49.32		0.78
2AB1	5152	210(99)	1.488	43.80	2620	0.79
3AB1U	5086	183(84)	1.356	43.60	2445	0.67
3AB1L	5185	215(102)	1.359	43.60	2445	0.70

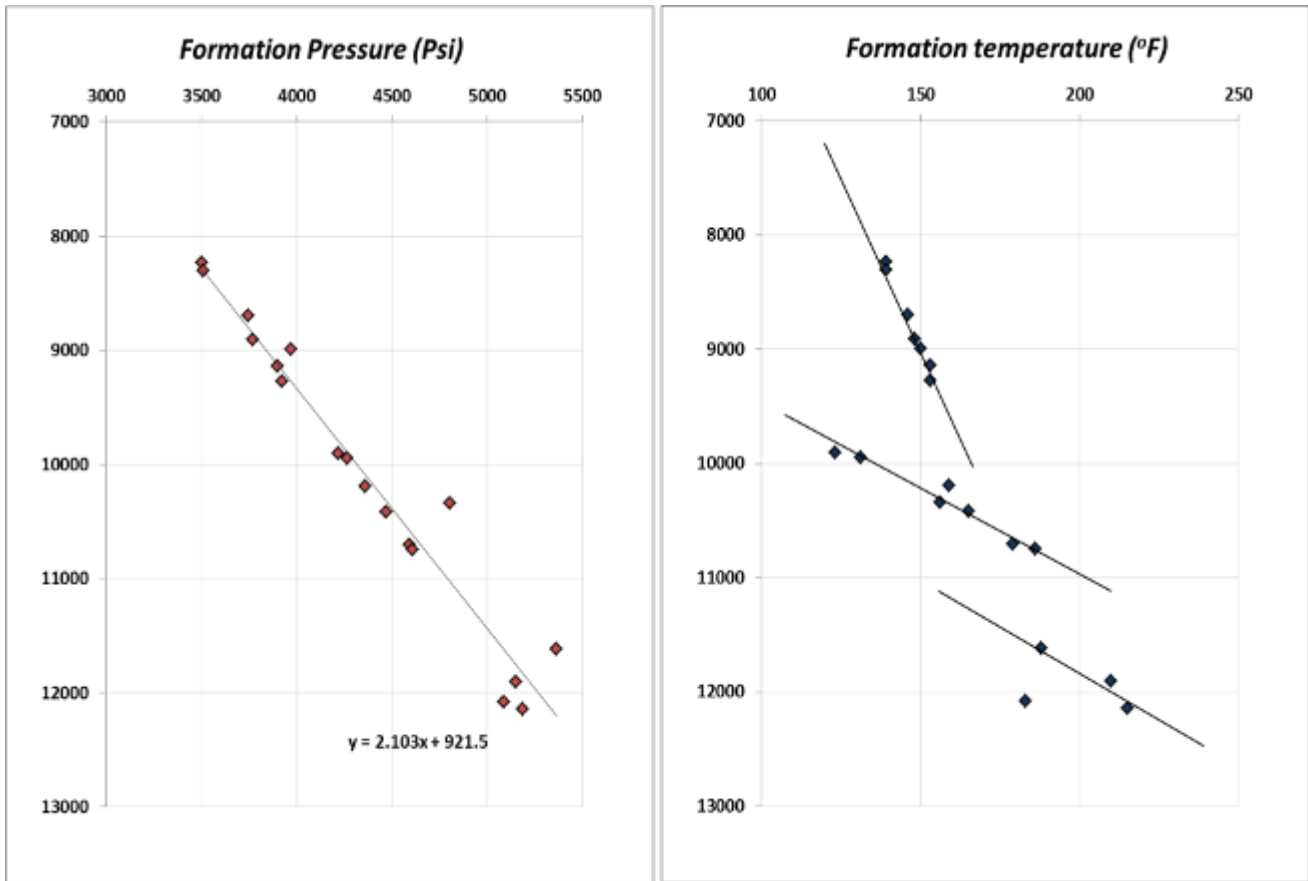


Fig. 3.17 Formation Pressure vs temperature F

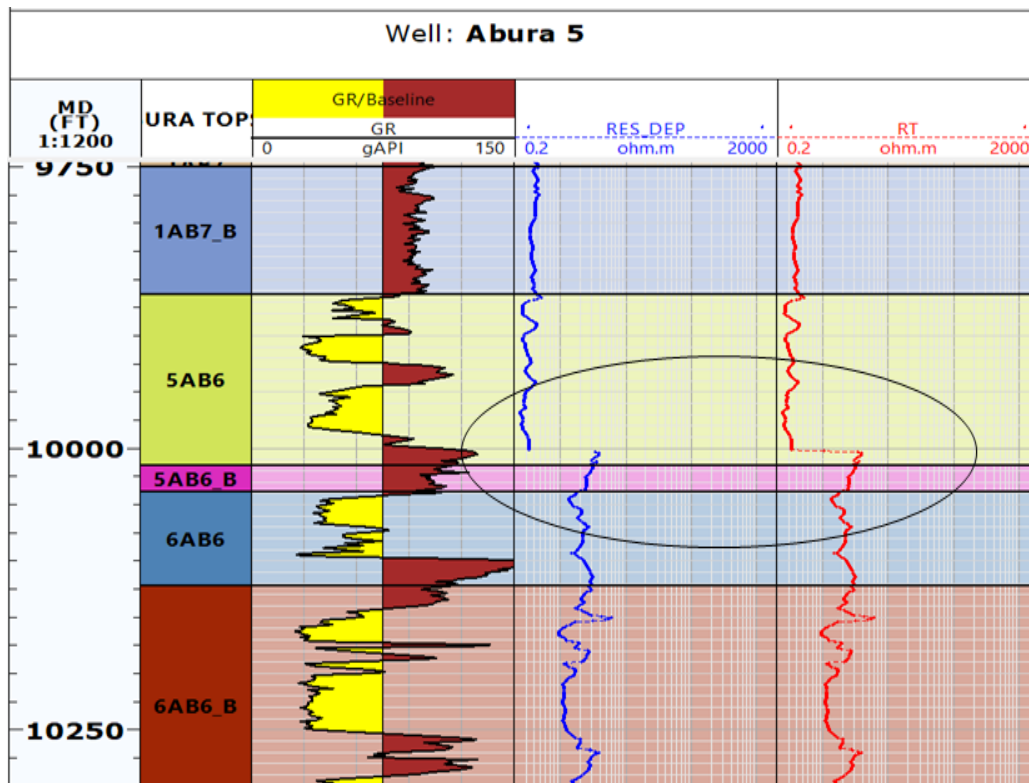


Fig. 3.18 Some BHT logs interpreted

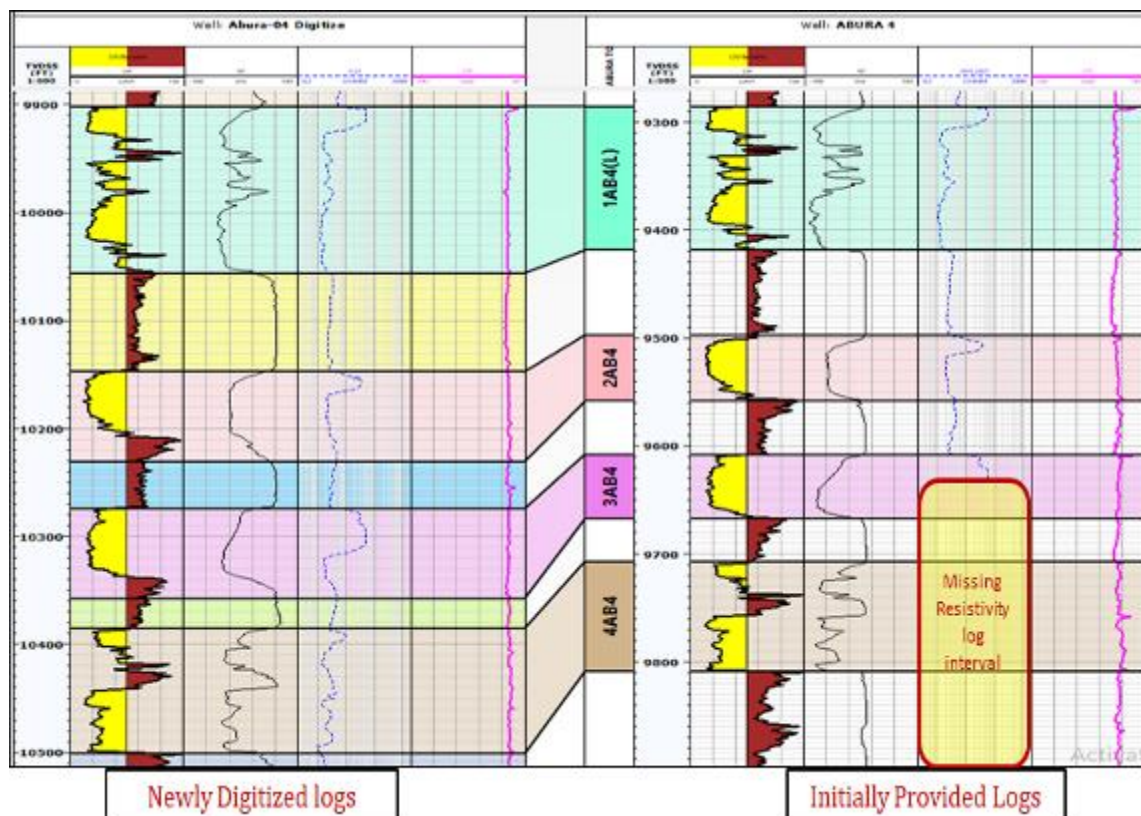
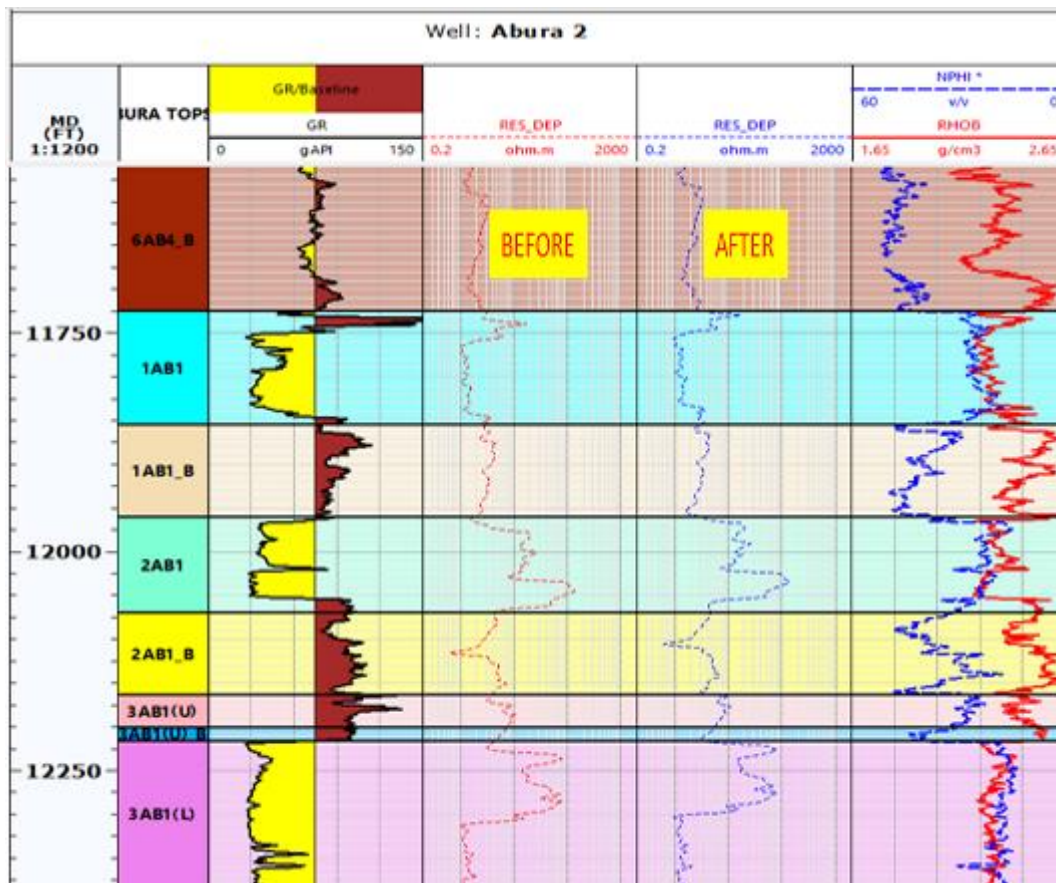


Table 12: Calculation of Formation Temperature from Abura Field Onshore Niger Delta:

	Reservoirs	BHT °C	TWD(m)	Thermal Resources
	6AB 4	86	3566	Hyperthermal
Abura 2	1AB 1	87	3613	Hyperthermal
	2AB 1	99	3682	Hyperthermal
	3AB 1 (U)	84	3717	Hyperthermal
	3AB 1 (L)	102	3780	Hyperthermal
Abura 4	1AB 4L	55	3063	Hyperthermal
	2AB 4	71	3115	Hyperthermal
	3AB 4	69	3160	Hyperthermal
	4AB 4 (U)	74	3200	Hyperthermal
Abura 5	5AB 6	66	3056	Hyperthermal
	6AB 6	67	3086	Hyperthermal
	6AB 6 B	77	3139	Hyperthermal
Owepele 2	A-1	82	2435	Hyperthermal
	B-2	85	3067	Hyperthermal
	C-3	91	3347	Hyperthermal
	D-4	79	2808	Hyperthermal

3.5 South Eastern Nigeria Geology and Hydrogeology

3.5.1 Geology of Okigwe and Afikpo

Okigwe and **Afikpo** are located in Imo State and Ebonyi, Nigeria respectively. The two locations lies within the southern part of Benue Trough. It is underlain by sandstone, shale, mudstone, and limestone (Fig.3.19). Along Okigwe and Uturu road, the outcrop section of Ajali Sandstone exposes. The outcrop (Fig. 3.19a and b) consists of unconsolidated, poorly sorted, coarse–fine-grained sandstone, poorly cemented mudstone and siltstone, with a thickness with herring-bone cross beds (Fig. 3.19 a) as the dominant sedimentary structure of the Formation. It is associated with reactivation surfaces, mud drapes, tidal bundles, backflowripple channels, cut and fills, lateral accretion surfaces, and Ophiomorpha Burrows (Fig.3.19 b)

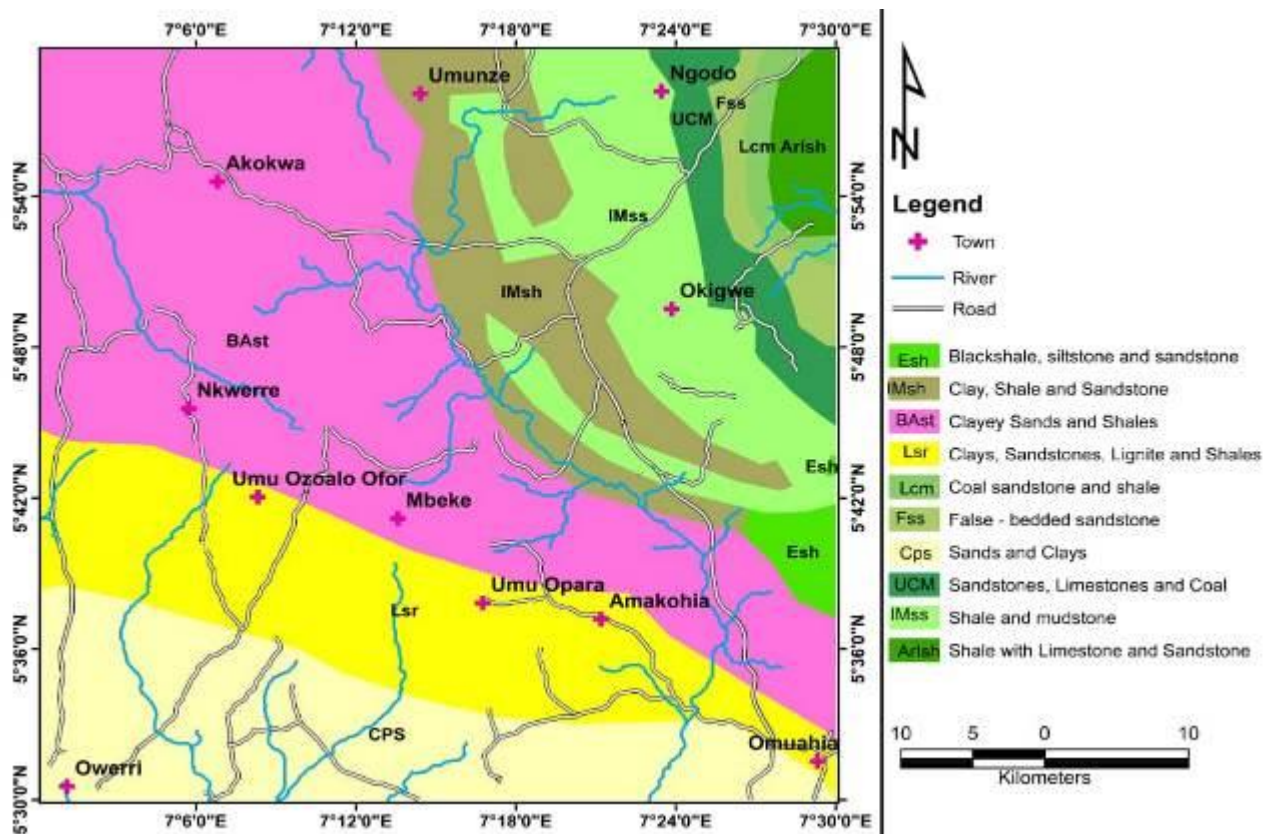


Fig. 3.19: Regional Geological map of part of Imo State showing Okigwe where the study area falls



Fig.3.19: (a) Outcrop exposure of Ajali Sandstone in Uturu-Okigwe Road showing herring-bone cross beds (b) Outcrop exposure of Ajali Sandstone in Uturu-Okigwe Road showing Ophiomorpha burrows.

3.5.2 Hydrogeology of Okigwe

The temperature of the river across the area was measured as 29°C throughout the river channels in the study area shows that the thermal resources are hypothermal.

Table 13: Point of water collection, conditions, rock unit and water temperature along the springs flow in Uturu-Okigwe, Imo, Nigeria

S/N	Geothermal Site	Point along the spring	Rock units	Temperature (°C)	Thermal Resources
1	Uturu-Okigwe Road	Along the stream	Sandstone	29	Hypothermal
2	Uturu-Okigwe Road	10m away from the stream	Sandstone	29	Hypothermal
3	Uturu-Okigwe Road	30m away from the stream	Sandstone	29	Hypothermal
4	Uturu-Okigwe Road	50m away from the stream	Sandstone	28	Hypothermal
5	Uturu-Okigwe Road	70m away from the stream	Sandstone	27.6	Hypothermal

** The Geothermal resources of Uturu -Okigwe hyper thermal, might be prospective for geothermal energy utilization.*

3.5.3 Geology of Nsukka

Nsukka is located in Enugu State. It lies within the Anambra Basin. The basin is an inland basin that is sandwiched between the Southwestern part of the Benue Trough and the Niger Delta. It is underlain by Nsukka Formation which comprises ironstone, mudstone, sandstone and shale with coal seam (Fig. 3.20). The shale is black to dark grey (Fig 3.20. a). Beneath the Nsukka Formation lies Ajali Sandstone consists of unconsolidated, poorly sorted, fine–coarse-grained sandstone (Fig. 3.20. b), with pronounce cross-beddings dominating the bed. It is associated with reactivation surfaces, mud drapes and tidal bundles,

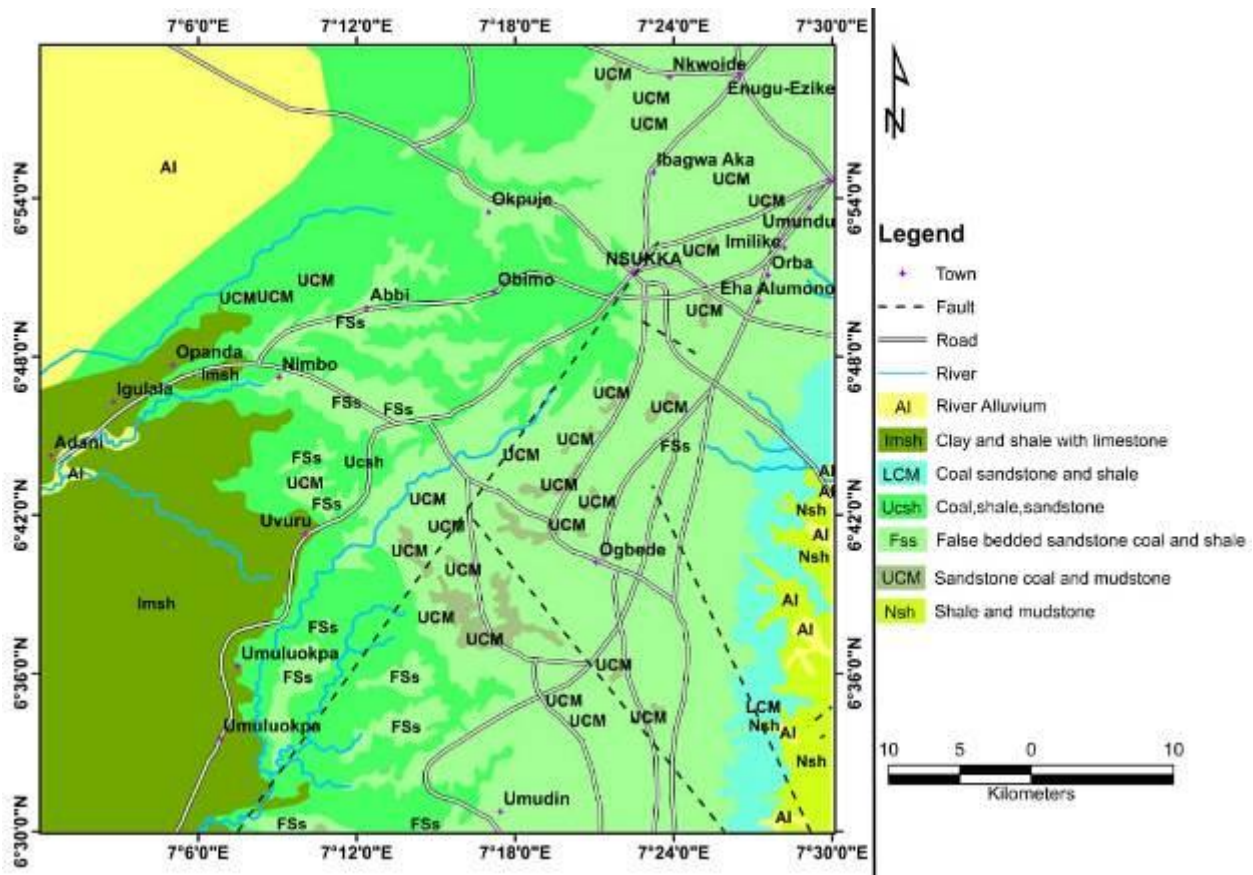


Fig. 3.20a: Regional Geological map of part of Enugu State showing Nsukka and environs where the study area falls

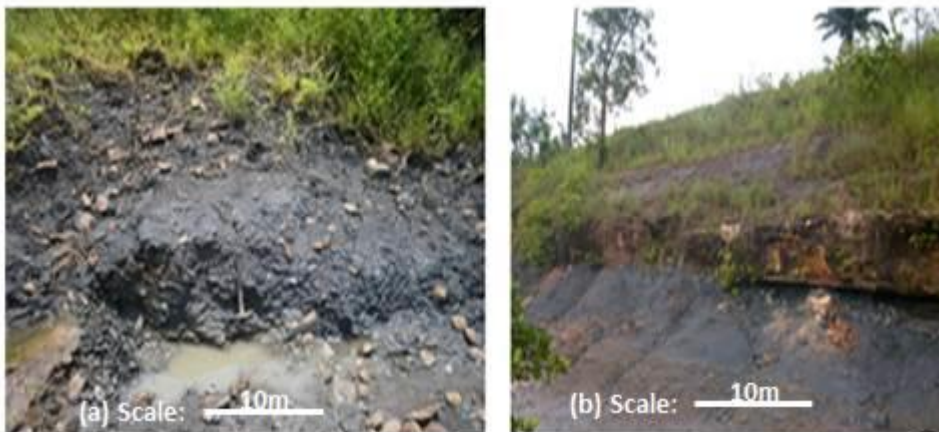


Fig.3.21: (a) Outcrop exposure of black shale in Nsukka (b) Section of Nsukka Formation showing the shale unit and the sandstone unit in Nsukka.

3.5.4 Hydrogeology of Nsukka

In Nsukka main town there is no river drainage but towards Ibagwa in EzimoRiver Akpaala drains area from the northern to the southern part of the study area. The topography is a low to slightly above low land, ranging from 710ft to 770ft forming into undulating surface. The action of the river in the northern part of the area has resulted to erosion processes that opens up the regolith thus, exposes the coal seam along some portion of the river and creating a very steep surface with high angle in the northern part. The water temperature along some portions across River Akpalla varies from 26°C to 30°C which indicates that the water thermal resource is hypothermal in nature (Table 14).

Table 14: Point of water collection, conditions, rock unit and water temperature along the springs flow in River Akpalla, Nsukka, Nigeria

S/N	Geothermal Site	Point along the spring	Rock units	Temperature (°C)	Thermal Resources
1	River Akpalla	Along the stream	Sandstone/siltstone	30	Hypothermal
2	River Akpalla	10m away from the stream	Shale	29	Hypothermal
3	River Akpalla	30m away from the stream	Mudstone/shale	28	Hypothermal
4	River Akpalla	50m away from the stream	Shale	27	Hypothermal
5	River Akpalla	70m away from the stream	Mudstone/shale	26	Hypothermal

** The Geothermal resources of River Akpalla hyper thermal, might be prospective for geothermal energy utilization within 5m radius from the source.*

CHAPTER FOUR

4.0 Analyses and interpretation of airborne gravity data of some locations in Nigeria for Geothermal Exploration

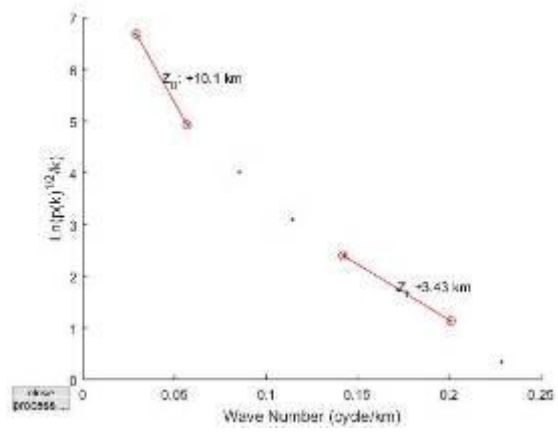
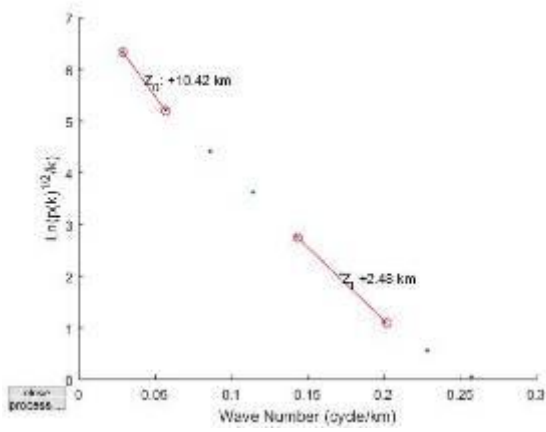
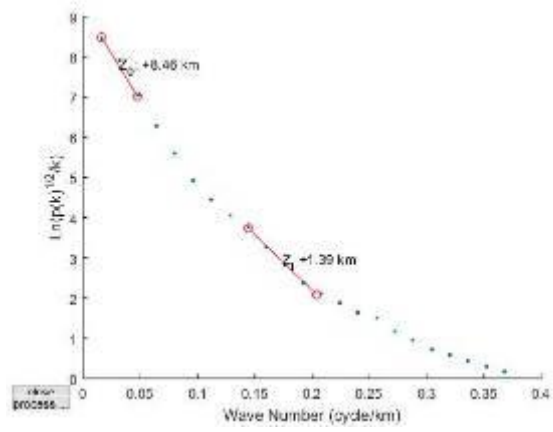
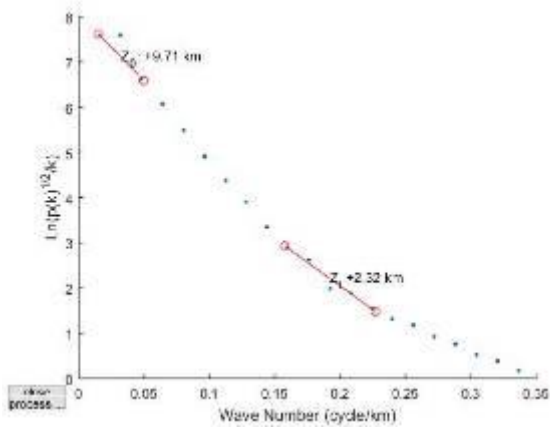
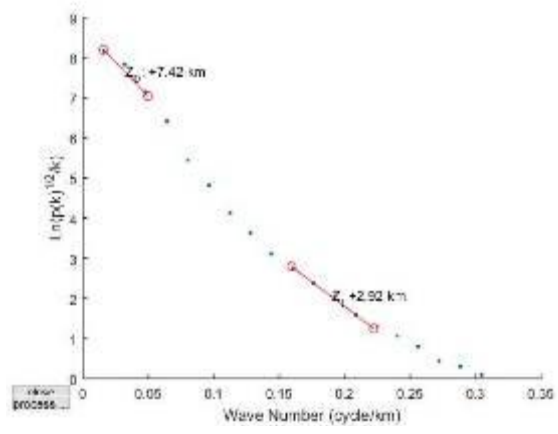
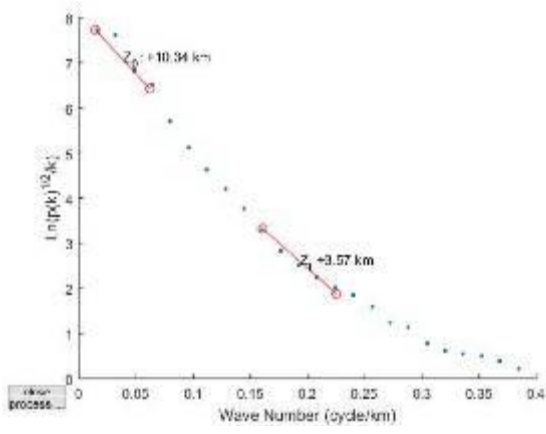
4.1 Materials and Methods

The spectral analysis was carried out on the bouguer of the gravity anomaly data of the study areas. The gravity data sets of the following locations: Toro (Sheet 147), Kaltungo (Sheet 173), Numal (Sheet 196), Kotonkarfi (Sheet 227), Akiri (Sheet 232), Ado (Sheet 244), Lokoja (Sheet 247), Auchi (Sheet 266), Nsukka (Sheet 287), Onitsha (Sheet 300), Okigwe (Sheet 312) and Pennigton Rivers (Sheet 326) were analysed using Geosoft Oasis montaj software. Each bouguer map was divided into eight overlapping sub-sheets of 27.5 X 27.5 km sizes. The spectral analysis by FFT was performed on each overlapping blocks and the plots of the logarithm of spectral energy $\ln(E)$ against the wave number (cycle/km) was produced using a Matlab program specifically designed to obtain the gradients for deepest depth (centroid depth) and depth to top of magnetic source.

Each sub-sheet was further subjected to Fast Fourier Transform, a process that decomposes the gravity data into its energy spectrum and wave number components. The locations were labelled A-L(Sheet 232; A, Sheet 244; B, sheet 247; C, sheet 266; D, sheet 287; E, sheet 300; F, sheet 147; G, sheet 173; H, sheet 196; I; sheet 227; J, sheet 326; K and sheet 312; L).The energy spectrum was plotted against wave number components using MatLab software (Fig4. 1a-l). This process deduced gradients in the form of depth to the top (Z_T) and centroid (Z_0) of sources.

The depth to top of basement and centroid were used to evaluate Curie point depth (Z_b) and thereafter estimate the geothermal gradient and heat flow of study area. Curie point depths varies with geological situations (Ross *et al.*, 2006). Tanaka *et al.* (1999) established that CPD ranging below 10 km are attributable to volcanic and geothermal regions, 10 km to 15 km are attributable to Island arch and ridges, 20 km and above are attributable to Plateaus and 30 km and above are attributable to trenches.

The heat flow value between 80mWm^{-2} and 100mWm^{-2} has been established to indicate geothermal anomalous conditions in an area for geothermal prospecting (Jessop *et al.*, 1976 ; Abraham *etal*,2014, Aliu, and Mazian, 2018)). It can therefore be deduced from this study that regions that fall within the range of 80 to 100 mWm^{-2} are good spots for geothermal energy resources.



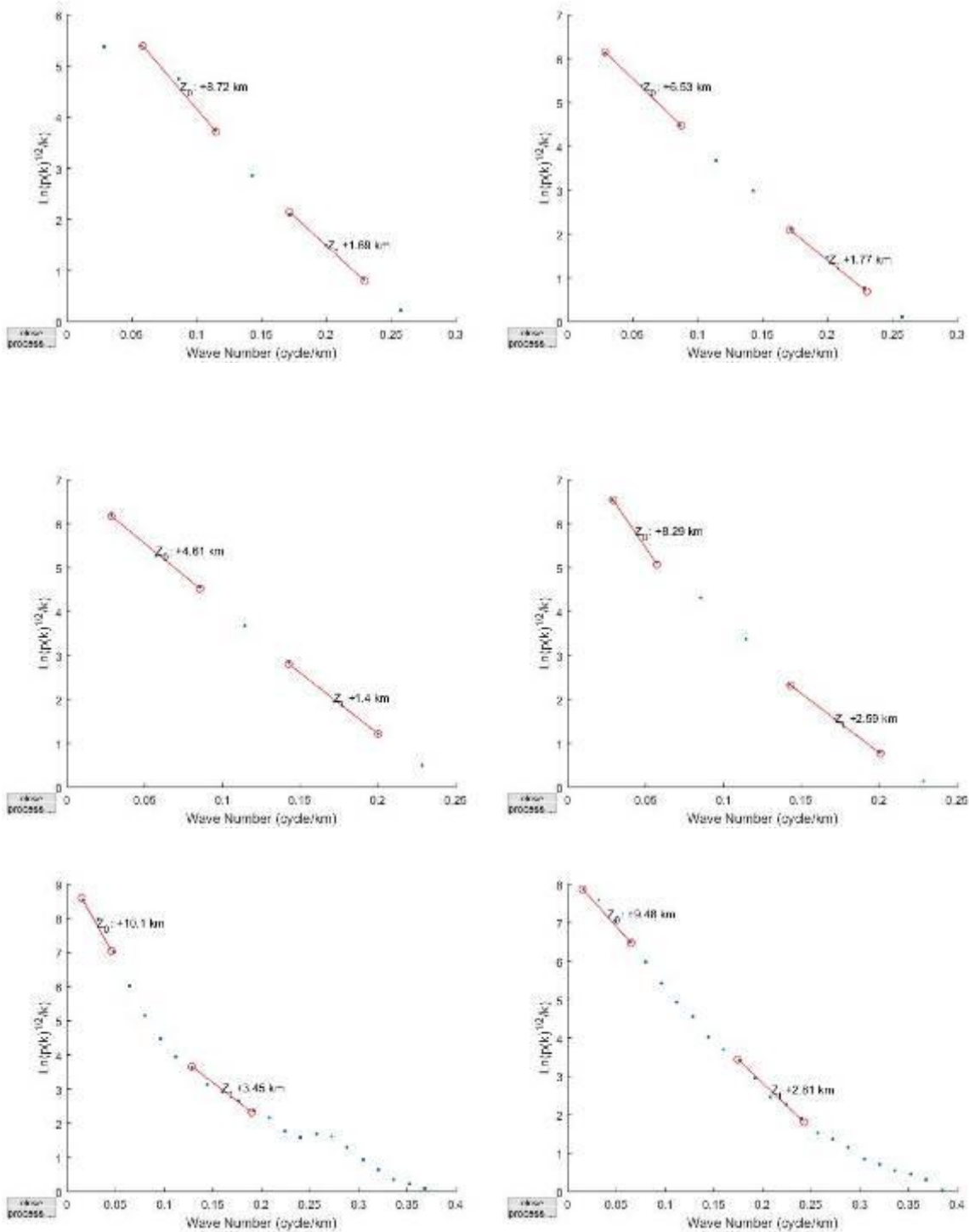


Fig.4.1: Plots of spectrum energy against wave number (a) spectral block A1 (b) spectral block B1 (c) Spectral block C1 (d) spectral block D1 (e) spectral block E1 (f) spectral block F1 (g) spectral block G1 (h) spectral block H1 (i) spectral I1 (j) spectral block J1 (k) spectral block K1 and (L) spectral block L1

4.2 Akiri - Sheet 232

Results of spectral analysis for study area revealed the occurrence of geothermal parameters: Curie point depth varied between 7.39 to 20.71 km, geothermal gradient varied between 28.01 to 78.48 °C/km and heat flow values varied between 70.29 to 197.99 mW/m². Table 15 presents the summary of the results of the centroid depth, depth to basement, curie depth, geothermal gradient and the heat flow. A general trend of low to peak geothermal gradient and heat flow values is observed from the southern to northern region of study area respectively (Fig.4. 2). An inverse trend is observed for Curie point depth. A recommended threshold value of heat flow for a good source of geothermal energy is set at 80 to 100 mW/m². These ranges of values can be observed between the light blue colours depicted within southern regions of the heat flow contour map. Values of heat flow above the stated range is considered as excess, however, the entire study area with exception of the extreme Southern parts can be considered in locating potential geothermal reservoirs. Only heat flow results in excess of 80 mW/m² indicating anomalous geothermal conditions can be utilized in geothermal electricity generation. The shallow curie depths with corresponding heat flow are observed around the Akiri and Awe hot springs. The observed anomalies geothermal conditions can be attributed to the intense cenozoic magmatic activities with numerous volcanic intrusions within the Benue trough.

Table 15: summary of the results of the centroid depth, depth to basement, curie depth, geothermal gradient and the heat flow

Blocks	Longitude (Deg)	Latitude (Deg)	Centroid Z _o (km)	Depth to basement Z _t (km)	Curie depth Z _B (km)	Geothermal gradient dT/dZ _b (°C/km)	Heat Flow (mWm ⁻²)
A1	9.125	8.375	8.29	2.59	13.99	41.46	104.06
A2	9.207	8.375	4.48	1.57	7.39	78.48	197.00
A3	9.290	8.370	4.58	1.48	7.68	75.52	189.56
A4	9.124	8.380	5.03	1.79	8.27	70.13	176.03
A5	9.125	8.125	11.7	2.69	20.71	28.01	70.29
A6	9.207	8.125	8.51	1.65	15.37	37.74	94.72
A7	9.207	8.125	9.1	2.01	16.19	35.82	89.92
A8	9.380	8.125	11.6	2.79	20.41	28.42	71.33
<i>*Heat Flow ranged from 70.29 – 197.00 (mWm⁻²)</i>				<i>13.75</i>	<i>55.39</i>	<i>144.4</i>	

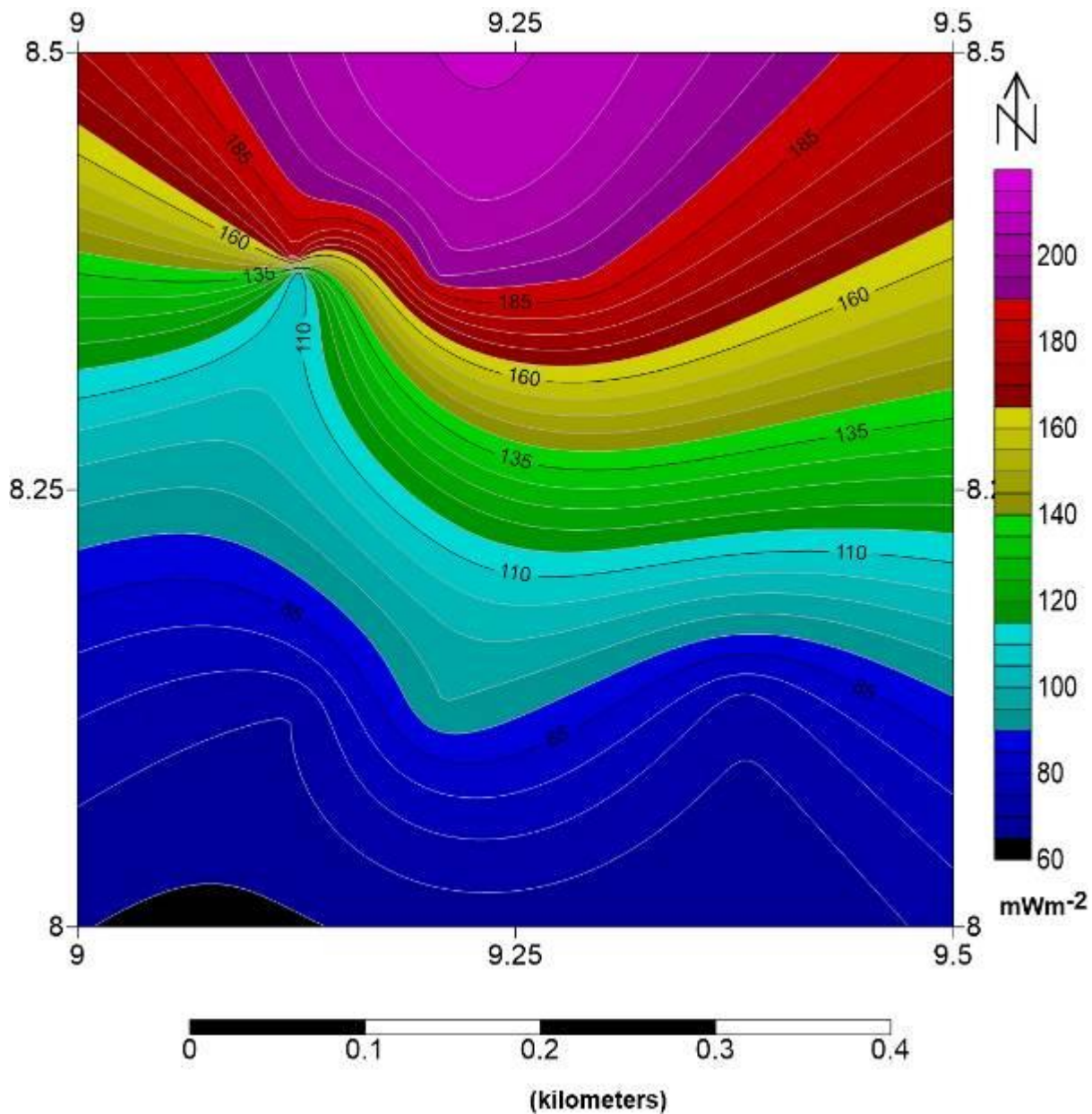


Fig.4. 2 Heat flow contour map of sheet 232 corresponding to Akiri

4.3 Ado Ekiti- Sheet 244

In order to access the geothermal parameters of study area, the gravity data (sheet 244) was subjected to spectral analysis and the results as follows: the Curie point depth values ranges from 7.0 to 14.92 km, geothermal gradient values ranges from 39.90 to 82.85 °C/km and heat flow values ranges from 97.63 to 207.97 mW/m² (Table 16). Heat flow values from 95 to 110 mW/m² is seen in black to light blue colours within the SE regions while values from 120 and above 200 mW/m² is observed largely in NW regions and partly in the SW regions depicted in green to purple colours. The entire study area could be said to be prospective for geothermal energy exploration since no value of heat flow falls below the recommended range of 80 to 100 mW/m² for a good source of geothermal energy. Also heat flow

values above the stated threshold of 80 to 100 mW/m² existing in the NW and SW regions can be said to be in excess abundance.

Table 16: summary of the results of the centroid depth, depth to basement, curie depth, geothermal gradient and the heat flow

Blocks	Longitude (Deg).	Latitude (Deg).	Centroid Zo(km)	Depth to basement Zt (km)	Curie depth Zb (km)	Geothermal Gradient (oC/km)	Heat Flow (mWm⁻²)
B1	5.125	7.875	4.61	1.4	7.82	74.17	186.16
B2	5.207	7.875	4.11	1.22	7	82.86	207.97
B3	5.291	7.875	4.81	1.13	8.49	68.32	171.47
B4	5.375	7.875	5.53	0.91	10.15	57.14	143.43
B5	5.125	7.625	4.19	0.94	7.44	77.96	195.67
B6	5.205	7.625	6.73	1.41	12.05	48.13	120.81
B7	5.291	7.625	7.99	1.77	14.21	40.82	102.45
B8	5.425	7.625	8.04	1.17	14.91	38.90	97.64
*Heat Flow ranged from 97.64 –207.97 (mWm⁻²)				10.26	61.04	153.2	

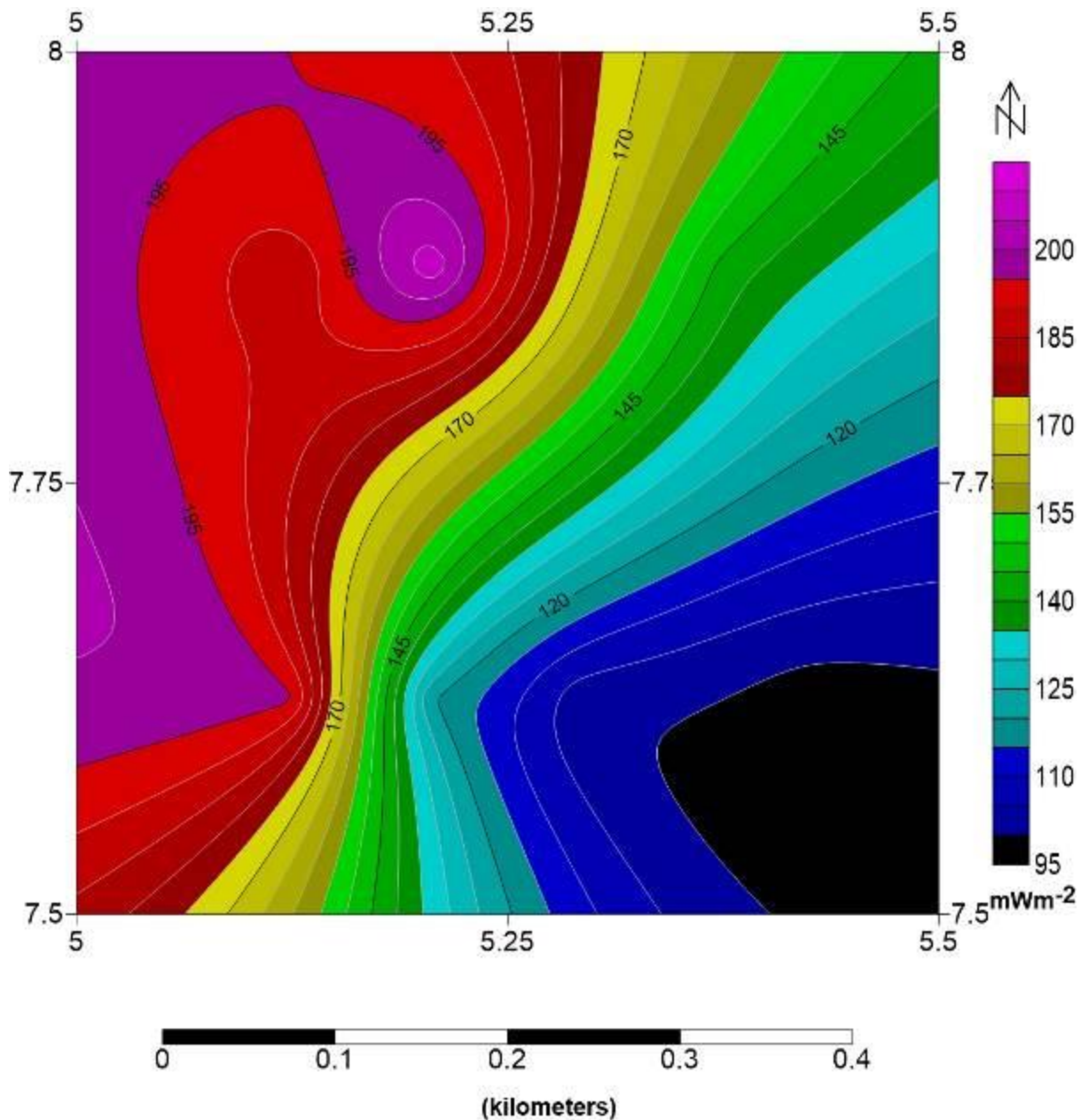


Fig.4. 3 Heat flow contour map of sheet 244 corresponding to Ado

4.4 Ijebu-Ode - (Sheet 280)

Delineating the geothermal potential of Ijebu – Ode in Ogun State, Nigeria from the calculated geothermal parameters using gravity data of the study area. The gravity data of the study area was subjected to spectral analysis and the results as follows: the Curie point depth values ranges from 13.34 to 17.32 km, geothermal gradient values ranges from 34.44 to 43.47°C/km and heat flow values ranges from 84.24 to 109.13 mW/m^2 (Table 16a). Heat flow values from 80 to 100 mW/m^2 is seen virtually in all the study area with an exception of the northeastern part of the study area with $>100 \text{ mWm}^{-2}$ (Fig.4.3a) The entire study area could be said to be prospective for geothermal energy exploration since

no value of heat flow falls below the recommended range of 80 to 100 mW/m² for a good source of geothermal energy. Also heat flow values above the stated threshold of 80 to 100 mW/m² existing in the NE regions is an indication of anomalous geothermal conditions (excellent) in the study area.

Table 16a: summary of the results of the centroid depth, depth to basement, curie depth, geothermal gradient and the heat flow

Blocks	Longitude (Deg)	Latitude (Deg)	Centroid depth Z_o (km)	Depth to basement Z_t(km)	Curie depth Z_b(km)	Geothermal Gradient (oC/km)	Heat flow (mWm⁻²)
M1	3.625	6.875	9.65	2.46	16.84	34.44	86.44
M2	3.708	6.875	8.97	2.41	15.53	37.34	93.74
M3	3.788	6.875	10.31	3.34	17.28	33.56	84.24
M4	3.875	6.875	7.67	2	13.34	43.47	109.13
M5	3.625	6.625	7.67	1.88	13.46	43.09	108.15
M6	3.708	6.625	9.52	2.33	16.71	34.70	87.12
M7	3.788	6.625	10.37	3.42	17.32	33.48	84.05
M8	3.875	6.625	8.92	3.76	14.08	41.19	103.39

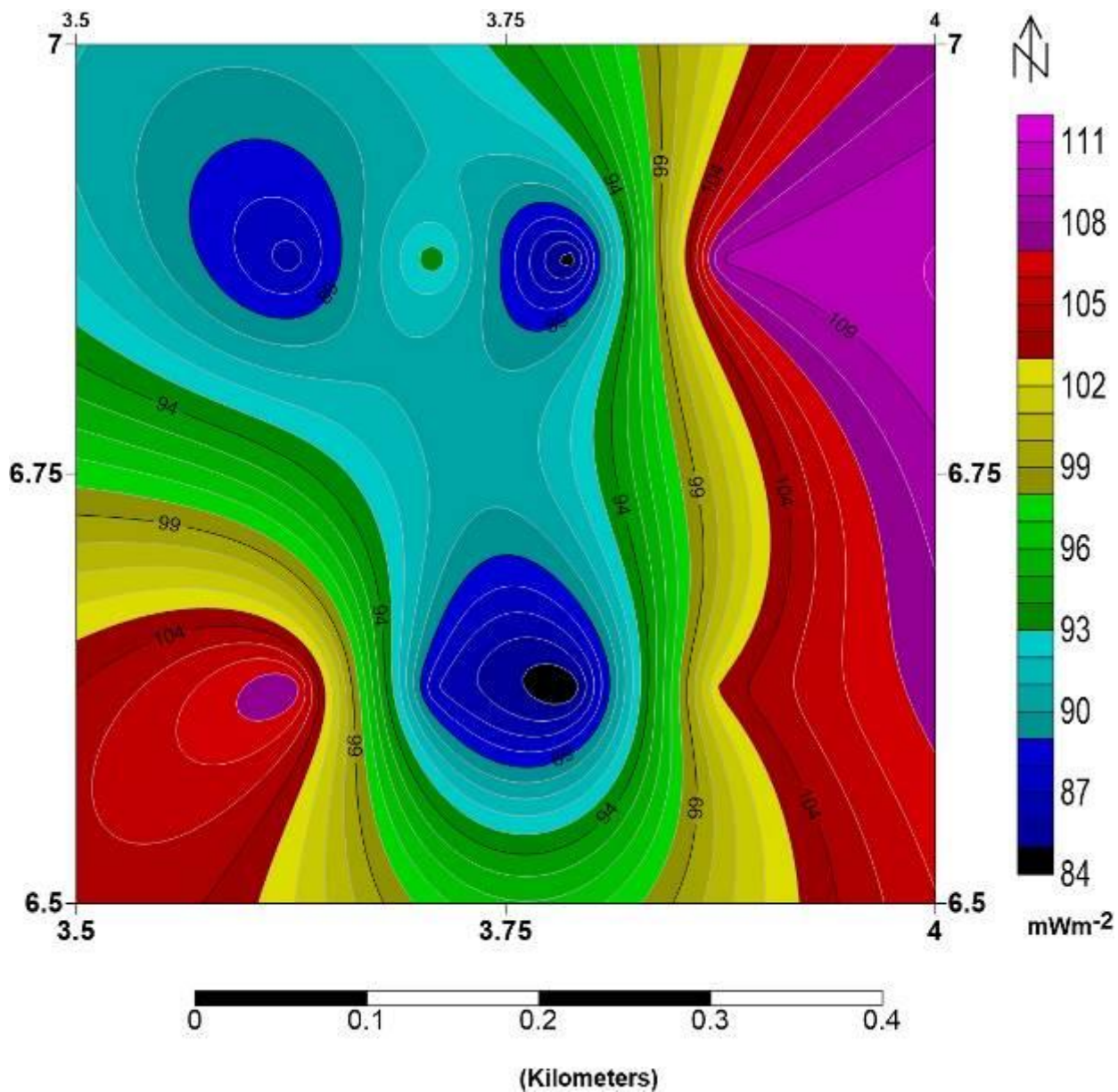


Fig. 4.3a: Heat flow contour map of sheet 280 corresponding to Ijebu – Ode (Ogun State)

4.5 Lokoja - Sheet 247

Spectral analysis performed on gravity data of study area generally showed the Curie point depth values varying inversely to the geothermal gradient and heat flow values. Curie point depth values ranges from 7.78 to 15.56 km with average of 11.65 km, geothermal gradient values ranges from 31.13 to 74.55 °C/km with average of 53.59 °C/km and heat flow values ranges from 78.14 to 187.12 mW/m² with average of 134.52 mW/m² (Table 17). The south eastern edge hosts the highest values of heat flow and geothermal gradient with corresponding shallowest values of Curie point depth (Fig.4.4). Generally, for a viable geothermal reservoir, a heat flow range of 80 to 100 mW/m² is recommended, hence it can be

inferred that every region on the study area could be considered as having good prospect except two isolated points at the northern regions depicted in dark blue colours.

Table 17: summary of the results of the centroid depth, depth to basement, curie depth, geothermal gradient and the heat flow

Blocks	Longitude (Deg).	Latitude (Deg)	Centriod Depth Zo (km)	Depth to basement Zt (km)	Curie depth Zb (km)	Geothermal gradient (oC/km)	Heat Flow (mWm⁻²)
C1	6.625	7.875	6.53	1.77	11.29	51.37	128.95
C2	6.708	7.875	9.91	1.19	18.63	31.13	78.14
C3	6.791	7.875	6.17	1.98	10.36	55.98	140.52
C4	6.875	7.875	8.6	1.64	15.56	37.28	93.56
C5	6.625	7.625	5.48	0.46	10.5	55.24	138.65
C6	6.708	7.625	6.01	1.31	10.71	54.15	135.93
C7	6.791	7.625	4.24	0.7	7.78	74.55	187.12
C8	6.875	7.625	4.66	0.92	8.4	69.05	173.31
*Heat Flow ranged from 78.14 – 187.12 (mWm⁻²)					11.65	53.59	134.50

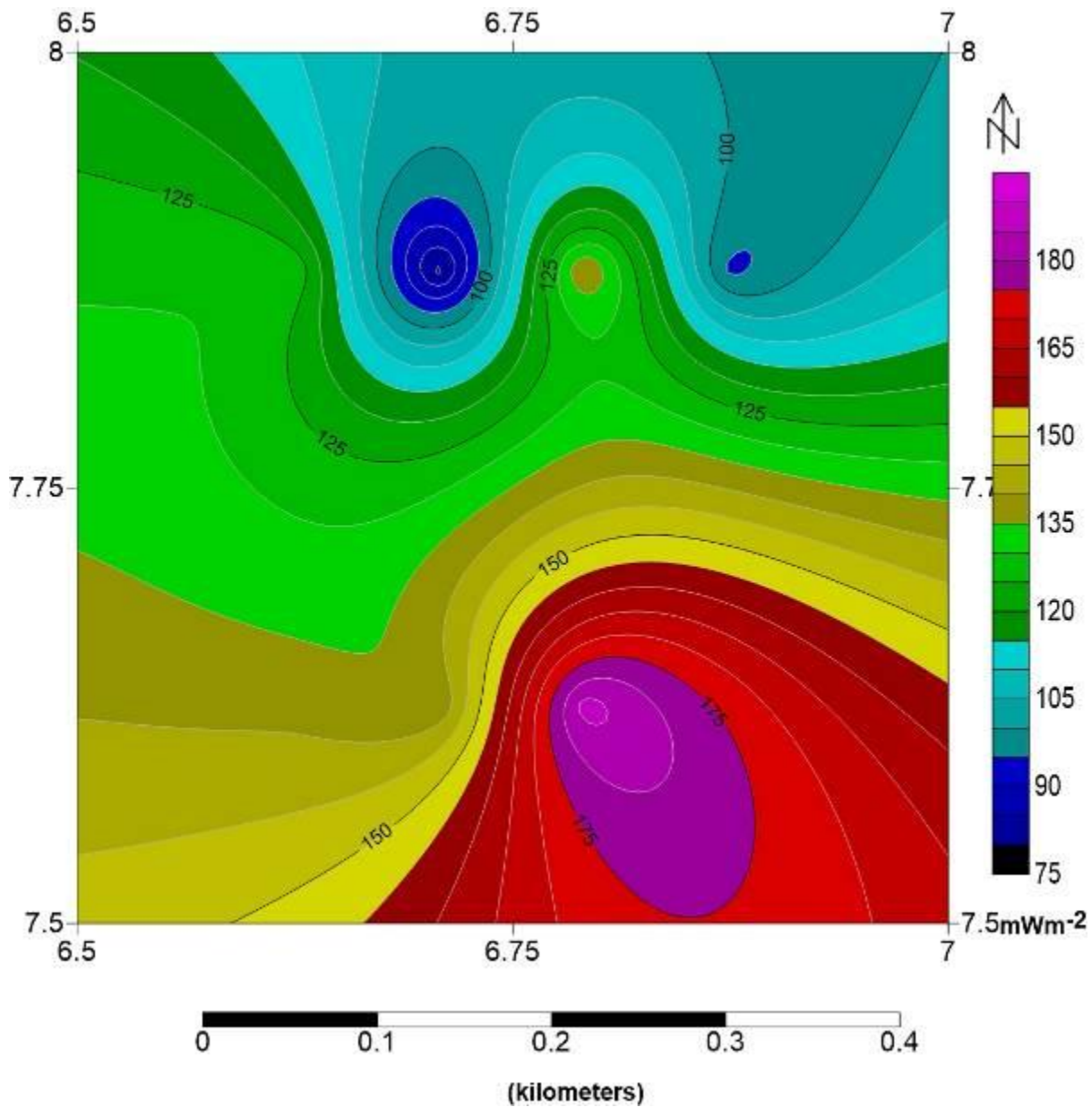


Fig. 4.4 Heat flow contour map of sheet 247 corresponding to Lokoja

4.6 Auchi - Sheet 266

Mappings from spectral analysis for gravity data of study area gives a clear view of the geothermal make up of study area. The geothermal gradient and heat flow values are distributed across the study area with low values occurring at the western half in dark to light blue colours and high values occurring at the eastern sides in green to purple colours. Shallow Curie point depth is observed at the south eastern edge and increases progressively outward towards the western regions. Values of curie point depth ranges from 10.48 to 17.47 km with an average of 14.31 km, geothermal gradient values ranges from 32.58 to 55.34 $^{\circ}\text{C}/\text{km}$ with an average of 42.18 $^{\circ}\text{C}/\text{km}$ and values of heat flow ranges from 81.78 to 138.91 mW/m^2 with average of 105.88 mW/m^2 (Table 18). A threshold range of heat flow values recommended for a prospective geothermal reservoir is 80 to 100 mW/m^2 , it there for implies

that all regions of the study area could be considered for geothermal energy exploration especially at regions of shallow Curie point depth (Table18).

Table 18: summary of the results of the centroid depth, depth to basement, curie depth, geothermal gradient and the heat flow

Blocks	Longitude (Deg).	Latitude (Deg)	Centroid depth Z_o (km)	Depth to basement Z_t (km)	Curie depth Z_b (km)	Geothermal Gradient (oC/km)	Heat Flow (mWm⁻²)
D1	6.125	7.375	8.72	1.69	15.75	36.83	92.43
D2	6.207	7.375	9.34	2.93	15.75	36.83	92.43
D3	6.291	7.375	6.54	1.58	11.5	50.43	126.59
D4	6.375	7.375	9.33	2.73	15.93	36.41	91.39
D5	6.125	7.125	8.9	1.33	16.47	35.22	88.39
D6	6.208	7.125	9.94	2.08	17.8	32.58	81.79
D7	6.291	7.125	6.02	1.56	10.48	55.34	138.91
D8	6.375	7.125	6.5	2.23	10.77	53.85	135.17
*Heat Flow ranged from 81.79 – 138.91 (mWm ⁻²)					14.31	42.19	105.8

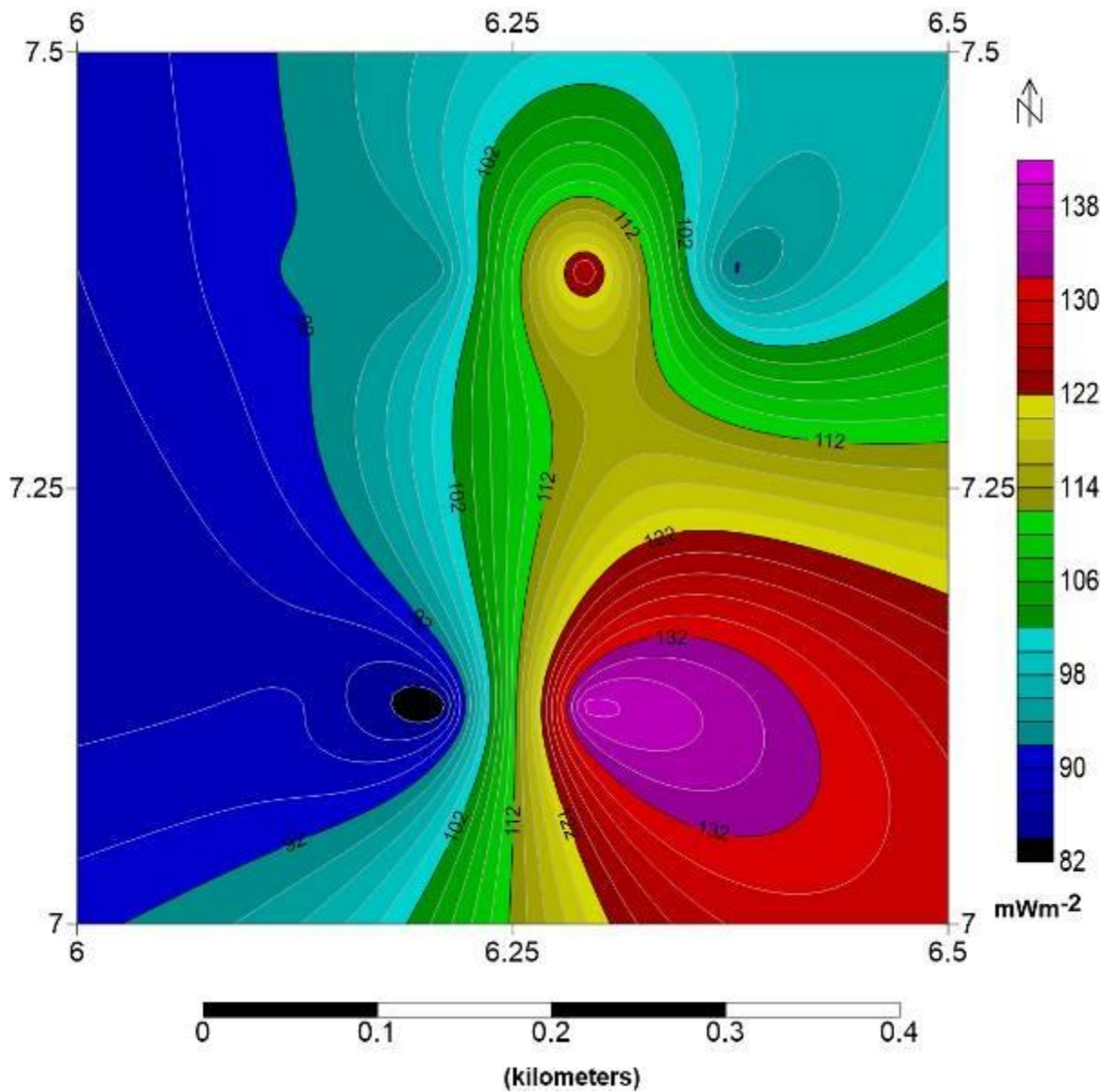


Fig.4. 5 Heat flow contour map of sheet 266 corresponding to Auchi

4.7 Nsukka - Sheet 287

The geothermal properties of study area were revealed from the spectral analysis of gravity data. The curie point depth which shows the depth to potential geothermal reservoirs varied between 14.78 to 20.81 km with an average value of 17.04 km, the geothermal gradient varied between 27.87 to 39.24 °C/km with an average value of 34.46 °C/km while the heat flow varied between 73.12 to 98.47 mW/m² with an average value of 86.49 mW/m² (Table 20). Heat flow values ranging from 80 to 98 mWm⁻² can be observed from the central regions extending to the northern regions depicted in green to purple colours (Fig.4. 6). The regions depicted in green to purple on the heat flow map also represents

the prospective regions for a viable geothermal source since from a conventional perspective, heat flow values between 80 to 100 mW/m² is regarded as sufficient for a viable geothermal reservoir.

Table 19: summary of the results of the centroid depth, depth to basement, curie depth, geothermal gradient and the heat flow

Blocks	Longitude (Deg).	Latitude (Deg)	Centroid Depth Z_o(km)	Depth to basement (Z_t)	Curie Depth (Z_b)	Geothermal gradient (oC/km)	Heat Flow (mWm⁻²)
E1	7.125	6.875	10.1	3.43	16.77	34.59	86.81
E2	7.208	6.725	8.76	2.74	14.78	39.24	98.50
E3	7.291	6.725	9.35	2.44	16.26	35.67	89.53
E4	7.375	6.725	11.52	3.13	19.91	29.13	73.12
E5	7.125	6.725	11.66	2.51	20.81	27.87	69.96
E6	7.208	6.725	8.37	1.31	15.43	37.59	94.35
E7	7.291	6.725	9.68	2.88	16.48	35.19	88.34
E8	7.375	6.725	8.88	1.83	15.93	36.41	91.39
*Heat Flow ranged from 73.12 – 98.50 (mWm⁻²)					17.05	42.72	86.50

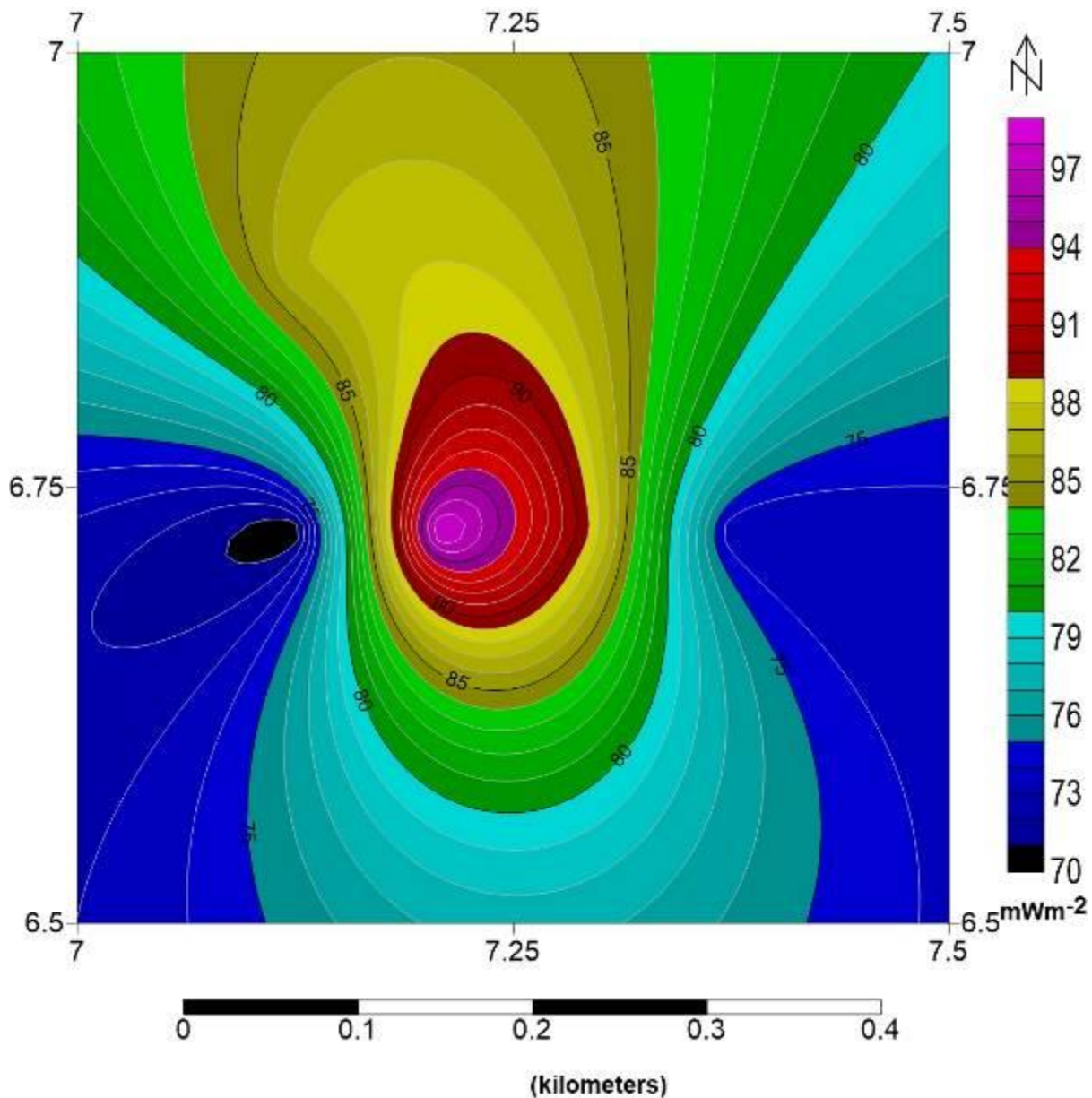


Fig.4.6 Heat flow contour map of sheet 287 corresponding to Nsukka

4.8 Onitsha - Sheet 300

The results from spectral analysis performed on gravity data of study area revealed the curie point depth varies between 13.69 to 21.26 km with average value of 16.71 km, the geothermal gradient varies between 27.28 to 42.36 °C/km with average value of 35.34 °C/km while heat flow varies between 68.47 to 106.34mW/m² with average value of 88.70mW/m². (Table 21). All the values of heat flow with study area falls within and slightly above the threshold range of 80 to 100 mW/m²pegged as prospective for a viable source of geothermal energy. With an exception of a small portion on the northern western edge depicted in blue, the remaining regions of study area recorded values in the range of 80 to 108 mW/m² and could be considered for exploration of possible geothermal reservoir (Fig.4. 7a).

Table 20: summary of the results of the centroid depth, depth to basement, curie depth, geothermal gradient and the heat flow

Blocks	Longitude (Deg)	Latitude (Deg)	Centriod depth Zo (km)	Depth to basement Zt (km)	Curie depth Zb (km)	Geothermal Gradient (oC/km)	Heat Flow (mWm⁻²)
F1	6.625	6.375	10.42	2.48	18.36	31.59	79.29
F2	6.708	6.375	12.51	3.76	21.26	27.28	68.48
F3	6.791	6.375	8.75	2.76	14.74	39.35	98.77
F4	6.785	6.125	10.05	2.67	17.43	33.28	83.52
F5	6.625	6.125	8.69	3.69	13.69	42.37	106.34
F6	6.708	6.125	9.8	2.87	16.73	34.67	87.02
F7	6.791	6.125	8.46	2.45	14.47	40.08	100.61
F8	6.875	6.125	9.99	2.98	17	34.12	85.64
<i>*Heat Flow ranged from 68.48 – 106.34 (mWm⁻²)</i>					<i>16.71</i>	<i>39.67</i>	<i>88.59</i>

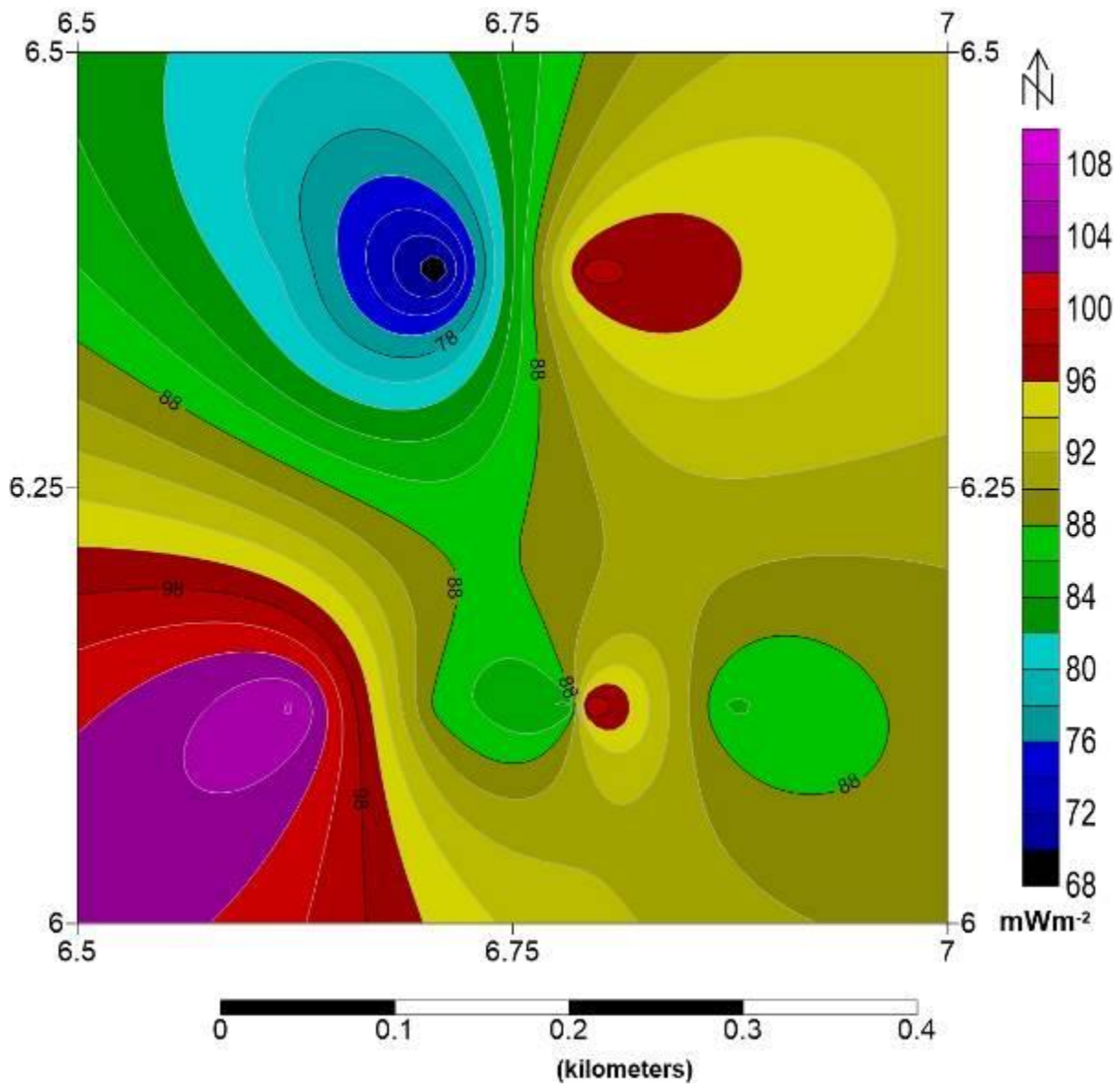


Fig.4.7a Heat flow contour map of sheet 300 corresponding to Onitsha

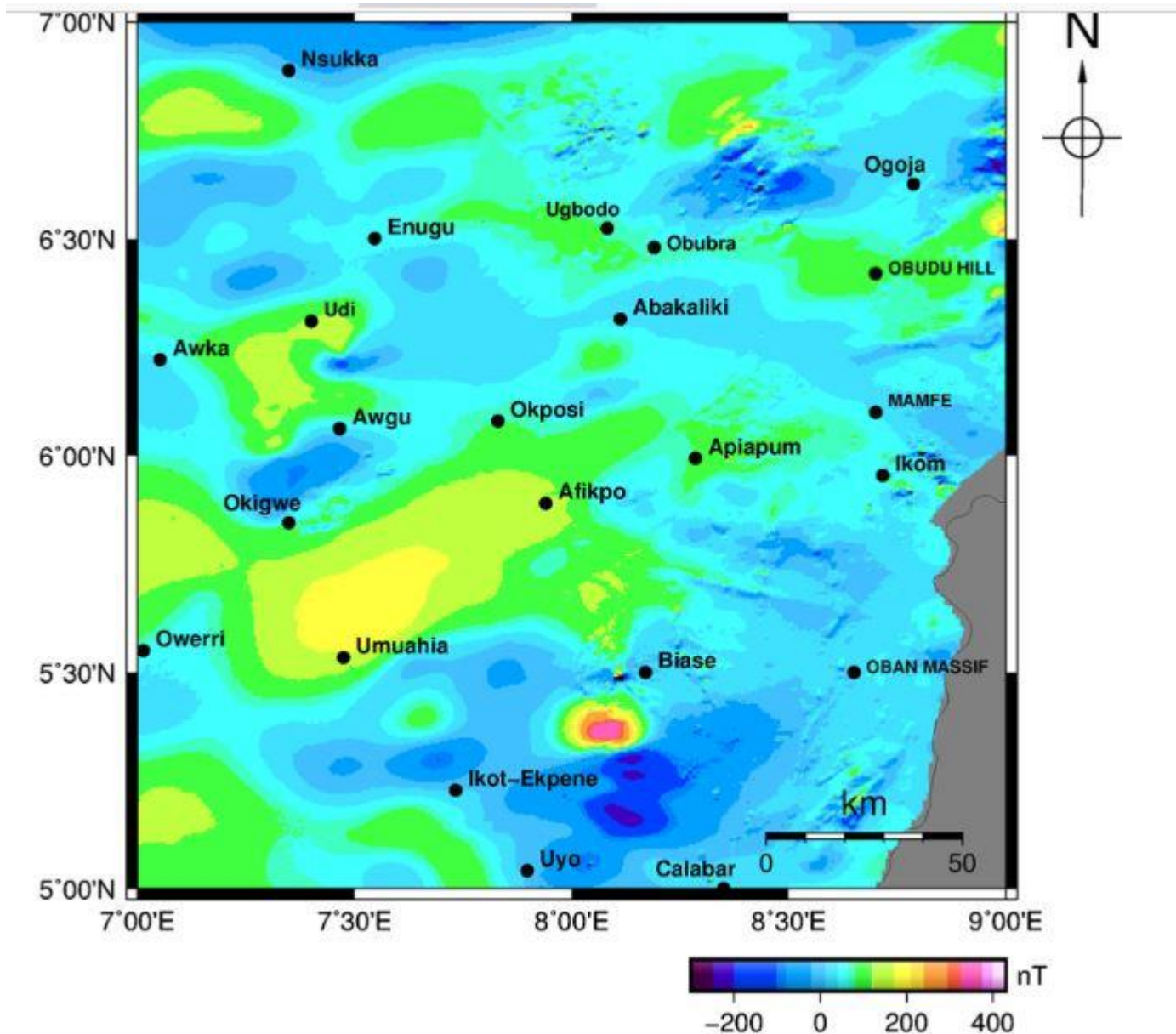


Fig. 4.7b: Anomaly map of Eastern Nigeria showing the anomalies in the central and southwestern regions of Afikpo and Umuahia Geothermal Gradient map CND map and heat flow map.

4.9 Geothermal potential of Abakaliki (Sheet 303)

The airborne gravity data Abakaliki in Ebonyi state was subjected to spectral analysis with the aim of accessing the geothermal potential of the study area. The Curie point depth values ranges from 12.57 to 19.16km, the geothermal gradient values ranges from 30.27 to 46.14°C/km and the heat flow values ranges from 75.98 to 115.81mW/m² (Table 21a). The SE edge hosts the highest values of heat flow and geothermal gradient with corresponding shallowest values of Curie point depth (Fig.4.7 c). Generally, for a viable geothermal reservoir, a heat flow range of 80 to 100 mW/m²is recommended, hence it can be inferred that every region on the study area could be considered as having good prospect except with

the NW edge regions of the study area with low heat flow below the recommended threshold (80 – 100) mWm^{-2} .

Table 21a: summary of the results of the centroid depth, depth to basement, curie depth, geothermal gradient and the heat flow

Blocks	Longitude (Deg)	Latitude (Deg)	Centroid depth Z_o (km)	Depth to basement Z_t(km)	Curie depth Z_b(km)	Geothermal Gradient ($^{\circ}\text{C}/\text{km}$)	Heat flow (mWm^{-2})
N1	8.125	6.375	11.32	3.48	19.16	30.27	75.98
N2	8.2065	6.375	9.03	2.71	15.35	37.78	94.84
N3	8.291	6.375	8.68	3.81	13.55	42.80	107.43
N4	8.375	6.375	10.04	3.33	16.75	34.62	86.91
N5	8.125	6.125	9.64	3.59	15.69	36.96	92.78
N6	8.2065	6.125	8.84	2.4	15.28	37.95	95.27
N7	8.291	6.125	7.48	2.39	12.57	46.14	115.81
N8	8.375	6.125	8.21	3.61	12.81	45.27	113.64
					15.145	38.97375	97.8325

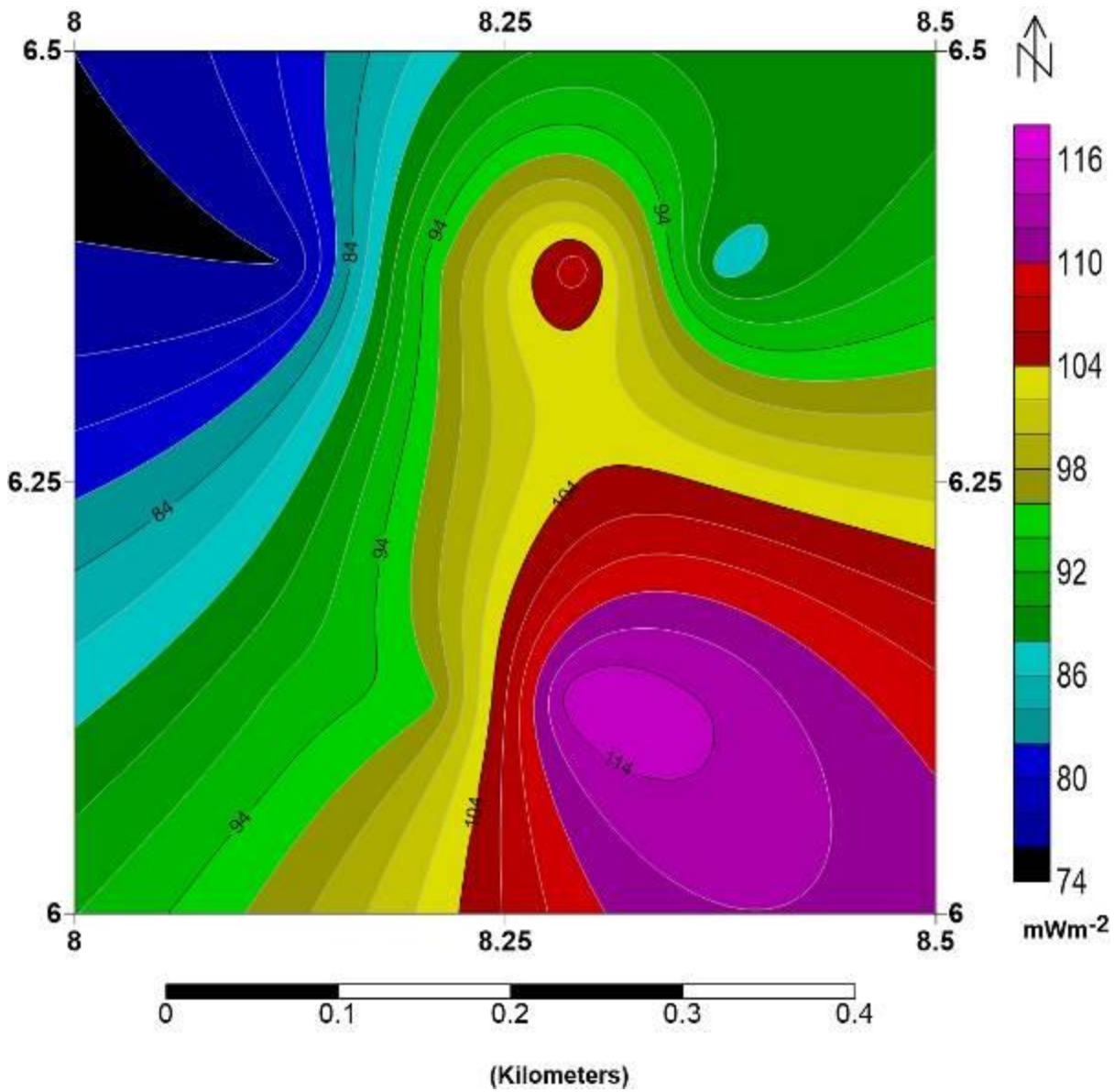


Fig.4.7c: Heat flow contour map of sheet 303 corresponding to Abakaliki (Ebonyi State)

4.10 Toro-Sheet 147

The result of geothermal parameters across the area of study shows the occurrence of Curie point depth values ranging from 12.71 km to 22.08 km. Geothermal gradient values ranges from 26.27 $^{\circ}\text{C}/\text{km}$ to 45.63 $^{\circ}\text{C}/\text{km}$. Corresponding values of heat flow ranges from 65.93 mW/m^2 to 114.54 mW/m^2 (Table 22) Peak values of heat flow is observed at the North-east and South-western edges of the study area. Heat flow values in the range of 86 mW/m^2 to 114 mW/m^2 is observed in green to purple colours respectively spreading out from a middle region of lower values toward the NE and SW edges having higher values (Fig 4.8). These range of values (86 to 114 mW/m^2) meet the recommended values of 80 to 100 mW/m^2 usually considered for a good source of geothermal energy. Hence the entire study area shows favourable range of heat flow recommended for a good source of geothermal energy except the middle portion depicted in light to dark blue (Western region) with values below 80 mW/m^2 .

Table 22: summary of the results of the centroid depth, depth to basement, curie depth, geothermal gradient and the heat flow

Blocks	Longitude (Deg).	Latitude (Deg)	Centroid depth Zo (km)	Depth to basement Zt (km)	Curie depth Zb (km)	Geothermal Gradient (oC/km)	Heat Flow mWm⁻²
G1	8.625	10.375	8.46	1.39	15.53	37.35	93.74
G2	8.875	10.375	7.62	1.85	13.39	43.32	108.72
G3	8.625	10.125	7.34	1.97	12.71	45.63	114.54
G4	8.875	10.125	9.92	2.72	17.12	33.88	85.04
G5	8.75	10.375	7.62	1.43	13.81	42.00	105.42
G6	8.75	10.125	10.03	2.69	17.37	33.39	83.81
G7	8.625	10.25	11.9	1.72	22.08	26.27	65.93
G8	8.875	10.25	9.87	1.8	17.94	32.33	81.15
*Heat Flow ranged from 65.93 – 114.54 (mWm⁻²)					16.24	36.77	92.29

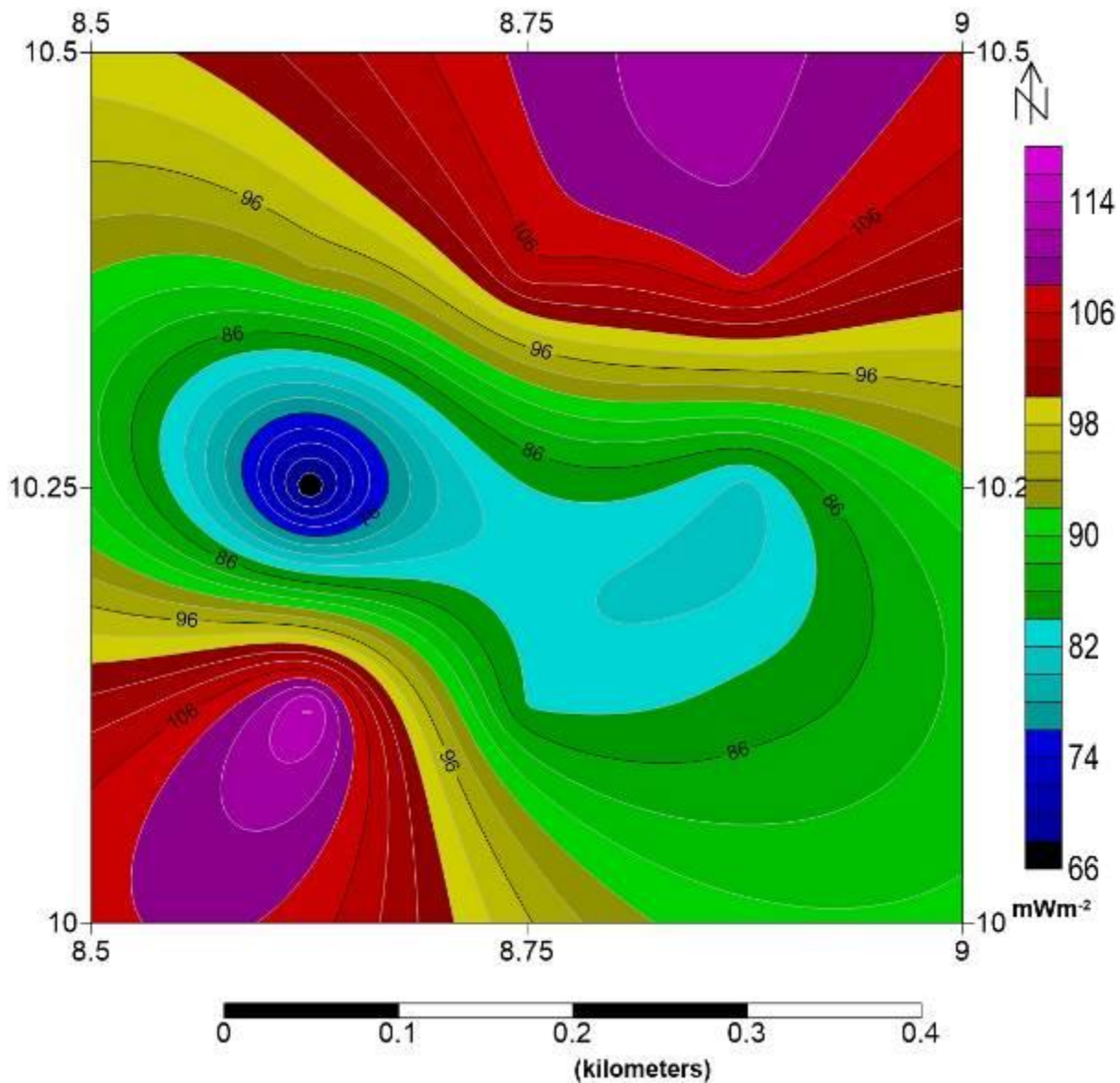


Fig. 4.8 Heat flow contour map of sheet 147 corresponding to Toro

4.11 Kaltungo - Sheet 173

The spectral analysis of sheet 173 shows the distribution and variation of geothermal parameters across the study area. Table 23 presents the summary of the results of the centroid depth, depth to basement, curie depth, geothermal gradient and the heat flow. The Curie point depth values ranges from 13.5 to 21.59 km with an average value of 17.29 km. The geothermal gradient ranges from 26.89 to 42.96 °C/km with an average value of 34.34 °C/km. The heat flow values varied between 67.42 to 107.83 mW/m² with an average value of 86.20 mW/m². High and peak values of geothermal gradient and heat flow is observed at the Northern and Southern regions while the western and eastern edges are depicted in low values (Fig.4.9.1). The shallowest Curie point depths also occurs within the Northern and Southern regions (Fig.4.9.1). A record of geothermal parameters favourable for explorable geothermal energy can be seen at the northern and southern regions with heat flow range of 82 to 106 mW/m²

depicted in green to purple colours on the contour map. The high values of heat flow correspond to recommended range of 80 to 100 mW/m² suitable for good source of geothermal energy.

Table 23: summary of the results of the centroid depth, depth to basement, curie depth, geothermal gradient and the heat flow

Blocks	Longitude (Deg).	Latitude (Deg)	Centroid depth Z_o (km)	Depth to basement Z_t (km)	Curie depth Z_b (km)	Geothermal Gradient (oC/km)	Heat Flow mWm⁻²
H1	11.125	9.875	9.71	2.32	17.1	33.92	85.13
H2	11.375	9.875	10.04	2.6	17.48	33.18	83.28
H3	11.125	9.625	10.7	2.36	19.04	30.46	76.46
H4	11.375	9.625	9.82	2.8	16.84	34.44	86.45
H5	11.25	9.875	7.64	1.53	13.75	42.18	105.88
H6	11.25	9.625	8.12	2.74	13.5	42.96	107.84
H7	11.125	9.75	10.54	2.21	18.87	30.74	77.15
H8	11.375	9.75	12	2.41	21.59	26.86	67.43
*Heat Flow ranged from 67.43 – 107.84 (mWm⁻²)				17.27	34.34	86.20	

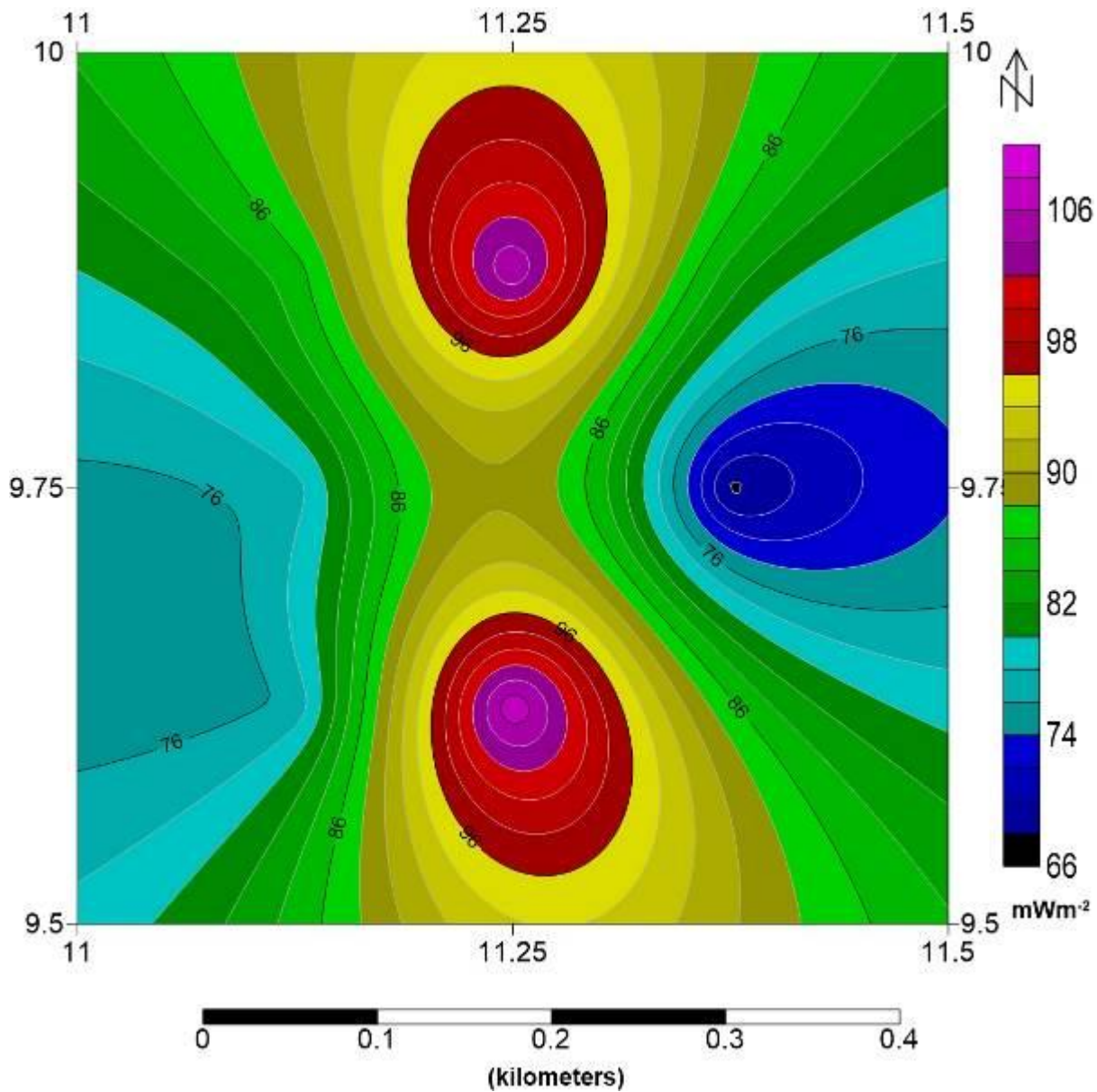


Fig.4.9 Heat flow contour map of sheet 173 corresponding to Kaltungo

4.12 Numal - Sheet 196

Results of analysis from sheet 196 showed curie point depth occurrence ranges from 11.92 to 21.84 km. Geothermal gradient values ranges from 26.55 to 48.65 °C/km. Heat flow values ranges from 66.65 to 122.13 mW/m². Table 24 presents the summary of the results of the centroid depth, depth to basement, curie depth, geothermal gradient and the heat flow. A trend of low values spreading out to high values of geothermal gradient and heat flow is observed from the North-eastern region to South-western region respectively (Fig. 4.91). This trend is observed inversely for Curie point depth. An occurrence of heat flow values in the range of 80 to 100 mW/m² is considered indicative of a viable geothermal energy source; it can therefore be inferred that all regions of the study area (NWS) with exception of

the North-Eastern edge shows trend of values for heat flow that is suitable for geothermal energy exploration.

Table 24: summary of the results of the centroid depth, depth to basement, curie depth, geothermal gradient and the heat flow

Blocks	Longitude (Deg).	Latitude (Deg)	Centroid depth Z_o (km)	Depth to basement Z_t (km)	Curie depth Z_b (km)	Geothermal Gradient (oC/km)	Heat Flow mWm⁻²
I1	12.125	9.375	7.42	2.92	11.92	48.66	122.13
I2	12.375	9.375	12.7	3.56	21.84	26.56	66.66
I3	12.125	9.125	7.35	2.48	12.22	47.46	119.13
I4	12.375	9.125	8.98	2.73	15.23	38.08	95.59
I5	12.25	9.375	11.84	3.56	20.12	28.83	72.36
I6	12.25	9.125	8.22	2.71	13.73	42.24	106.03
I7	12.125	9.25	8.81	2.56	15.06	38.51	96.67
I8	12.375	9.25	11.38	3.25	19.51	29.73	74.62
*Heat Flow ranged from 66.66 – 122.13 (mWm⁻²)					16.20	37.51	94.15

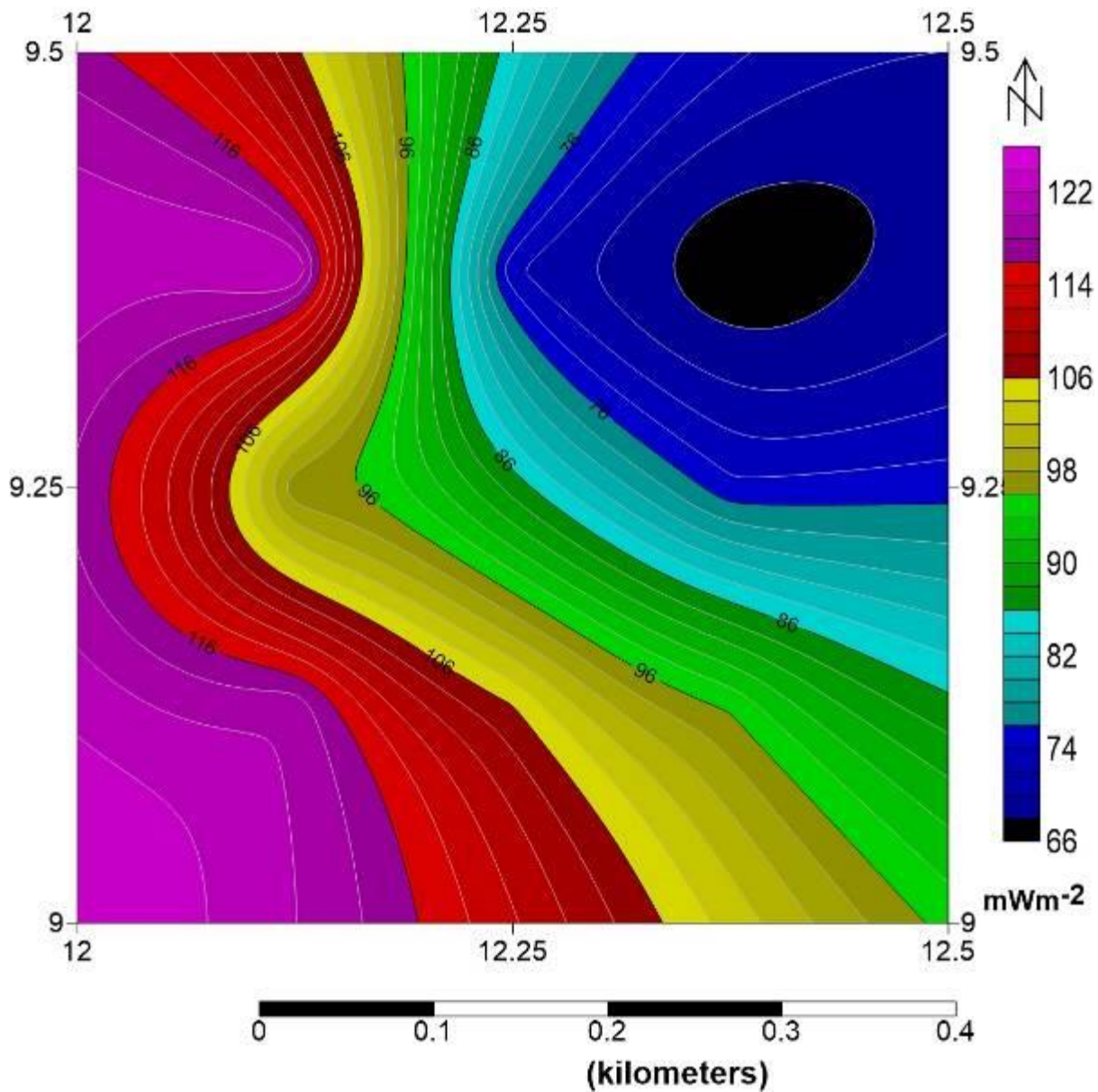


Fig. 4.9.1 Heat flow contour map of sheet 196 corresponding to Numal

4.13 Kotonkarfi - Sheet 227

The spectral analysis performed on the gravity data of study area showed the distribution of Curie point depth, Geothermal gradient and Heat flow values across the regions of study area. Table 25 presents the summary of the results of the centroid depth, depth to basement, curie depth, geothermal gradient and the heat flow. Curie point depth varied between 11.93 to 19.84 km with an average value of 15.82 km. Geothermal gradient values varied between 29.77 to 48.61 °C/km with average value of 38.01 °C/km. a record of heat flow values varied between 74.73 to 122.02 mW/m² with average value of 95.41 mW/m². Peak values of geothermal gradient and heat flow with corresponding shallow Curie point depth is observed at the North-eastern and South-western edges of study area. The North-west and

South-east regions recorded lower values of heat flow and geothermal gradient (Fig. 4.92). A General and conventional values of heat flow recommended for a viable geothermal reservoir is between 80 to 100 mW/m². The range of heat flow values within stated threshold is hosted at the NE and SW regions which also represents the regions with prospective geothermal energy sources.

Table 25: summary of the results of the centroid depth, depth to basement, curie depth, geothermal gradient and the heat flow

Blocks	Longitude (Deg).	Latitude (Deg)	Centroid depth Z_o (km)	Depth to basement Z_t (km)	Curie depth Z_b (km)	Geothermal Gradient (oC/km)	Heat Flow mWm⁻²
J1	6.625	8.375	9.48	2.81	16.15	35.91	90.14
J2	6.875	8.375	7.32	2.71	11.93	48.62	122.03
J3	6.625	8.125	6.86	1.06	12.66	45.81	114.99
J4	6.875	8.125	11.1	2.36	19.84	29.23	73.38
J5	6.75	8.375	10.98	3.14	18.82	30.82	77.35
J6	6.75	8.125	7.44	1.66	13.22	43.87	110.12
J7	6.625	8.25	7.85	1.22	14.48	40.06	100.54
J8	6.875	8.25	10.9	2.32	19.48	29.77	74.73
*Heat Flow ranged from 73.34 – 122.03 (mWm⁻²)					15.82	38.01	95.41

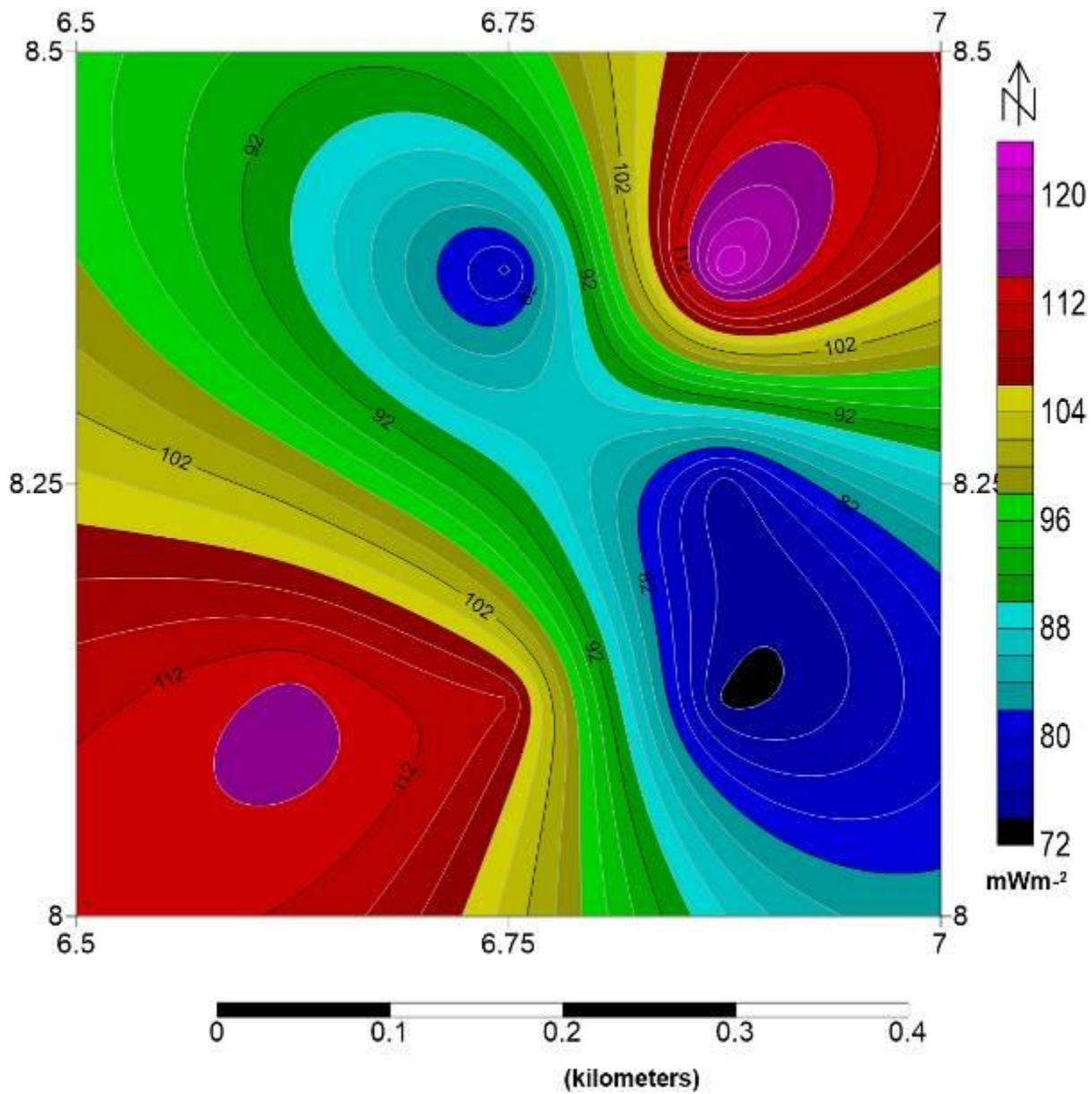


Fig. 4.9.2 Heat flow contour map of sheet 227 corresponding to Kotonkarfi

4.14 Pennigton Rivers_Bayelsa - Sheet 326

The gravity data of study area was subjected to spectral analysis; the result shows that Curie point depth ranges from 14.07 to 21.77 km, the geothermal gradient ranges from 26.64 to 41.22 °C/km and the heat flow ranges from 66.87 to 103.46 mW/m² (Tabe 26). High occurrence of geothermal gradient and heat flow values is observed across the entire regions of study area depicted in green to purple colours with an exception of lower values occurring at the southern regions depicted in blue to light blue colours. While peak values of geothermal gradient and heat flow can be seen on eastern regions, a record of shallow curie point depth is equally observed across the eastern regions making it favourable for

possible geothermal energy exploration (Fig. 4.93). This is because the values of heat flow in the region is in conformity with a recommended range of 80 to 100 mW/m².

Table 26: summary of the results of the centroid depth, depth to basement, curie depth, geothermal gradient and the heat flow

Blocks	Longitude (Deg).	Latitude (Deg)	Centroid depth Z₀ (km)	Depth to basement Z_t (km)	Curie depth Z_b (km)	Geothermal Gradient (oC/km)	Heat Flow mWm⁻²
K1	5.526	4.875	10.34	3.57	17.11	33.90	85.08
K2	5.875	4.875	9.34	2.9	15.78	36.76	92.26
K3	5.625	4.625	10.9	4.16	17.64	32.88	82.53
K4	5.875	4.625	10.24	3.62	16.86	34.40	86.35
K5	5.750	4.875	10.5	3.16	17.84	32.51	81.60
K6	5.750	4.625	12.8	3.83	21.77	26.64	66.87
K7	5.625	4.750	9.96	2.7	17.22	33.68	84.54
K8	5.875	4.750	8.17	2.27	14.07	41.22	103.47
*Heat Flow ranged from 66.87 – 103.47 (mWm⁻²)					17.29	34.0	85.34

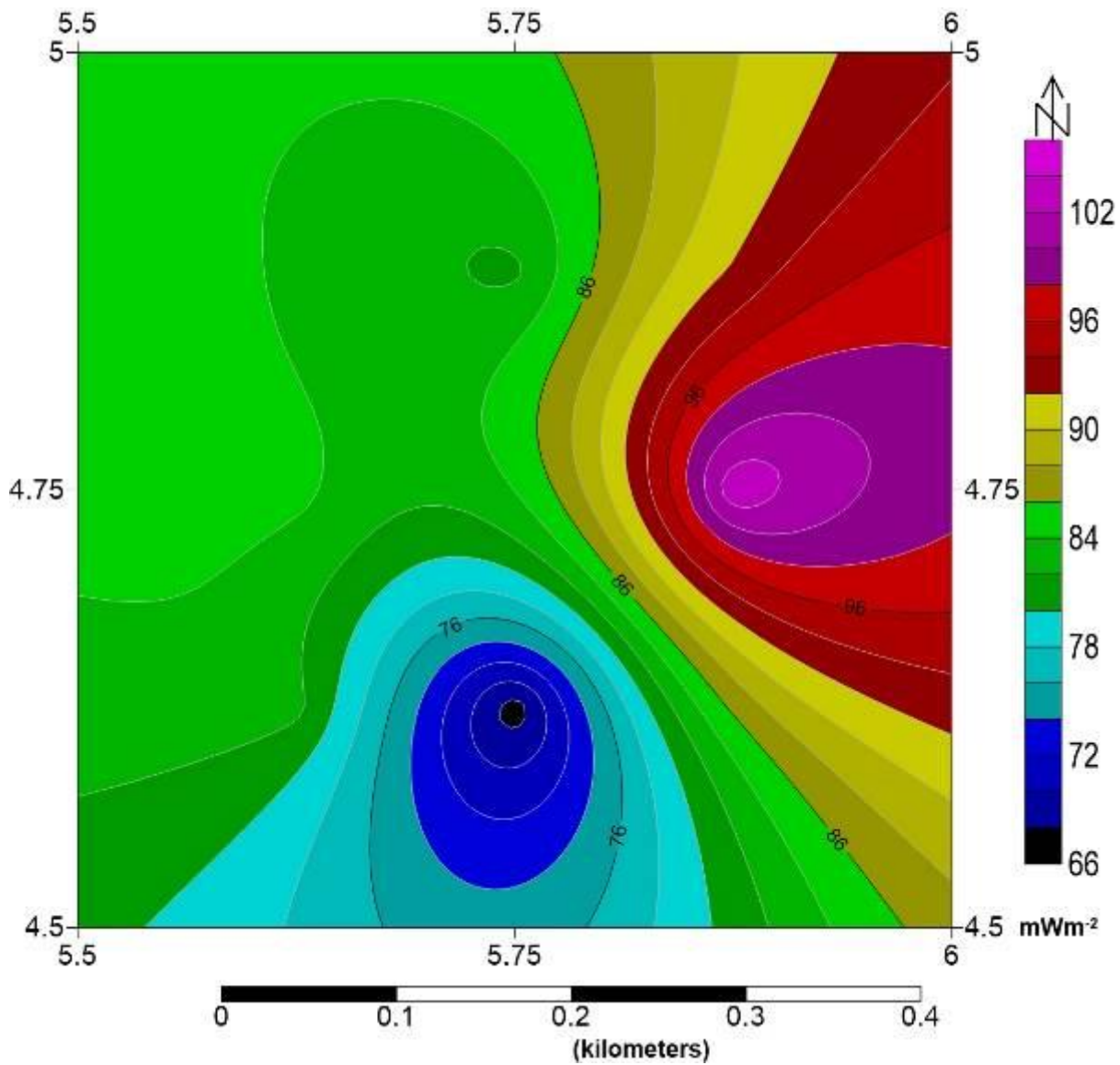


Fig. 4.9.3 Heat flow contour map of sheet 326 corresponding to Pennington Rivers

4.15 Okigwe - Sheet 312

The distribution of geothermal parameters within the study area can be seen through the contour maps of the Curie point depth, geothermal gradient and heat flow. The value of Curie point depth ranges from 15.83 to 22.36 km, geothermal gradient values ranges from 25.93 to 36.63 $^{\circ}\text{C}/\text{km}$ while heat flow values ranges from 65.11 to 91.96 mW/m^2 (Table 27). A contrast of the parameters shows that the Curie point depth varies inversely to the geothermal gradient and heat flow. This implies that regions of shallow Curie point depth corresponds to high occurrence of geothermal gradient and heat flow. On the heat flow map (Fig. 4.94) Peak values in the range of 86 to 92 mW/m^2 depicted in red to purple colours is observed at the northern regions while average to lower values depicted in black to yellow colours is in middle regions extending down to southern parts of study area. The northern regions depicted in

yellow to purple colours can be considered for a viable geothermal source when comparing the heat flow values with conventional threshold of 80 to 100 mW/m² usually recommended as prospective good source.

Table 27: summary of the results of the centroid depth, depth to basement, curie depth, geothermal gradient and the heat flow

Blocks	Longitude (Deg).	Latitude (Deg)	Centroid depth Z_o (km)	Depth to basement Z_t (km)	Curie depth Z_b (km)	Geothermal Gradient (oC/km)	Heat Flow mWm⁻²
L1	7.125	5.875	10.1	3.45	16.75	34.63	86.91
L2	7.375	5.875	9.76	3.69	15.83	36.64	91.96
L3	7.125	5.625	11.35	5.52	17.18	33.76	84.74
L4	7.375	5.625	11.59	3.86	19.32	30.02	75.35
L5	7.250	5.875	12.31	4.56	20.06	28.91	72.57
L6	7.250	5.625	13.1	3.84	22.36	25.94	65.11
L7	7.125	5.750	12.5	3.21	21.79	26.62	66.81
L8	7.375	5.750	12.5	5.05	19.95	29.07	72.97
*Heat Flow ranged from 65.11 – 91.96 (mWm⁻²)					19.16	30.70	77.05

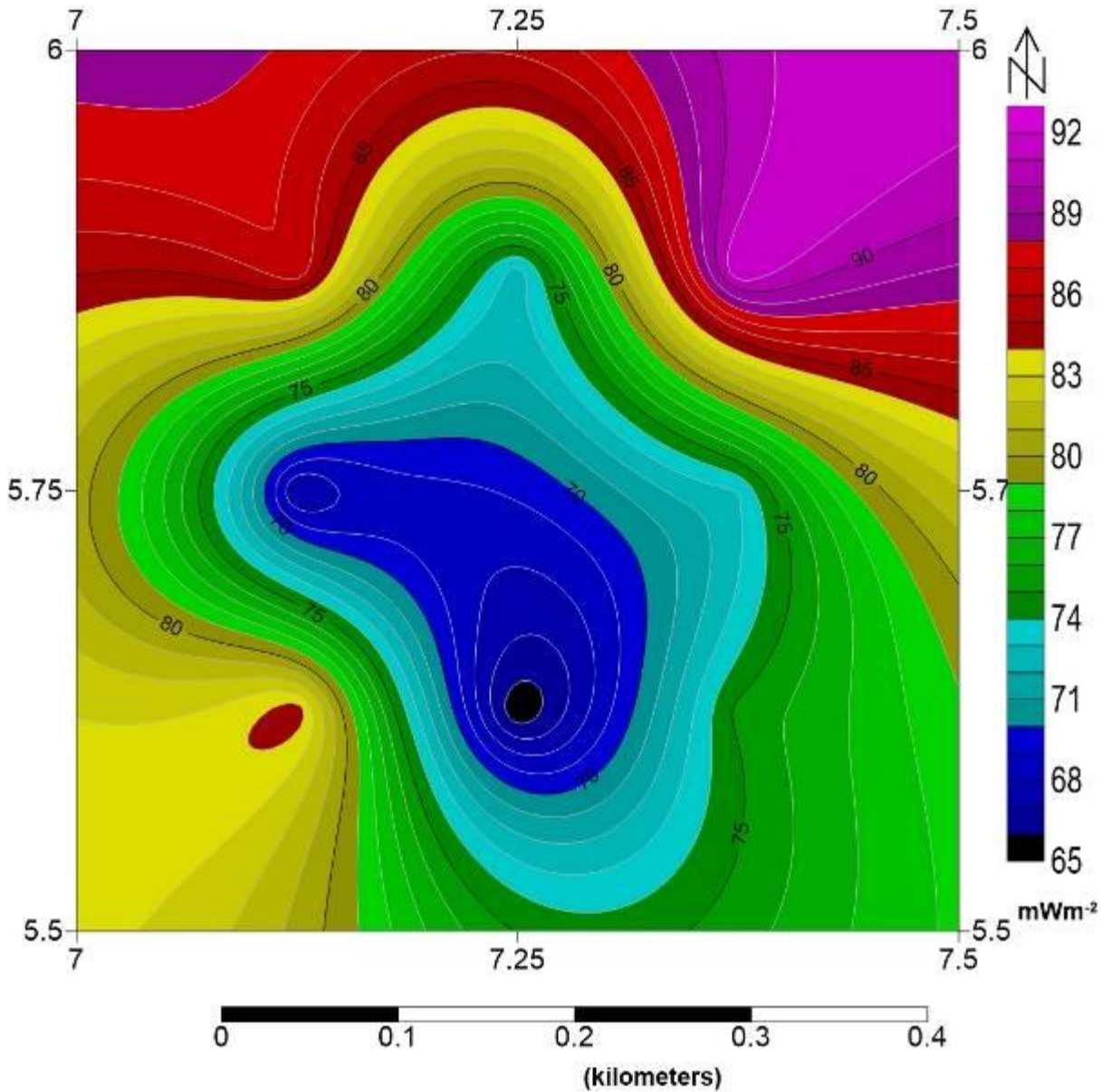


Fig. 4.9.4 Heat flow contour map of sheet 312 corresponding to Okigwe

4.16 Geothermal potential of Chad Basin North Eastern Nigeria (Karriwa Sheet 24)

The airborne gravity data of chad basin, karriwa sheet 24 was subjected to spectral analysis with the aim of accessing the geothermal potential of the study area. The Curie point depth values ranges from 15.14 to 30.78km, and the heat flow values ranges from 40.00 to 98.78mW/m² (Table 28). The NE edge hosts the highest values of heat flow and geothermal gradient with corresponding shallowest values of Curie point depth (Fig.4.95). Generally, for a viable geothermal reservoir, a heat flow range of 80 to 100 mW/m² is recommended, hence it can be inferred that every region on the study area could be considered as having good prospect except with the NW regions of the study area with low heat flow below 80 – 100 mWm⁻².

Table 28: summary of the results of the centroid depth, depth to basement, curie depth, geothermal gradient and the heat flow

Blocks	Long(°E)	Lat. (°N)	Depth to the Top (Z_t) (km)	Depth to the centroid (Z_o) (km)	Curie depth (Z_b) (km)	Heat flow (m/Wm^2)
1	10.50	12.50	2.91	12.83	22.75	65.81
2	11.00	12.50	3.12	14.76	26.52	56.00
3	11.50	12.50	3.64	9.39	15.14	98.78
4	11.50	12.88	4.99	11.34	17.69	83.01
5	10.50	12.00	1.48	13.82	26.16	57.04
6	11.00	12.00	3.47	16.92	30.33	48.02
7	11.50	12.00	2.72	16.75	30.78	59.05
8	10.50	11.50	3.59	14.25	24.91	40.00

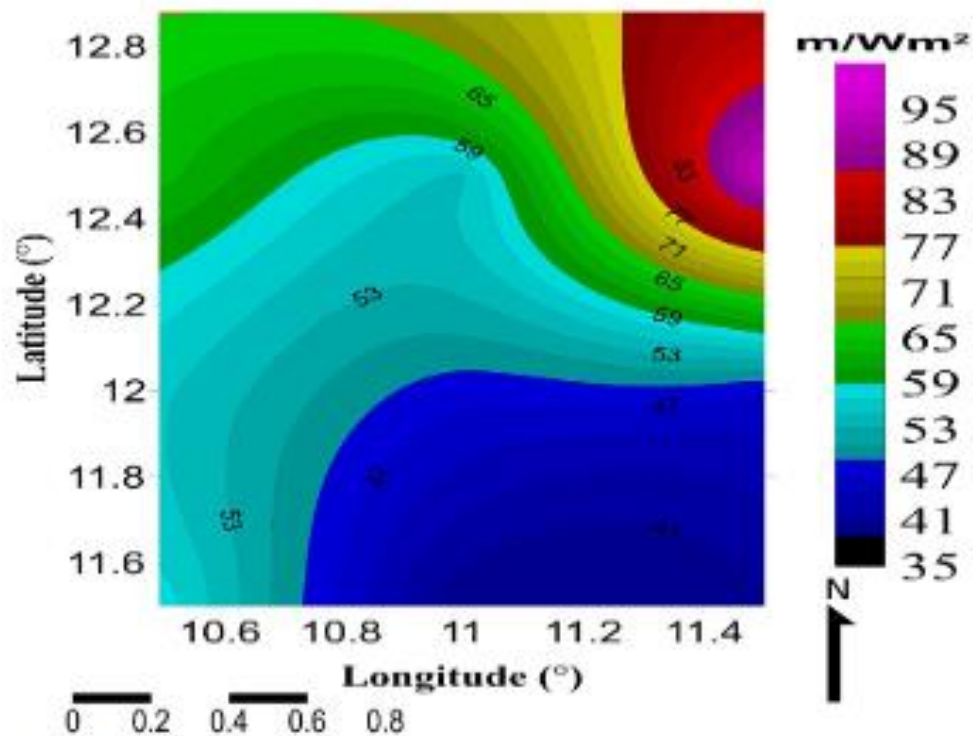


Fig. 4.9.5: Heat flow contour map of Chad Basin North Eastern Nigeria (Karriwa Sheet 24)

CHAPTER FIVE

5.0

Material and Methods

Source of Data: Aeromagnetic

The Nigerian Geological Survey Agency provided the aeromagnetic data (Sheets) used for this research. The data was obtained as part of the NGSAsponsored nationwide aeromagnetic survey in 2009 and the data were collected along a series of 200-meter-spaced NE SW flight lines with an average flight elevation of about 80 meters, with tie lines every 500 meters. Using the International Geomagnetic Reference Field (IGRF), 2005, the geomagnetic gradient was removed from the data. Also, the data was made available in the form of grids with a scale of 1:100,000. The total area covered in this study is approximately 55 by 55 km², extending from Latitude 7° N to 7° 30' N and Longitude 6° E to 6° 30' N.

This study's procedures include creating a Total Magnetic Intensity (TMI) map with OASIS MONTAJ software, separating regional and residual anomalies, dividing the residual map into eight overlapping blocks, performing spectral analysis on each block, evaluating the depth to the magnetic source with spectral analysis, and estimating the geothermal gradient and heat flow.

5.1 Theory of Methods

Calculation of Curie-point depth, geothermal gradient, and heat flow.

The centroid depth is calculated from the low wave number part of the scaled power spectrum as

$$\ln [P(k)^{1/2} / k] = A - |k| Z_0 \quad (6)$$

where \ln is the natural logarithm, $P(k)$ is the radially averaged power spectrum, k is the wave properties magnetization and its orientation and Z_0 is the centroid depth of the magnetic sources (Tanaker *et al.*, 1999; Abraham *etal*,2014). For the high wave number part, the lower spectrum can be related to the top of the magnetic sources by a similar equation:

$$\ln [P(k)^{1/2} / k] = B - |k| Z_t \quad (7)$$

where B is a constant: Z_t is the depth to the top of the magnetic sources. The depth of the bottom of magnetization Z_b is:

$$Z_b = 2Z_0 - Z_t \quad (8)$$

Summarily, the depth to the base of the magnetic source (the Curie point depth) is calculated in four steps (Tanaka *et al.*, 1999):

- i. Calculate the radially averaged power spectrum of the magnetic data in each window
- ii. Estimate the depth to the top of the magnetic source (Z_t) using the high wave number portion of the magnetic anomaly power spectra
- iii. Estimate the depth to the centroid of the magnetic source (Z_0) using a lower wave number portion of the magnetic anomaly power spectra.
- iv. Calculate the depth to the base of the magnetic source (Z_b) using $Z_b = 2Z_0 - Z_t$. The value of the Z_b is the Curie point depth/DBMS.

Therefore, the geothermal gradient in relation to the heat flow q is (Tanaka *et al.*, 1999; Nwankwo, *et al.*, 2009 Akinnubi and Adetona, 2018)

$$q = k \theta^\circ C d \quad (9)$$

The surface temperature is θ^0 C and dT/dZ will remain constant provided there are no heat sources or heat sinks depth. The Curie temperature depends on magnetic mineralogy. For example, although the Curie temperature of magnetite (Fe_3O_4) is at approximately 580oC, an increase of Titanium (Ti) contents of titanomagnetite ($Fe_{2-x}Ti_xO_3$) will cause a reduction of the Curie temperature. A curie temperature of 580°C and thermal conductivity of 2.5 W m⁻¹ °C⁻¹ which is the average thermal conductivity for igneous rocks will be used in the study as standard (Nwankwo (2015); Tanaka *et al.*, 1999), we then calculate the value for K the geothermal gradient in the study area using the empirical relation between Curie point, Curie temperature and geothermal gradient.

Heat flow estimates on the crust can thus be made using depth and thickness information. The Curie point temperature at which rocks lose their ferromagnetic properties connects thermal models and

models based on magnetic source analysis. Temperature influences the magnetic susceptibility and strength of the materials that make up the crust (Chukwu *et al* ,2017). Magnetic ordering becomes loose at temperatures above the Curie point, and both induced and remanent magnetization disappear, while temperatures above 580°C cause ductile deformation in the materials.

The basic relation for conductive heat transport is based on the assumption that the direction of the temperature variation is vertical and the temperature gradient dT/dZ is

$$q = -k (dT/dZ) \quad (10)$$

where q is heat flow and k is thermal conductivity. The Curie temperature $\theta^\circ\text{C}$ can also be defined as:

$$\theta^\circ\text{C} = (dT/dZ) d \quad (11)$$

where d is the Curie point depth (as obtained from the spectral magnetic anomaly).

5.2 Aeromagnetic Results and Discussion across Nigeria: Stages 3 and 4 Deliverables

Results and Discussion

5.3 Geothermal Potential of Lere_Farin Ruwa_Sheet 147

Results of analysis from **Lere_Farin Ruwa_Sheet 147** showed Curie point depth occurrence ranges from (12.55 - 20.6) km. Geothermal gradient values ranges from (28.15- 46.21) °C/km. Heat flow values ranges from 70.38to 115.52 mW/m². Table 29 presents the summary of the results of the centroid depth, depth to basement, curie depth, geothermal gradient and the heat flow. The anomaly spans numerous towns such as from the North-Eastern (NE) region to South-western region respectively covering Barakin Yelwa Rishi and Mariri (Figs. 5.1a-c). This trend is observed inversely for Curie point depth. An occurrence of heat flow values in the range of (80 - 100) mW/m² is considered indicative of a viable geothermal energy source; it can therefore be concluded that all regions of the study area with exception of the Western portion, (Blue and black) covering right of Doka town (which shows trend of low values for heat flow) are suitable for geothermal energy exploration.

Table 29: Summary of the results of the centroid depth, depth to basement, curie depth, geothermal gradient and the heat flow

Lere_Farin Ruwa_Sheet 147

Blocks	X	Y	Centroid Depth	Depth to basement	Curie depth	Geothermal Gradient	Heat Flow (mWm ⁻²)
A	8.625	10.375	8.2	1.38	15.02	38.61	96.52
B	8.875	10.375	7.51	1.9	13.12	44.2	110.5
C	8.625	10.125	7.25	1.95	12.55	46.21	115.52
D	8.875	10.125	9.47	2.95	15.99	36.27	90.67
E	8.75	10.375	7.85	1.23	14.47	40.08	100.2
F	8.75	10.125	10.29	2.72	17.86	32.47	81.17
G	8.625	10.25	11.21	1.82	20.6	28.15	70.38
H	8.875	10.25	9.66	1.75	17.57	33.01	82.52

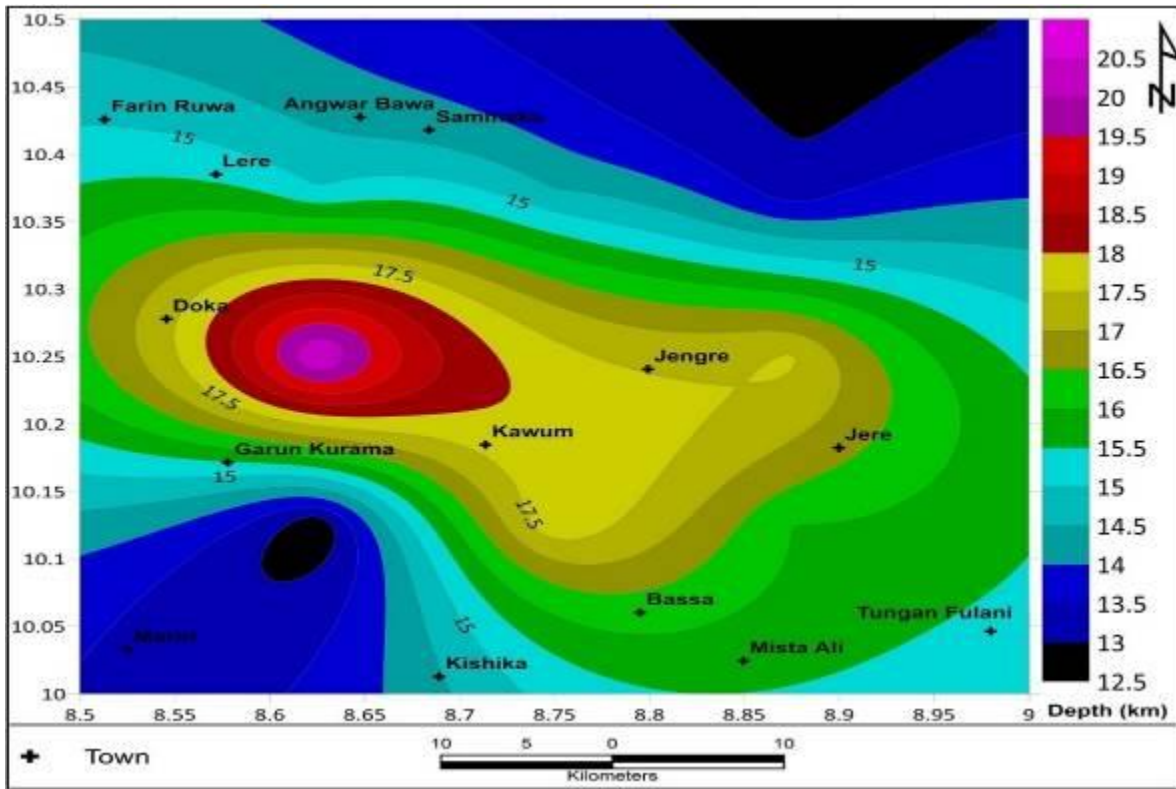


Fig 5.1a: Curie Point Depth Geological Map of (Sheet 147) corresponding to Lere_ Farin Ruwa

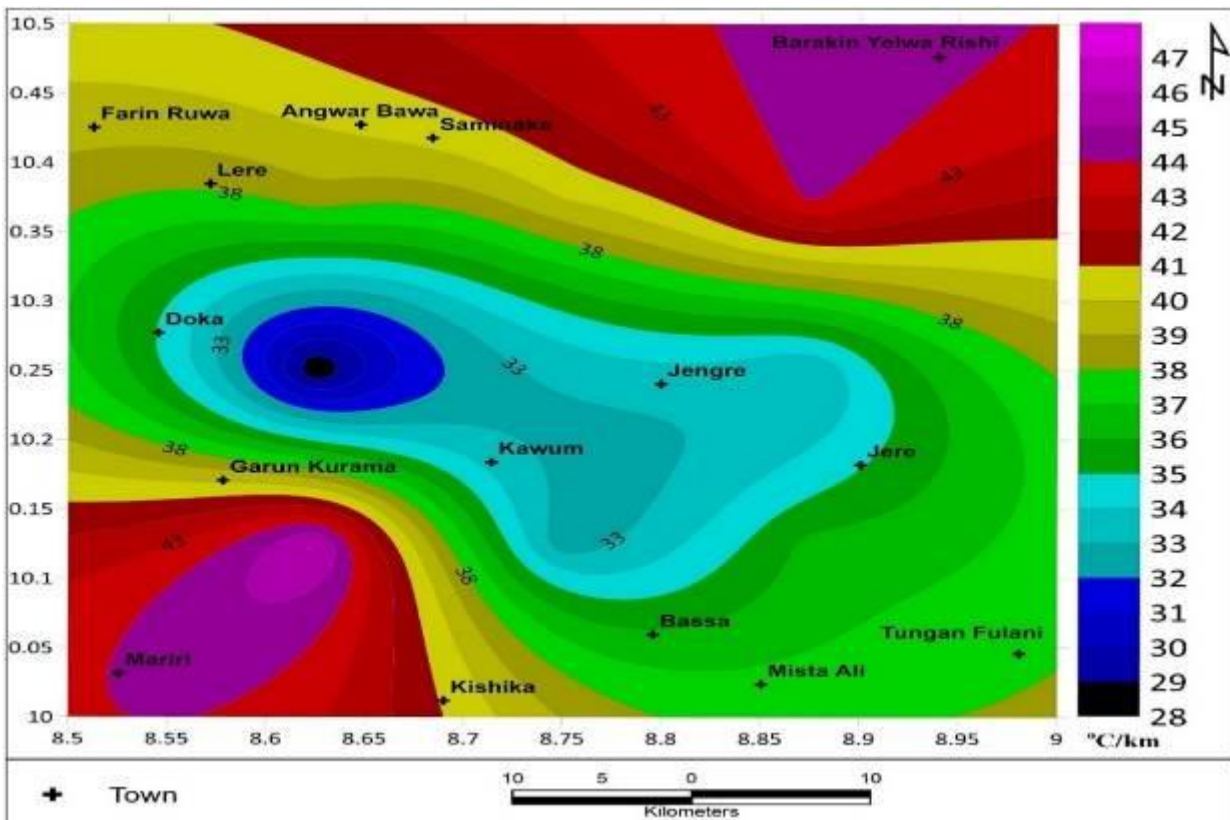


Fig 5.1b: Geothermal Gradient Geological Map of (Sheet 147) corresponding to Lere_ Farin Ruwa

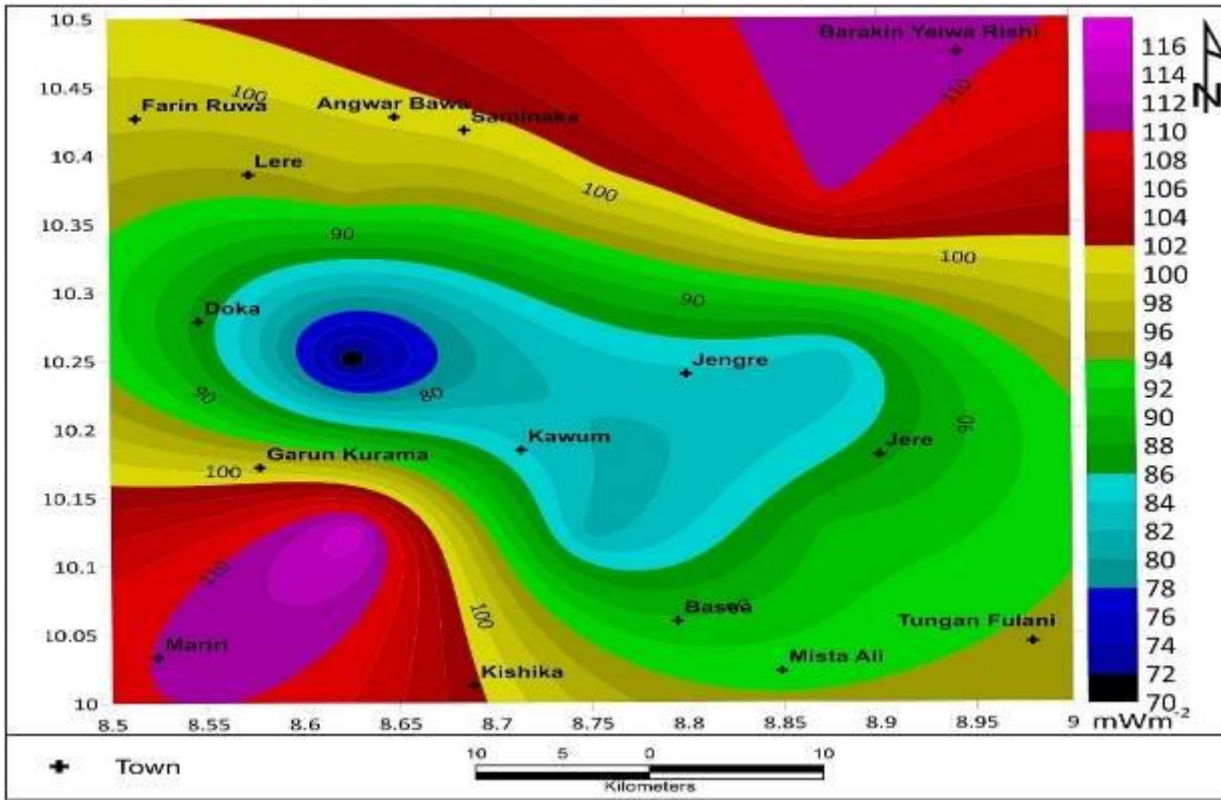


Fig 5.1c: Heat flow Geological Map of (Sheet 147) corresponding to Lere_ Farin Ruwa

5.4 Geothermal potential of Kaltungo_ (Sheet 173)

The aeromagnetic data of Kaltungo_ Sheet173 was subjected to spectral analysis with the aim of accessing the geothermal potential of the study area. The Curie point depth values ranges from (13.1- 20.46) km, the geothermal gradient values ranges from (29.8 - 44.27) °C/km and the heat flow values ranges from (74.5- 110.67) mW/m² (Table 30). The North edge and South covering Billiri and Burak hosts' anomalous values of heat flow and geothermal gradient with corresponding shallowest values of Curie point depth. The NW, central, SE and NE all show geothermal manifestations covering Kashere, Kongo, Kaltungo, Bambuka, Sabonlayi Awak (Fig. 5.2 a-c). Generally, for a viable geothermal reservoir, a heat flow range of 80 to 100 mW/m² is recommended, hence it can be inferred that every region on the study area could be considered as having good prospect except regions EW and Eastern edge covering Filliya, Ture Balam and Lakweme like of the study area with low heat flow below 80 mWm⁻².

Table 30 Summary of the results of the centroid depth, depth to basement, curie depth, geothermal gradient and the heat flow

Kaltungo_ (Sheet 173)

Blocks	X	Y	Centroid	Depth to basement	Curie depth	Geothermal gradient	Heat Flow (mWm ⁻²)
A	11.125	9.875	9.31	2.56	16.06	36.11	90.27
B	11.375	9.875	10.29	2.8	17.78	32.62	81.55
C	11.125	9.625	10.86	2.26	19.46	29.8	74.5
D	11.375	9.625	9.25	2.73	15.77	36.77	91.92
E	11.25	9.875	7.37	1.64	13.1	44.27	110.67
F	11.25	9.625	8.25	2.78	13.72	42.27	105.68
G	11.125	9.75	10.6	2.2	19	30.52	76.3
H	11.375	9.75	11.57	2.68	20.46	28.34	70.85

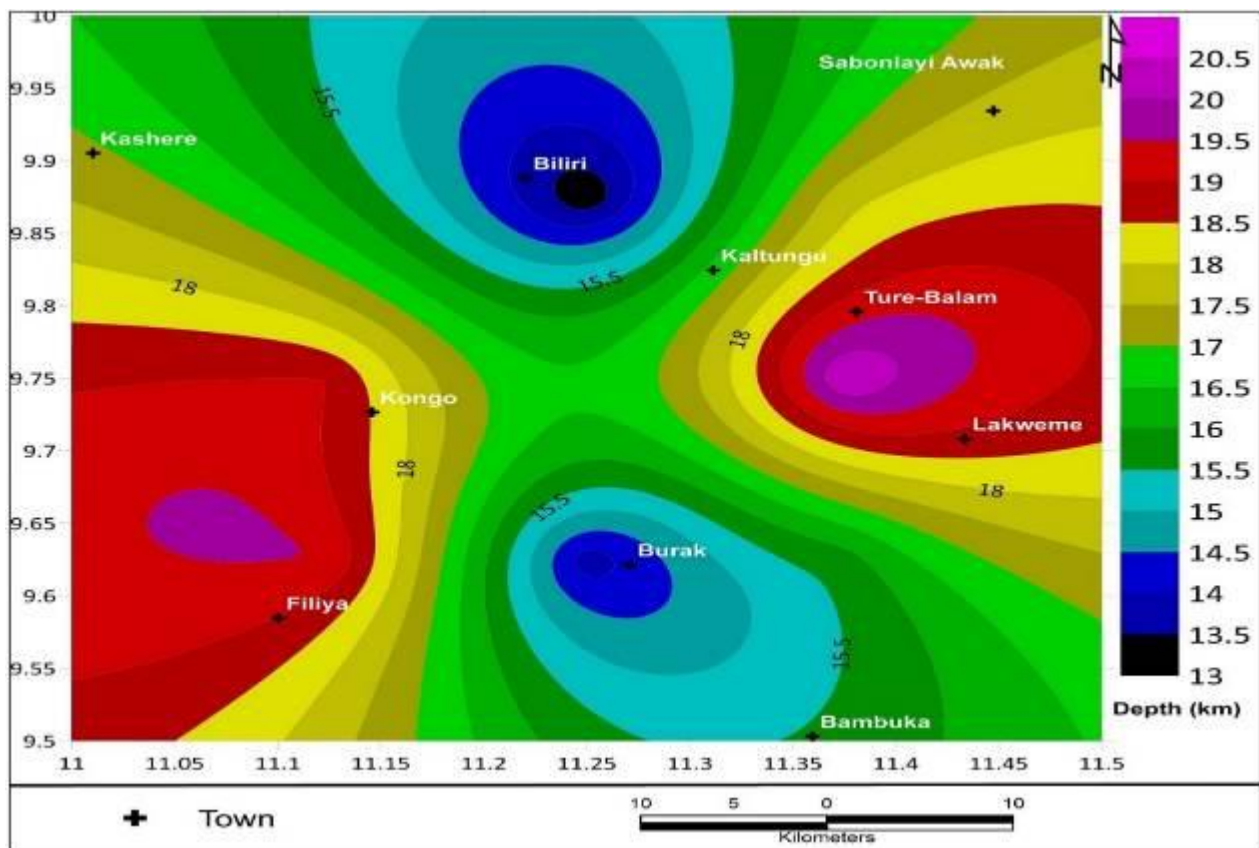


Fig 5.2a: Curie Point Depth (CPD) Geological Map of (Sheet 173) corresponding to Kaltungo

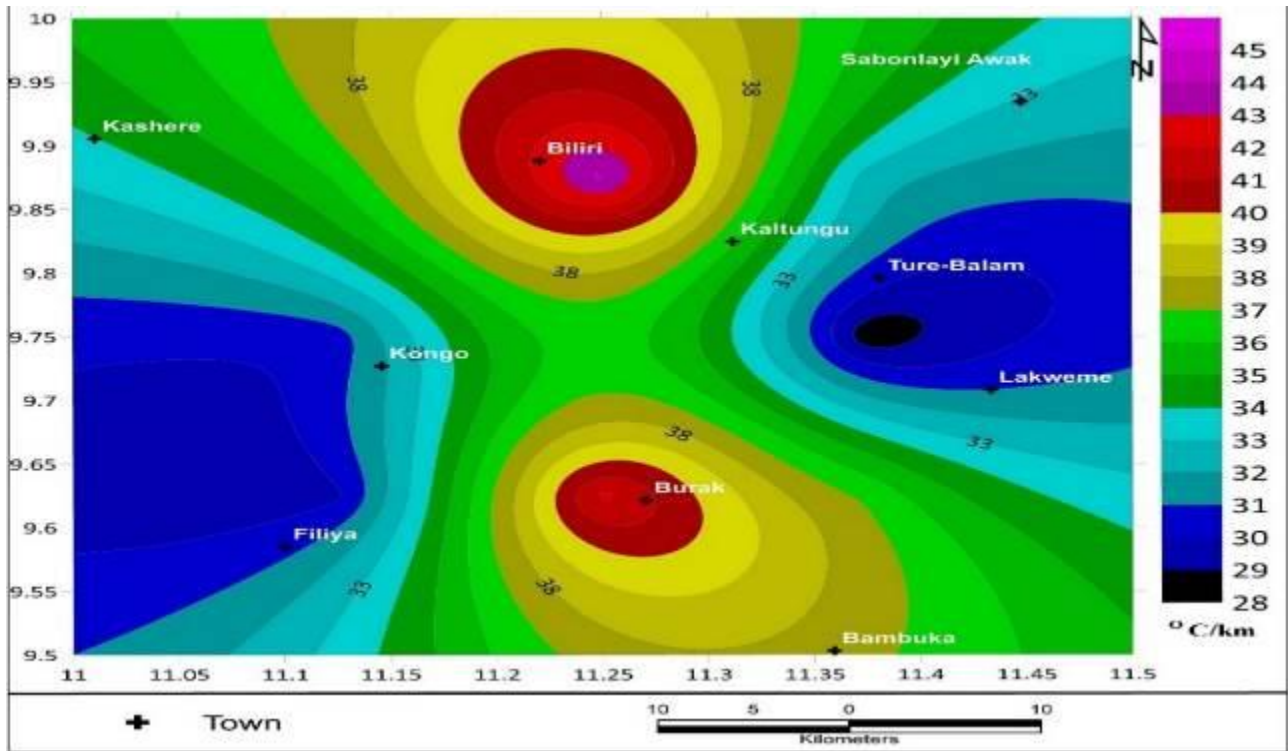


Fig 5.2b: Geothermal Gradient map of (Sheet 173) corresponding to Kaltungu

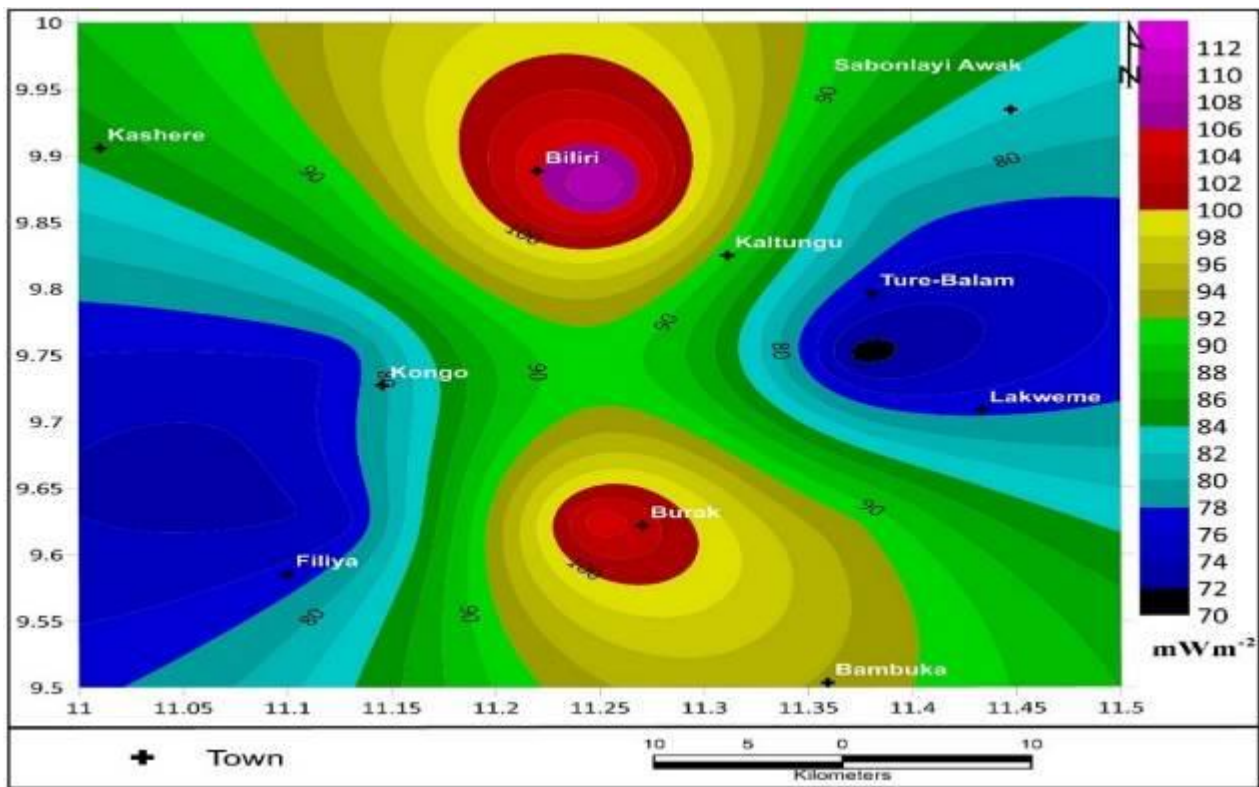


Fig 5.2c: Heat flow map of (Sheet 173) corresponding to Kaltungu

5.5 Geothermal potential of Numal_ (Sheet 196)

The aeromagnetic data of Numal_ (Sheet 196) was subjected to spectral analysis with the aim of accessing the geothermal potential of the study area. The Curie point depth values ranges from (11.92-20.51) km, the geothermal gradient values ranges from (30.00– 48.65) °C/km and the heat flow values ranges from (70.7- 121.62) mW/m² (Table 31). The NWS edge covering Numan, Mayo Belwa, hosts the highest values of heat flow and geothermal gradient with corresponding shallowest values of Curie point depth. Other areas like new Dansa, Laide, Jilli, Dadin Kowa and Dulumi have geothermal manifestations (Fig 5.3 a-c). Generally, for a viable geothermal reservoir, a heat flow range of 80 to 100 mW/m² is recommended, hence it can be inferred that every region on the study area could be considered as having good prospect except the NE edge regions of Kwo, Wafango, labondo, Jabura, and Yola the study area with low heat flow below the recommended threshold value (80 mWm⁻²-100).

Table 31 Summary of the results of the centroid depth, depth to basement, curie depth, geothermal gradient and the heat flow

Numal_ (Sheet 196)

Blocks	X	Y	Centroid	Depth to basement	Curie depth	Geothermal Gradient	Heat Flow (mWm ⁻²)
A	12.125	9.375	7.43	2.82	12.04	48.17	120.42
B	12.375	9.375	12.7	3.56	20.51	28.28	70.7
C	12.125	9.125	7.14	2.36	11.92	48.65	121.62
D	12.375	9.125	8.67	2.65	14.69	39.48	98.7
E	12.25	9.375	11.41	3.49	19.33	30	75
F	12.25	9.125	8.32	2.66	13.98	41.48	103.7
G	12.125	9.25	8.79	2.44	15.14	38.31	95.77
H	12.375	9.25	11.18	3.15	19.21	30.19	75.47

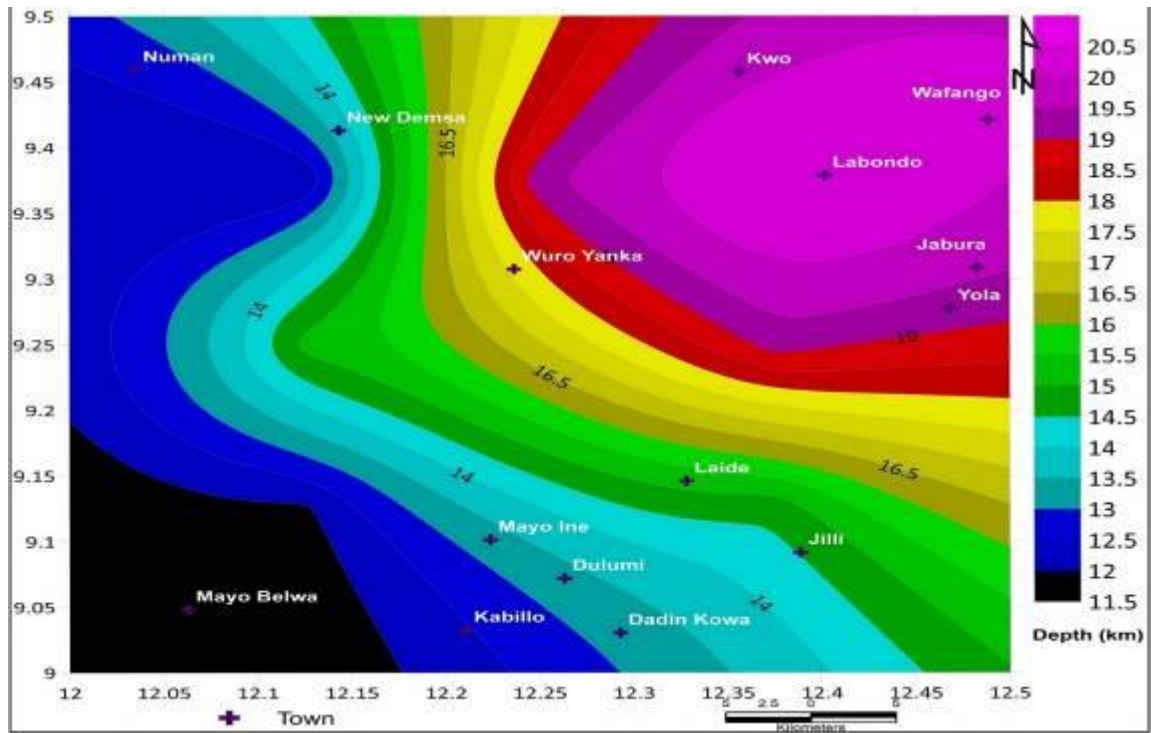


Fig 5.3a. CPD contour map of Sheet 196 corresponding to Numal

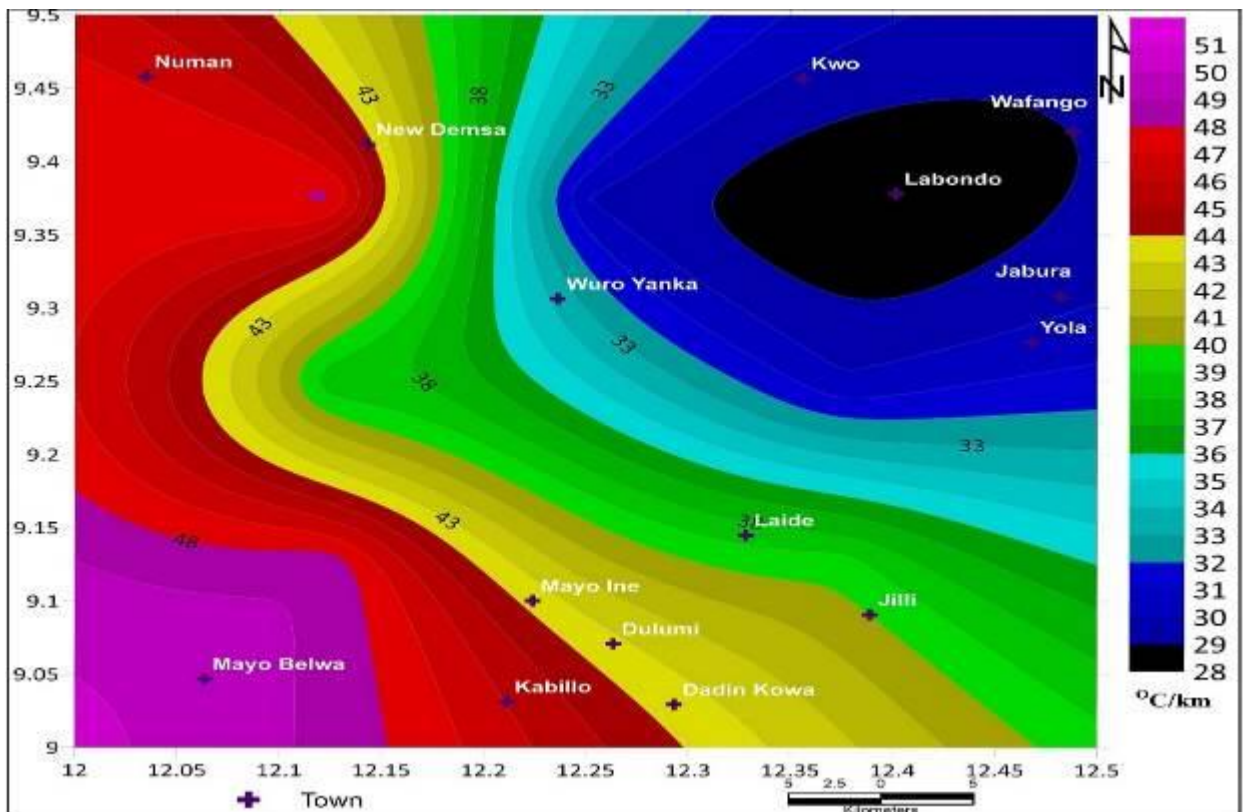


Fig.5.3b Geothermal Gradient contour map of Sheet 196 corresponding to Numal

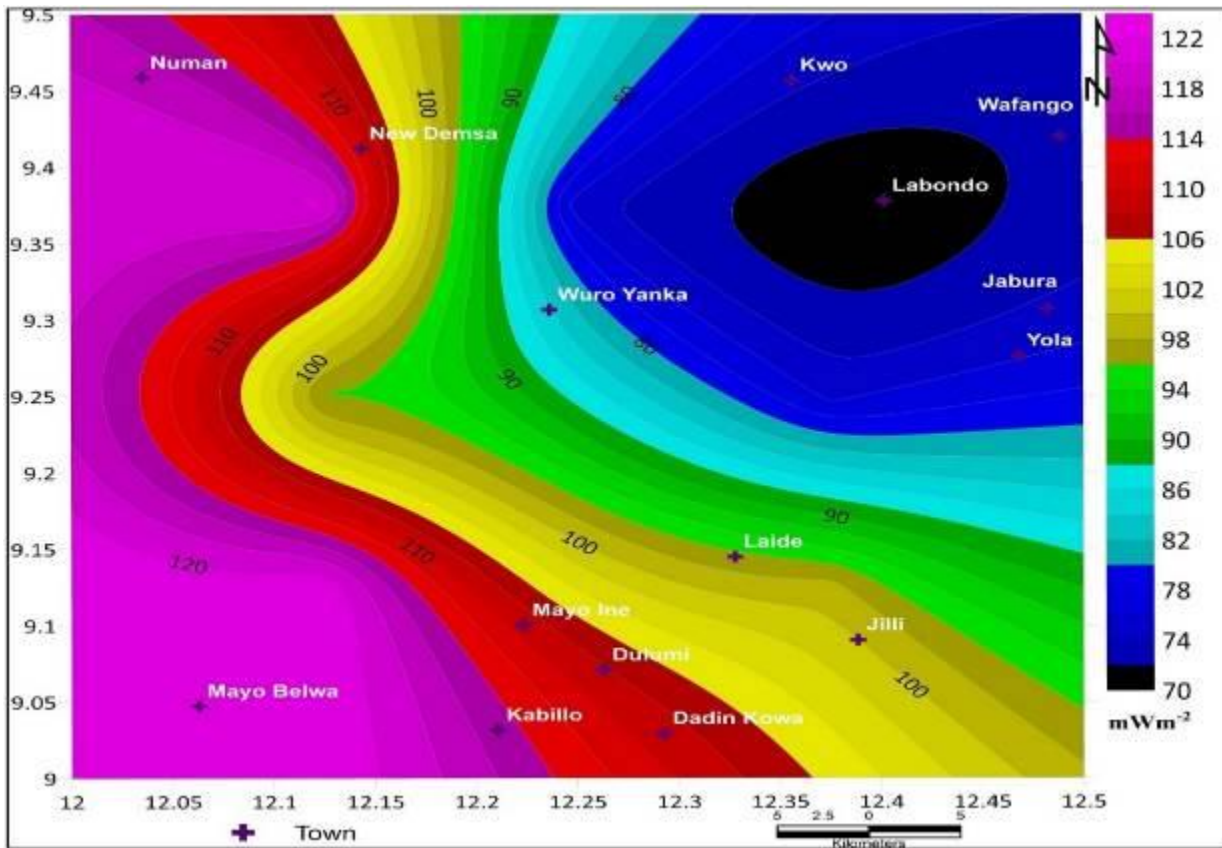


Fig 5.3c. Heat flow contour map of Sheet 196 corresponding to Numal

5.6 Geothermal potential of Kotonkarfi_ (Sheet 227)

The aeromagnetic data of Kotonkarfi_ (Sheet 227) was subjected to spectral analysis with the aim of accessing the geothermal potential of the study area. The Curie point depth values ranges from (12.04-18.5) km, the geothermal gradient values ranges from (31.35– 48.17)°C/km and the heat flow values ranges from(78.37- 120.42) mW/m² (Table..). The NE and SW edge covering areas like Abaji, Shedamu and Atsawa hosts the highest values of heat flow and geothermal gradientith corresponding shallowest values of Curie point depth (Fig...). Generally, for a viable geothermal reservoir, a heat flow range of 80 to 100 mW/m²is recommended, hence it can be inferred that every region on the study area could be considered as having good prospect for geothermal power generation except a small portion of Gegu area in East central portion.

Table 32 Summary of the results of the centroid depth, depth to basement, curie depth, geothermal gradient and the heat flow

Kotonkarfi _ (Sheet 227)

Blocks	X	Y	Centroid	Depth to basement	Curie depth	Geothermal Gradient	Heat Flow (mWm ⁻²)
A	6.625	8.375	9.06	2.91	15.21	38.13	95.32
B	6.875	8.375	7.43	2.82	12.04	48.17	120.42
C	6.625	8.125	6.87	1.17	12.57	46.14	115.35
D	6.875	8.125	10.49	2.54	18.44	31.45	78.62
E	6.75	8.375	10.77	3.04	18.5	31.35	78.37
F	6.75	8.125	7.45	1.55	13.35	43.44	108.6
G	6.625	8.25	7.73	1.2	14.26	40.67	101.67
H	6.875	8.25	10.86	2.12	19.6	29.59	73.98

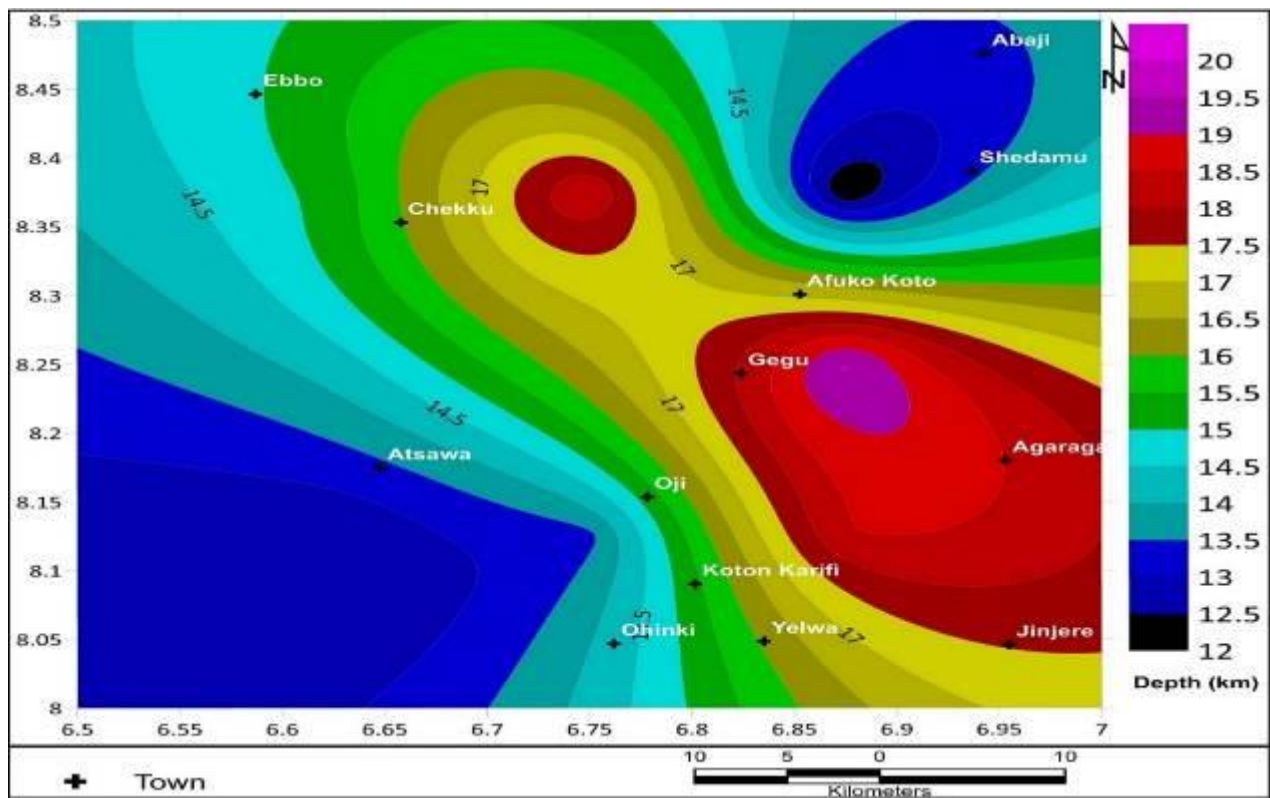


Fig 5.4a. CPD contour map of Sheet 227 corresponding to Kotonkarfi

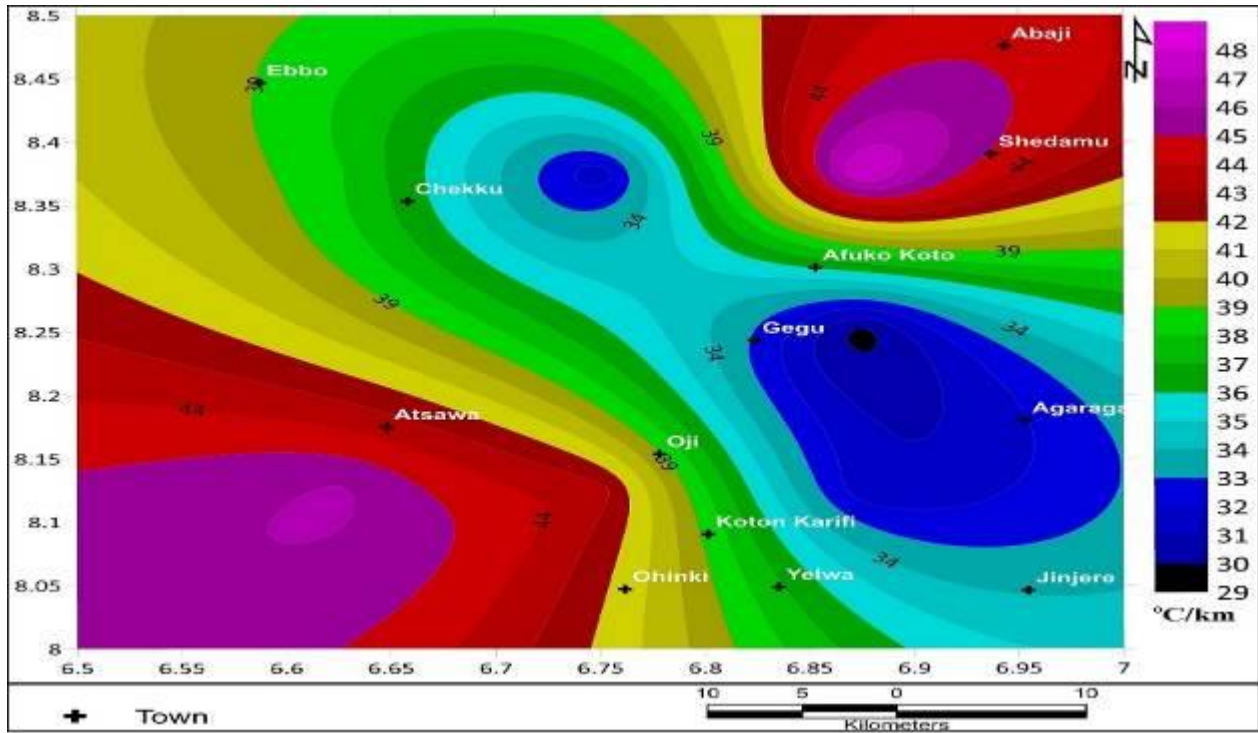


Fig. 5.4b Geothermal Gradient contour map of Sheet 227 corresponding to Kotonkarfi

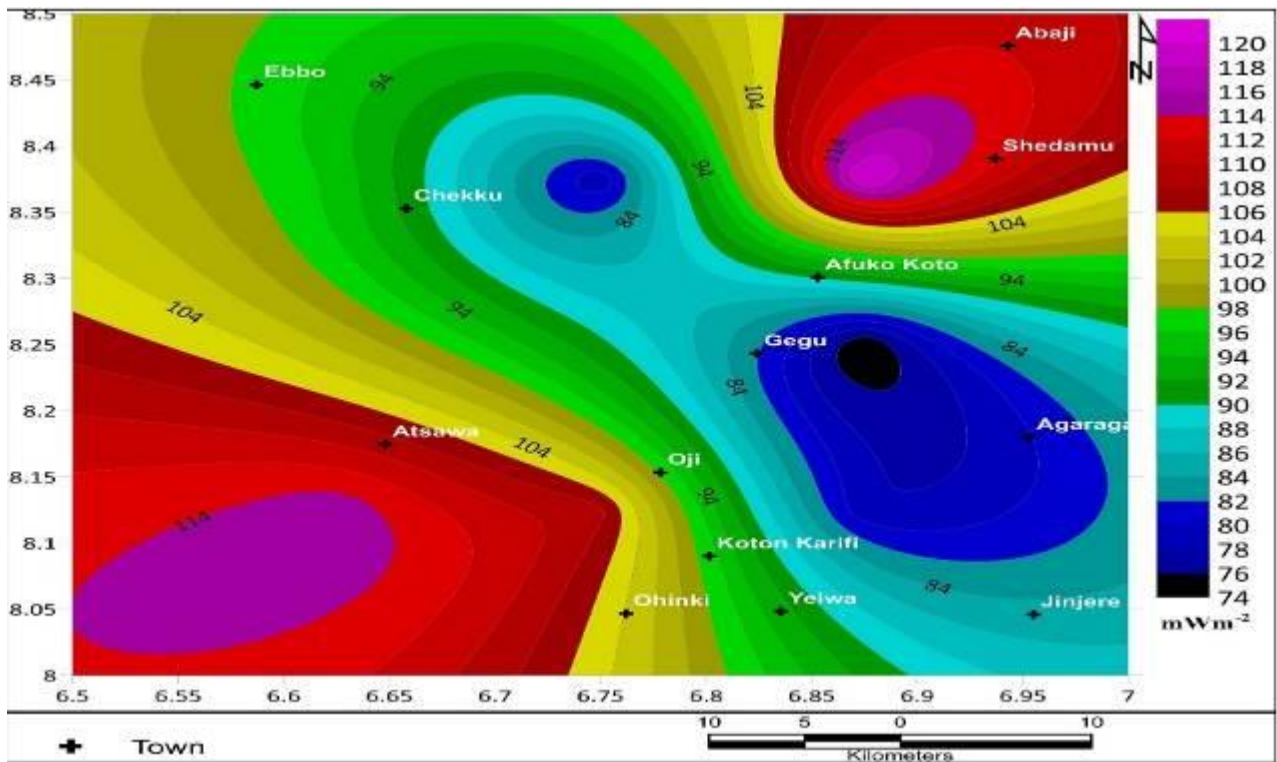


Fig. 5.4c Heat flow contour map of Sheet 227 corresponding to Kotonkarfi

5.7 Geothermal Potential of Akiri_ (Sheet 232)

The aeromagnetic data of Akiri_ (Sheet 232) was subjected to spectral analysis with the aim of accessing the geothermal potential of the study area and environs. The Curie point depth values ranges from (7.44- 20.81) km, the geothermal gradient values ranges from (27.87– 77.95) °C/km and the heat flow values ranges from (69.68- 194.87) mW/m² (Table33). The NE edge covering Jangwa, Azara, Akiri, and Ribbi hosts the anomalous heat flow and geothermal gradient with corresponding shallowest values of curie point depth (Fig 5.5 a-c). Other regions like Kumar, Jutu, Kanje, Adawa, Atakoro, and Kaza also show good geothermal manifestations, except few areas in SW covering Tunga with low heat flow below the recommended threshold value of (80 - 100)mW/m².

Table 33 Summary of the results of the centroid depth, depth to basement, curie depth, geothermal gradient and the heat flow

Akiri_ (Sheet 232)							
Blocks	X	Y	Centroid	Depth to basement	Curie depth	Geothermal Gradient	Heat Flow (mWm ⁻²)
A	9.125	8.375	8.1	2.4	13.8	42.02	105.05
B	9.207	8.375	4.47	1.5	7.44	77.95	194.87
C	9.29	8.37	4.65	1.34	7.96	72.86	182.15
D	9.124	8.38	4.98	1.49	8.47	68.47	171.17
E	9.125	8.125	11.4	2.56	20.81	27.87	69.68
F	9.207	8.125	8.24	1.52	14.96	38.77	96.92
G	9.207	8.125	9.12	2.54	15.7	36.94	92.35
H	9.38	8.125	11.2	2.7	19.7	29.44	73.6

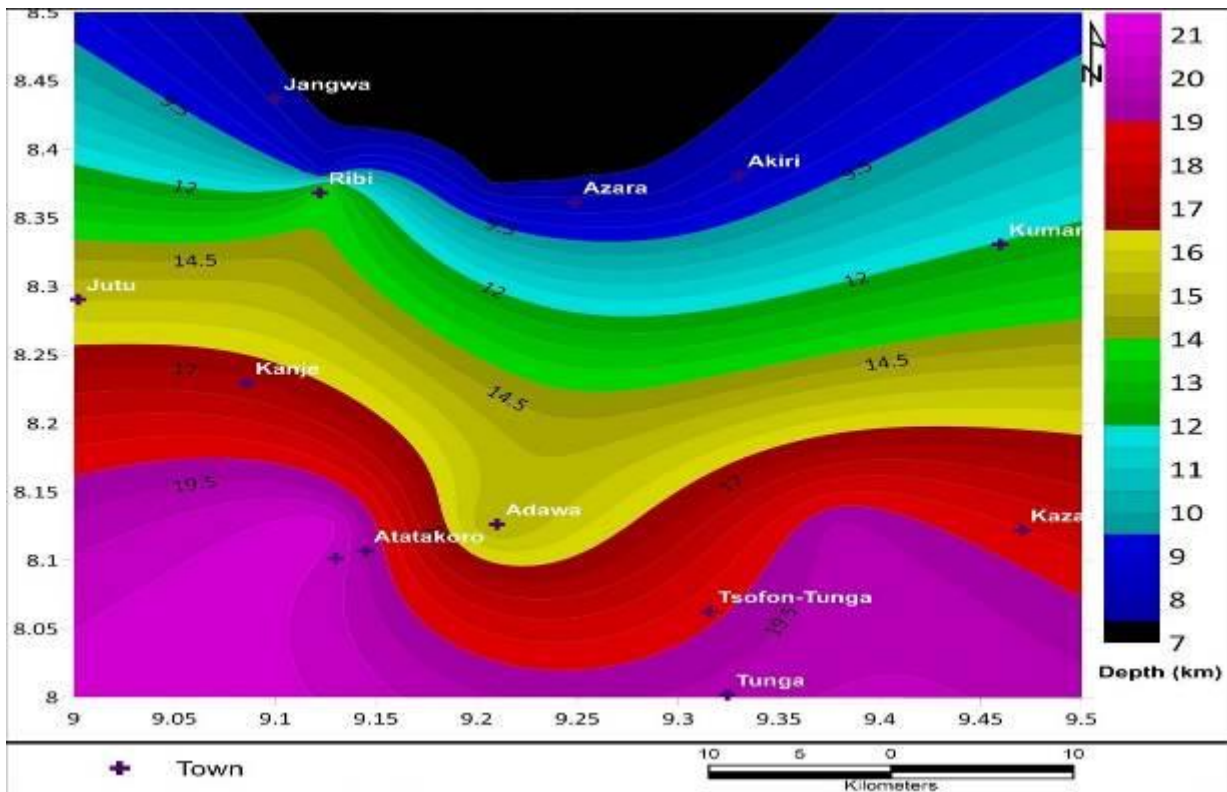


Fig. 5.5a CPD contour map of Sheet 232 corresponding to Akiri

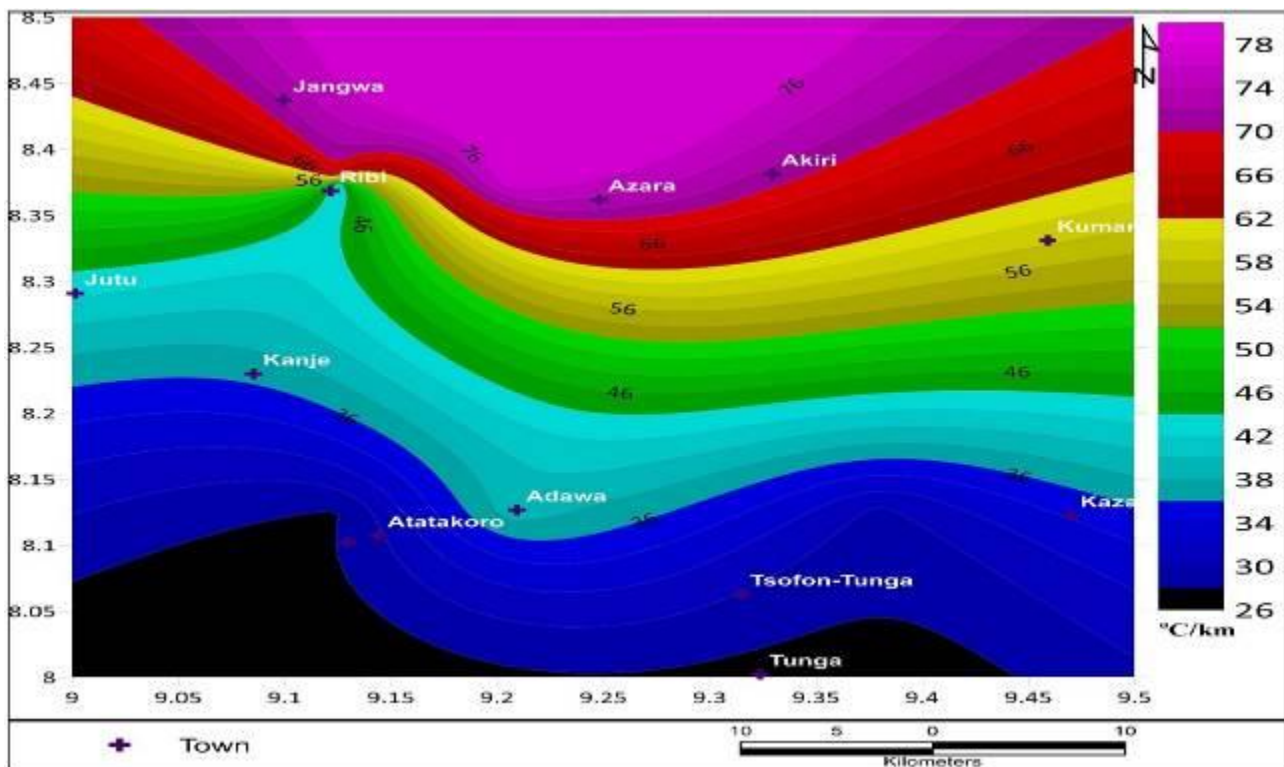


Fig. 5.5b Geothermal Gradient contour map of Sheet 232 corresponding to Akiri

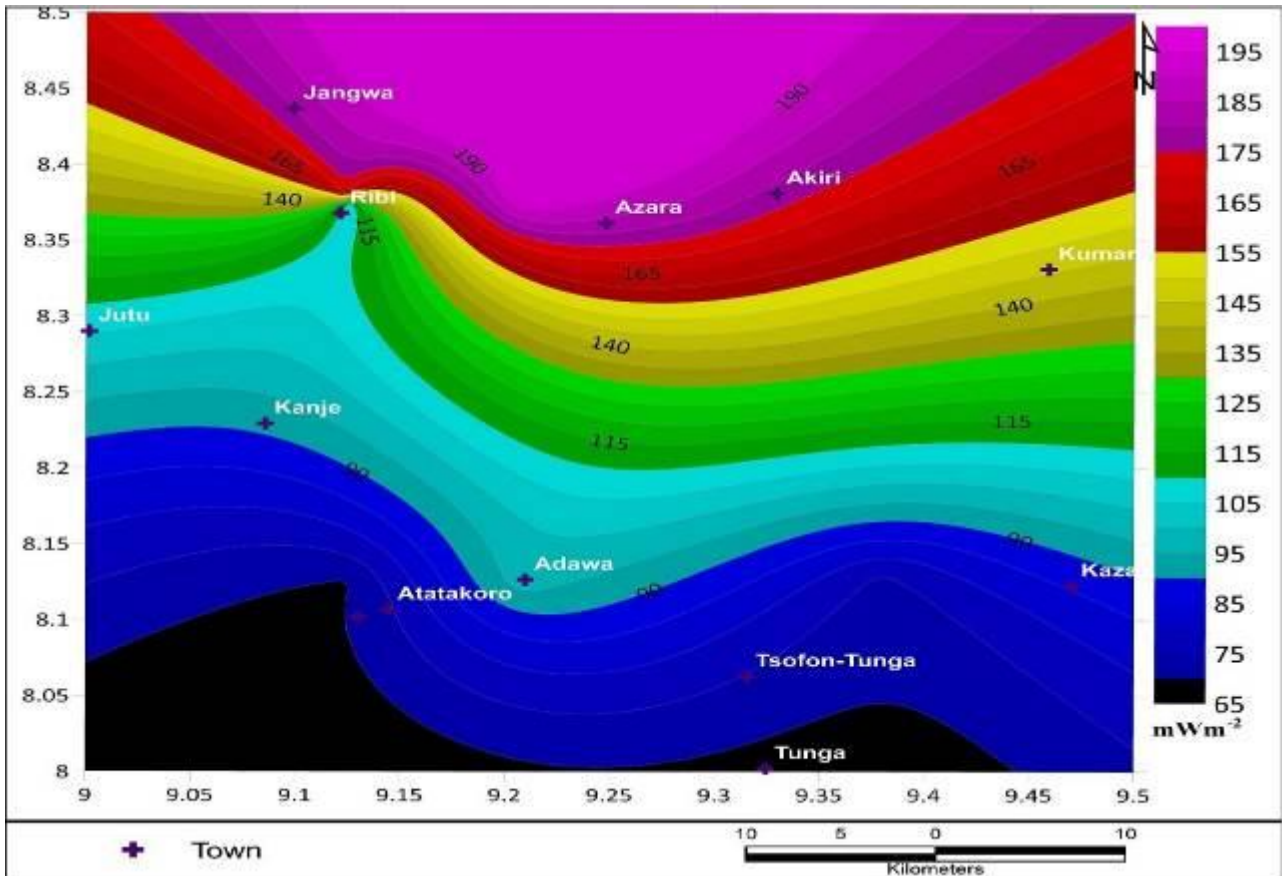


Fig. 5.5c Heat flow contour map of Sheet 232 corresponding to Akiri

5.8 Geothermal Potential of Ado-Ekiti (Sheet 244)

The aeromagnetic data of **Ado-Ekiti (Sheet 244)** was subjected to spectral analysis with the aim of accessing the geothermal potential of the study area and environs. The Curie point depth values ranges from (7.01- 15.14) km, the geothermal gradient values ranges from (38.3– 82.73) °C/km and the heat flow values ranges from (95.75- 206.82) mW/m² (Table 34). The NW edge covering Ofale, Iye, Ifere, Iddo-Ekiti, Ijero-Ekiti, Aramoko, and Ikogosi hosts the highest anomalous values of heat flow and geothermal gradient with corresponding shallowest values of Curie point depth (Fig. 5.6 a-c). Generally, for a viable geothermal reservoir, a heat flow range of 80 to 100 mW/m² is recommended, hence it can be inferred that every region on the study area could be considered as having good prospect of the study area with high heat flow above 80 – 100 mWm⁻².

Table 34 Summary of the results of the centroid depth, depth to basement, curie depth, geothermal gradient and the heat flow

Ado (Sheet 244)

Blocks	X	Y	Centroid	Depth to basement	Curie depth	Geothermal Gradient	Heat Flow (mWm ⁻²)
A	5.125	7.875	4.59	1.5	7.68	75.52	188.8
B	5.207	7.875	4	0.99	7.01	82.73	206.82
C	5.291	7.875	4.71	1.03	8.39	69.06	172.65
D	5.375	7.875	5.6	0.89	10.31	56.25	140.62
E	5.125	7.625	4.15	0.92	7.38	78.59	196.47
F	5.205	7.625	6.48	1.38	11.58	50.08	125.2
G	5.291	7.625	8.03	1.68	14.38	40.33	100.82
H	5.425	7.625	8.15	1.16	15.14	38.3	95.75

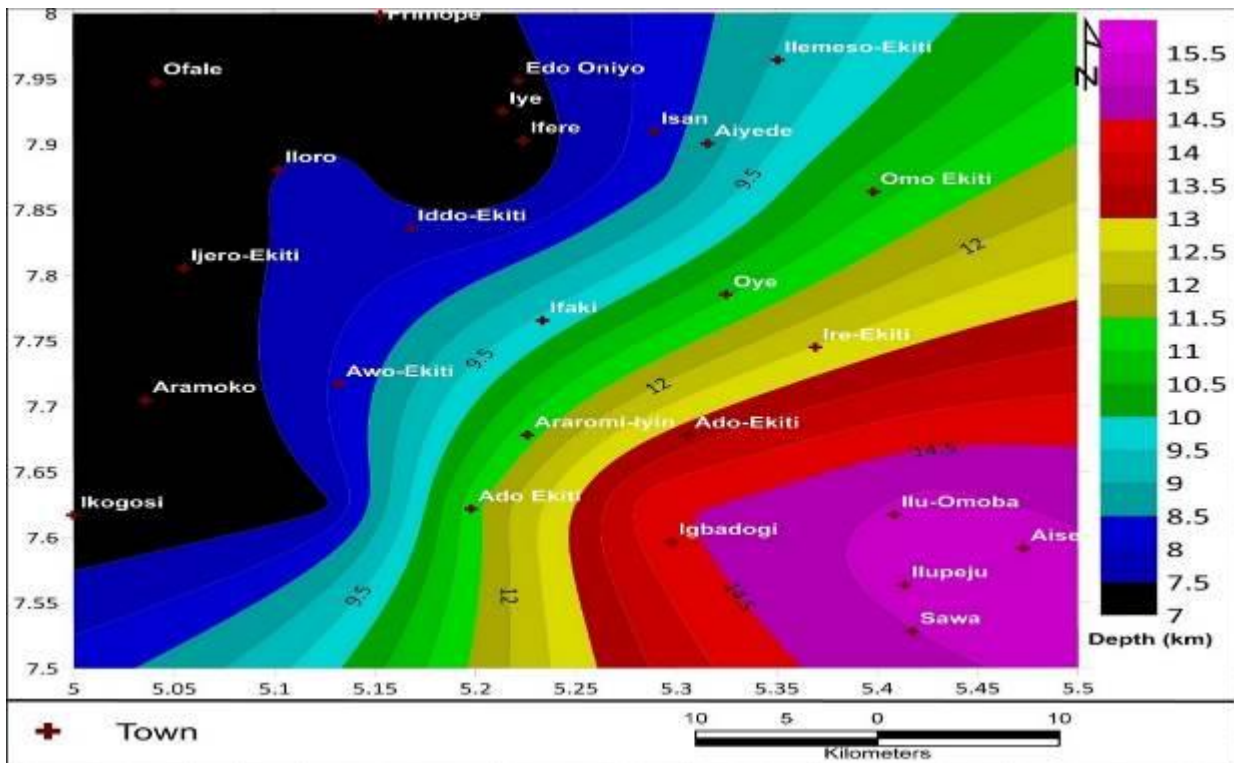


Fig.5.6a CPD contour map of Sheet 244 corresponding to Ado-Ekiti

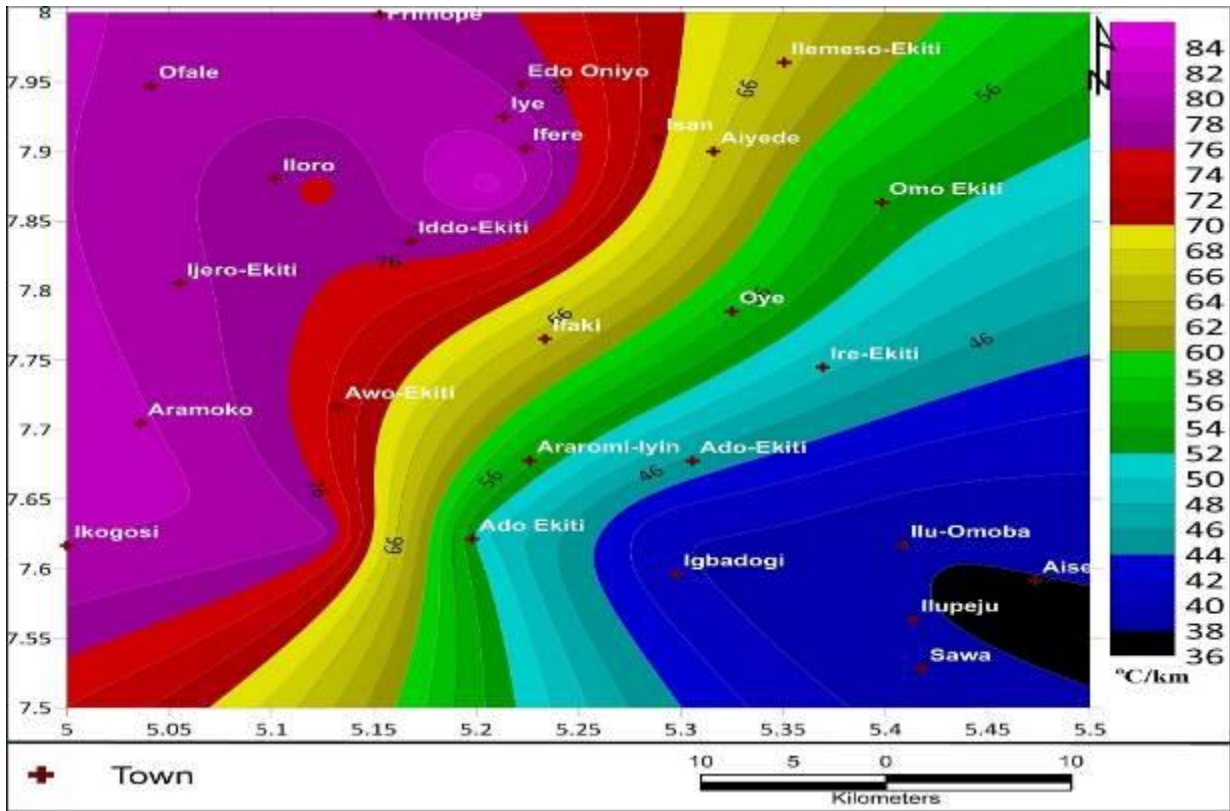


Fig. 5.6b Geothermal gradient contour map of Sheet 244 corresponding to Ado-Ekiti

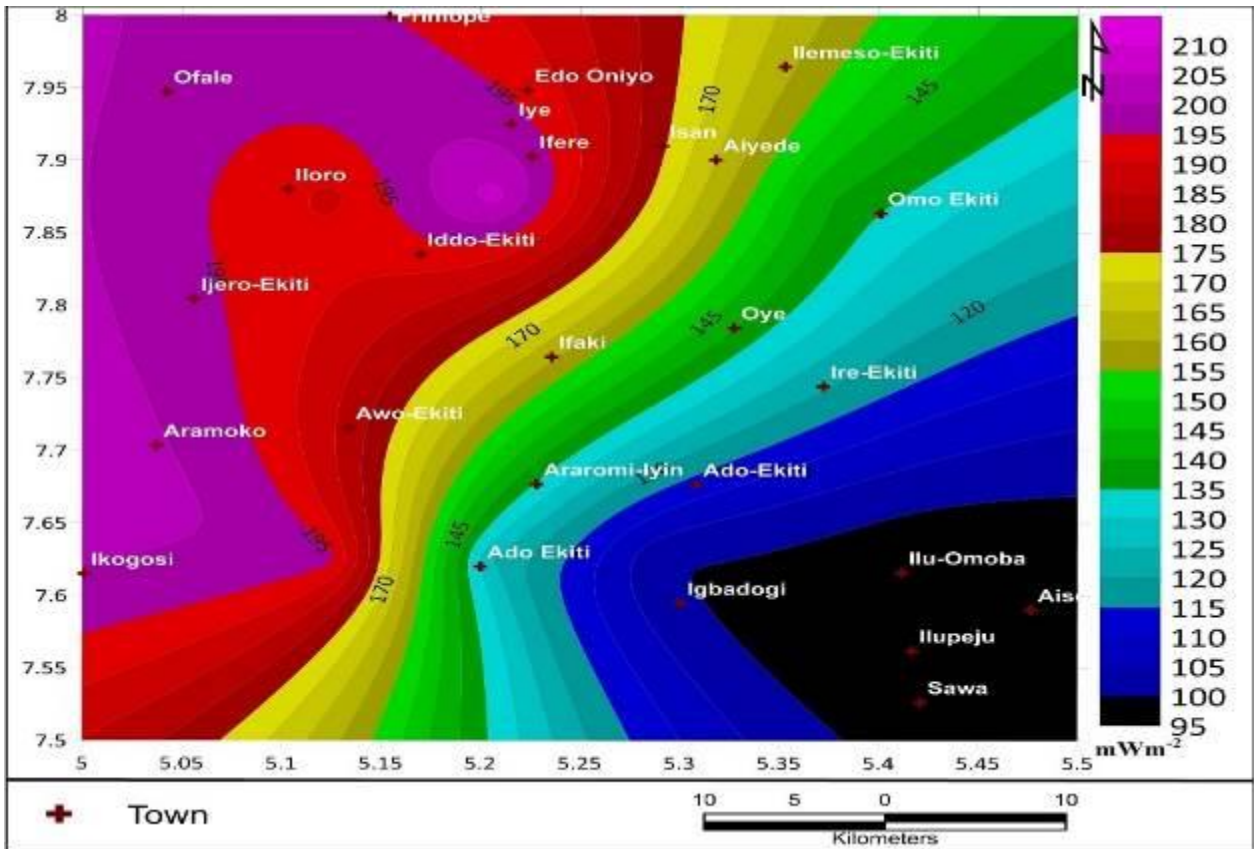


Fig 5.6c. Heat flow contour map of Sheet 244 corresponding to Ado- Ekiti

5.9 Geothermal Potential of Lokoja _ (Sheet 247)

The aeromagnetic data of **Lokoja _ (Sheet 247)** was subjected to spectral analysis with the aim of accessing the geothermal potential of the study area and environs. The Curie point depth values ranges from (10.4- 18.03) km, the geothermal gradient values ranges from (32.16– 76.21) °C/km and the heat flow values ranges from (80.4- 190.52) mW/m² (Table35). The SE edge hosts the highest values of heat flow and geothermal gradient with corresponding shallowest values of Curie point depth (Fig. 5.7 a-c). Generally, for a viable geothermal reservoir, a heat flow range of 80 to 100 mW/m² is recommended, hence it can be inferred that every other region on the study area could be considered as having good prospect in the study area with high heat flow above 80 – 100 mWm⁻².

Table 35 Summary of the results of the centroid depth, depth to basement, curie depth, geothermal gradient and the heat flow

Lokoja (Sheet 247)							
Blocks	X	Y	Centroid	Depth to basement	Curie depth	Geothermal gradient	Heat Flow (mWm ⁻²)
C1	6.625	7.875	6.43	1.75	11.11	52.2	130.5
C2	6.708	7.875	9.63	1.23	18.03	32.16	80.4
C3	6.791	7.875	6.1	1.75	10.45	55.5	138.75
C4	6.875	7.875	8.4	1.65	15.15	38.28	95.7
C5	6.625	7.625	5.58	0.48	10.68	54.3	135.75
C6	6.708	7.625	5.9	1.4	10.4	55.76	139.4
C7	6.791	7.625	4.16	0.71	7.61	76.21	190.52
C8	6.875	7.625	4.67	0.96	8.38	69.21	173.02

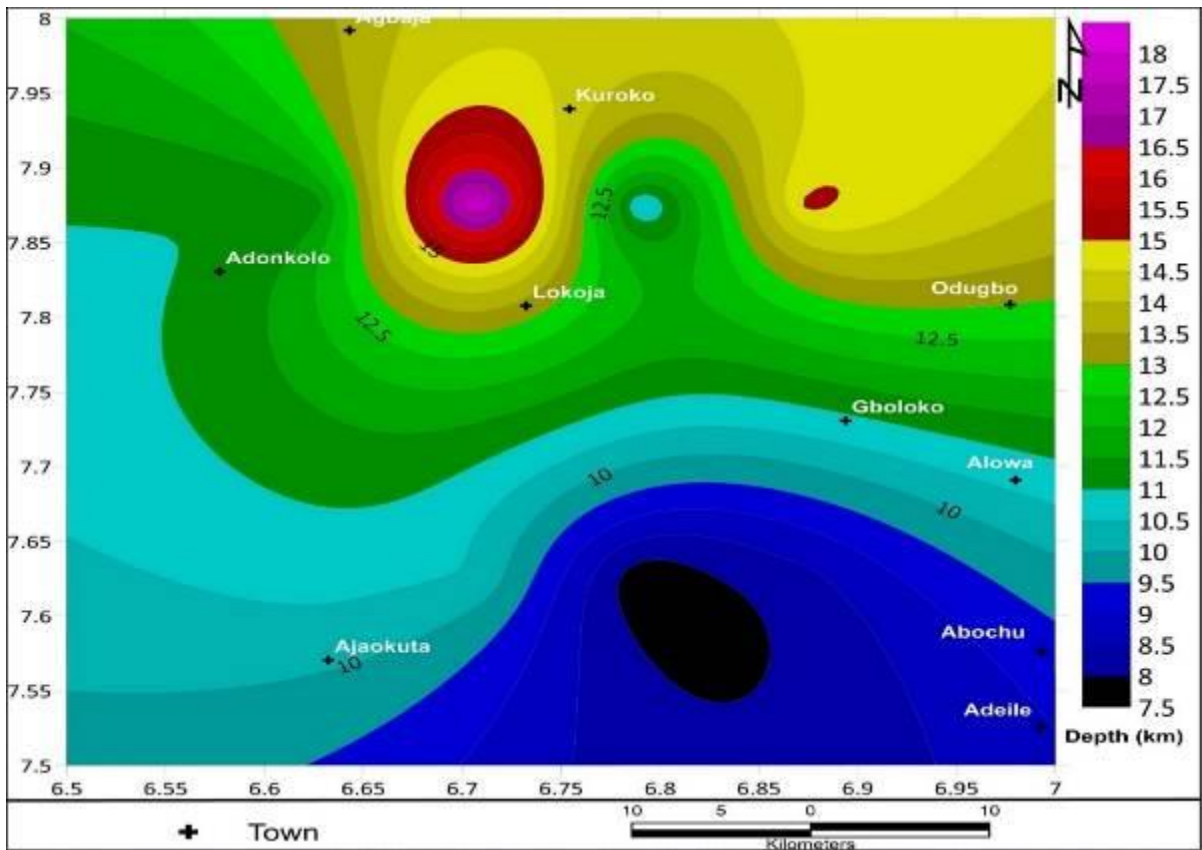


Fig.5.7a CPD contour map of Sheet 247 corresponding to Lokoja

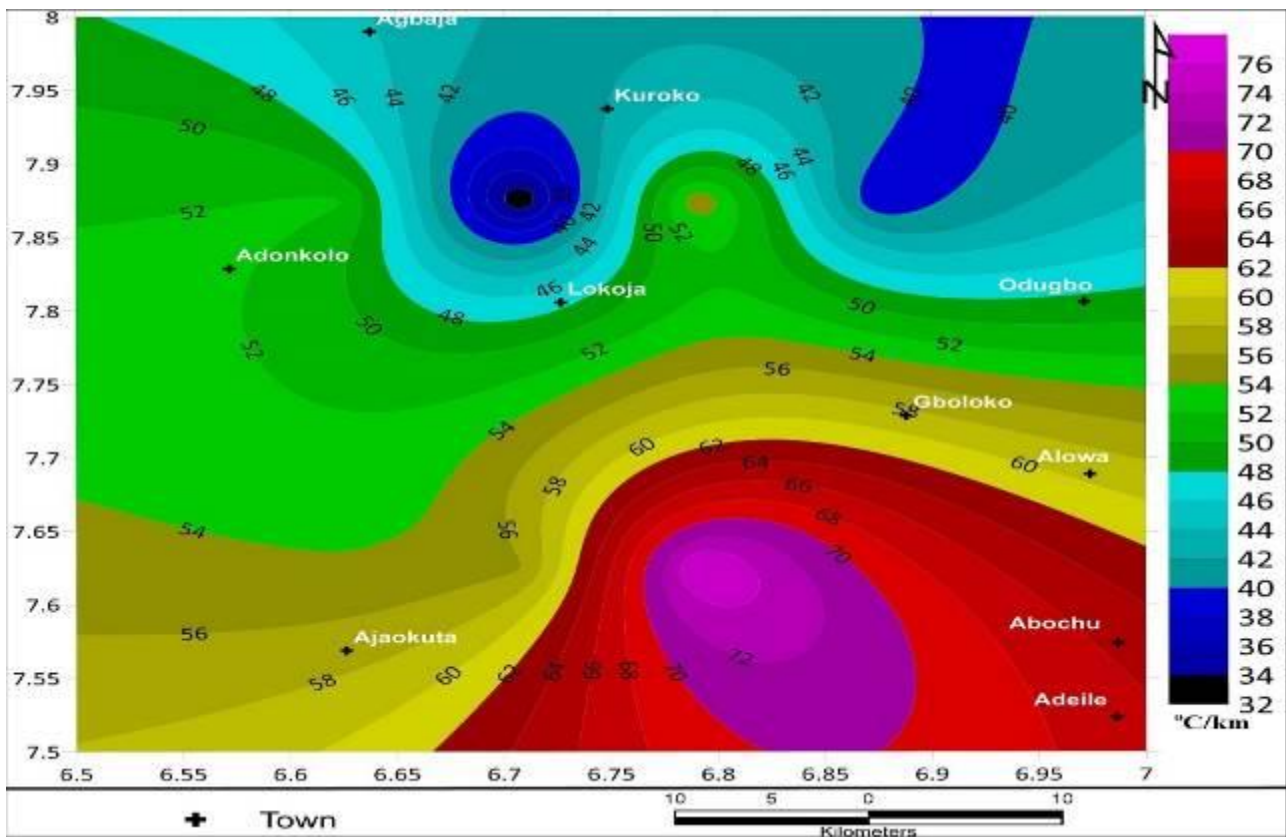


Fig. 5.7b Geothermal Gradient contour map of Sheet 247 corresponding to Lokoja

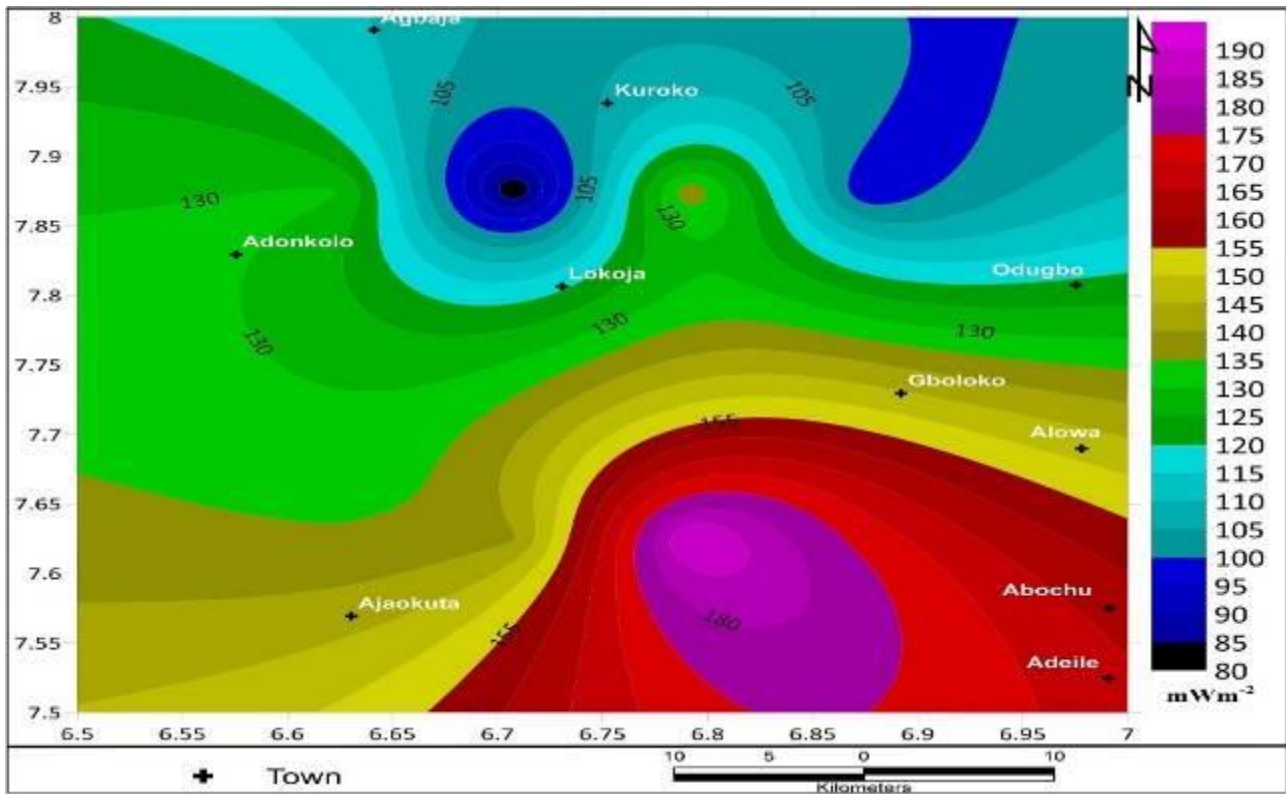


Fig. 5.7c Heat flow map contour map of Sheet 247 corresponding to Lokoja

5.10 Geothermal Potential of Auchi _ (Sheet 266)

The aeromagnetic data of **Auchi _ (Sheet 266)** was subjected to spectral analysis with the aim of accessing the geothermal potential of the study area and environs. The Curie point depth values ranges from (10.8- 17.93) km, the geothermal gradient values ranges from (32.35– 56.2) °C/km and the heat flow values ranges from (80.88- 140.5) mW/m² (Table 36). The SE region corresponding to Auchi, Avbiele, Iyerekwo and Azukala edge hosts the highest values of heat flow and geothermal gradient with corresponding shallowest values of curie point depth (Fig.5.8 a-c). Generally, for a viable geothermal reservoir, a heat flow range of 80 to 100 mW/m² is recommended, hence it can be inferred that every region on the study area could be considered as having good prospect within the regions of the study area with high heat flow above 80 – 100 mWm⁻².

Table 36 Summary of the results of the centroid depth, depth to basement, curie depth, geothermal gradient and the heat flow

Auchi (Sheet 266)

Blocks	X	Y	Centroid	Depth to basement	Curie depth	Geothermal gradient	Heat Flow (mWm ⁻²)
A	6.125	7.375	8.45	1.77	15.13	38.33	95.82
B	6.207	7.375	9.33	2.86	15.8	36.71	91.78
C	6.291	7.375	6.4	1.69	11.11	52.2	130.5
D	6.375	7.375	9.35	2.68	16.02	36.2	90.5
E	6.125	7.125	8.7	1.37	16.03	36.18	90.45
F	6.208	7.125	9.95	1.97	17.93	32.35	80.88
G	6.291	7.125	6.03	1.74	10.32	56.2	140.5
H	6.375	7.125	6.56	2.32	10.8	53.7	134.25

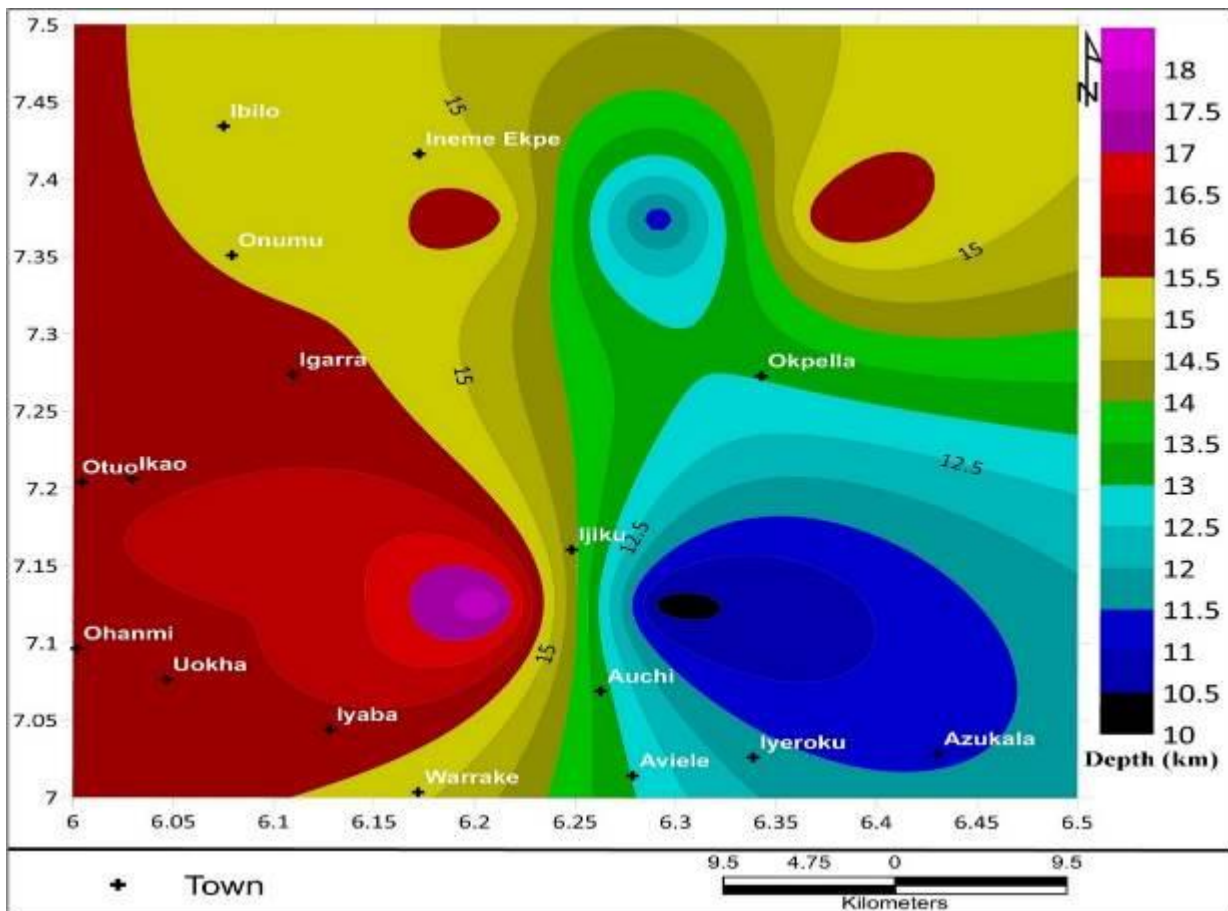


Fig 5.8a. CPD contour map of Sheet 266 corresponding to Auchi

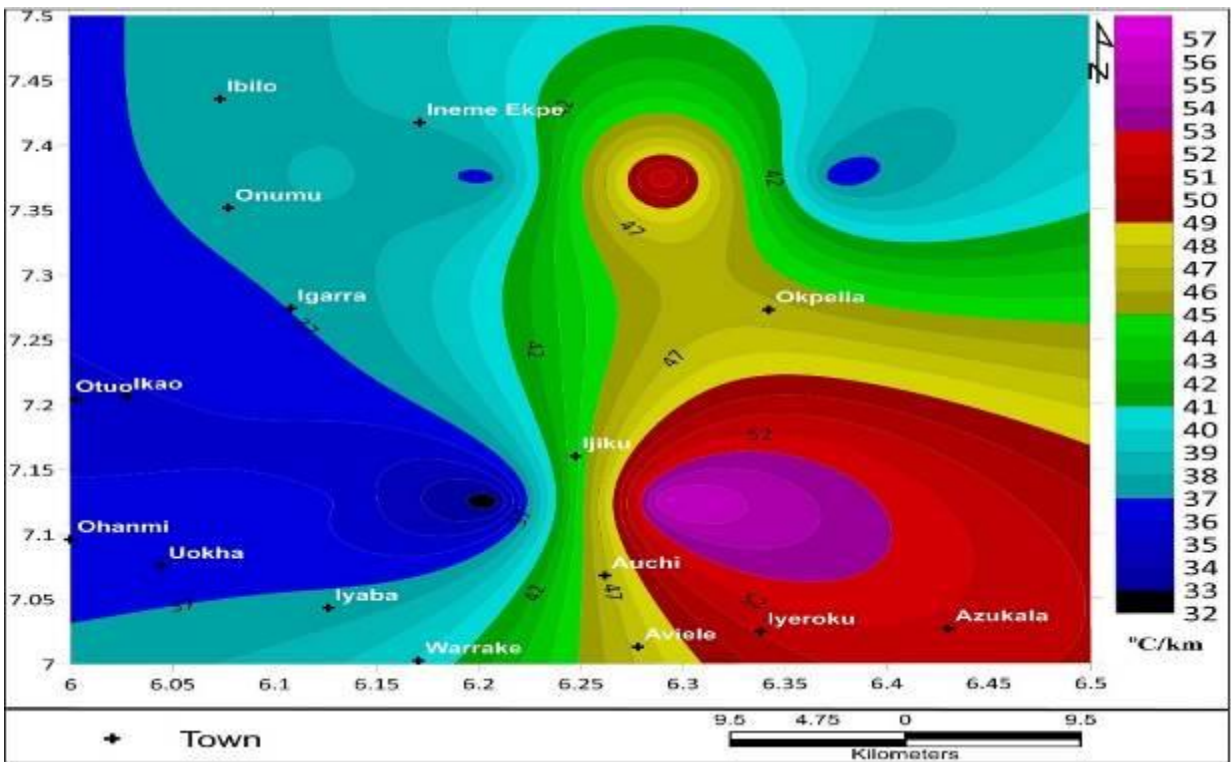


Fig.5.8b Geothermal Gradient contour map of Sheet 266 corresponding to Auchi

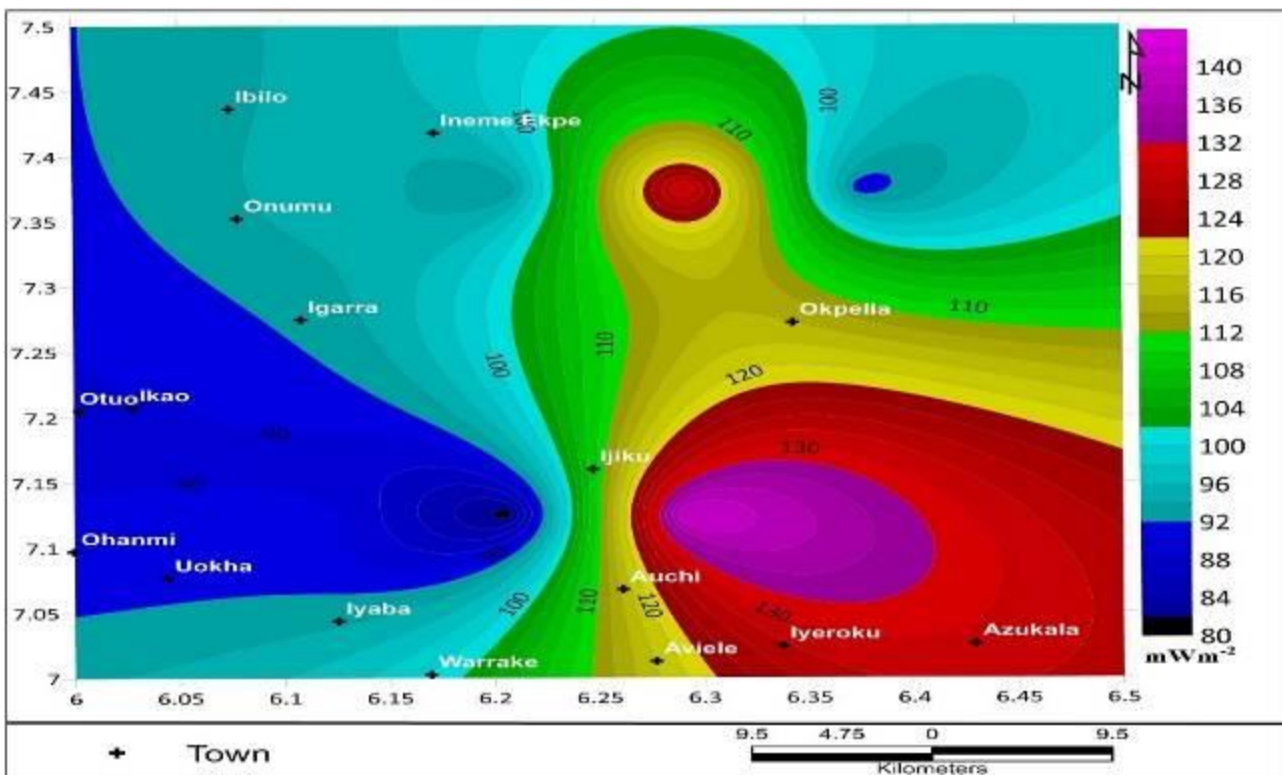


Fig.5.8c Heat flow contour map of Sheet 266 corresponding to Auchi

5.11 Geothermal Potential of Nsukka _ (Sheet 287)

The aeromagnetic data of **Nsukka_ Sheet 287** was subjected to spectral analysis with the aim of accessing the geothermal potential of the study area and environs. The Curie point depth values ranges from (15.0- 21.37) km, the geothermal gradient values ranges from (27.14– 39.78) °C/km and the heat flow values ranges from (67.85- 99.45) mW/m² (Table 37). The North central region covering Abbi, Okpuje, Obimo and Nimbo hosts the highest values of heat flow and geothermal gradient with corresponding shallowest values of Curie point depth (Fig. 5.9 a-c). Generally, for a viable geothermal reservoir, a heat flow range of 80 to 100 mW/m² is recommended, hence it can be inferred that every region on the study area could be considered as having good prospect except in SW and SE regions of the study area corresponding to Ogbode, Umudin, Umuluopa and Adani with heat flow below 80 – 100 mWm⁻².

Table 37 Summary of the results of the centroid depth, depth to basement, curie depth, geothermal gradient and the heat flow

Nsukka (Sheet 287)

Blocks	X	Y	Centroid	Depth to basement	Curie depth	Geothermal gradient	Heat Flow (mWm ⁻²)
A	7.125	6.875	9.47	3.94	15	38.66	96.65
B	7.208	6.725	8.7	2.82	14.58	39.78	99.45
C	7.291	6.725	9.33	2.66	16	36.25	90.63
D	7.375	6.725	11.36	3.47	19.25	30.13	75.33
E	7.125	6.725	12	2.63	21.37	27.14	67.85
F	7.208	6.725	8.16	1.35	14.97	38.74	96.85
G	7.291	6.725	9.94	2.98	16.9	34.32	85.8
H	7.375	6.725	8.69	2.03	15.35	37.78	94.45

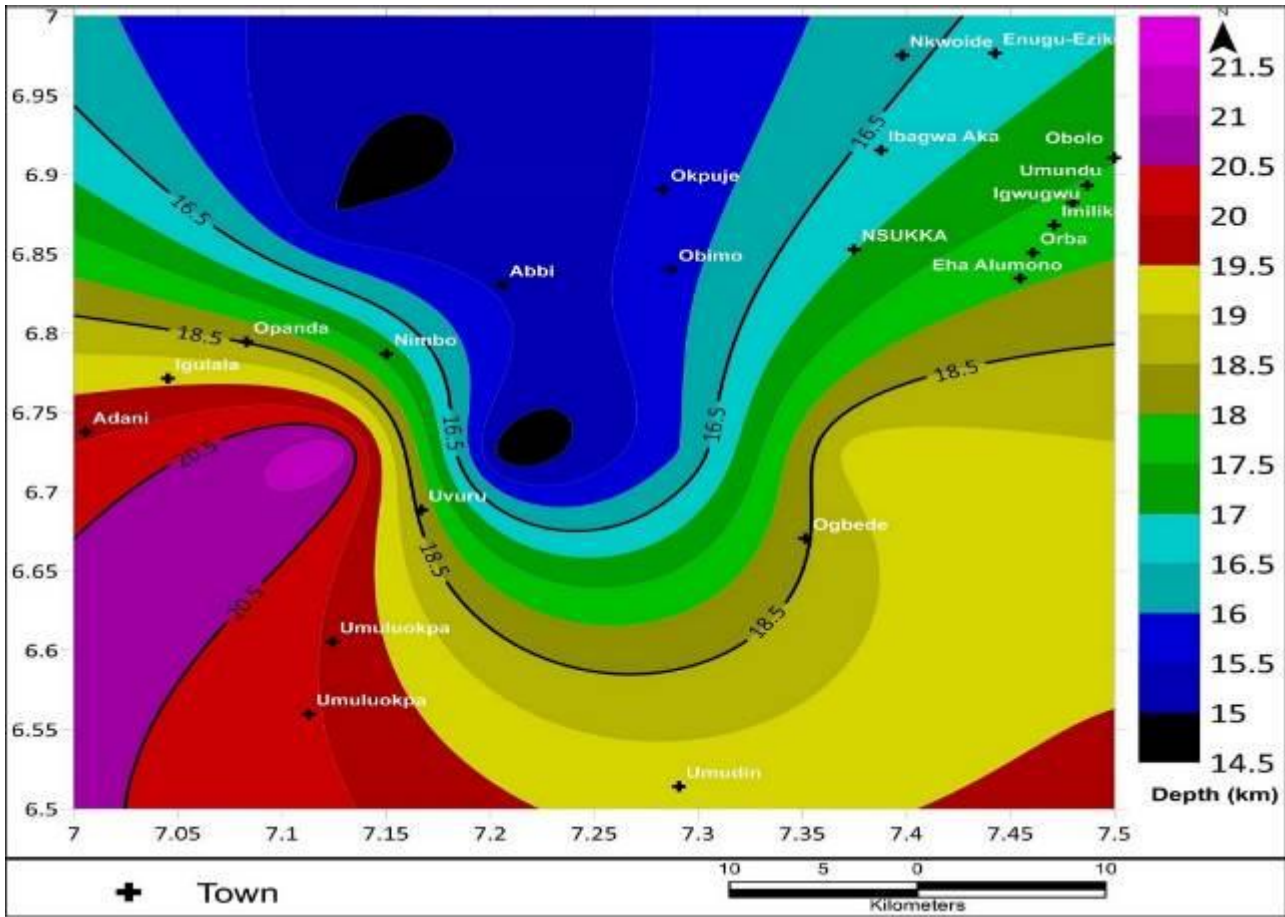


Fig. 5.9a CPD contour map of Sheet 287 corresponding to Nsukka

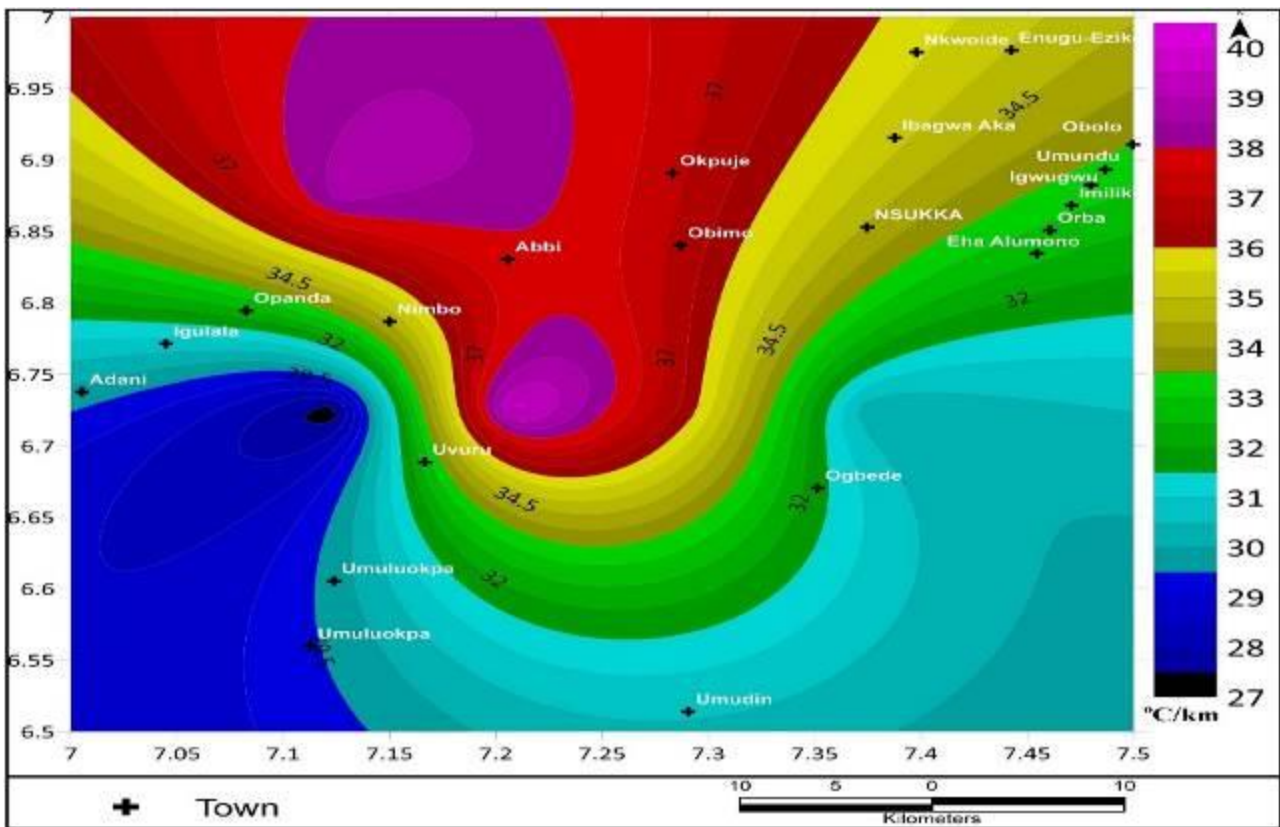


Fig.5.9b Geothermal Gradient contour map of Sheet 287 corresponding to Nsukka

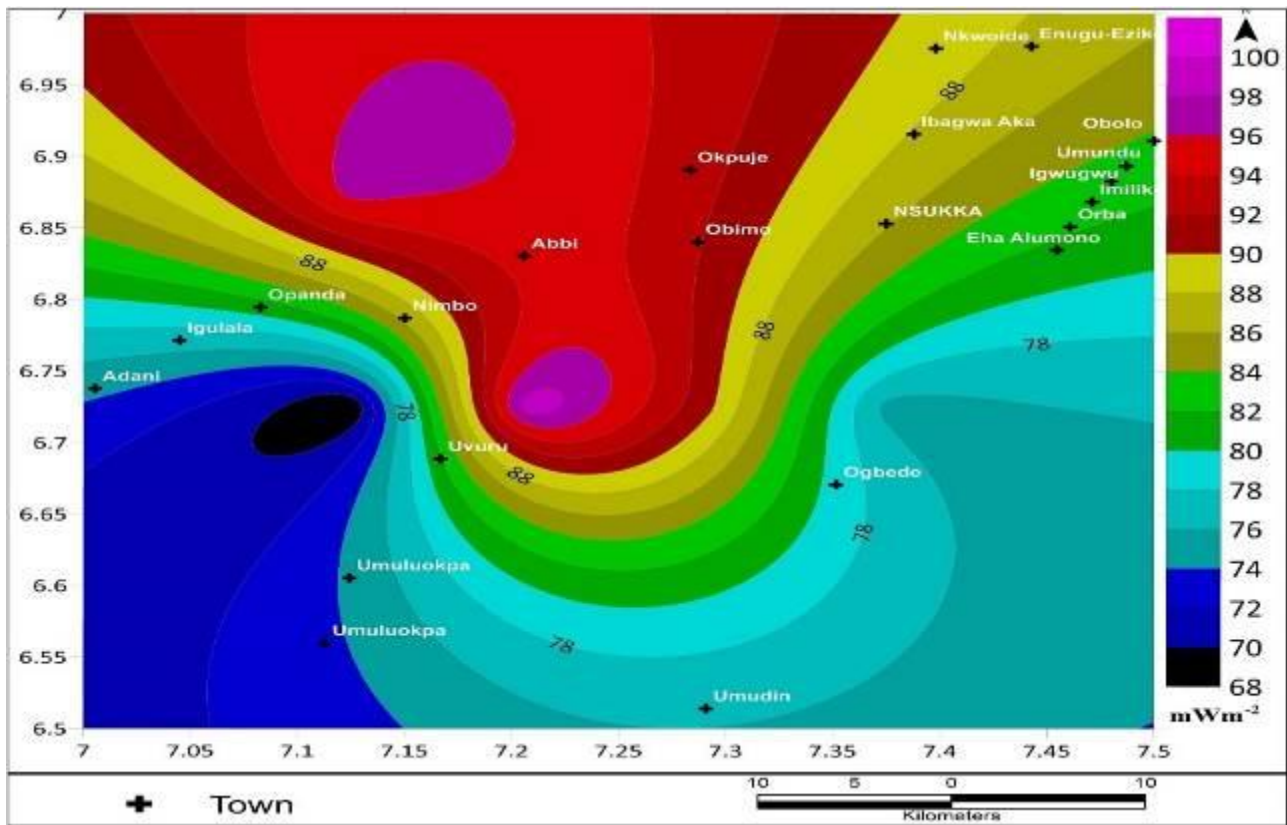


Fig.5.9c Heat flow contour map of Sheet 287 corresponding to Nsukka

5.12 Geothermal Potential of Onitsha_ (Sheet 300)

The aeromagnetic data of **Onitsha_ (Sheet 300)** was subjected to spectral analysis with the aim of accessing the geothermal potential of the study area and environs. The Curie point depth values ranges from (13.1- 20.58) km, the geothermal gradient values ranges from (28.18– 40.36) °C/km and the heat flow values ranges from (70.45- 110.68) mW/m² (Table 38). The SW edge corresponding to Ishiagu, Ogwashi Olor and Ogwasi Ukwu hosts the highest values of heat flow and geothermal gradient with corresponding shallowest values of Curie point depth (Fig.6.1a-c). Generally, for a viable geothermal reservoir, a heat flow range of 80 to 100 mW/m² is recommended, hence it can be inferred that every region on the study area could be considered as having good prospect except with the North central regions of the study area, Illah with heat flow below 80 – 100 mWm⁻².

Table 38 Summary of the results of the centroid depth, depth to basement, curie depth, geothermal gradient and the heat flow

Onitsha (Sheet 300)

Block s	X	Y	Centroi d (Z_0)	Depth to basement (Z_t)	Curie depth CPD (km)	Geothermal Gradient (C/km)	Heat Flow (mWm^{-2})
A	6.62 5	6.37 5	10.24	2.47	18.01	32.2	80.5
B	6.70 8	6.37 5	12.12	3.66	20.58	28.18	70.45
C	6.79 1	6.37 5	8.59	2.73	14.45	40.13	100.33
D	6.78 5	6.12 5	9.97	2.97	16.97	34.17	85.42
E	6.62 5	6.12 5	8.4	3.7	13.1	44.27	110.68
F	6.70 8	6.12 5	9.63	2.83	16.43	35.3	88.25
G	6.79 1	6.12 5	8.46	2.45	14.37	40.36	100.9
H	6.87 5	6.12 5	9.61	2.79	16.43	35.3	88.25

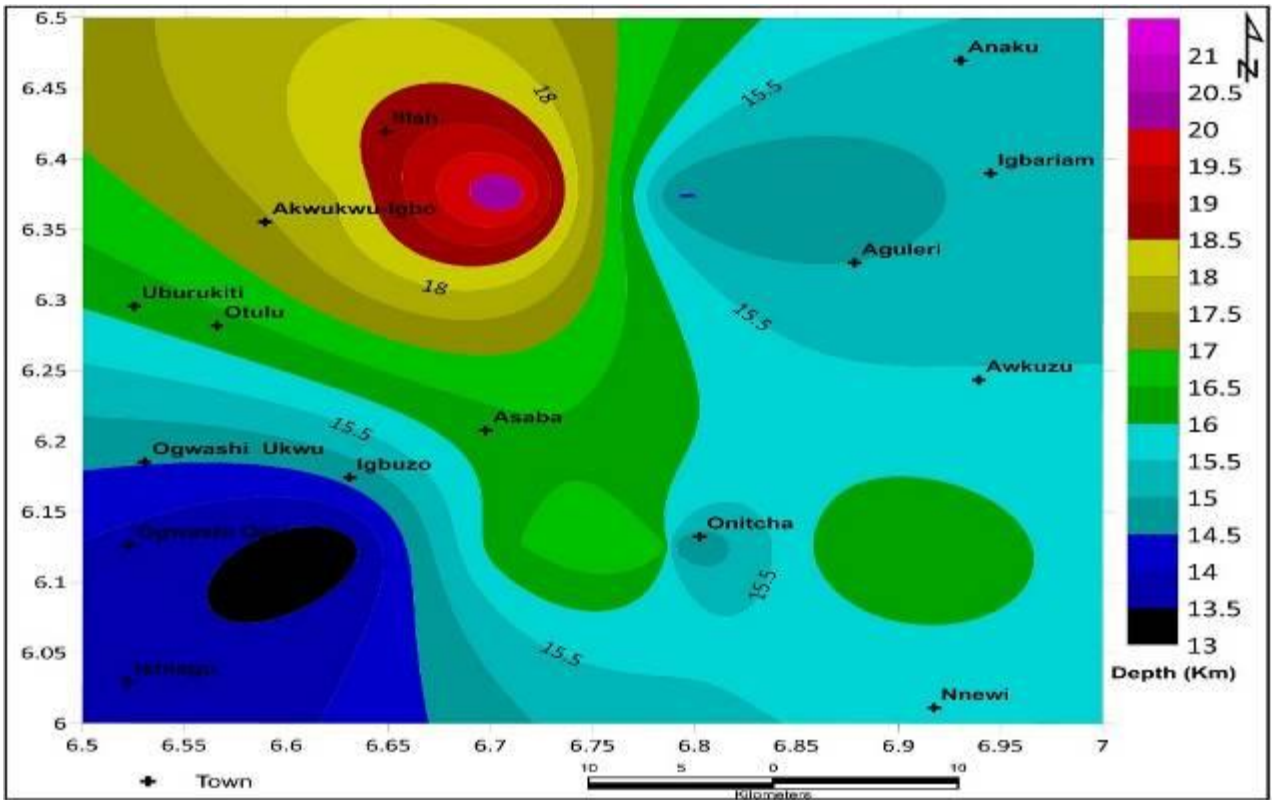


Fig. 6.1a CPD contour map of Sheet 300 corresponding to Onitsha

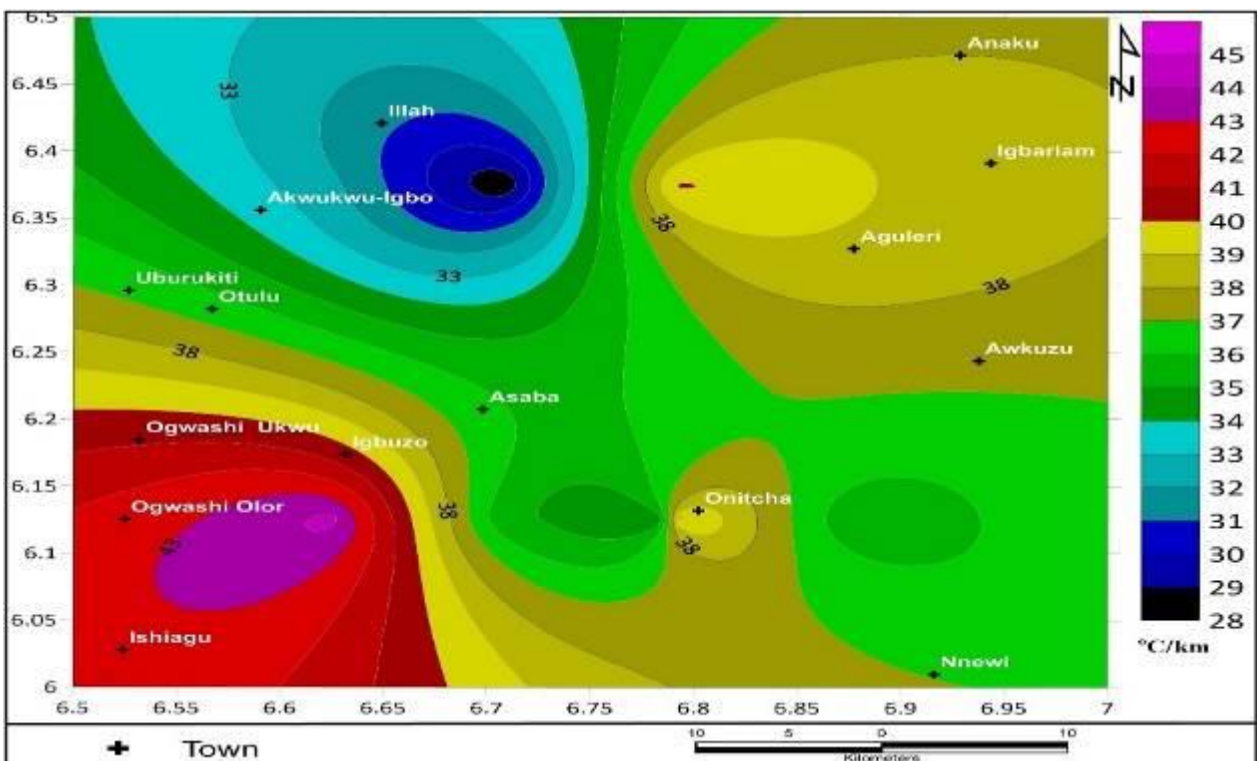


Fig.6.1b Geothermal Gradient contour map of Sheet 300 corresponding to Onitsha

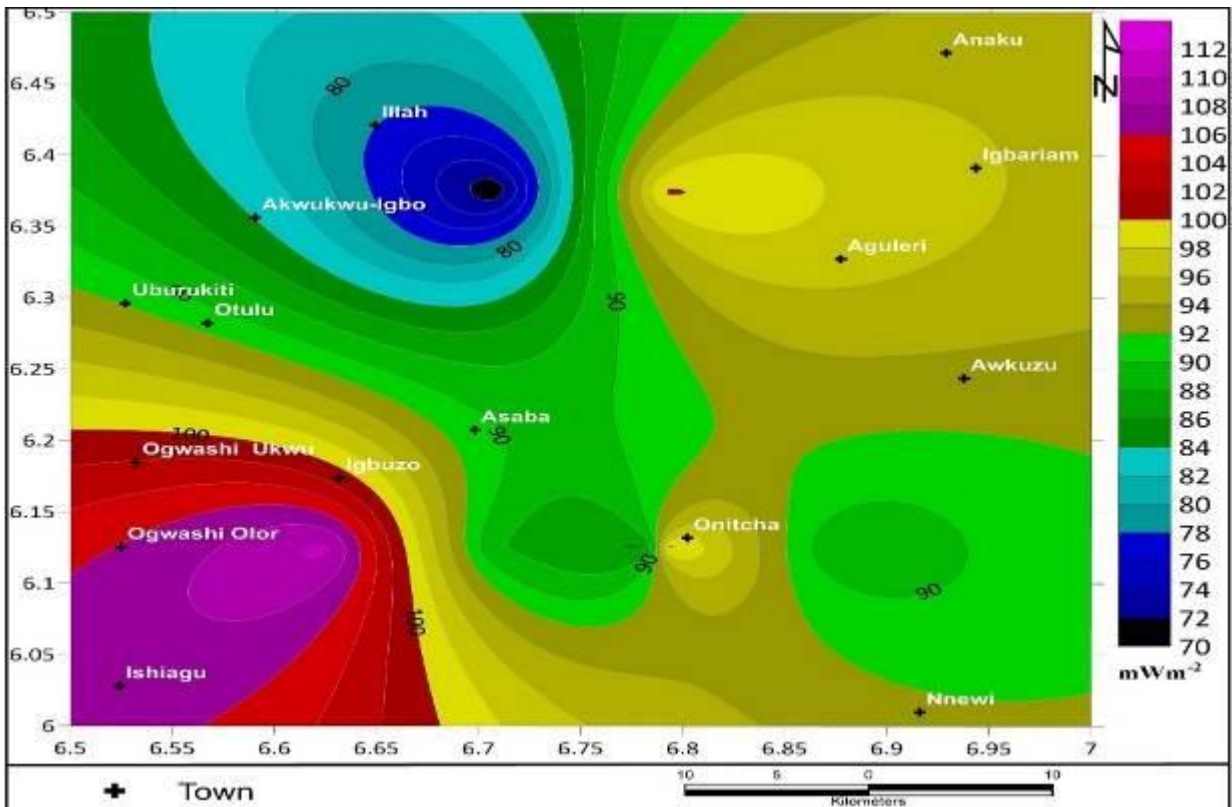


Fig.6.1c Heat flow contour map of Sheet 300 corresponding to Onitsha

5.13 Geothermal potential of Okigwe_Sheet312

The aeromagnetic data of **Okigwe_ (Sheet 312)** was subjected to spectral analysis with the aim of accessing the geothermal potential of the study area and environs. The Curie point depth values ranges from (15.14- 23.81) km, the geothermal gradient values ranges from (24.35– 38.3) °C/km and the heat flow values ranges from (70.45- 95.75) mW/m² (Table 39). The NE edge hosts the highest values of anomalous heat flow and geothermal gradient with corresponding shallowest values of Curie point depth (Fig. 6.2a-c). Generally, for a viable geothermal reservoir, a heat flow range of 80 to 100 mW/m² is recommended, hence it can be inferred that every region on the study area could be considered as having good prospect except the central portion of the South corresponding to Umu opara of the study area with low heat flow below 80 – 100 mWm⁻².

Table 39 Summary of the results of the centroid depth, depth to basement, curie depth, geothermal gradient and the heat flow

Okigwe (Sheet 312)

Blocks	X	Y	Centroid	Depth to basement	Curie depth	Geothermal gradient	Heat Flow (mWm ⁻²)
A	7.125	5.875	10.12	3.36	16.88	34.36	85.9
B	7.375	5.875	9.36	3.58	15.14	38.3	95.75
C	7.125	5.625	10.92	5.41	16.43	35.3	88.25
D	7.375	5.625	11.56	4.49	18.63	31.13	77.82
E	7.25	5.875	11.24	4.46	18.02	32.18	80.45
F	7.25	5.625	13.8	3.79	23.81	24.35	60.87
G	7.125	5.75	12.4	4.22	20.58	28.18	70.45
H	7.375	5.75	12.36	5.1	19.62	29.56	73.9

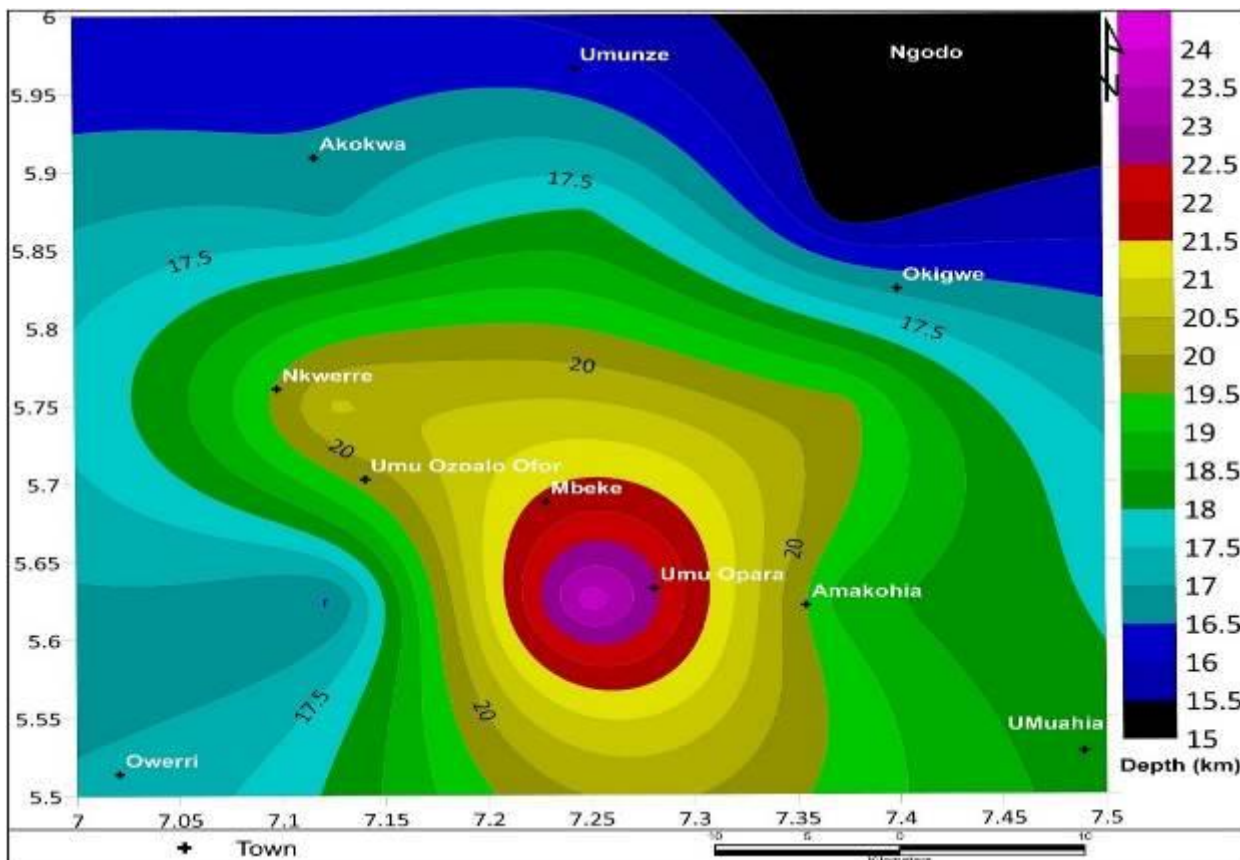


Fig.6.2a CPD contour map of Sheet 312 corresponding to Okigwe

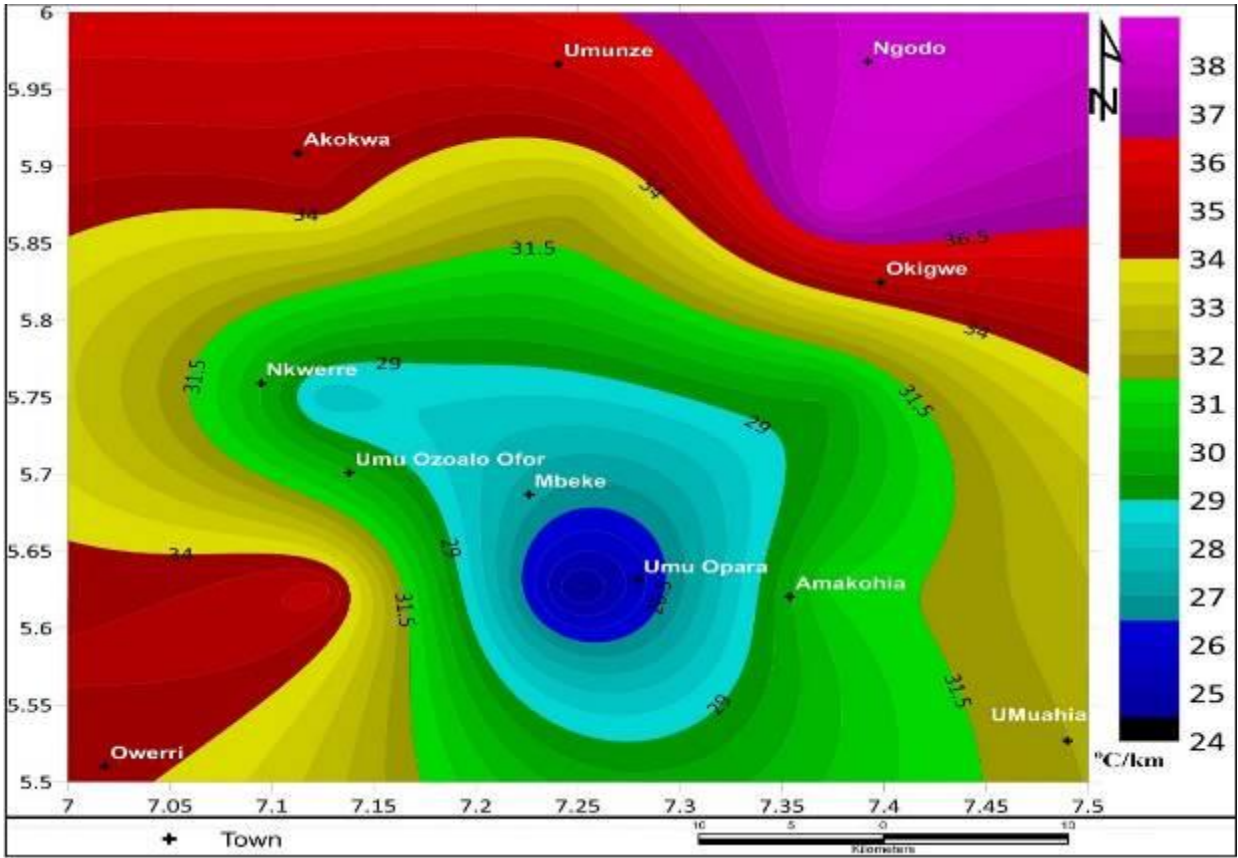


Fig.6.2b Geothermal Gradient contour map of Sheet 312 corresponding to Okigwe

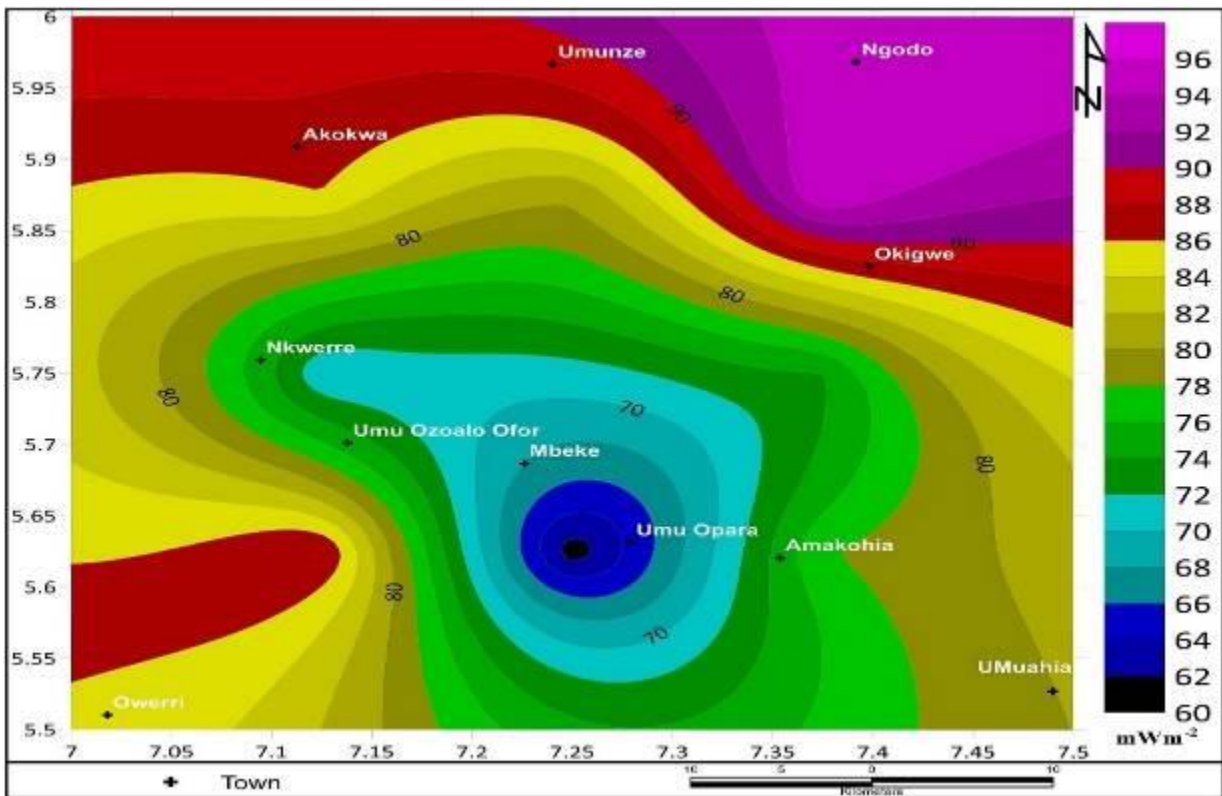


Fig. 6.2c Heat flow contour map of Sheet 312 corresponding to Okigwe

5.14 Geothermal potential of Bauchi _Sheet 148

The aeromagnetic data of **Bauchi _Sheet 148** was subjected to spectral analysis with the aim of accessing the geothermal potential of the study area and environs. The Curie point depth values ranges from (15.14- 23.81) km, the geothermal gradient values ranges from (8.23– 19.504) °C/km and the heat flow values ranges from (74.344- 176.183) mW/m² (Table 40). The SE edge hosts the highest values of anomalous heat flow and geothermal gradient with corresponding shallowest values of Curie point depth (Fig. 6.3 a-c). Generally, for a viable geothermal reservoir, a heat flow range of 80 to 100 mW/m² is recommended, hence it can be inferred that every region on the study area could be considered as having good prospect except the portion of NW regions of the study area covering Zalau with low heat flow below 80 – 100 mWm⁻².

Table 40 Summary of the results of the centroid depth, depth to basement, curie depth, geothermal gradient and the heat flow

Bauchi Sheet 148

Blocks	X	Y	Z0	Zt	Curie Depth	Geothermal gradient	Heat Flow
A	9.125	10.375	10	0.496	19.504	29.504	74.344
B	9.208	10.375	9.82	0.575	19.065	30.422	76.055
C	9.291	10.375	8.46	0.785	16.135	35.95	89.875
D	9.375	10.375	8.34	0.717	15.963	36.334	90.835
E	9.125	10.125	7.38	0.85	13.91	41.697	104.243
F	9.208	10.125	8.94	0.482	17.398	32.333	80.83
G	9.291	10.125	5.28	0.773	9.787	59.262	148.155
H	9.375	10.125	4.44	0.65	8.23	70.473	176.183

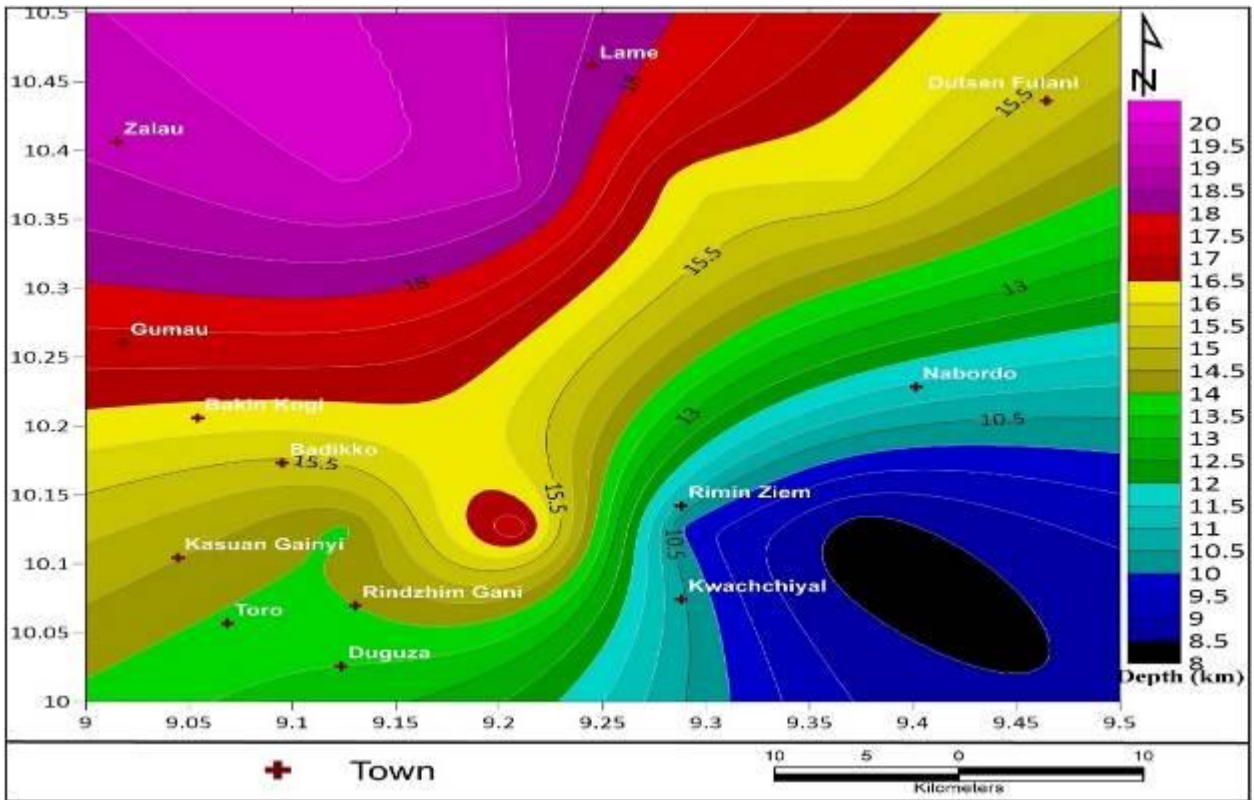


Fig. 6.3a CPD contour map of Sheet 418 corresponding to Bauchi

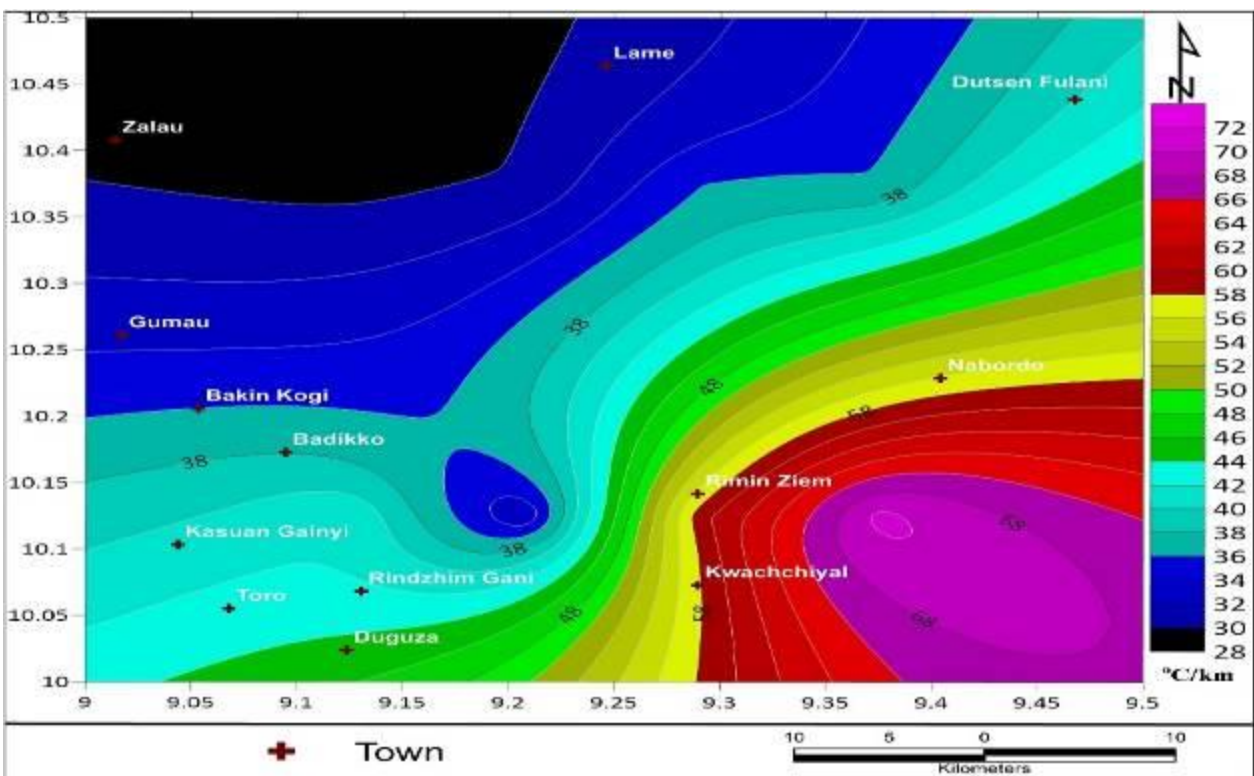


Fig. 6.3b Geothermal gradient contour map of Sheet 418 corresponding to Bauchi

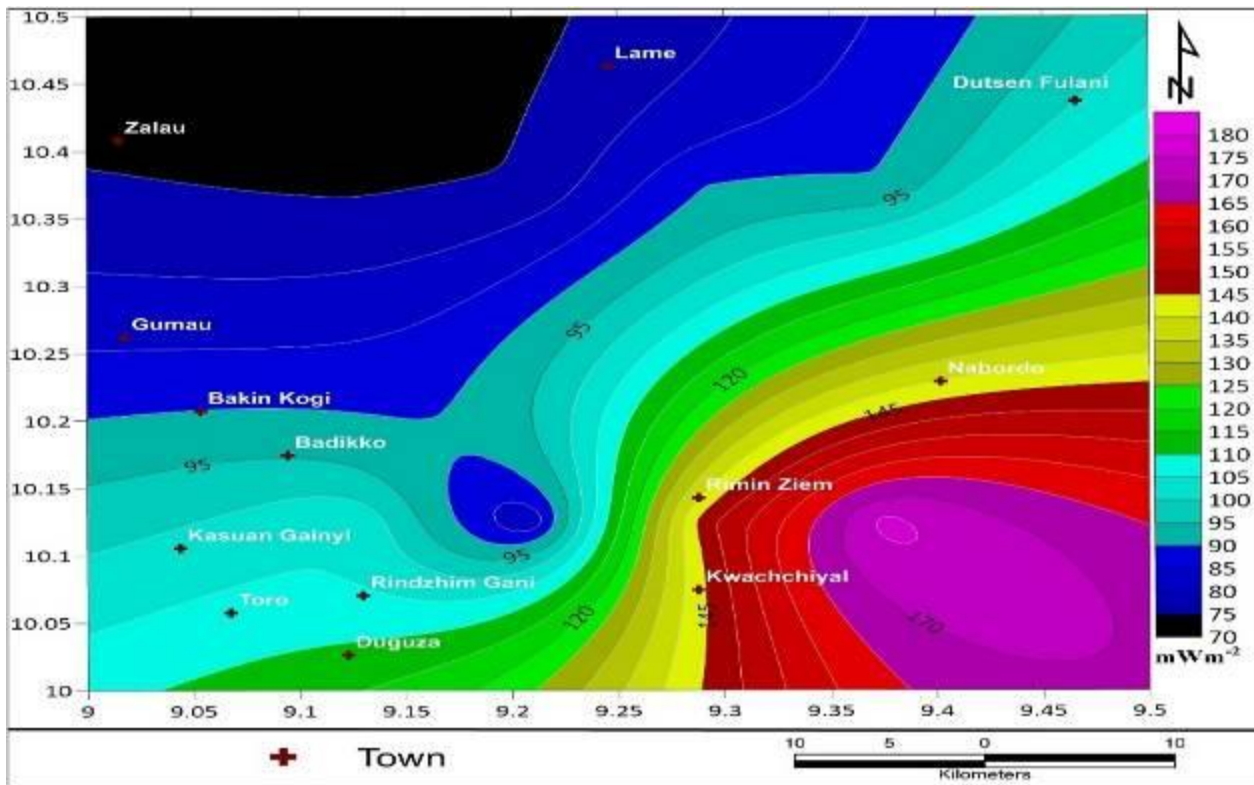


Fig.6.3c Heat flow contour map of Sheet 418 corresponding to Bauchi

5.15 Geothermal potential of Jalingo_Sheet215

The aeromagnetic data of **Jalingo_ (Sheet 215)** was subjected to spectral analysis with the aim of accessing the geothermal potential of the study area and environs. The Curie point depth values ranges from (6.929- 17.062) km, the geothermal gradient values ranges from (33.994– 59.003) °C/km and the heat flow values ranges from (84.985- 209.265) mW/m² (Table 41). The NE edge covering Jalingo and Kogin Maliki hosts the highest values of heat flow and geothermal gradient anomalies with corresponding shallowest values of Curie point depth (Fig. 6.4 a-c). Generally, for a viable geothermal reservoir, a heat flow range of 80 to 100 mW/m² is recommended, hence it can be inferred that every region on the study area could be considered as having good prospect.

Table 41 Summary of the results of the centroid depth, depth to basement, curie depth, geothermal gradient and the heat flow

Jalingo Sheet 215

Blocks	X	Y	Centroid Depth Zo	Depth to Basement Zt	Curie Point Depth (km)	Geothermal gradient (°C/km)	Heat Flow mWm ⁻²
A	11.125	8.875	6.74	0.455	13.025	44.53	111.325
B	11.208	8.875	5.2	0.475	9.925	58.438	146.095
C	11.291	8.875	5.1	0.37	9.83	59.003	147.508
D	11.375	8.875	3.68	0.431	6.929	83.706	209.265
E	11.125	8.625	7.6	0.325	14.875	38.991	97.48
F	11.208	8.625	8.72	0.378	17.062	33.994	84.985
G	11.291	8.625	7.38	0.251	14.509	39.951	99.878
H	11.375	8.625	8.06	0.532	15.588	37.208	94.52

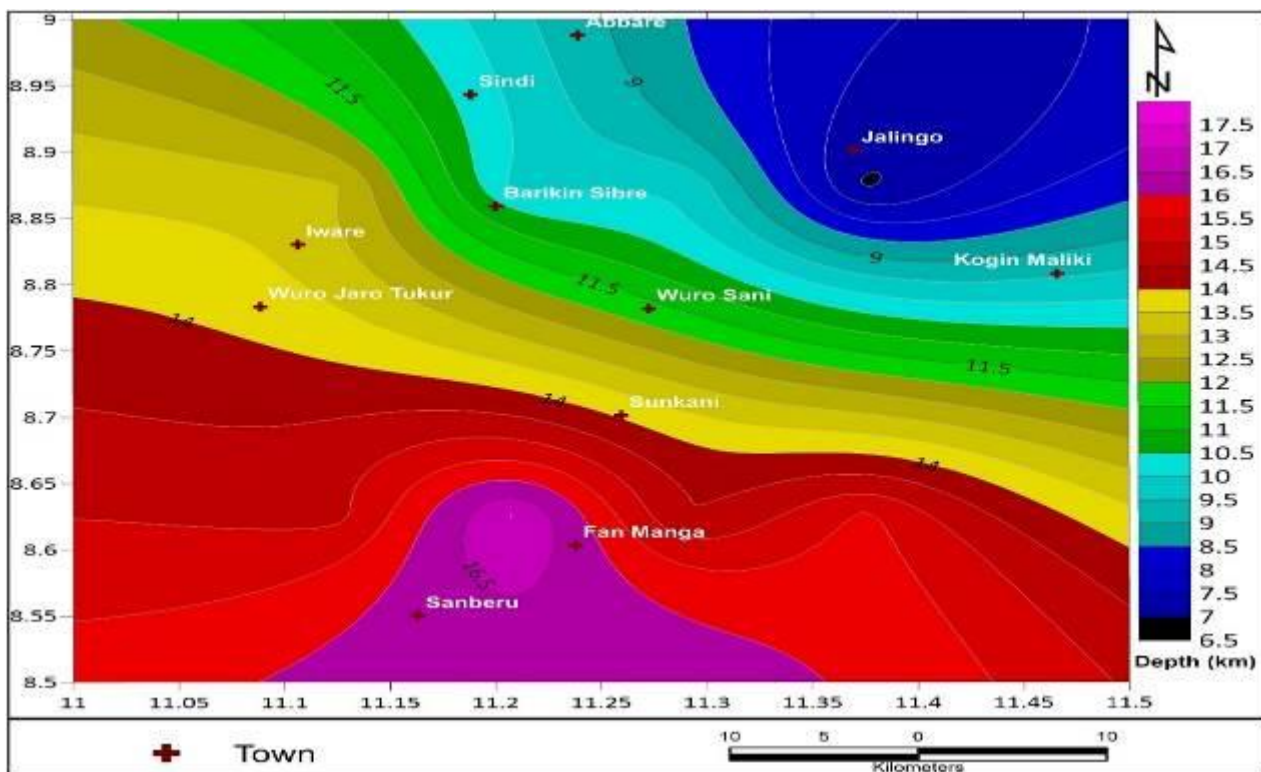


Fig. 6.4a CPD contour map of Sheet 215 corresponding to Jalingo

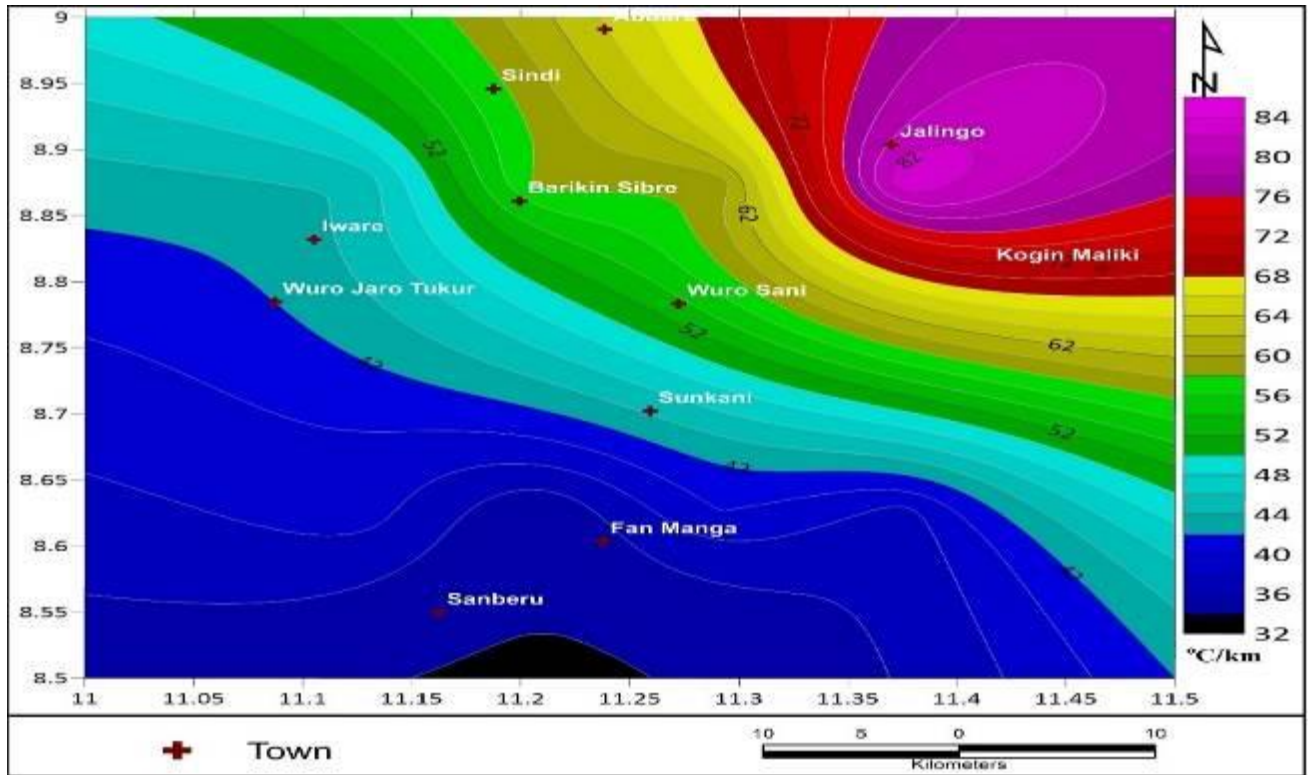


Fig. 6.4b Geothermal Gradient contour map of Sheet 215 corresponding to Jalingo

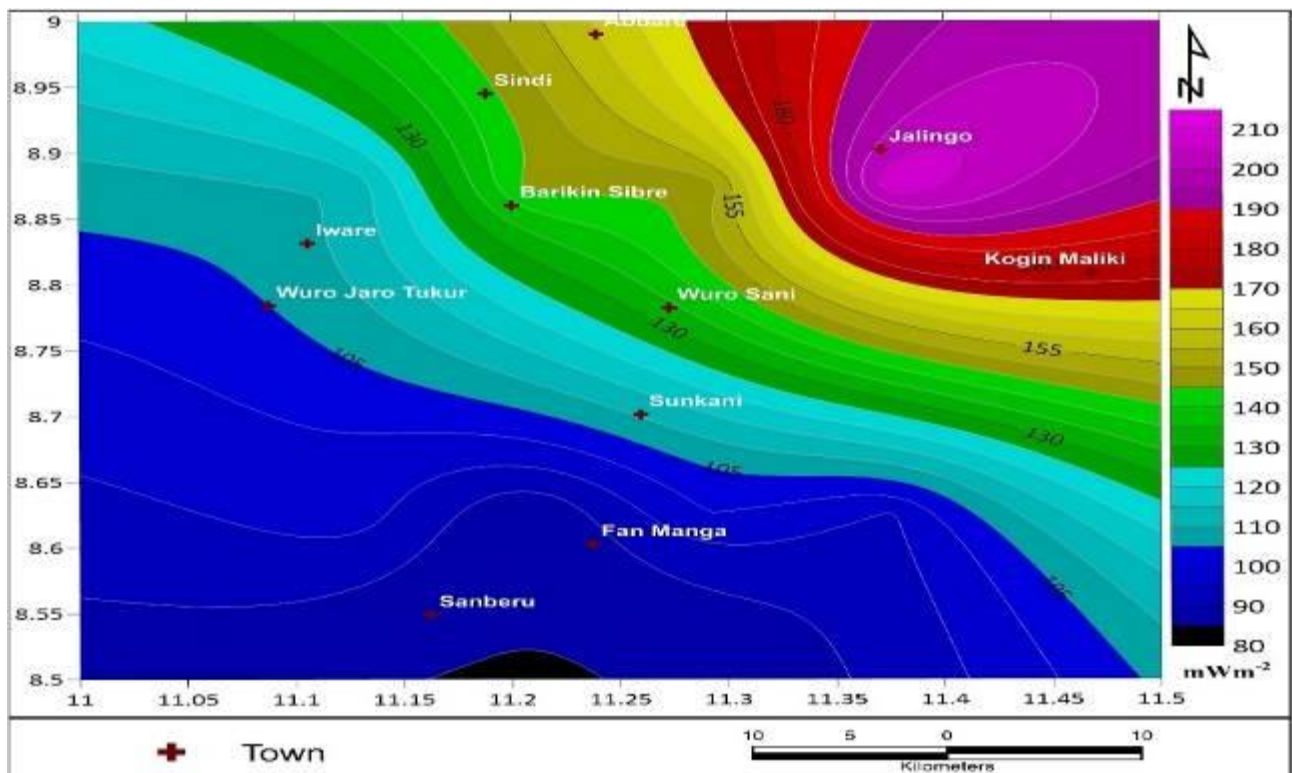


Fig. 6.4c Heat flow contour map of Sheet 215 corresponding to Jalingo

5.16 Geothermal Potential of Ilesha Sheet 243

The aeromagnetic data of **Ilesha_ (Sheet 243)** was subjected to spectral analysis with the aim of accessing the geothermal potential of the study area and environs. The Curie point depth values ranges from (15.14- 23.81) km, the geothermal gradient values ranges from (14.639– 21.924) °C/km and the heat flow values ranges from (67.196- 100.635) mW/m² (Table 42). The Northern and the central portion covering Ikirun and Ilerin edge hosts the highest values of heat flow and geothermal gradient with corresponding shallowest values of curie point depth (Fig. 6.5a-c). Generally, for a viable geothermal reservoir, a heat flow range of 80 to 100 mW/m² is recommended, hence it can be inferred that every region on the study area could be considered as having good prospect except with the SW region of the study area covering Ife with the lowest heat flow below the recommended threshold (80 – 100) mWm⁻².

Table 42 Summary of the results of the centroid depth, depth to basement, curie depth, geothermal gradient and the heat flow

Ilesha Sheet 243

Blocks	X	Y	Zo	Zt	Curie point depth	Geothermal gradient	Heat Flow
A	4.625	7.875	8.34	0.864	15.816	36.667	93.134
B	4.708	7.875	7.681	0.723	14.639	39.62	100.635
C	4.791	7.875	7.98	0.812	15.148	38.289	97.254
D	4.875	7.875	8.847	0.854	16.84	34.442	87.483
E	4.625	7.625	11.562	1.2	21.924	26.455	67.196
F	4.708	7.625	10.435	0.678	20.192	28.724	72.969
G	4.791	7.625	7.866	0.745	14.987	38.7	98.298
H	4.875	7.625	9.55	0.765	18.335	31.633	79.023

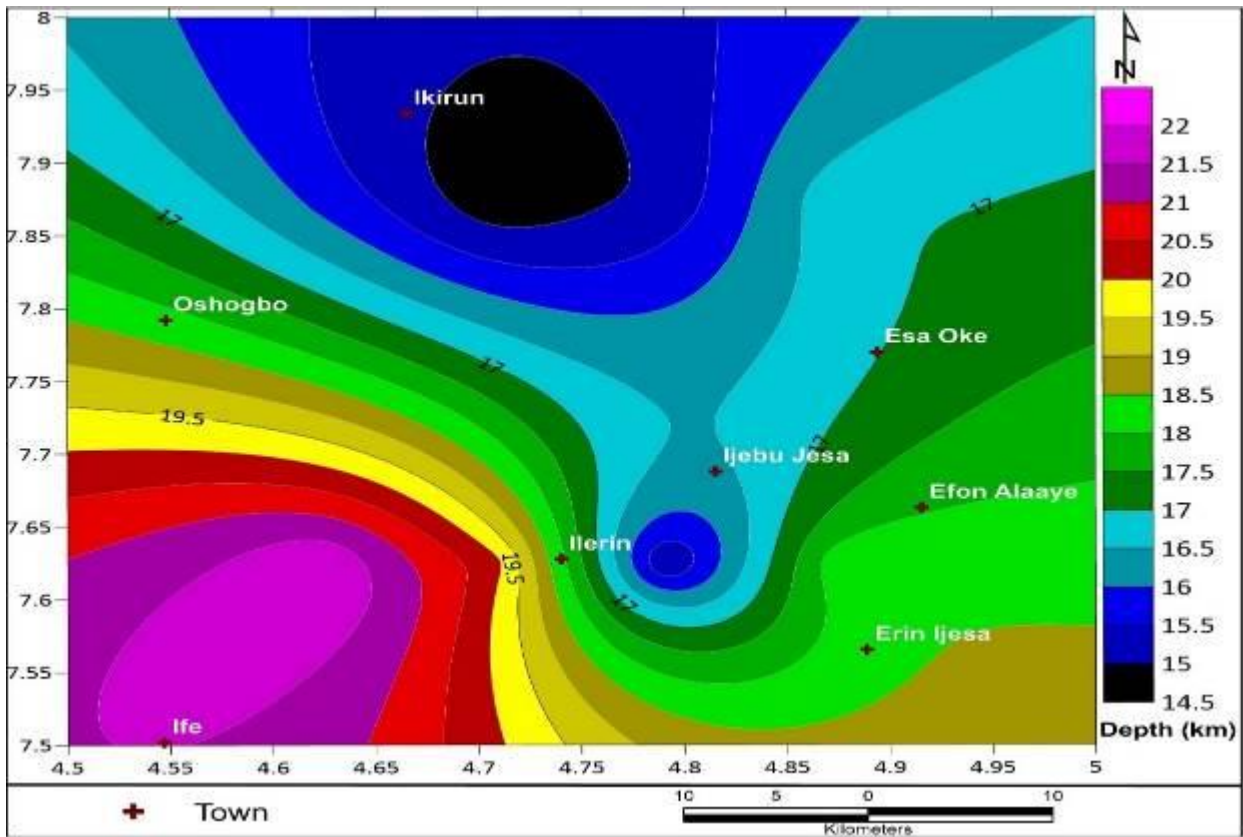


Fig.6.5a CPD contour map of Sheet 243 corresponding to Ilesha

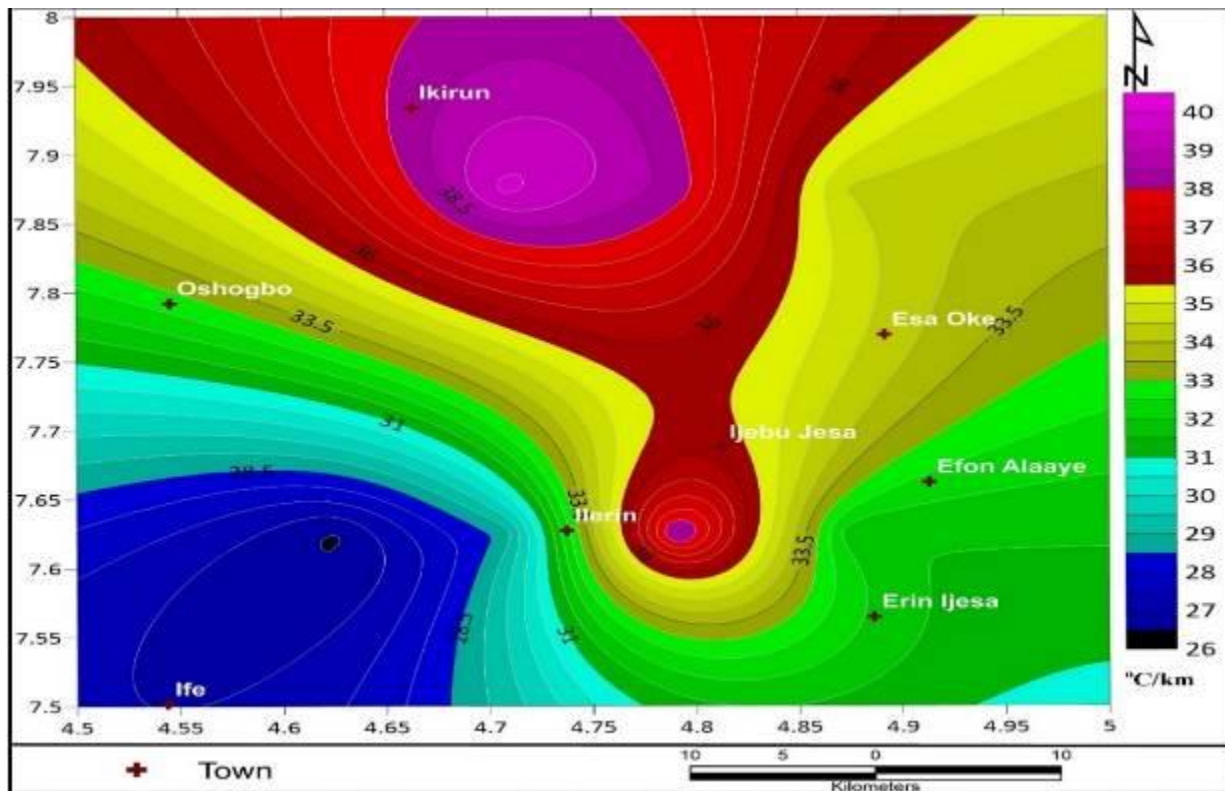


Fig. 6.5b Geothermal gradient contour map of Sheet 243 corresponding to Ilesha

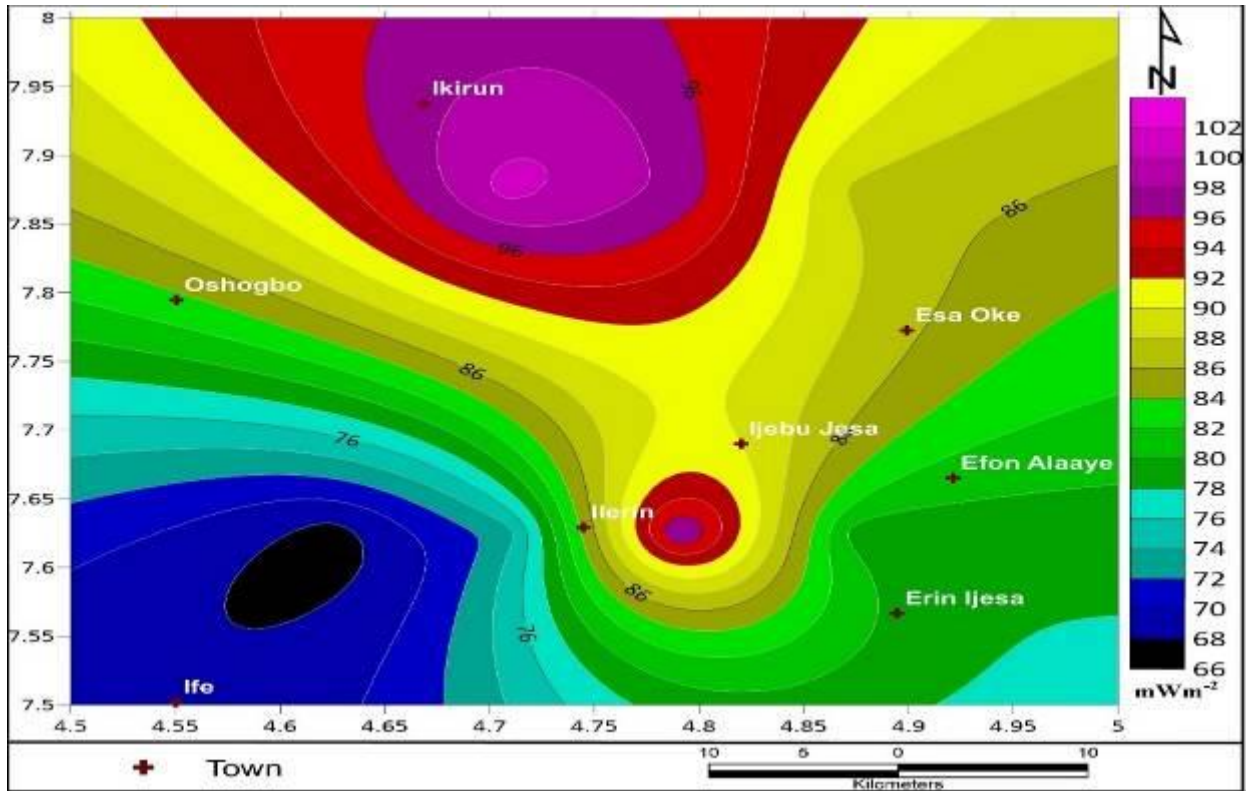


Fig. 6.5c Heat flow contour map of Sheet 243 corresponding to Ilesha

5.17 Geothermal Potentials of Ijebu-Ode_280

The aeromagnetic data of **Ijebu-Ode_ (Sheet 280)** was subjected to spectral analysis with the aim of accessing the geothermal potential of the study area and environs. The Curie point depth values ranges from (11.768- 15.358) km, the geothermal gradient values ranges from (33.978– 49.286) °C/km and the heat flow values ranges from (84.945- 125.186) mW/m² (Table 43). The NS edge hosts the highest values of heat flow and geothermal gradient with corresponding shallowest values of Curie point depth (Fig. 6.6 a-c). Generally, for a viable geothermal reservoir, a heat flow range of 80 to 100 mW/m² is recommended, hence it can be inferred that every region on the study area could be considered as having good prospect

Table 43 Summary of the results of the centroid depth, depth to basement, curie depth, geothermal gradient and the heat flow

Ijebu-Ode Sheet 280

Blocks	X	Y	Zo	Zt	CPD	Geothermal gradient	Heat Flow
A	3.625	6.875	6.3	0.76	11.84	48.986	124.424
B	3.708	6.875	6.38	0.992	11.768	49.286	125.186
C	3.791	6.875	7.26	1.168	13.352	43.439	110.335
D	3.875	6.875	8.24	1.192	15.288	37.938	96.363
E	3.625	6.791	8.88	0.688	17.07	33.978	84.945
F	3.708	6.791	6.52	1.214	11.826	49.0447	124.573
G	3.791	6.791	6.78	0.808	12.752	45.438	123.033
H	3.875	6.791	8.06	0.762	15.358	37.765	95.847

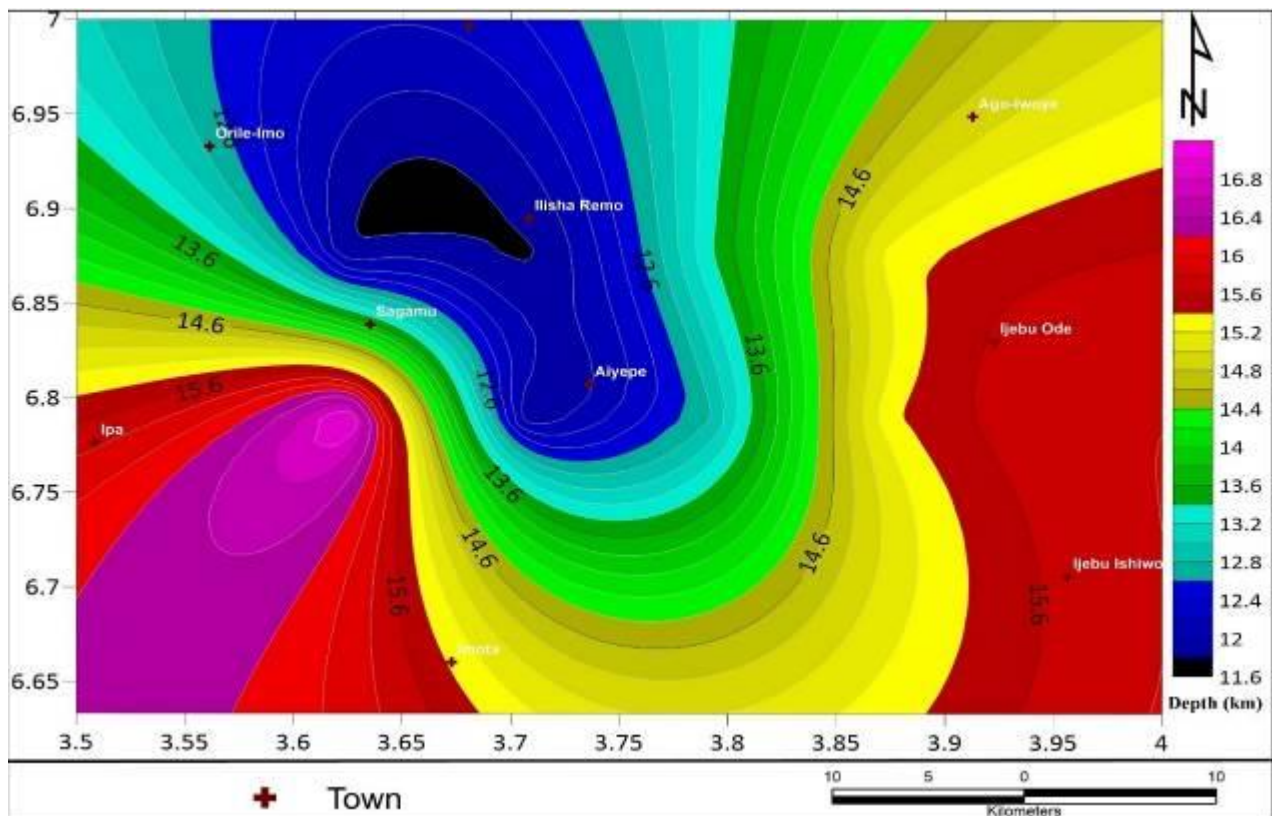


Fig. 6.6a: CPD contour map of Sheet 280 corresponding to Ijebu-Ode

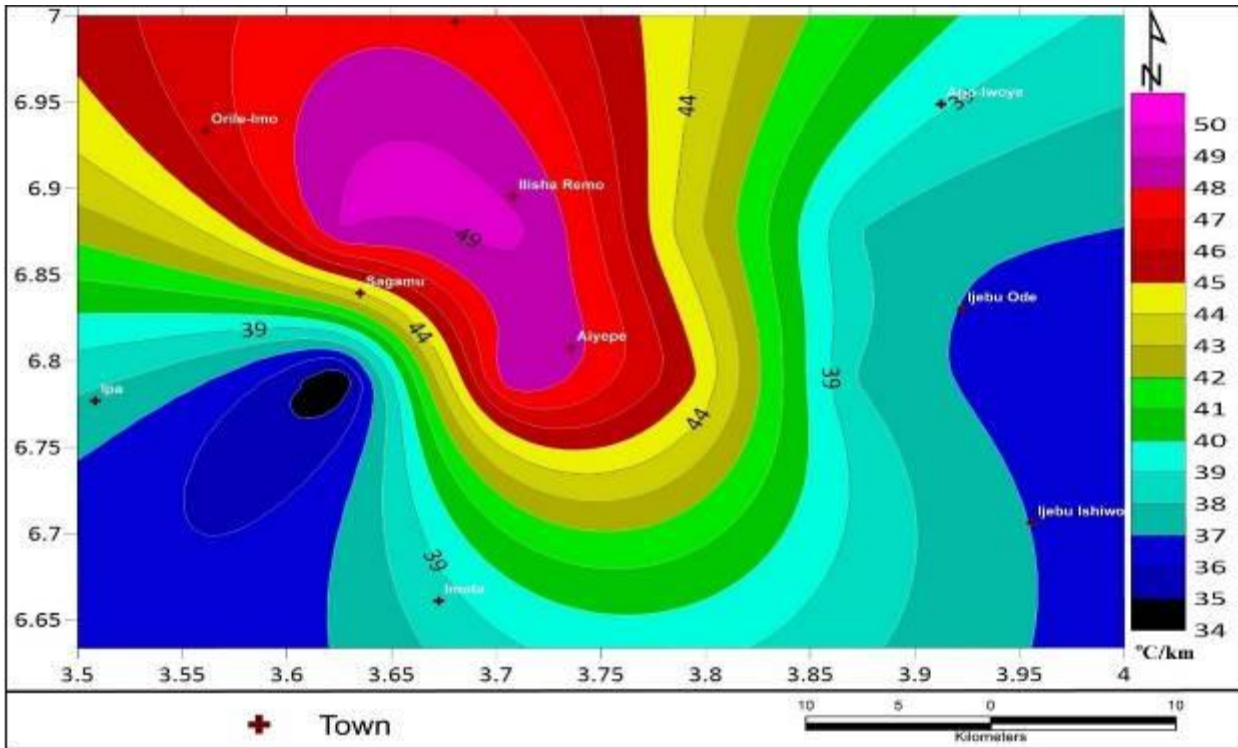


Fig 6.6b: Geothermal Gradient contour map of Sheet 280 corresponding to Ijebu-Ode

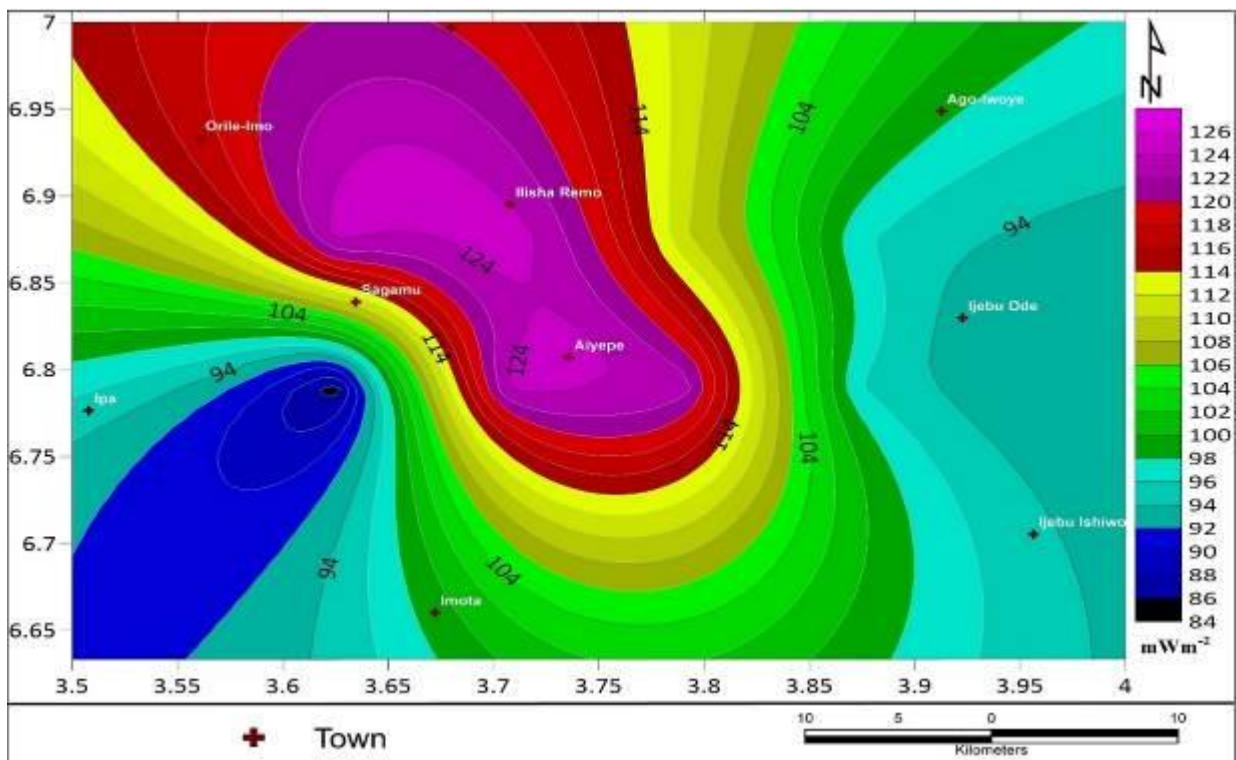


Fig.6.6 c: Heat flow contour map of Sheet 280 corresponding to Ijebu-Ode

5.18 Geothermal Potentials of Ijebu-Ife_281

The aeromagnetic data of **Ijebu-Ife_ (Sheet 281)** was subjected to spectral analysis with the aim of accessing the geothermal potential of the study area and environs. The Curie point depth values ranges from (13.224- 22.343) km, the geothermal gradient values ranges from (25.959– 38.113) °C/km and the heat flow values ranges from (65.936- 110.089) mW/m² (Table 44). The SE edge, Abigi, Agbure, and Ilushin hosts the highest values of heat flow and geothermal gradient with corresponding shallowest values of curie point depth (Fig. 6.7 a-c). Regions like Omo, Oso, Kojala, Oniparaja also good geothermal manifestations. Generally, for a viable geothermal reservoir, a heat flow range of (80 - 100) mW/m² is recommended, hence it can be inferred that every region on the study area could be considered as having good prospect except within the Northern region, Gbamu of the study area with low heat flow below 80 mWm⁻².

Table 44 Summary of the results of the centroid depth, depth to basement, curie depth, geothermal gradient and the heat flow

Ijebu-Ife Sheet 281

Blocks	X	Y	Centroid Depth (Z _o)	Depth to Basement (Z _t)	Curie point Depth (km)	Geothermal gradient	Heat Flow (mWm ⁻²)
A	4.125	6.875	9.92	0.604	19.236	30.152	76.586
B	4.208	6.875	11.88	1.417	22.343	25.959	65.936
C	4.291	6.875	9.08	0.863	17.297	33.532	85.171
D	4.375	6.875	9.12	0.792	17.448	33.242	84.435
E	4.125	6.625	8.82	0.678	16.962	34.194	86.853
F	4.208	6.625	7.261	1.298	13.224	43.86	110.089
G	4.291	6.625	8.67	0.79	16.55	35.045	89.014
H	4.375	6.625	8.08	0.942	15.218	38.113	96.799

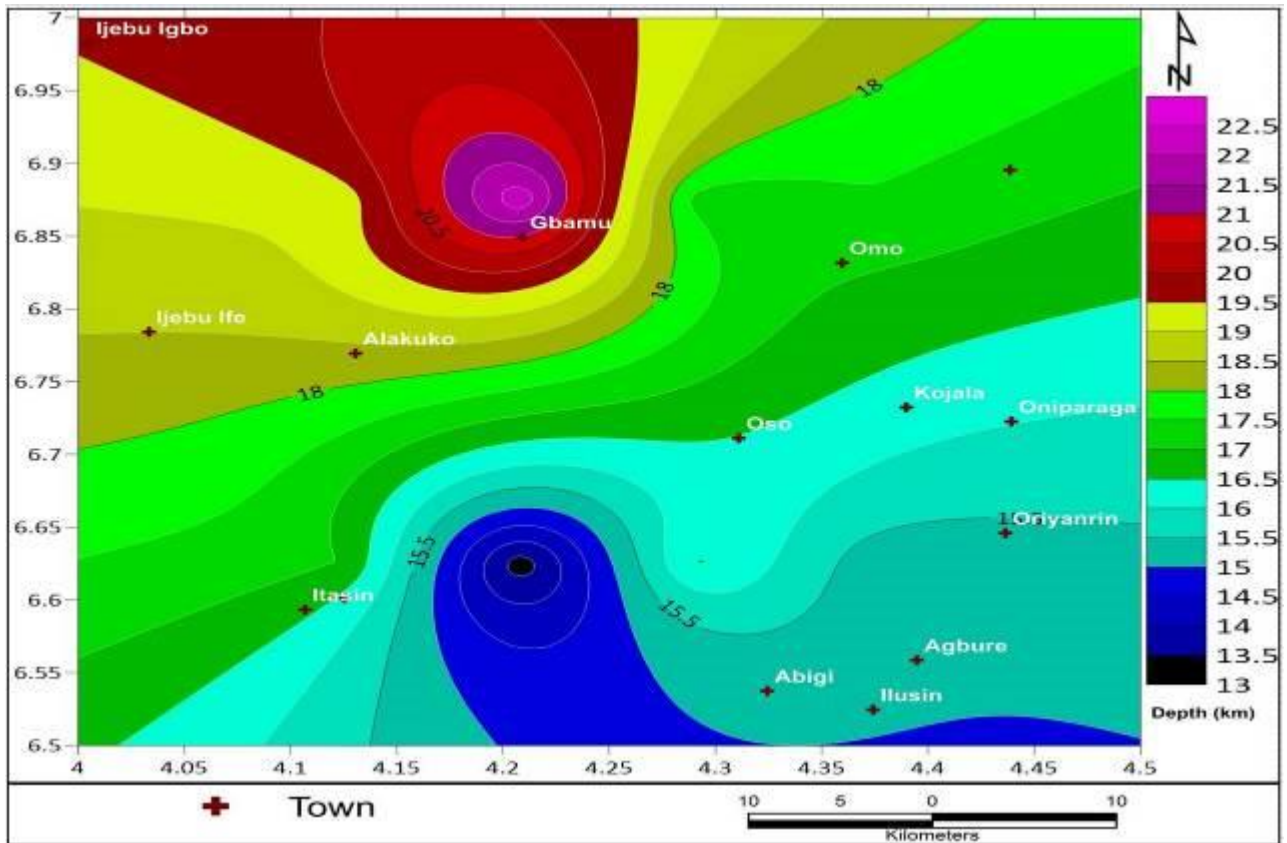


Fig.6.7 a: CPD contour map of Sheet 281 corresponding to Ijebu-Ife

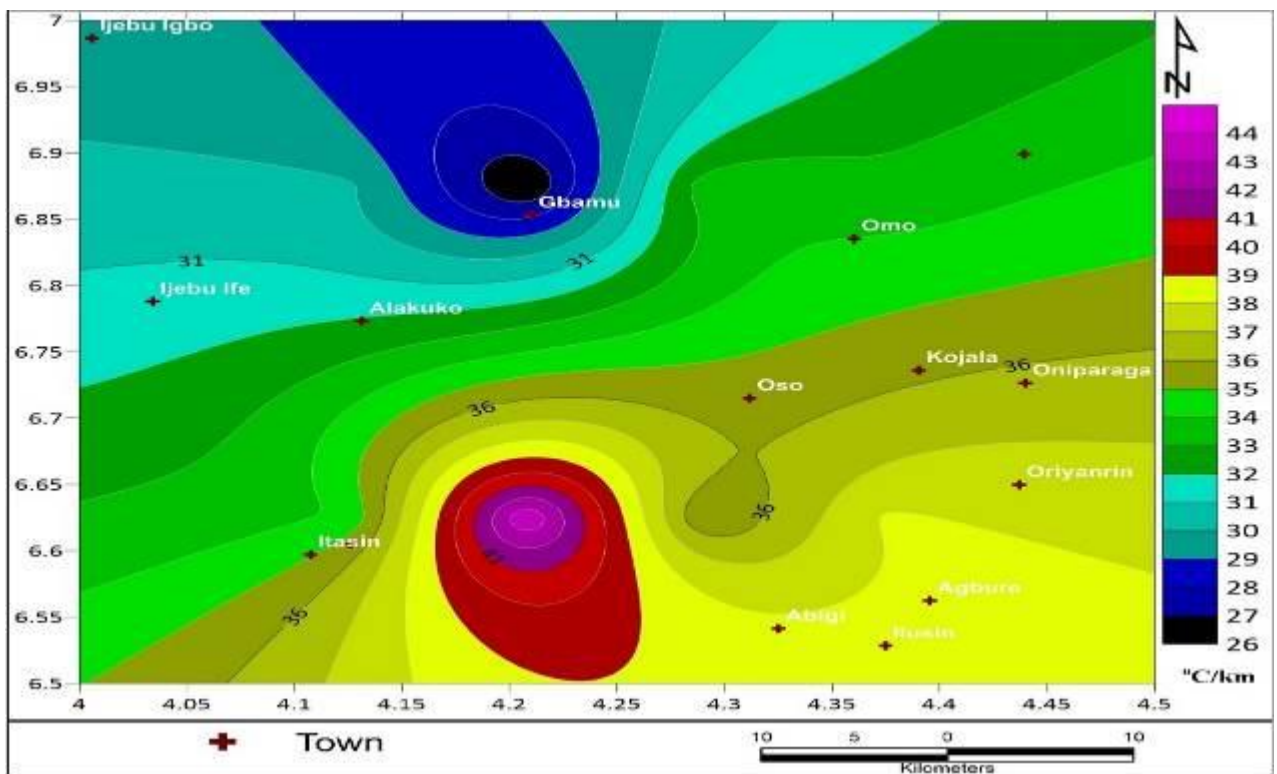


Fig. 6.7b: Geothermal Gradient contour map of Sheet 281 corresponding to Ijebu-Ife

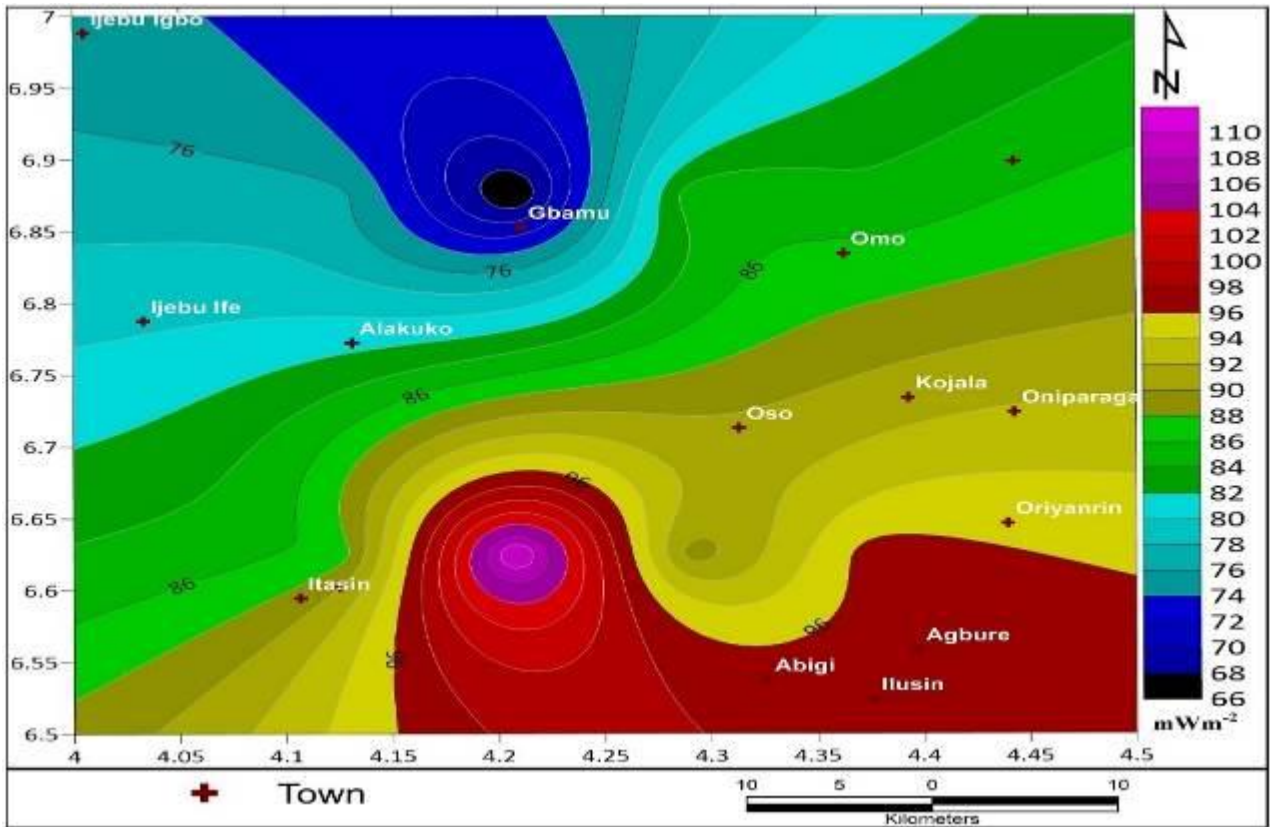


Fig.6.7 c: Heat flow contour map of Sheet 281 corresponding to Ijebu-Ife

5.19 Geothermal Potentials of Abo_311

The aeromagnetic data of Abo_ (Sheet 311) was subjected to spectral analysis with the aim of accessing the geothermal potential of the study area and environs. The Curie point depth values ranges from (11.88- 25.87) km, the geothermal gradient values ranges from (22.42– 48.82) °C/km and the heat flow values ranges from (56.95- 124) mW/m² (Table 45). The SE and NE portion covering Okija, Nnebuku, Mgbidi, Izombe, Obudi, Ndoni and Obofia hosts the highest values of heat flow and geothermal gradient with corresponding shallowest values of Curie point depth (Fig. 6.8a-c). Generally, for a viable geothermal reservoir, a heat flow range of 80 to 100 mW/m² is recommended, hence it can be inferred that every region on the study area could be considered as having good prospect except with the NW covering Anuabo and Abo regions of the study area with low heat flow below 80 – 100 mWm².

Table 45 Summary of the results of the centroid depth, depth to basement, curie depth, geothermal gradient and the heat flow

Abo Sheet 311

Blocks	X	Y	Zo	Zt	CPD	Geothermal gradient	Heat Flow
A	6.675	5.875	13.64	1.41	25.87	22.42	56.95
B	6.708	5.875	11.22	1.74	20.7	28.02	71.17
C	6.791	5.875	10.2	1.7	18.34	31.62	80.31
D	6.875	5.875	9.06	1.13	16.99	34.14	86.72
E	6.675	5.625	11.08	2.25	19.91	29.13	73.99
F	6.708	5.625	6.94	1.85	12.03	48.21	122.45
G	6.791	5.625	7.88	2.33	12.43	46.66	118.52
H	6.875	5.625	6.9	1.92	11.88	48.82	124

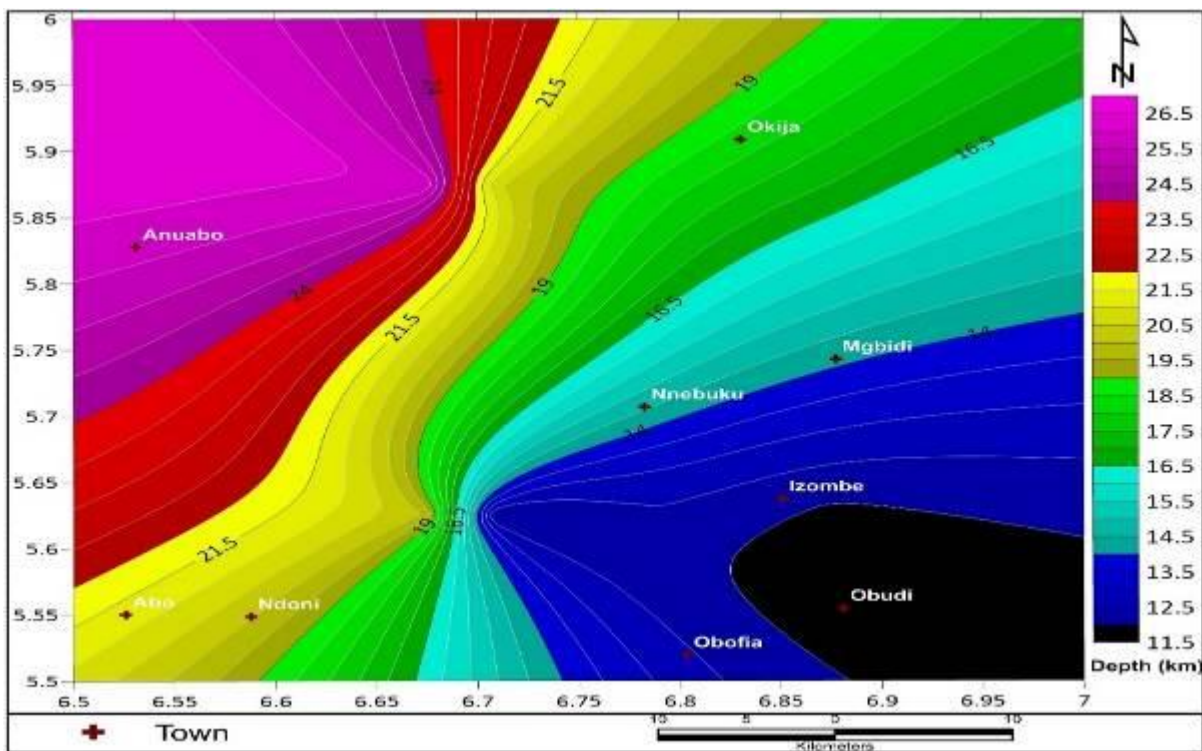


Fig.6.8a: CPD contour map of sheet 311 corresponding to Abo

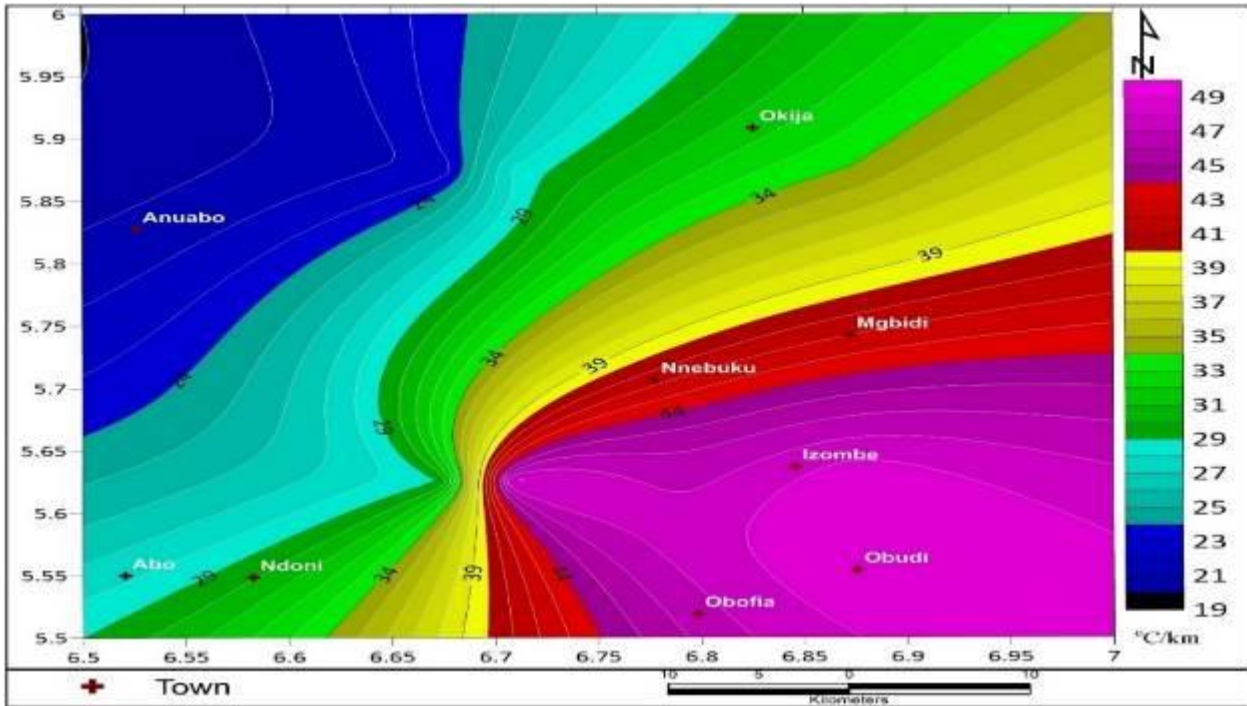


Fig. 6.8b: Geothermal gradient contour map of sheet 311 corresponding to Abo

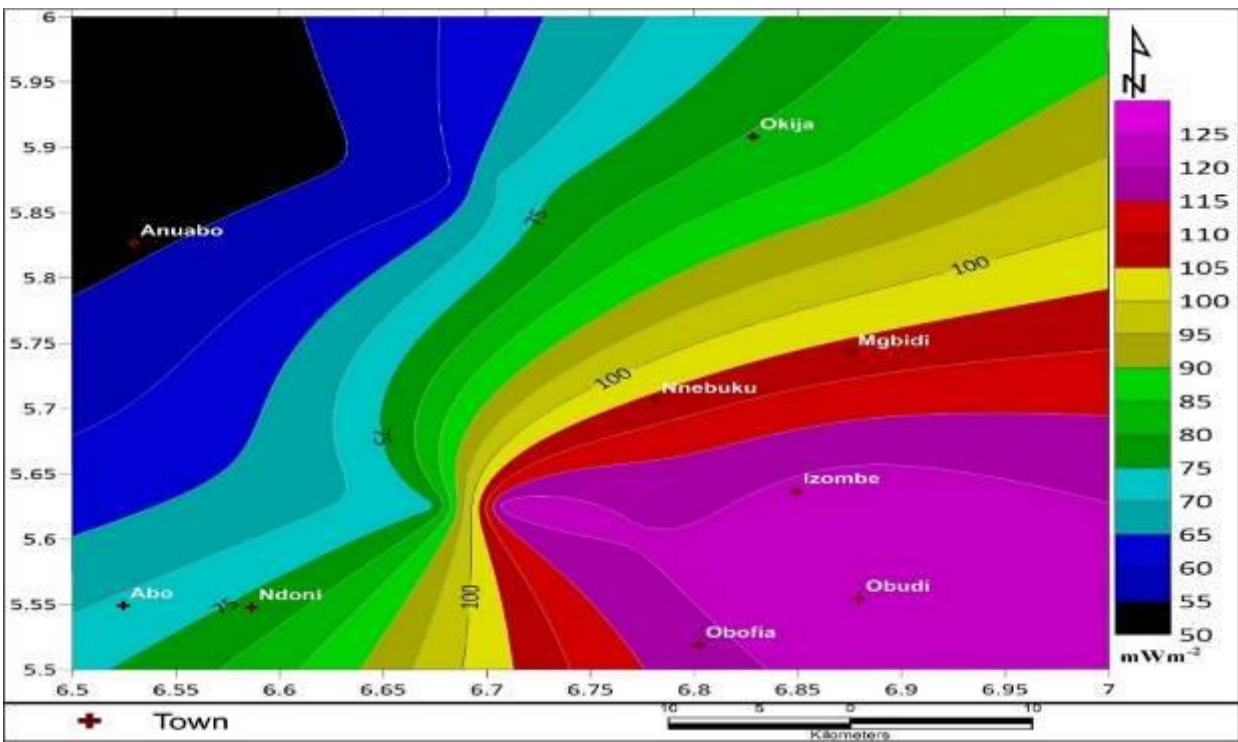


Fig.6.8c: Heat flow contour map of sheet 311 corresponding to Abo

5.20 Geothermal Potentials of Ugep_314

The aeromagnetic data of **Ugep_ (Sheet 314)** was subjected to spectral analysis with the aim of accessing the geothermal potential of the study area and environs. The Curie point depth values ranges from (7.7- 17.49) km, the geothermal gradient values ranges from (33.162– 75.325) °C/km and the heat flow values ranges from (80.45- 192.342) mW/m² (Table 46). The entire area of NE, SE, central portion, NW, SW have high geothermal anomalies, and hosts the highest values of heat flow and geothermal gradient with corresponding shallowest values of curie point depth (Fig. 6.9a-c). Generally, for a viable geothermal reservoir, a heat flow range of 80 to 100 mW/m² is recommended, hence it can be inferred that every region on the study area could be considered as having good anomalous prospect except within the western portion of Adin, Abini and Agwu -Agwuna regions of the study area with low heat flow below the threshold 80 – 100 mWm⁻².

Table 46 Summary of the results of the centroid depth, depth to basement, curie depth, geothermal gradient and the heat flow

Ugep Sheet 314

Blocks	X	Y	Zo	Zt	CPD	Geothermal gradient	Heat Flow
A	8.125	5.875	9.06	1.548	16.572	34.999	88.897
B	8.208	5.875	8.64	1.03	16.25	35.692	80.45
C	8.291	5.875	6.14	1.67	10.61	54.665	138.849
D	8.375	5.875	4.66	0.998	8.322	69.695	177.025
E	8.125	5.625	9.54	1.59	17.49	33.162	84.231
F	8.208	5.625	8.5	1.616	15.384	37.702	95.763
G	8.291	5.625	5.38	1.072	9.668	59.992	152.38
H	8.375	5.625	4.8	1.9	7.7	75.325	192.342

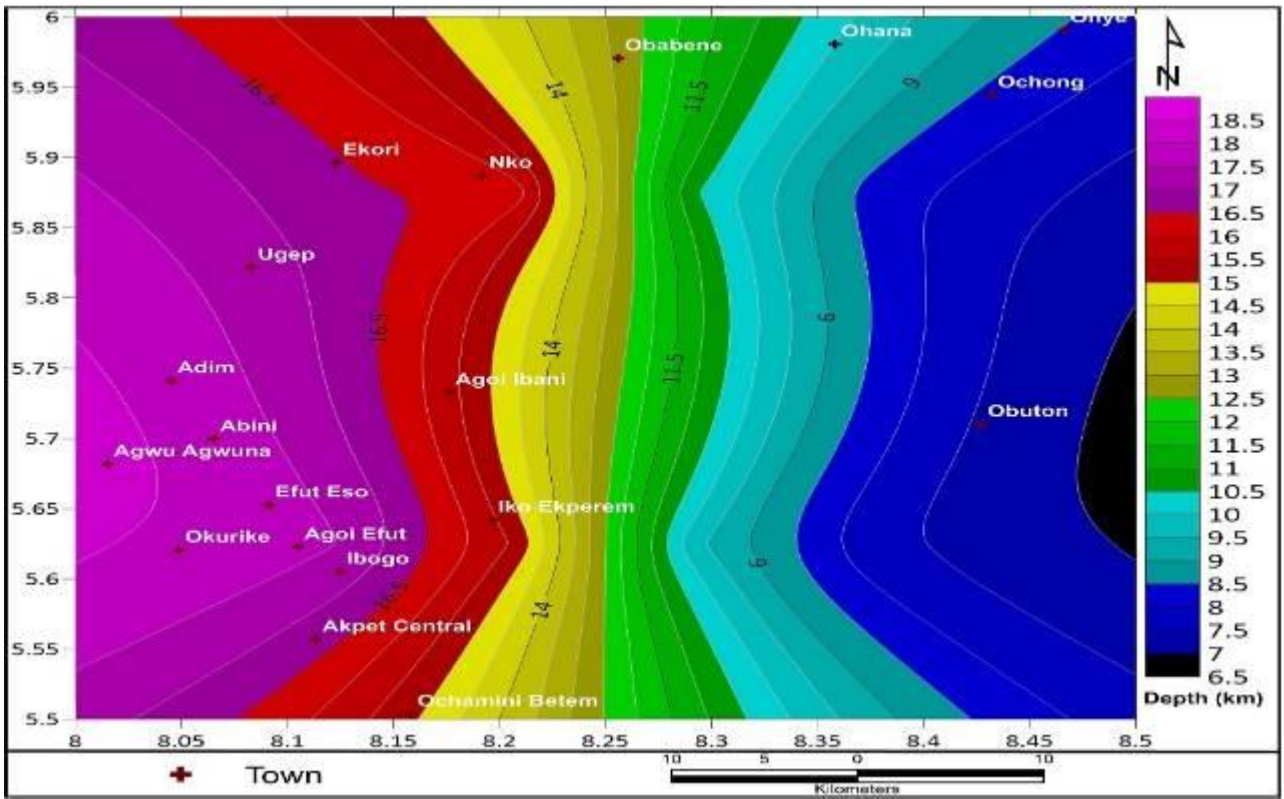


Fig.6.9 a: CPD contour map of sheet 314 corresponding to Ugep

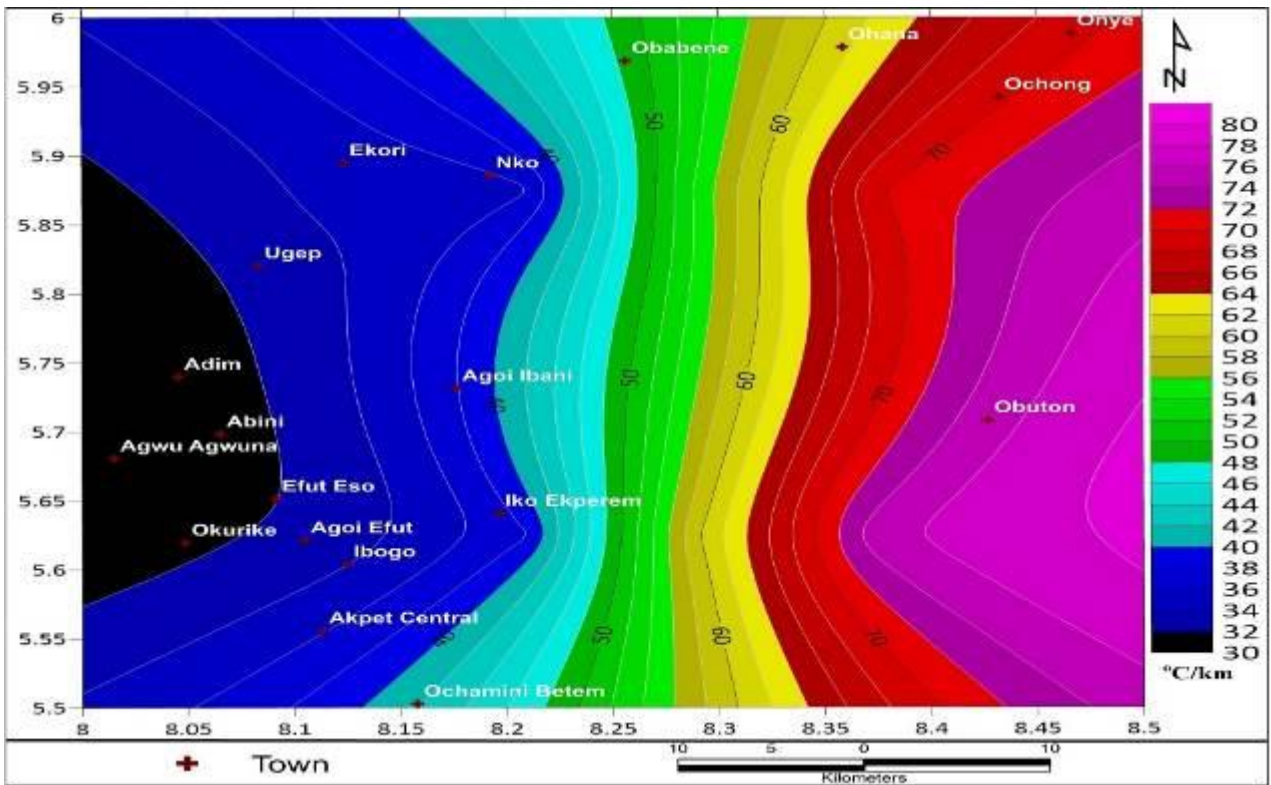


Fig. 6.9b: Geothermal gradient contour map of sheet 314 corresponding to Ugep

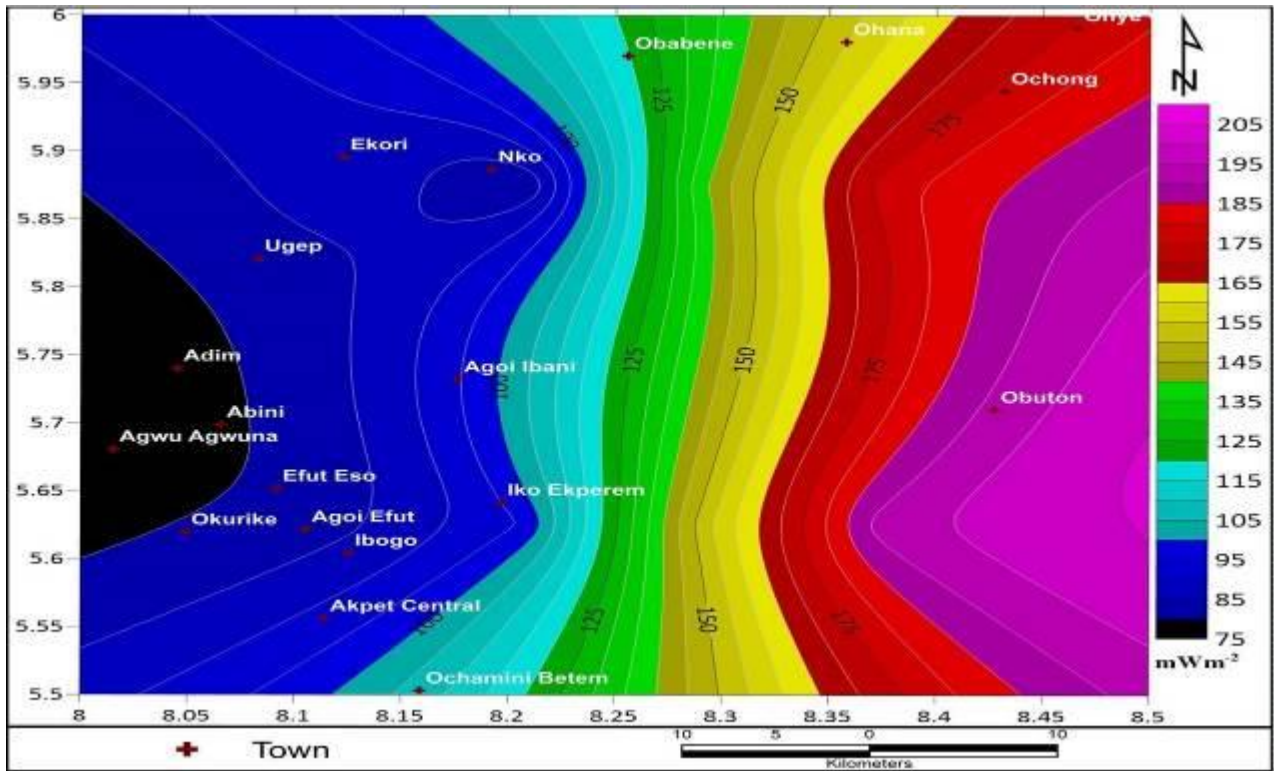


Fig.6.9c: Heat flow contour map of sheet 314 corresponding to Ugep

5.21 Geothermal Assessment of some selected BHT logs in Niger Delta

The lowest values of geothermal gradient were found in the center of Niger Delta within the thick Tertiary sediments as 1.1-2.1 °C/100 m or 2.4-2.5 °C/100 m in Edo South -Warri-Port Harcourt area. The values calculated in 8 points (wells) range from 3.5 to 5.6 °C/100 m and the heat flow estimated on the basis of these gradients was 82-96 mW/m² towards the Anambra Basin. By implication, a high geothermal gradient enhances the early formation of oil at relatively shallow burial depths, but causes the depth range of the oil window to be narrow, while low geothermal gradient causes the first formation of oil to begin at fairly deep subsurface levels, but makes the oil window broad.

Table 46a: Calculation Of The Geothermal Gradient And Formation Temperature From Abura Field Onshore Niger Delta: Tms = 80°f (27°c)

ABURA 2:

Reservoirs	BHT (°F) °C	TWD (ft) m	gG °C/100m
6AB 4	186 (86)	11700(3566)	5.6
1AB 1	188 (87)	11855(3613)	4.3
2AB 1	210 (99)	12080(3682)	4.1
3AB 1 (U)	183 (84)	12195(3717)	1.3
3AB 1 (L)	215 (102)	12400(3780)	2.1

ABURA b:

Reservoirs	BHT (°F)	TWD (ft) M	gG °C/100m
1AB 4L	131	10050(3063)	3.96
2AB 4	159	10220(3115)	3.60
3AB 4	156	10370(3160)	1.4
4AB 4 (U)	165	10500(3200)	1.2

ABURA c:

Reservoirs	BHT (°F)	TWD (ft) M	gG °C/100m
5AB 6	150	10025(3056)	5.2
6AB 6	153	10125(3086)	3.5
6AB 6	170	10300(3139)	1.2

TABLE d: Calculation Of the Geothermal Gradient and Formation Temperature from Northern field Offshore Delta: Tms = 80°F (27°C)

Reservoirs	BHT (°F)	TWD (ft) M	gG °C/100m
A-1	180	7989(2435)	3.2
B-2	185	10063(3067)	2.5
C-3	195	10982(3347)	1.4
D-4	175	9213(2808)	1.1

The geothermal gradients was estimated to range from (1.1-5.6°C)/100m.

5.22 Proposed Cost of Drilling Geothermal Well, 2-5KM

Geothermal wells are built into hot, deep rocks: basement, sedimentary or volcanic rocks. Developers drill wells 1 3 to 10 kilometers into the rocks, using conventional oil drills. The temperature down there measures (71 -315) degree Celsius. Geothermal power plant locations are **restricted by geological features**: they must be built at sites of volcanic or seismic activity, such as hot springs, geysers, and volcanoes.

A typical drilled well is 2-5 km deep with the scale of temperatures between 40°C and over 300°C (Bloomquist *et al.*, 1989) and an average cost of a 2 km geothermal borehole costs \$1-2 million (personal contact with Barker and Huges at NAPE, conference, Lagos), however the cost can vary depending on the drilling conditions) .Each well will take approximately 35 to 45 days to drill. To begin the well drilling process, large flat areas called 'well pads' are prepared so that the drilling rig can operate on a stable platform. The estimate cost for 2-5km geothermal power plant installation is 3,991 USD per kilowatt.

An open loop system relies on two wells, one supply well and one return well, and circulates water via pipes between the two.

THE KENYA MODEL

In Kenya 2.5km well is drilled for about 2 million USD. This model is recommended for the Nigeria government.

For deeper kms as at this year, 2023 the estimated cost today: \$50-100 million USD, Barker and Huges

- Need to reduce deep hard rock drilling costs by a factor of ~10.

Factors influencing the cost of 2-5km geothermal well:

The most expensive problem routinely encountered in geothermal drilling is **lost circulation**, which is the loss of drilling fluid to pores or fractures in the rock formations being drilled.

The main factors determining influence on location of geothermal power plants are: **the temperature and the capacity of the source, the depth of resources available and the degree of mineralization of water sources as well as their efficiency.**

Disadvantages of geothermal energy

- Surface instability (earthquakes) the construction of geothermal power plants can affect the stability of the land.
- Expensive.
- Sustainability issues.

The largest single disadvantage of geothermal energy is that it is **location specific**. Geothermal plants need to be built in places where the energy is accessible, which means that some areas are not able to exploit this resource.

The main environmental concern that comes with geothermal power plants is **the potential for surface instability**. Because geothermal plants remove water and steam from reservoirs within the earth, the land above those reservoirs can sometimes sink slowly over time.

CHAPTER SIX

6.0

Conclusion

This research has demonstrated the capability of BHT logs, Temperature measurements, aeromagnetic and airborne gravity as a vital tool that can integrate geological and hydrogeological data sources into a significant geothermal prospectivity map. It also provided the first set of information to geoscientists and other stakeholders in the sustainable and renewable energy sector (particularly the NCC) about the availability of geothermal prospects in Nigeria. Therefore, this contributes to the global sustainable energy drive via exploration for new areas of higher geothermal prospects.

This study have assessed various previous works conducted on geothermal prospect in Nigeria from the Geoscientific point of view. Geological and geophysical assessment reveals geothermal manifestations in both sedimentary and basement complex geothermal settings.

The distribution of these surface manifestations of Migmatite ,granites, basalts, and mud volcanoes along regional tectonic stress areas shows the relationship between the formation mechanism of the Northern, Eastern rift itself and schist belts in the South Western Nigeria. Furthermore, the expression of high geothermal potential anomaly in most areas (tables 3.2- 14 and Figs 3.1-3.21ab) respectively. Figs: 3.1.3.21ab , whose lithologic outcrops show the presence of older and younger granitic rocks as well as the locations of the warm springs which prove the correlation between the geology, tectonic structural features, and the areas of shallower CPD anomalies/high-temperature gradients. Hence, these surface geothermal indicators validate the accuracy of the potential CPD, geothermal and heat flow maps created (Figs. 4.2-6.9). The results of the Geological and hydrological studies across Nigeria to identify potential areas with viable thermal resources reveals that the warm springs in Ikogosi from the South-Western Nigeria have temperatures around (71°C) from the source and (41 °C) **1 km away** from the source ., Akiri (54 °C), Awe1-3 (41.5-32.7)°C , Farin Ruwa (43°C), and , Wikki warm springs (32 °C) Gwana (30.5°C), Malwulgo(30.5°C) , Ruwan Zafi (54 °C) Ruwan Dimil (26°C), Keana warm saline spring (34°C), Ribi warm saline spring (33.9 °C), Azara warm fresh water(32.7°C) and Kanje warm fresh water (34 °C) ,Numan, Rafin Ruwa (, Igbonla springs (54 °C) , Egeneja (43°C) from the North central; Ugep in Niger Delta area (45 °C) and *Azukala (37°C)in Edo State* have their thermal resources as hyper thermal, while other areas have either thermal or hypothermal (Olumirin water fall temperature (28°C) measurement was found to be hypothermal with no surface manifestation for geothermal, but with extended schist belt from the Ikogosi axis) ,River Akpalla (30°C) and Uturu-Okigwe (29 °C); (Tables 3.2 - 14 and Figs: 3.1.3.21ab). However, it is very possible for those areas with hypothermal like the Olumirin water falls to be viable but because the springs that manifested their viability did not have fault that cut deep into the region that can give viable thermal resources .

Only warm springs with hyper thermal and thermal resources are viable for the electricity generation (Tables 3.2 - 14).

Figs: 4.1(a-L, 7.1 a-h,8.1 a-h .) are samples of spectral plots used to compute depths to the top of magnetic sources (Z_t), which were obtained from the second slope/profile line breaks. Figures 4.1a-L 7.1 a-h,8.1 a-h) show samples utilized to compute depths to the centroid, Z_0 of magnetic sources in the region (z) from the first slope. Tables 15-46 Provides extended details on computational results for 55 x55 and the 27.5 x27.5km windows taken across the region. The results revealed that depth to the top of the magnetic source ranges as shown in tables 15-46. The estimated CPD, geothermal gradients, and heat flow, were obtained by applying centroid method for the blocks or windows.

The spectral analysis performed on the aeromagnetic and gravity data of study area which showed the distribution of Curie point depth, Geothermal gradient and Heat flow values across the regions of study areas in Nigeria for clean energy generation gave some geothermal evidence as shown in (Tables 15 - 46) and (Figs. 4.2- 6.9a-c).

The heat flow threshold values delineated (80-100) mW/m² within the study areas across Nigeria imply high potential of the occurrences of geothermal energy exploration (Tables 15-46). Heat flow values above the stated threshold of (80-100) mW/m² and anomalous geothermal gradients in the various regions can be said to be very good for geothermal power plant installations (Tables 15 -46) and (Figs. 4.2- 6.9a-c). These interpreted results from the Aeromagnetic and airborne gravity data confirm derived results from geological, hydrogeological and BHT measurements.

Deductions from the drawn geological / hydrogeological studies, BHT logs, Aeromagnetic and Airborne gravity maps and results for potential areas with viable thermal resources in the study areas across Nigeria are in good agreement.

On the premise of the BHT information from oil wells in the Niger Delta and Anambra Basin it has been observed that the lowest values of geothermal gradient were found in the center of Niger Delta within the thick Tertiary sediments as 1.1-2.1 °C/100 m or 2.4-2.5 °C/100 m in Edo- Ologbo -Warri-Port Harcourt areas. The values calculated in 6 points (wells) range from 3.5 to 5.6 °C/100 m and the heat flow estimated on the basis of these gradients was (82-96) mW/m² towards the Anambra Basin. By implication, a high geothermal gradient enhances the early formation of oil at relatively shallow burial depths, but causes the depth range of the oil window to be narrow, while low geothermal gradient causes the first formation of oil to begin at fairly deep subsurface levels, but makes the oil window broad.

Summarily, the results from the Geological, hydrogeological, BHT measurements, Aeromagnetic and airborne gravity interpretations correlated well and showed good manifestations of geothermal evidence for electricity generation (Tables 3.2- 14 abcd ; Figs 3.1-3.21ab) and (Tables 15- 46 ; Figs 4.2-6.9 a-c).

An effort has been made in this research to advocate a panacea to the prevailing energy crisis in Nigeria by estimating the country's geothermal energy resource potential from high resolution aeromagnetic, airborne, Temperature measurements of subsurface manifestations (geological and hydrogeological studies) and BHT logs calculations. There is widespread occurrence of warm/hot springs in Nigeria, which gives credence to the availability and abundance of geothermal reserves. Results of aeromagnetic and gravity investigations also confirm that areas with anomalous high heat flow exist in Nigeria, showing high prospects of employing geothermal energy for direct and indirect energy applications (Tables 3.2- 14 abcd ; Figs 3.1-3.21ab) and (Tables 15- 46 ; Figs 4.2-6.9 a-c).

This study have assessed various previous work conducted on the geothermal prospect in Nigeria from the geo scientific point of view. Geological and geophysical assessment reveals geothermal manifestations in both basement complex and the sedimentary geothermal settings.

In comparison to some similar researches done in Nigeria:

1. This research results on geothermal parameters for power generation reveals that our Ikogosi results heat flow range from (97.64 – 207.97) Wm^{-2} and geothermal gradient of 38.90 – 82.86 $^{\circ}\text{C}/\text{km}$ agrees with the similar research work of Fawale and Nwankwo, 2019 where the heat flow was estimated to be 93.79 – 209.54 10 Wm^{-2} and geothermal of 37.52-83.82 $^{\circ}\text{C}/\text{km}$. Most researches on Ikogosi showed that the surface temperature manifestations to be 41 $^{\circ}\text{C}$ or 38 $^{\circ}\text{C}$. Our results indicated with more information, that at the restricted point by the community that the temperature is 71 $^{\circ}\text{C}$ and 41 $^{\circ}\text{C}$ at the accessible point 1 km away from the source and 38 $^{\circ}\text{C}$ (Warm and cool water meeting point),table 3.2, in line with the study of Olurunfemi *et al*, 2011 that temperature is 38 $^{\circ}\text{C}$. The 38 $^{\circ}\text{C}$ of most researchers is the temperature at meeting point of the warm and cold water and not the source and 1km away temperature from the source as previously reported.
2. Tochukwu *et al*, 2022 estimated surface temperature of Awe2 spring in Nassarawa State to be 38 $^{\circ}\text{C}$ in conformity with our result of 39 $^{\circ}\text{C}$ and anomalous heat flow results,table4.
3. Aliu and Mazian 2018 on geothermal detection in South Central Bauchi concluded that geothermal manifestation exist in some parts of Central Bauchi and North Central. This results was validated by this research with high thermal resources in Yankari and Wikki axis of Bauchi (Section 3.3.4).

4. Odumodu and Mode, 2016 result on geothermal and heat flow in eastern Nigeria Delta on BHT data, estimated geothermal gradient to vary between 18-45⁰C/km in conformity with Abraham and Nkitnam and our research on geothermal results in Niger Delta on BHT as 1.1-2.1⁰C/100m or 2.4-2.50⁰C/100m in Warri Port Harcourt axis (Section 5.21).
5. On geothermal investigation in Ado –Ekiti which is the same geological setting of Ikogosi, Abraham *etal* 2014 opined. The average Curie point depth for the Ikogosi warm spring area is 15.1 ± 0.6 km and centres on the host quartzite rock unit. The computed equivalent depth extent of heat production provides a depth value (14.5 km) which falls within the Curie point depth margin and could indicate change in mineralogy. The low Curie point depth observed at the warm spring source is attributed to magmatic intrusions at depth. This is also evident from the visible older granite intrusion at Ikere - Ado-Ekiti area, with shallow Curie depths (12.37 ± 0.73 km). This results is in line with our research on Curie point depth of 14.91km and heat flow of (97.64-207.97) mW/m² (Table 34 and Figs 5.6a – 5.6c).
6. The research results using BHT and aeromagnetic data indicated that the geothermal and heat flow results of this research of 1.1-2.1 ⁰C/100m or 2.4-2.50 ⁰C/100m in Warri, Port Harcourt validated the results of Abraham and Nkitnam 2017 on BHT in Niger Delta and Anambra and Basin results (Section 5.21).
7. Our research study on Ruwa Zafi area and environs using Aeromagnetic and Airborne gravity integration showed that the temperature from at the source of the warm spring is 54 ⁰C (3.3.2) with high heat flow results for geothermal prospect, the heat flow values ranges from 66.65 to 122.13mW/m² (Section 4.12). This study further confirmed the works of Onyejiuwaka, & Iduma, (2020) on Assessment of Geothermal Energy Potential of Ruwan Zafi, Adamawa State and Environs, Northeastern Nigeria, using High Resolution Airborne Magnetic Data with temperature as 54⁰C and the associated mantle heat flow varies from about 84.48 to 172.53 mW/m² (Section 3.3.2).
8. Eko *etal*, 2022 on geothermal assessment around Akiri reveals moderate geothermal and heat flow results around Akiri and Awe as (31.9-79.7)mW/m² which is below our research work on four integrated methods with heat flow of (71.33-197) mW/m² .There is the need for Eko *etal*, 2022 to probe deeper into the earth's mantle since they applied ground magnetic method with limitations /resolutions.
9. Anyadiegwu and Aigbogun (2021) Estimated the Curie Point Depth, Heat Flow and Geothermal Gradient Determined from Analysis of Aeromagnetic Data over parts of the Lower Benue

Trough and Anambra Basin, Nigeria. The results revealed that the average Curie point Depth of the Study area is 8.07594 km, the Geothermal gradient obtained has an average value of 73 °C/km, The study area has an average heat flow of 170 mW/m². Results of airborne gravity spectral analysis for Akiri (middle Benue trough) study area revealed the occurrence of geothermal parameters: Curie point depth varied between 7.39 to 20.71 km, geothermal gradient varied between 28.01 to 78.48 °C/km and heat flow values varied between 70.29 to 197.99 mW/m². Table 15 presents the summary of the results of the centroid depth, depth to basement, curie depth, geothermal gradient and the heat flow. The aeromagnetic data of **Akiri_ (Sheet 232)** was subjected to spectral analysis with the aim of accessing tAkirihe geothermal potential of the study area and environs. The Curie point depth values ranges from (7.44- 20.81) km, the geothermal gradient values ranges from (27.87– 77.95) °C/km and the heat flow values ranges from (69.68- 194.87) mW/m² (Table33). The NE edge covering Jangwa, Azara, Akiri, and Ribi hosts the anomalous heat flow and geothermal gradient with corresponding shallowest values of curie point depth (Fig 5.5 a-c). Other regions like Kumar, Jutu, Kanje, Adawa, Atatakoru, and Kaza also show good geothermal manifestations, except few areas in SW covering Tunga with low heat flow below the recommended threshold value of (80 - 100)mW/m². In general the results for the area/ regions studied correlate well when compared as seen above .

The aeromagnetic data of **Bauchi _Sheet 148** was subjected to spectral analysis with the aim of accessing the geothermal potential of the study area and environs. The Curie point depth values ranges from (15.14- 23.81) km, the geothermal gradient values ranges from (8.23– 19.504) °C/km and the heat flow values ranges from (74.344- 176.183) mW/m² (Table 40). The SE edge hosts the highest values of anomalous heat flow and geothermal gradient with corresponding shallowest values of Curie point depth (Fig. 6.3 a-c). This results validated the works of Anyadiegwu and Aigbogun (2021).

The aeromagnetic, airborne gravity, geological and BHT data have been able to identify the fractured migmatite and quartzite/faulted zone as a result of the magnetic minerals contained in the areas of surface manifestations and other areas without surface manifestations. It was suspected that the fractured/faulted quartzite may have acted as conduits for the movement of warm groundwater from deep depth to the surface in most areas/ regions as shown in the geological maps. The depth to magnetic sources estimated in this research and its correlation with the faulting systems provides information about the geodynamic activities around all the warm springs studied. The estimated depth to magnetic anomaly which is probably an indicative of magma intrusion is relatively shallow and thus has several implications on the geothermal resources and tectonic activities in the areas. The heat flow

in the areas is high enough to cause the surface geothermal manifestation within Akiri- Awe, Farin Ruwa, Ruwan Zafi, Azukala, Yankari and Wikki, Keana, Kanje, Rib, Igbonla, Enemabia, Numan, Ugep and Ikogosi warm springs and other areas with heat flow range (80-100) W/m² (Tables 15-46 and Figs 4.2-6.9 a-c) respectively.

It can be concluded therefore from the interpreted data supported by existing literatures and other field observations that the manifestation of hot springs in most areas/regions of the study is largely supported by the presence of faults and that the areas and environs as indicated in the geological maps are promising for further geothermal exploration/development.

As part of our contributions to knowledge and further studies we have acquired, interpreted and have new results of CPD, geothermal gradients and heat flow for the following regions for possible clean electricity generations, Numal, Akiri, Farin Ruwa, Lokoja, Auch, Nsukka, Abo, Okigwe, Onitsha, Kotonkarfi, Jalingo, Kaltungo, Ugep, Ilesha, Ijebu Ode, Ijebu Ife, Ado- Ekiti, Pennington Rivers, Bayelsa, Bauchi, and Chad Basin (section 5.3-5.21, figs. 5.1-6.9 and tables 29-46a).

It is, therefore, imperative for Nigeria government to take a quantum leap in holistic renewable energy research and development through the NCC appropriate government science advice, policy and environmental management. However, the published article, conference/ workshops acceptance are also attached in this report with acknowledgements.

We strongly recommend from the geological and hydrogeological assessment that areas:

- (i) with hot springs water thermal temperatures of (>30– 40°C) or hyperthermal (>40°C) be explored for geothermal clean power generation across Nigeria (tables 3.2- 14 and Figs 3.1- 3.21ab) respectively.
- (ii) development/exploitation and geothermal power installations be carried out in areas where the heat flow values estimated falls within or above the threshold value 80 mW/m² across Nigeria, (high potential or anomaly of the occurrences of geothermal energy), (Tables 15-46 and Figs 4.2-6.9 a-c) respectively.

This research reveals information that can assist in deciding on locations with better geothermal prospects before power plant installations. Binary cycle power plant is recommended for the electricity generation due to its low temperature that can be heated up by the plant, 0.1-40MW units common and 10% efficient.

6.1 Further Recommendations

- (i) In order to achieve national climate goals, Nigeria can use geothermal resources (due to its spread across the country) through the NCC to generate electricity for utilizations in the industries, offices, homes, grow food in greenhouses and recycle plastics, . Furthermore, geothermal power plants have become a hotbed for innovation that deals directly with future challenges such as capturing carbon emissions.
- (ii) As more nations explore solutions to move from fossil fuels to more environmentally friendly energy alternatives, NCC should lead the way as usual in advocating for a geothermal-fueled future by going to the next stage with these innovation for the geothermal power generation as a source of clean energy.
- (iii) Nigerian Government should implement policies to encourage relevant agencies towards ensuring that more data and information relating to geothermal resource are obtained through Research and Development (R&D) programmes with a view to immediately commence utilizing this resource to generate power for her citizens.

By this Innovative clean energy through geothermal, Nigeria and NCC in particular will be able to have an outsized impact on the battle against climate change as the projects offer clean energy to larger populations.

ACKNOWLEDGMENTS

The researchers would like to thank the **Nigerian Telecommunications Commission (NCC)** for sponsoring this laudable project.

APPENDIX I

EXAMPLES OF ENERGY SPECTRUM AGAINST WAVE NUMBER COMPONENTS USING MATLAB SOFTWARE FROM THE AEROMAGNETIC DATA

RADIALLY AVERAGED POWER SPECTRUM

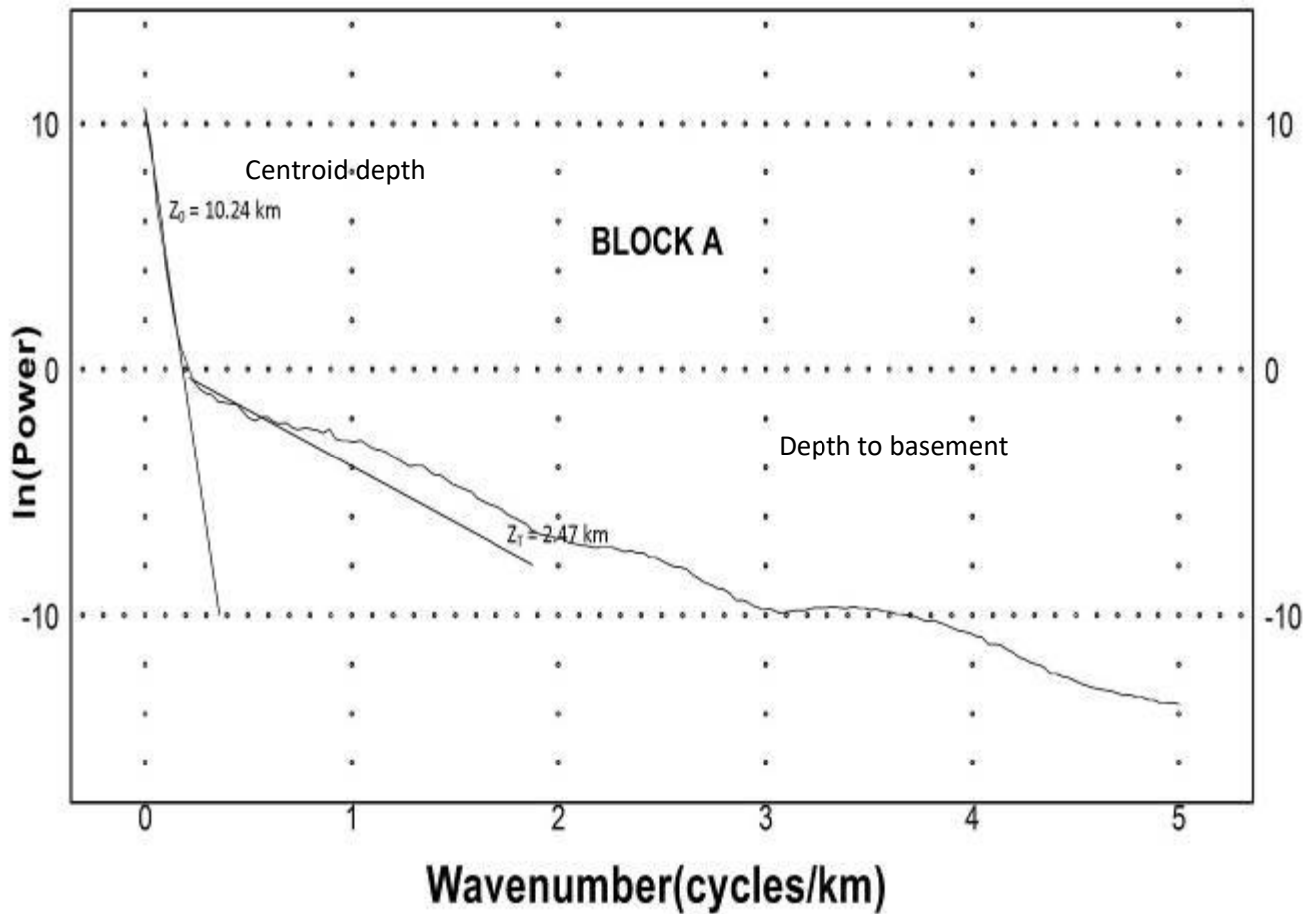


Fig 7.1a: Plots of spectrum energy against wave number (spectral block A **Sheet 300**)

Spectra plots utilized to compute depths to the centroid of magnetic sources in the region.

RADIALLY AVERAGED POWER SPECTRUM

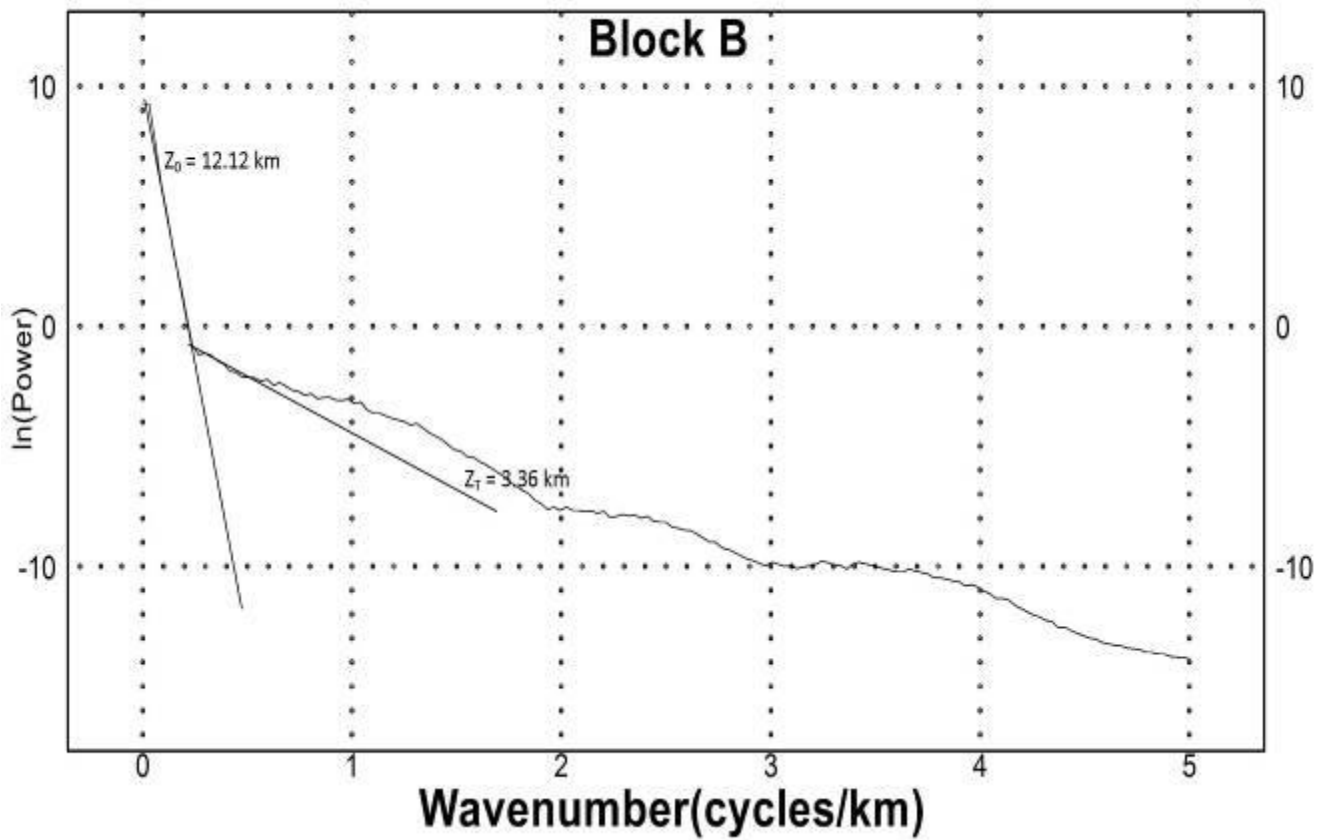


Fig 7.1b Plots of spectrum energy against wave number (spectral block B **Sheet 300**)

RADIALLY AVERAGED POWER SPECTRUM

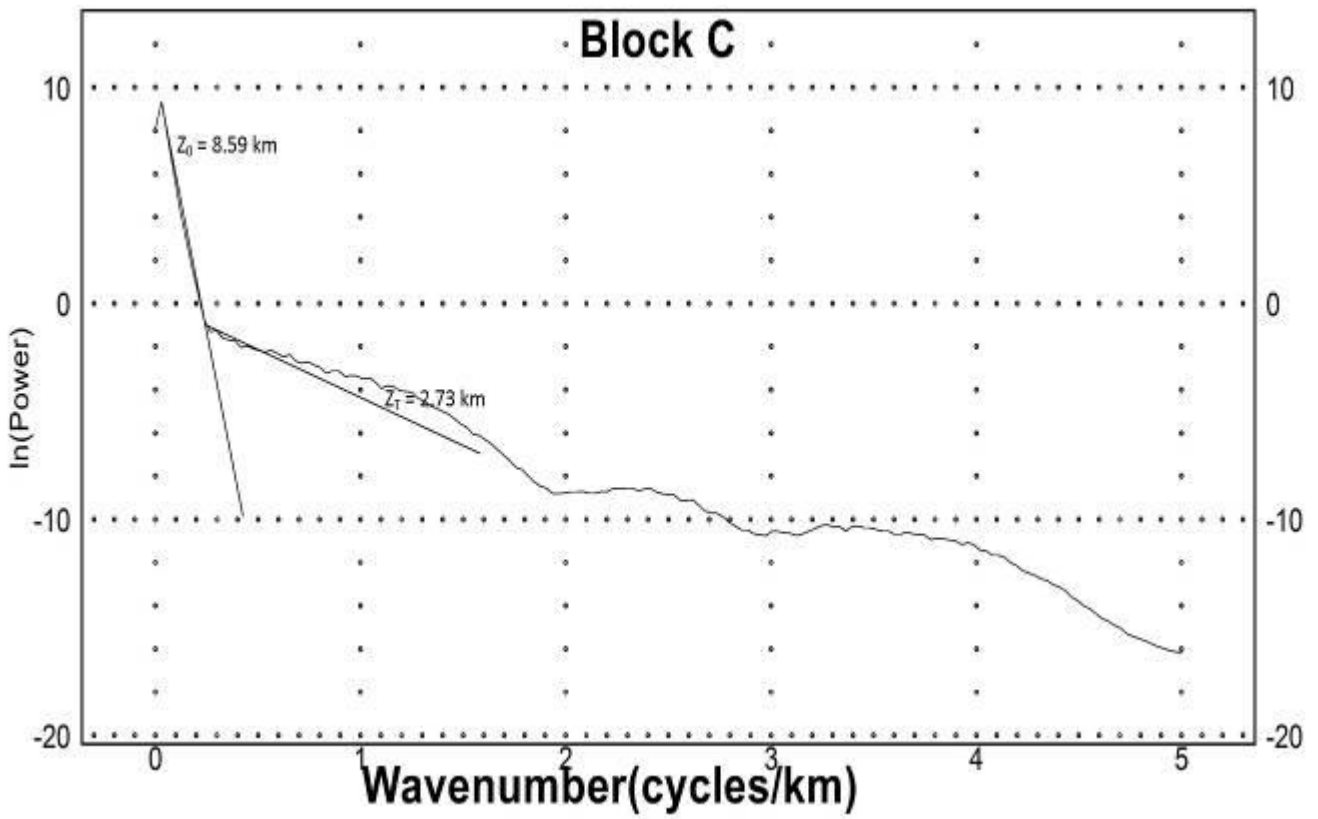


Fig 7.1c Plots of spectrum energy against wave number (spectral block C **Sheet 300**)

RADIALLY AVERAGED POWER SPECTRUM

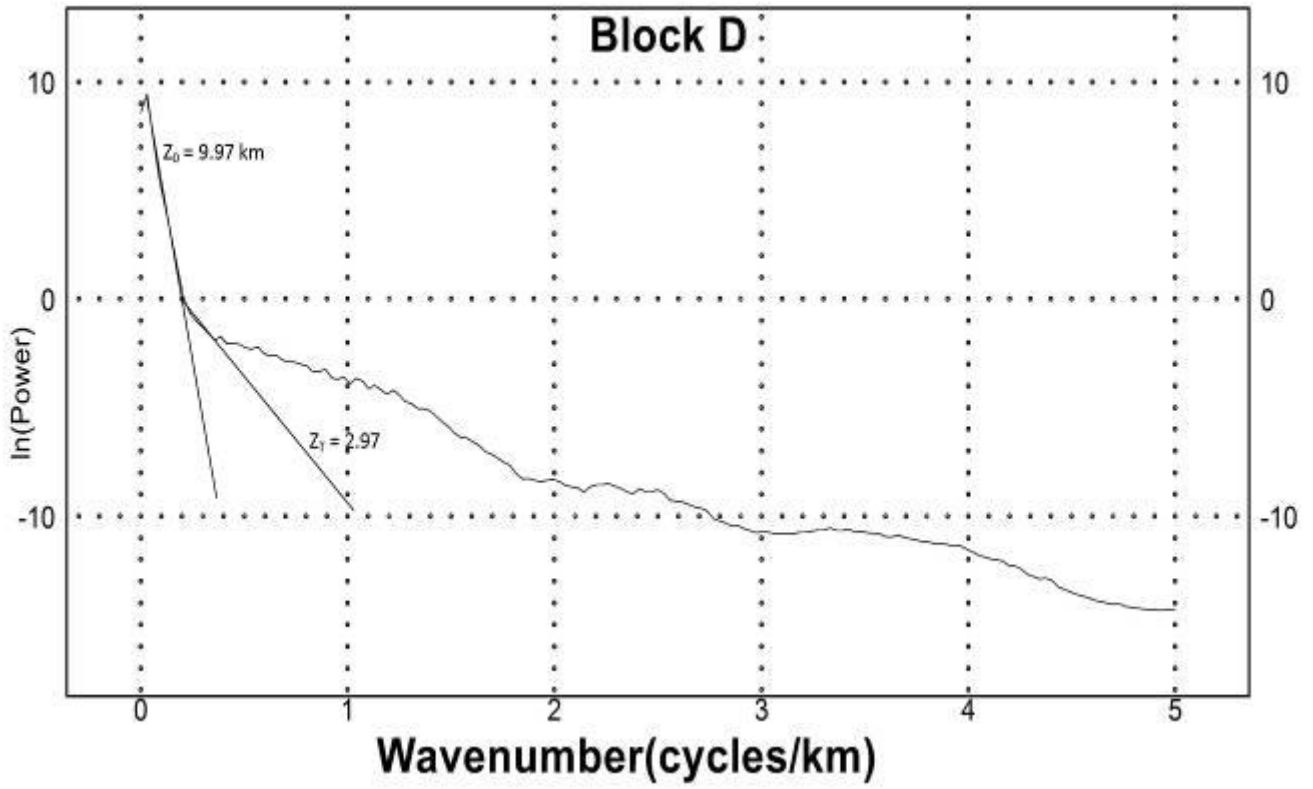


Fig 7.1d Plots of spectrum energy against wave number (spectral block D **Sheet 300**)

RADIALLY AVERAGED POWER SPECTRUM

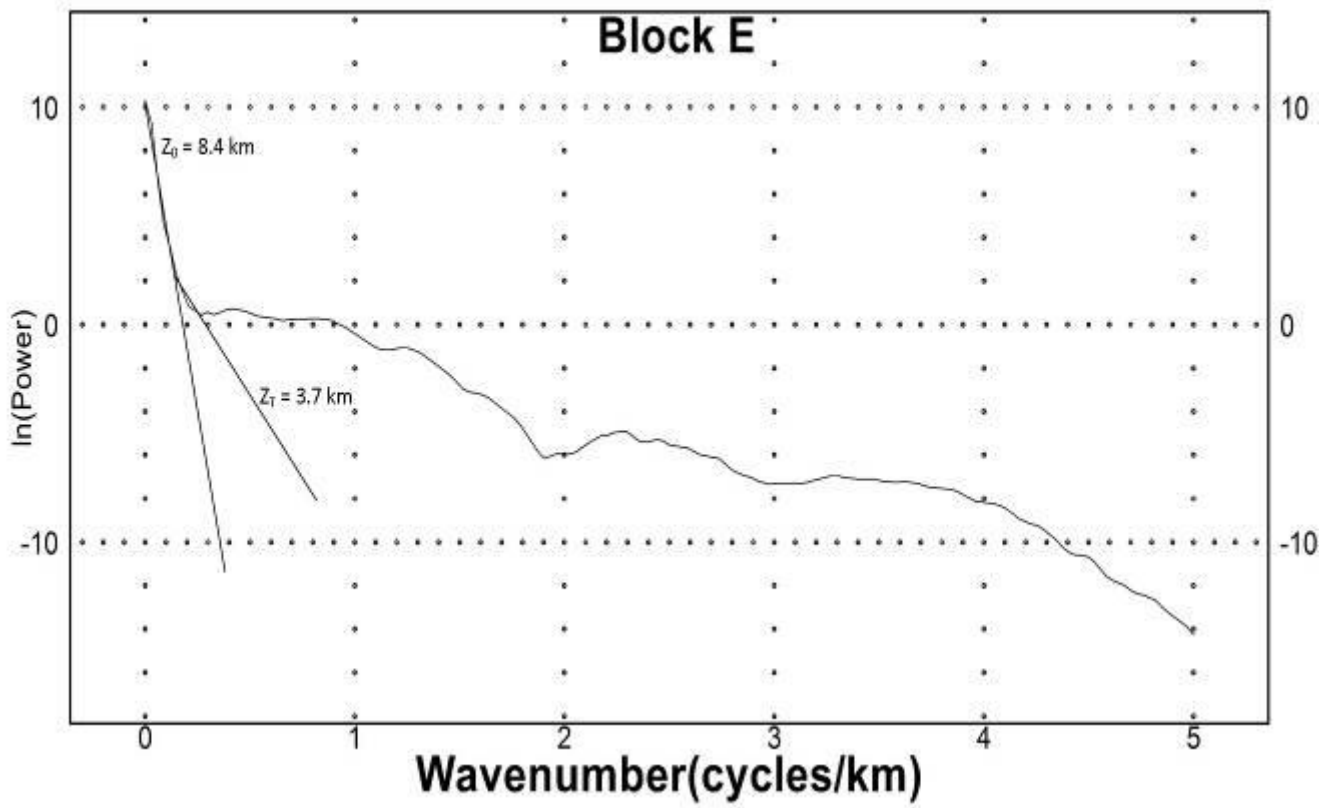


Fig 7.1e Plots of spectrum energy against wave number (spectral block E **Sheet 300**)

RADIALLY AVERAGED POWER SPECTRUM

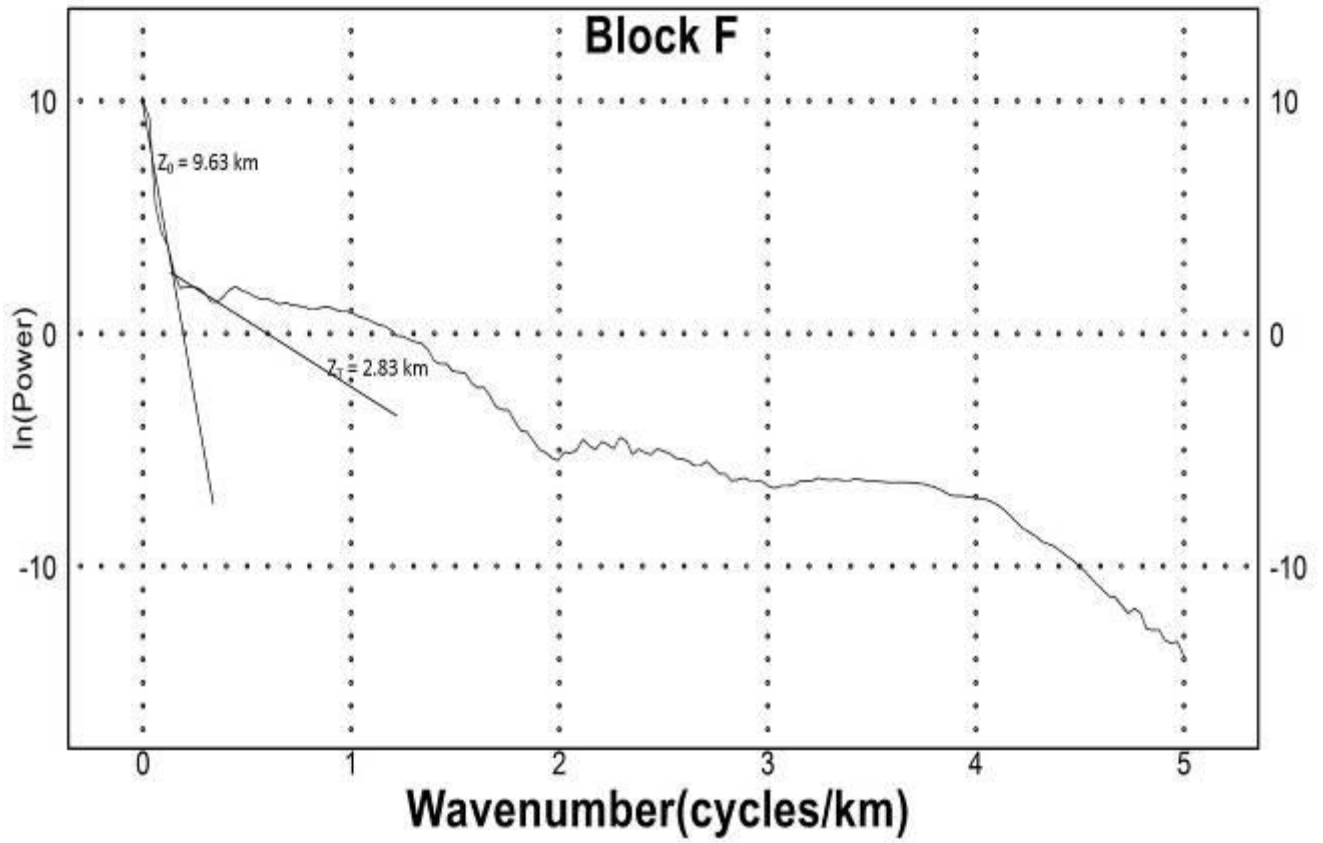


Fig 7.1f Plots of spectrum energy against wave number (spectral block F **Sheet 300**)

RADIALLY AVERAGED POWER SPECTRUM

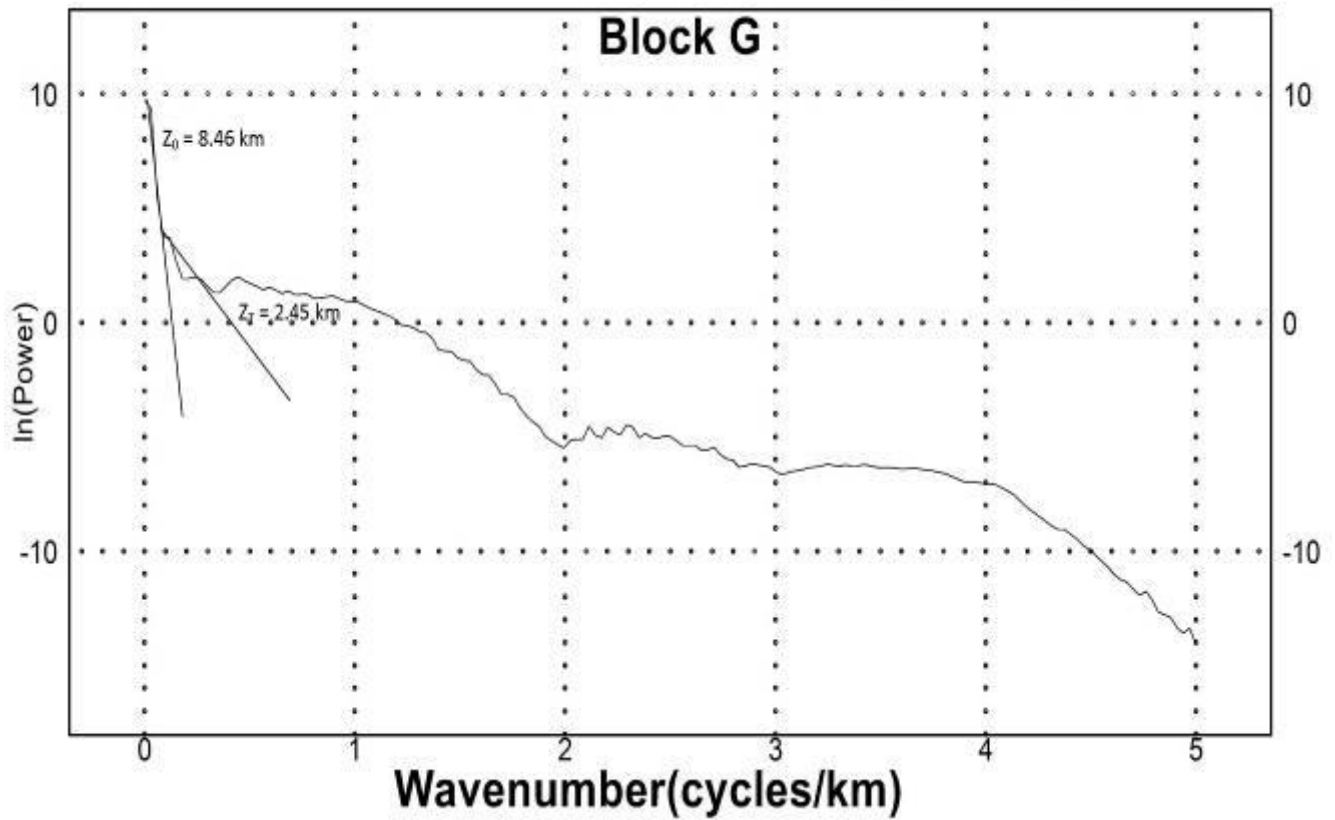


Fig 7.1g Plots of spectrum energy against wave number (spectral block G Sheet 300)

RADIALLY AVERAGED POWER SPECTRUM

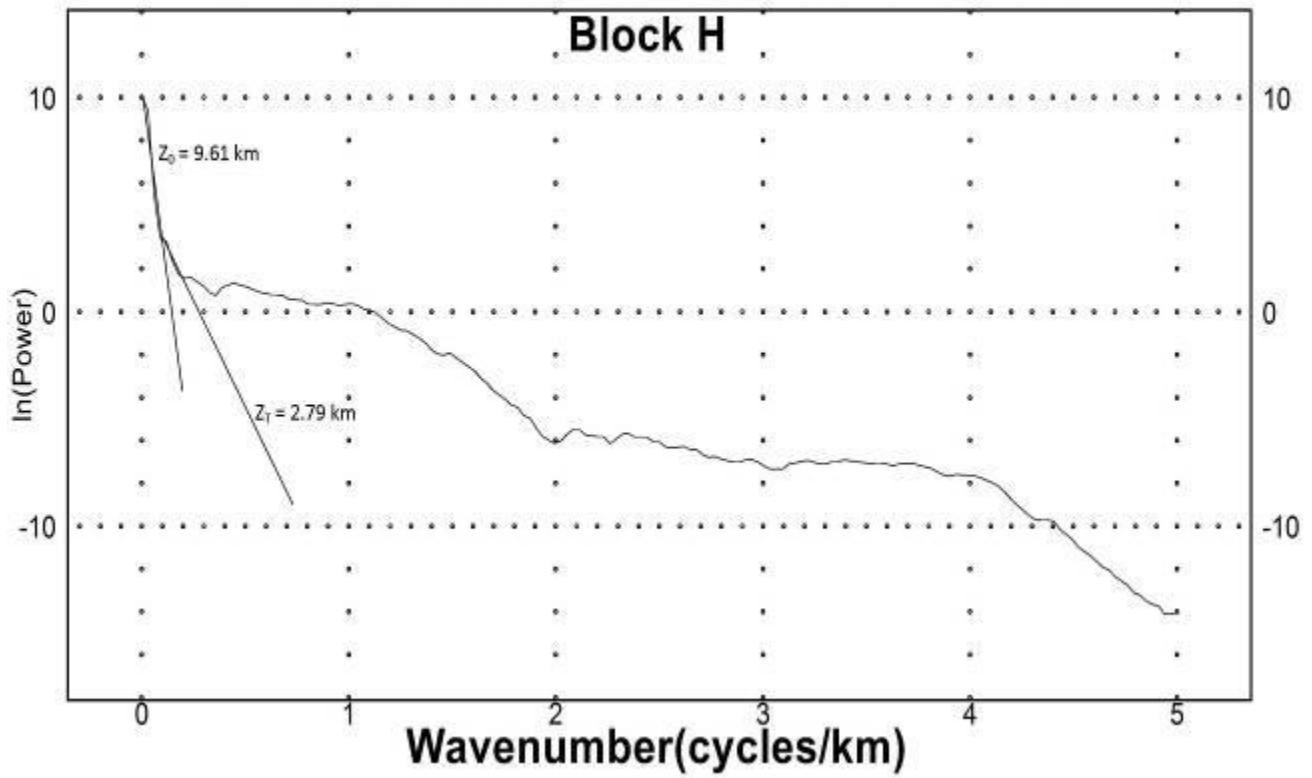


Fig 7.1h Plots of spectrum energy against wave number (spectral block G **Sheet 300**)

RADIALLY AVERAGED POWER SPECTRUM

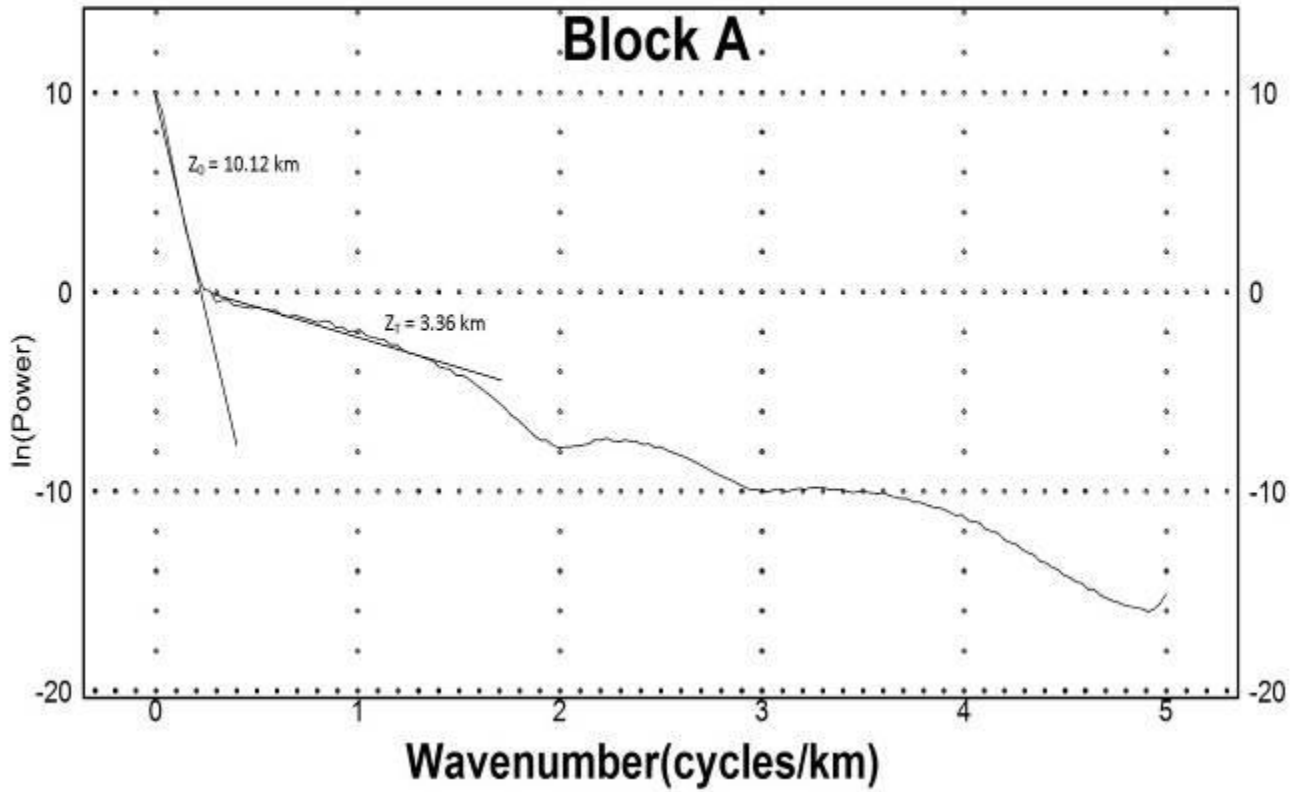


Fig 8.1a Plots of spectrum energy against wave number (spectral block A **Sheet 312**)

RADIALLY AVERAGED POWER SPECTRUM

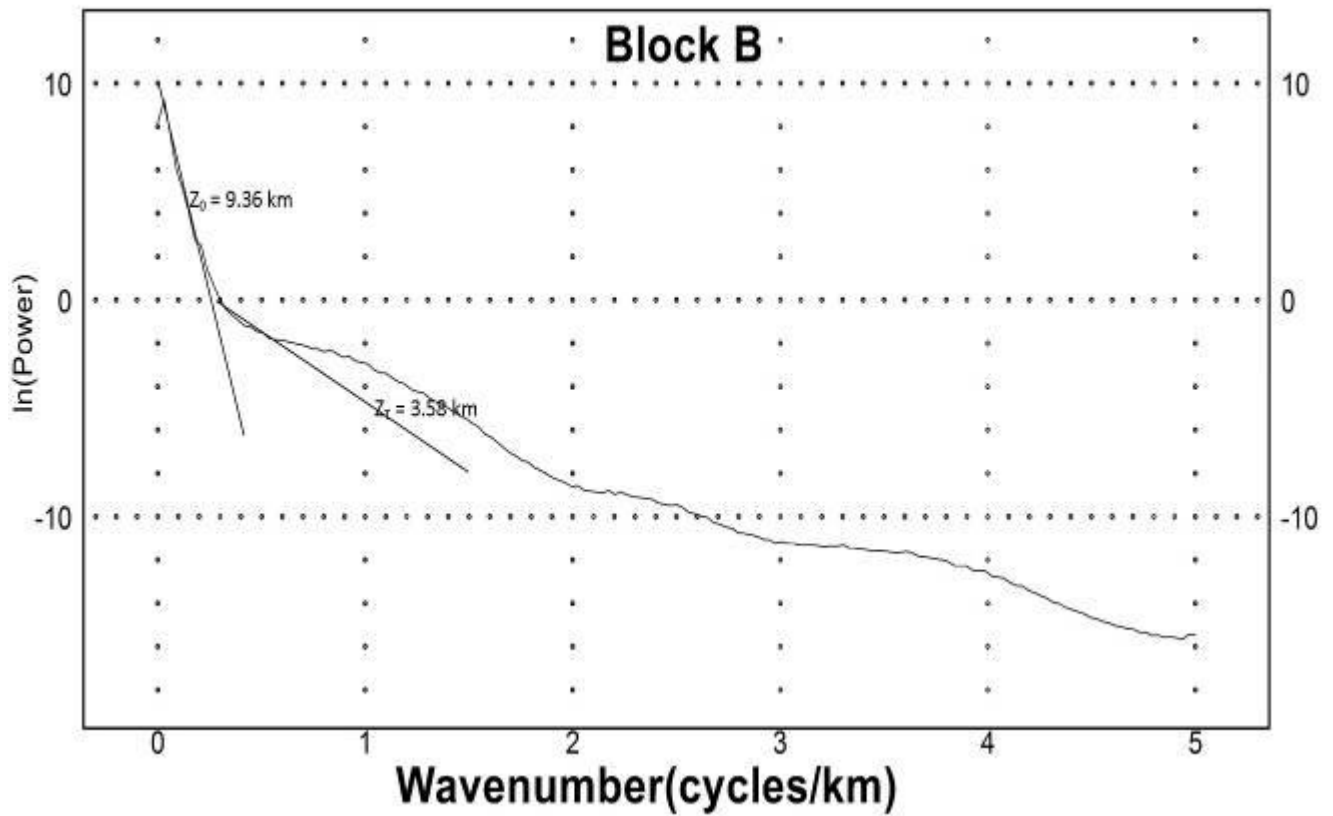


Fig 8.1b Plots of spectrum energy against wave number (spectral block **B Sheet 312**)

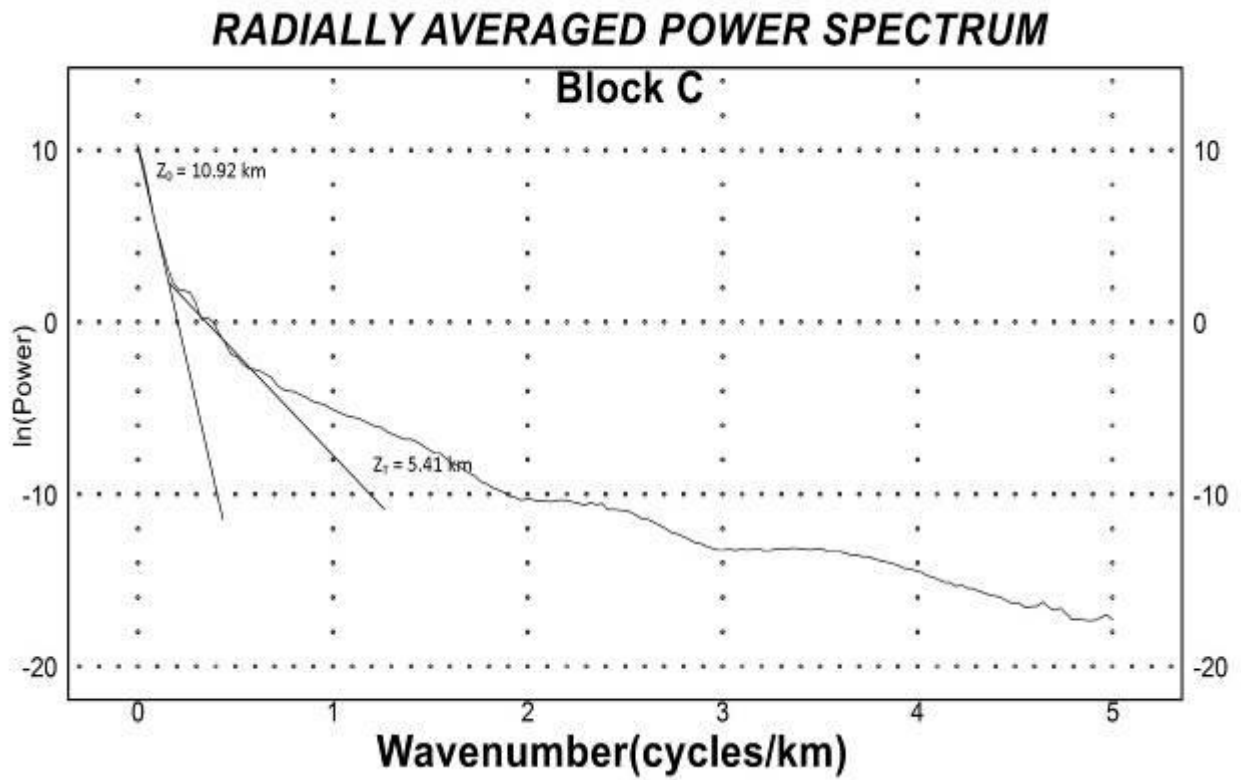


Fig 8.1c Plots of spectrum energy against wave number (spectral block C **Sheet 312**)

RADIALLY AVERAGED POWER SPECTRUM

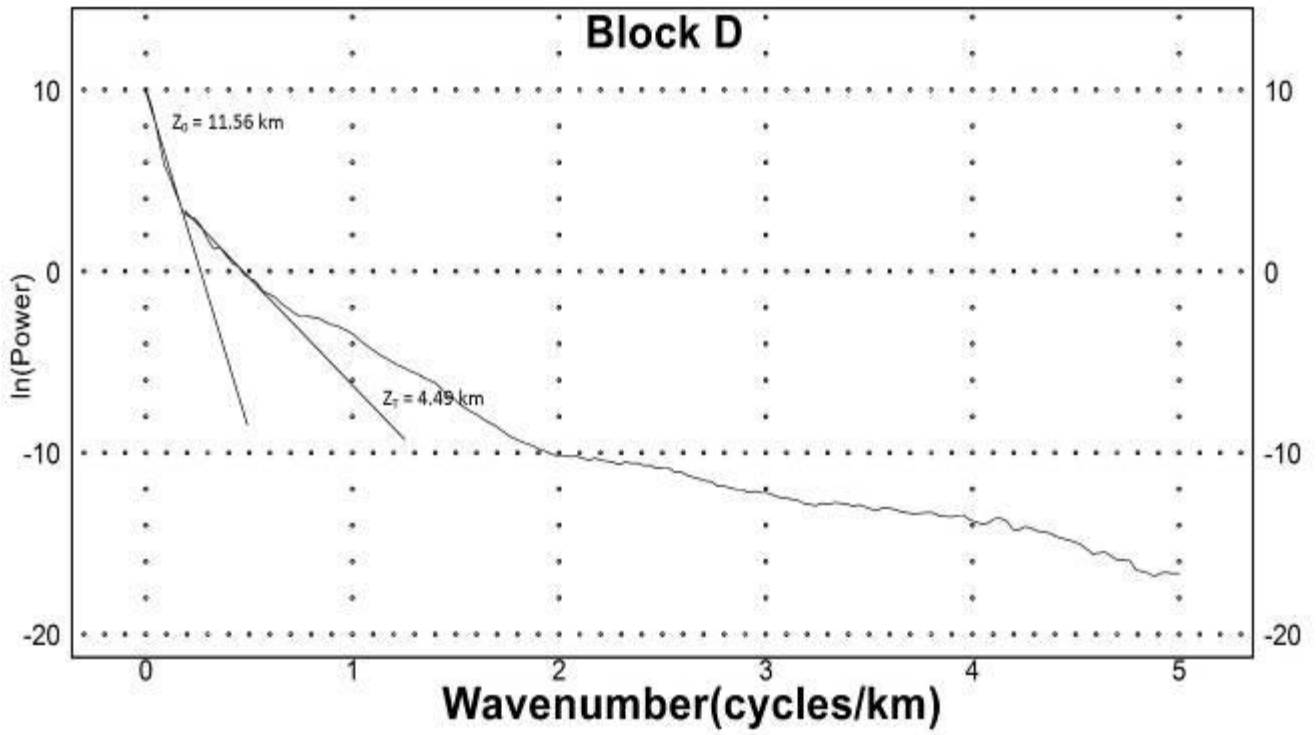


Fig 8.1d Plots of spectrum energy against wave number (spectral block D **Sheet 312**)

RADIALLY AVERAGED POWER SPECTRUM

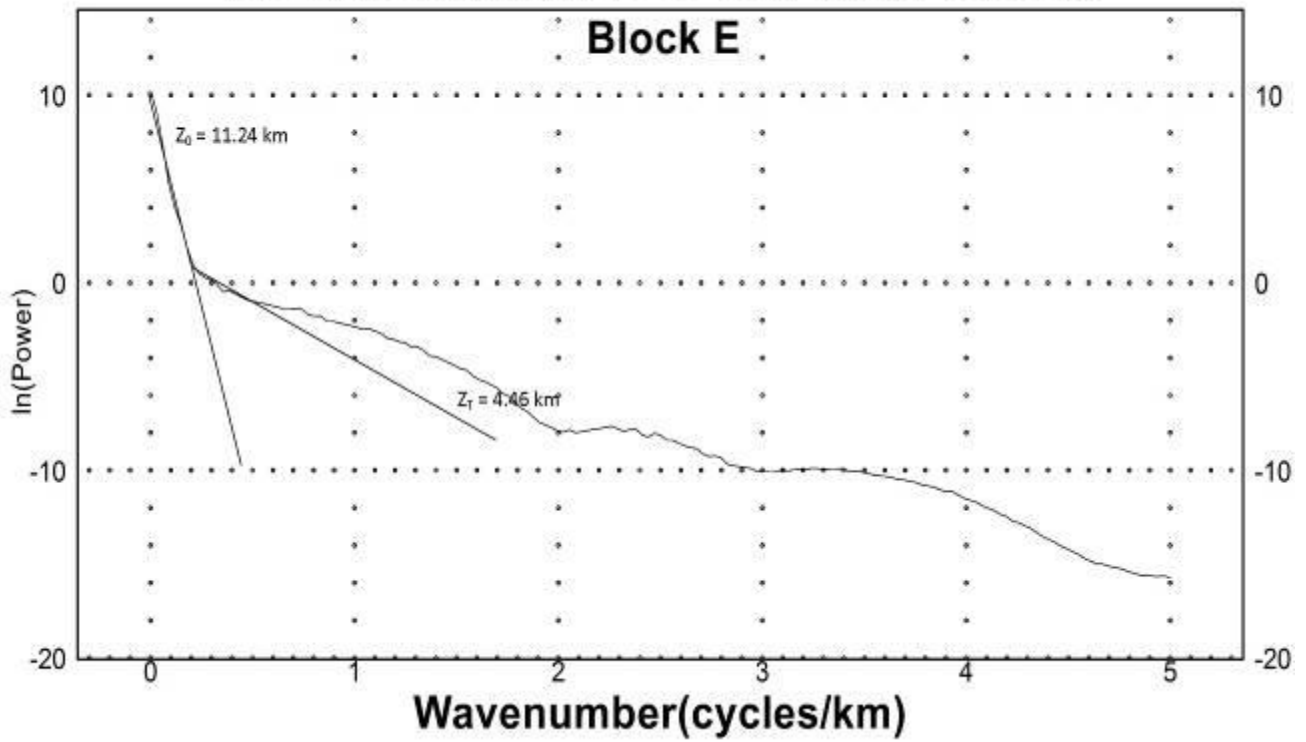


Fig 8.1e Plots of spectrum energy against wave number (spectral block E Sheet 312)

RADIALLY AVERAGED POWER SPECTRUM

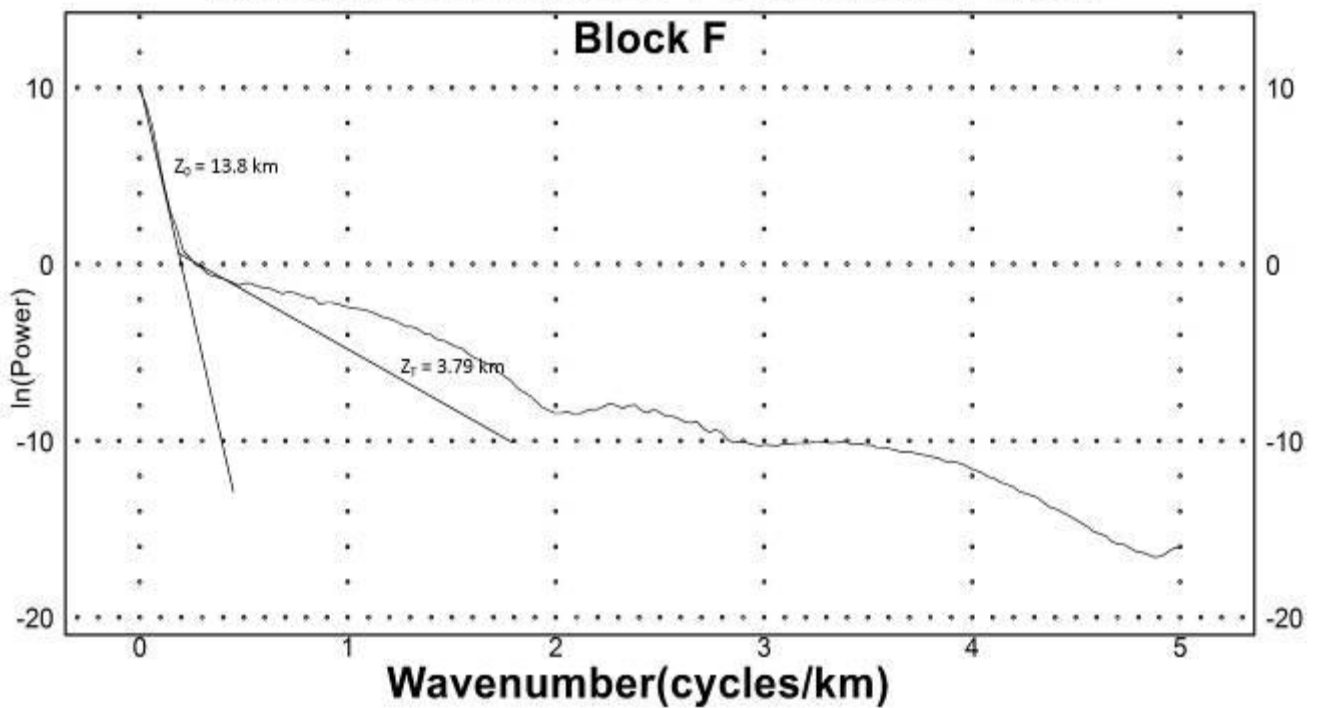


Fig 8.1f Plots of spectrum energy against wave number (spectral block F Sheet 312)

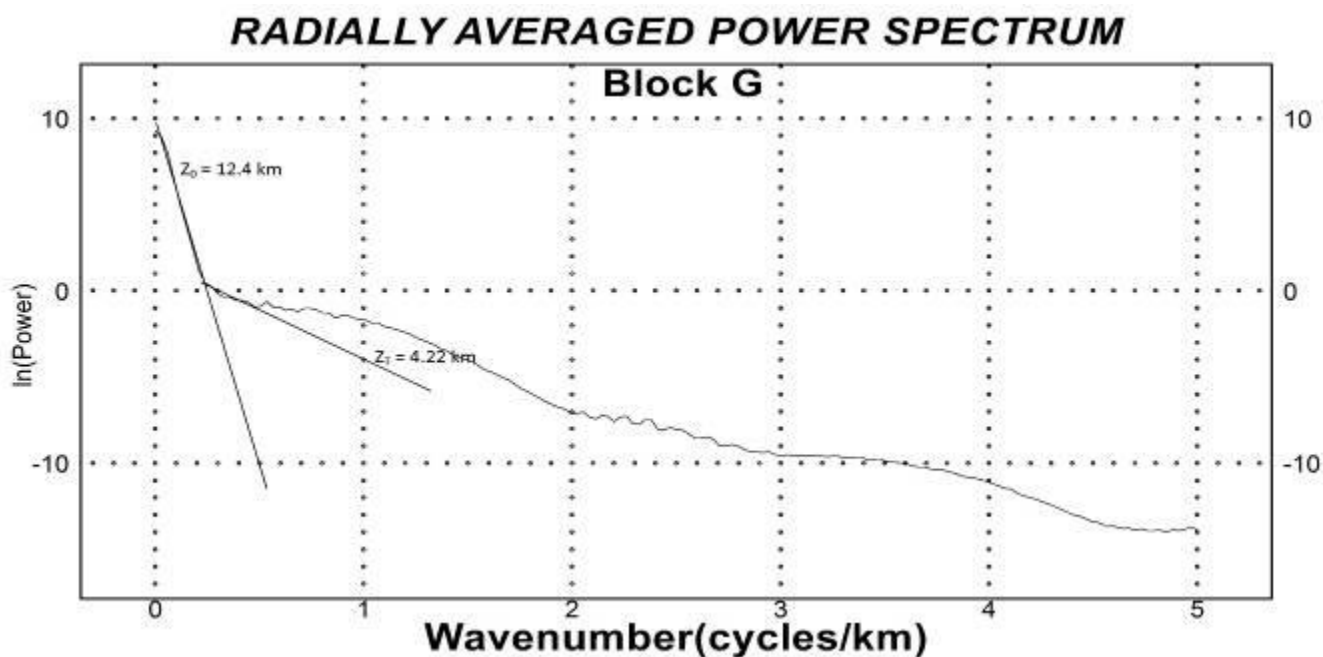


Fig 8.1g Plots of spectrum energy against wave number (spectral block G Sheet 312)

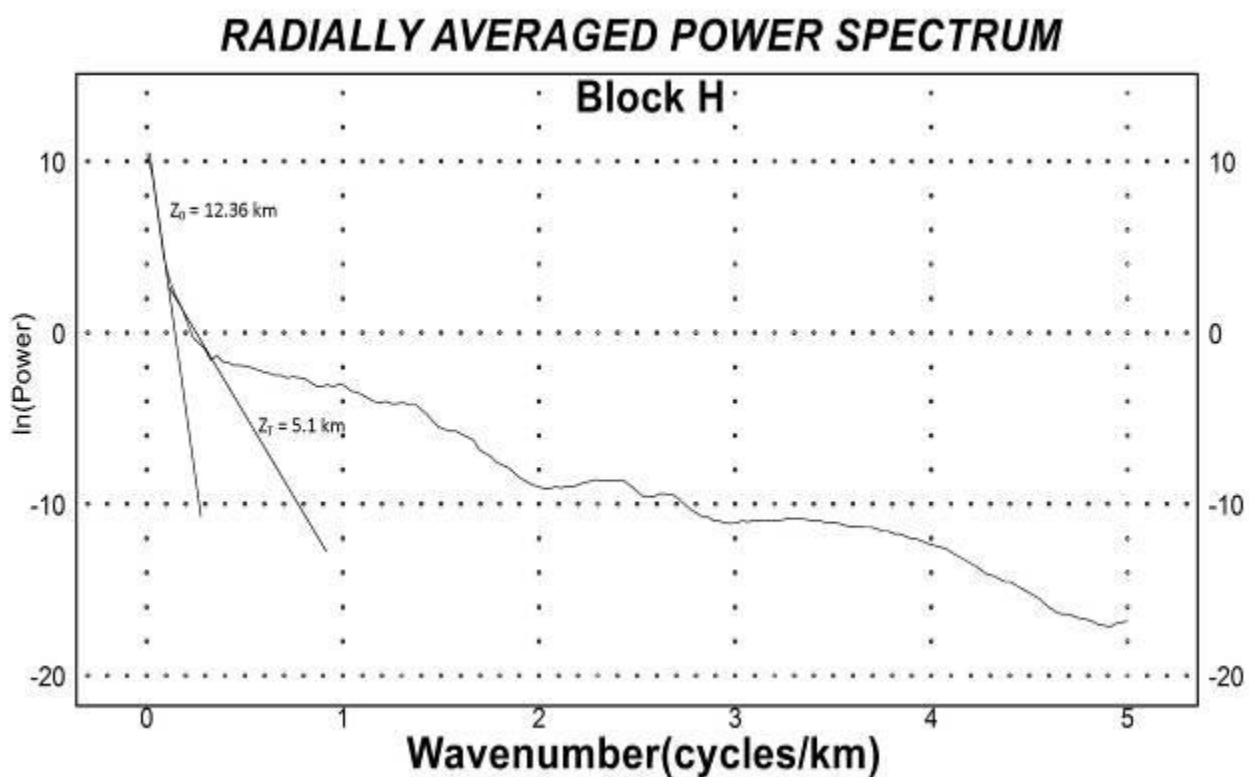


Fig 8.1h Plots of spectrum energy against wave number (spectral block H Sheet 312)

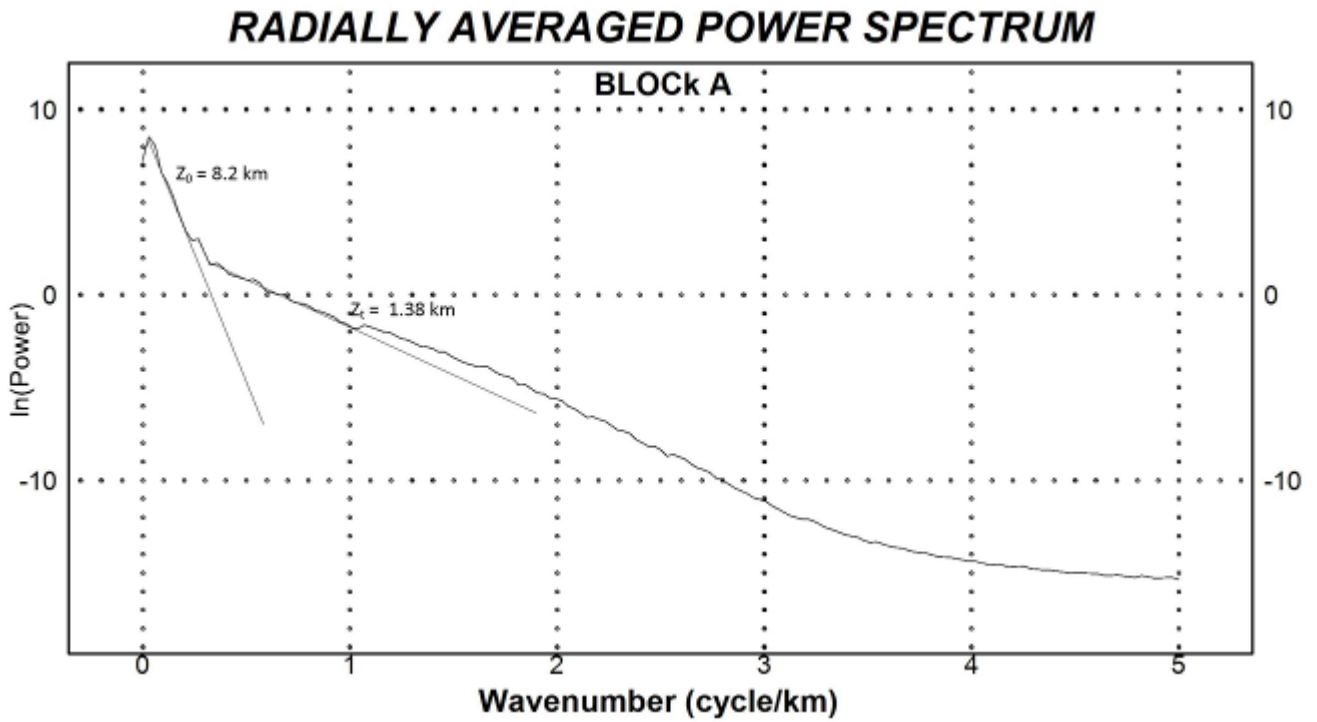


Fig 9.1a Plots of spectrum energy against wave number (spectral block H **Sheet 147A**)

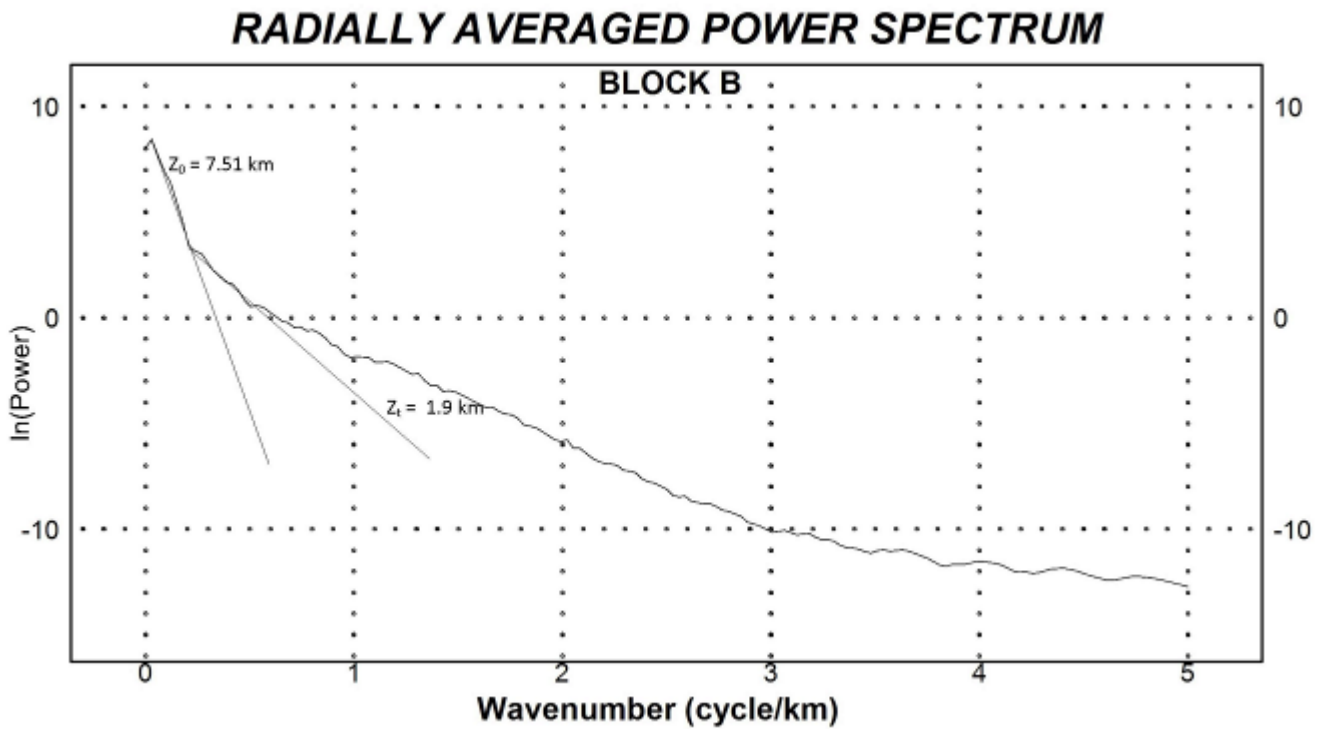


Fig 9.1b Plots of spectrum energy against wave number (spectral block H **Sheet 147B**)

RADIALLY AVERAGED POWER SPECTRUM

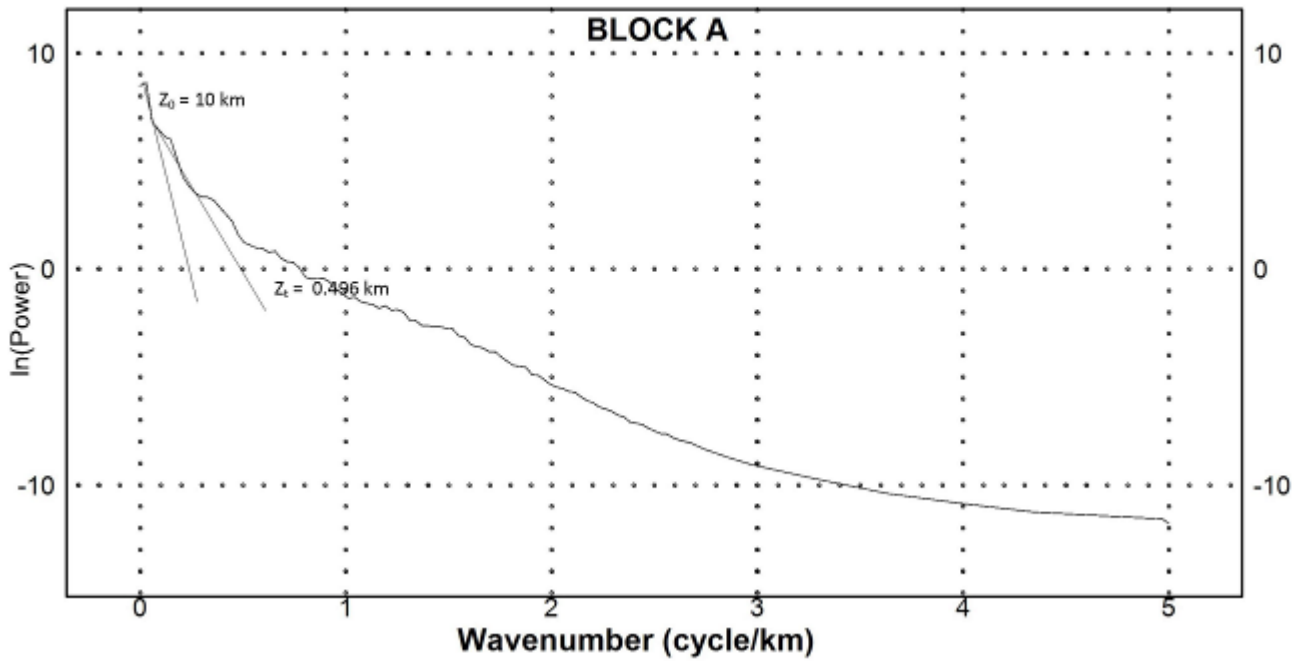


Fig 9.1c Plots of spectrum energy against wave number (spectral block H Sheet 148A)

RADIALLY AVERAGED POWER SPECTRUM

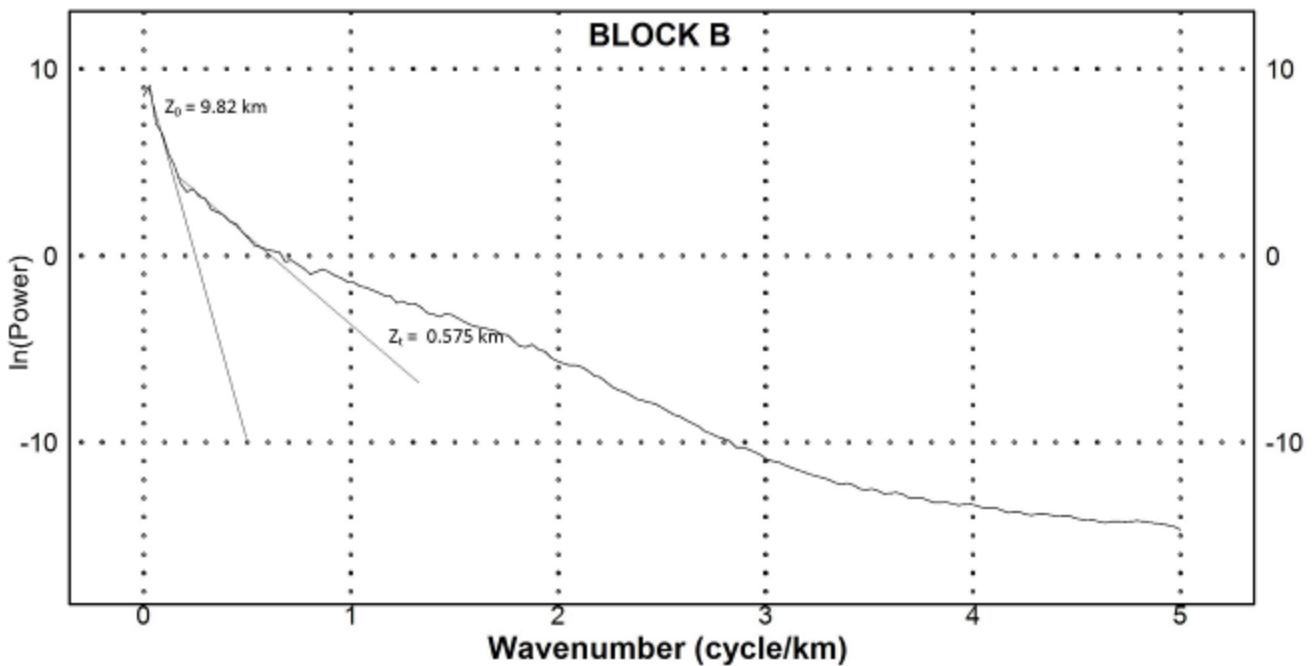


Fig 9.1d Plots of spectrum energy against wave number (spectral block H Sheet 148B)

RADIALLY AVERAGED POWER SPECTRUM

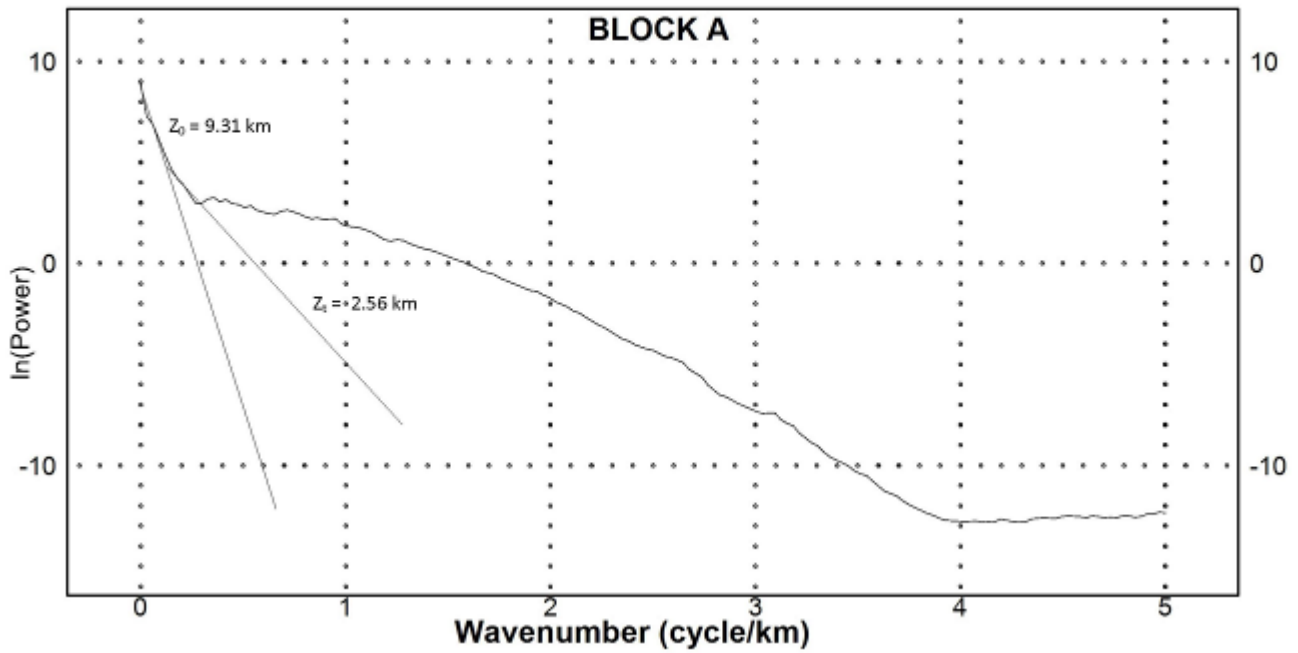


Fig 9.1e Plots of spectrum energy against wave number (spectral block H Sheet 173A)

RADIALLY AVERAGED POWER SPECTRUM

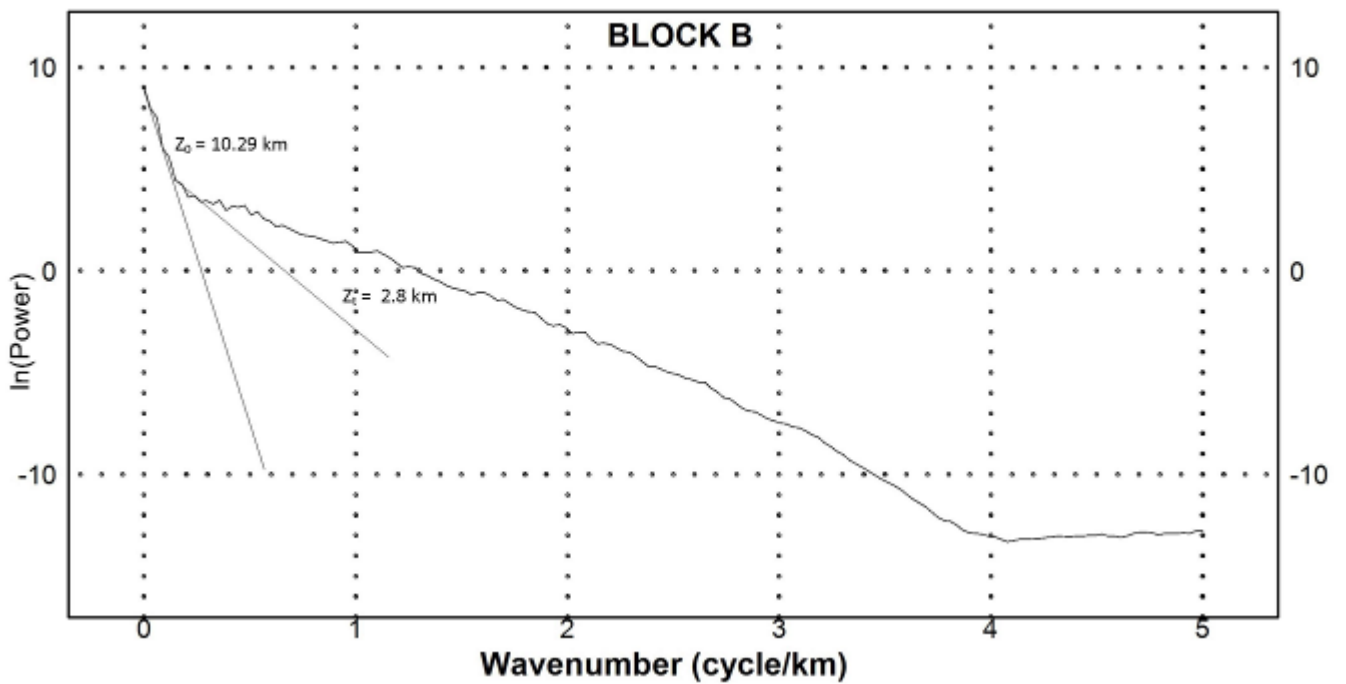


Fig 9.1f Plots of spectrum energy against wave number (spectral block H Sheet 173B)

RADIALLY AVERAGED POWER SPECTRUM

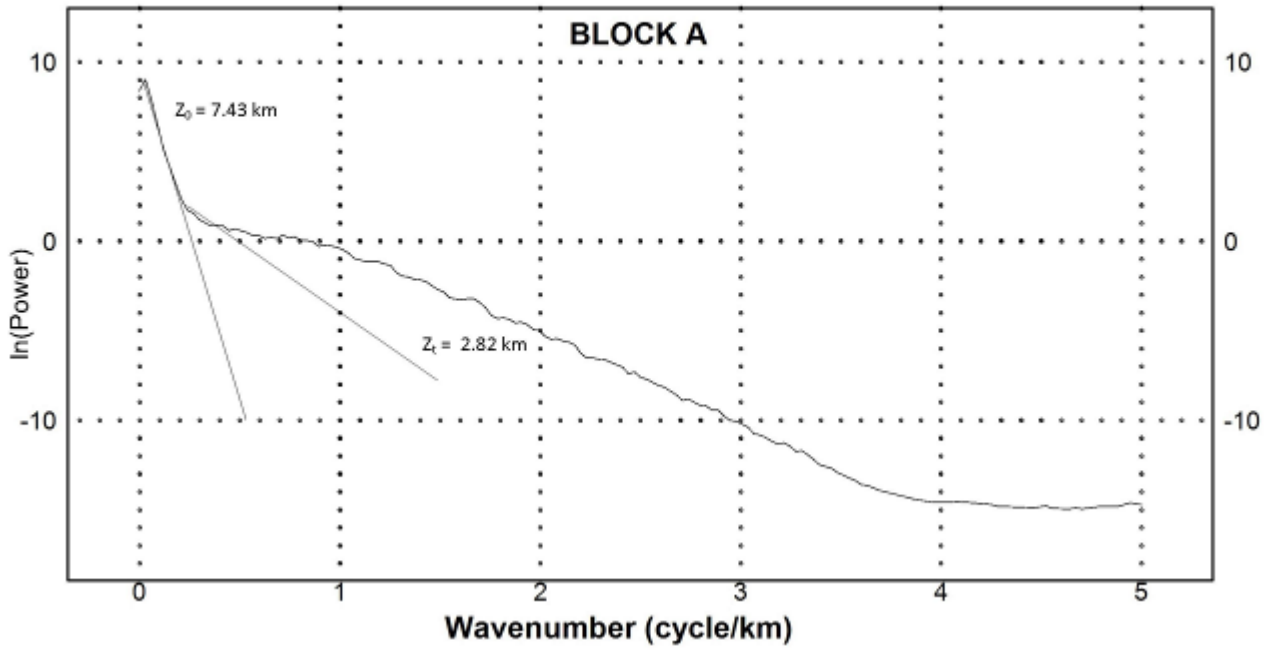


Fig 9.1h Plots of spectrum energy against wave number (spectral block H Sheet 196A)

RADIALLY AVERAGED POWER SPECTRUM

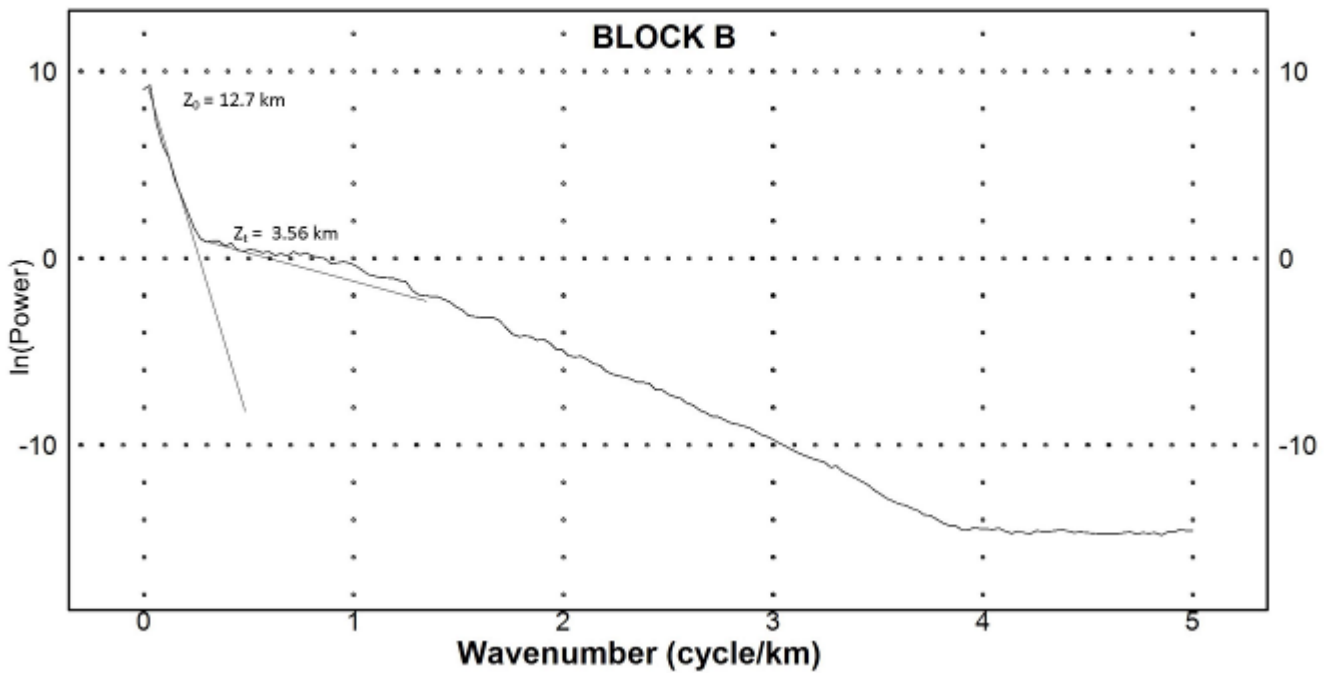


Fig 9.1i Plots of spectrum energy against wave number (spectral block H Sheet 196B)

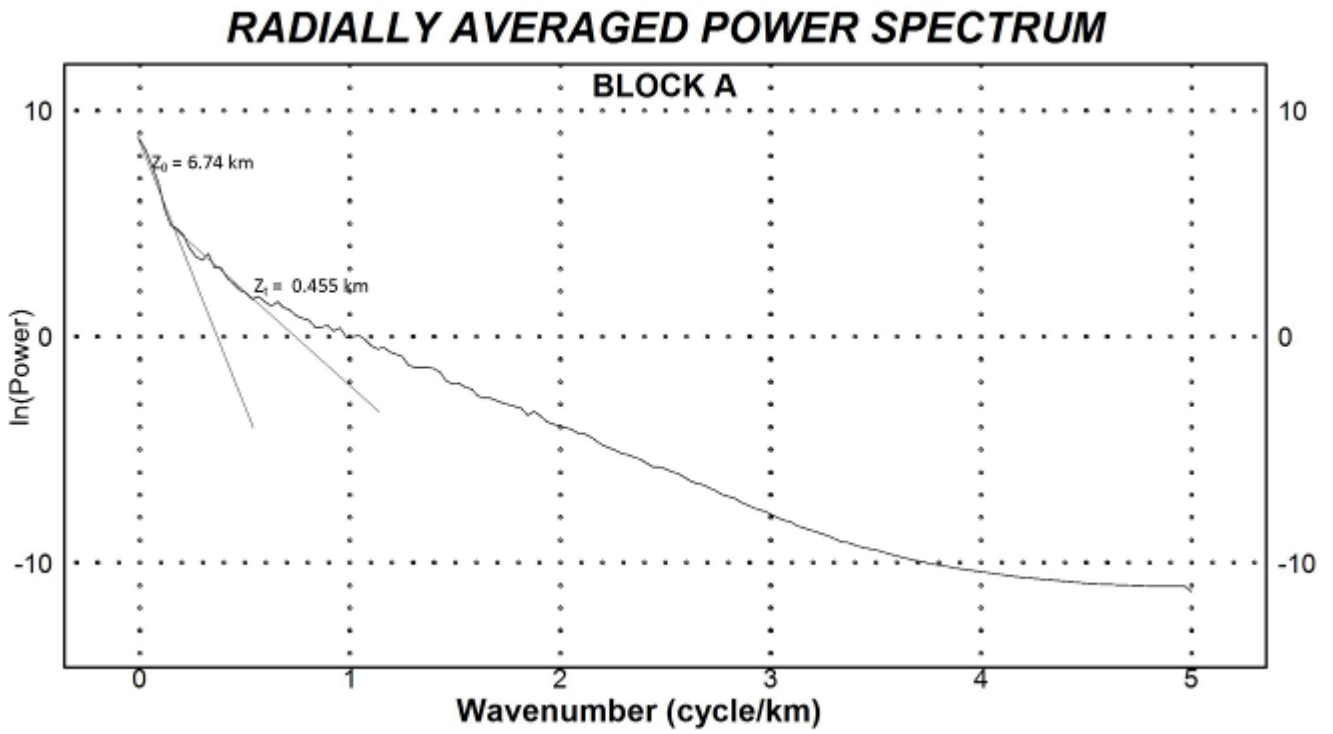


Fig 9.1j Plots of spectrum energy against wave number (spectral block H **Sheet 215A**)

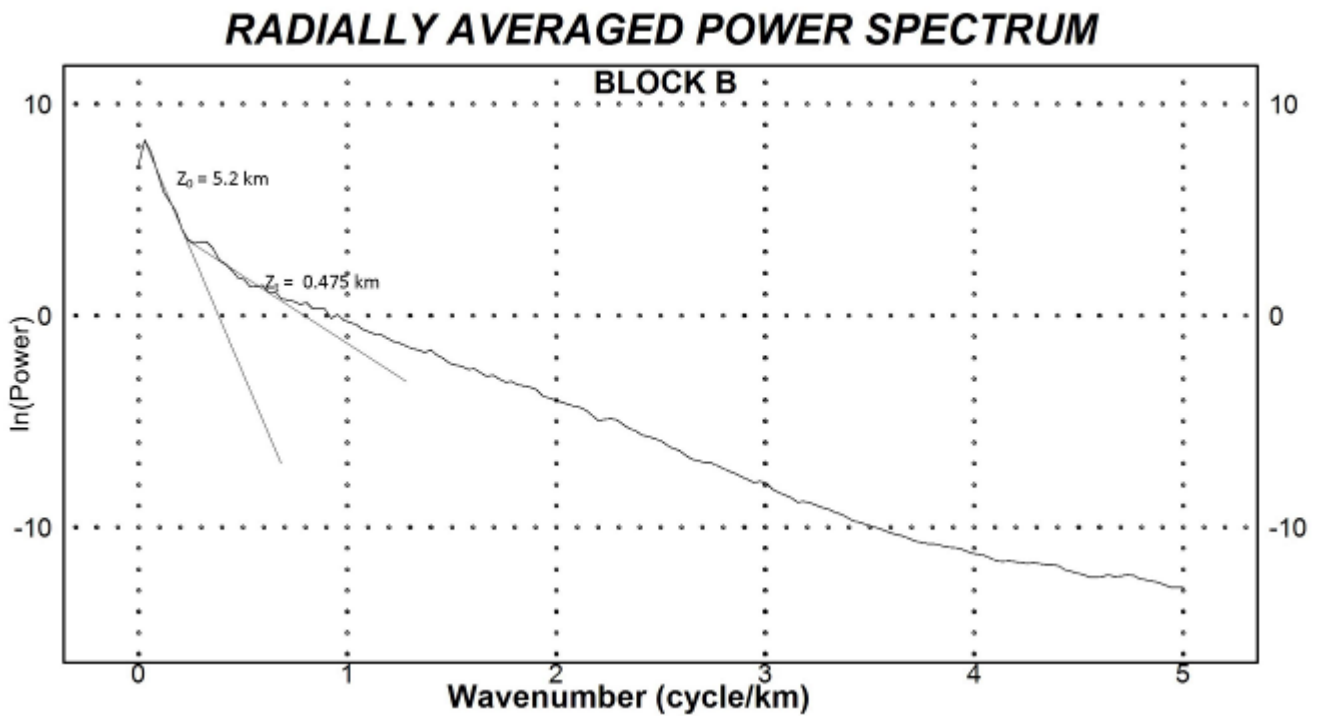


Fig 9.1k Plots of spectrum energy against wave number (spectral block H **Sheet 215B**)

RADIALLY AVERAGED POWER SPECTRUM

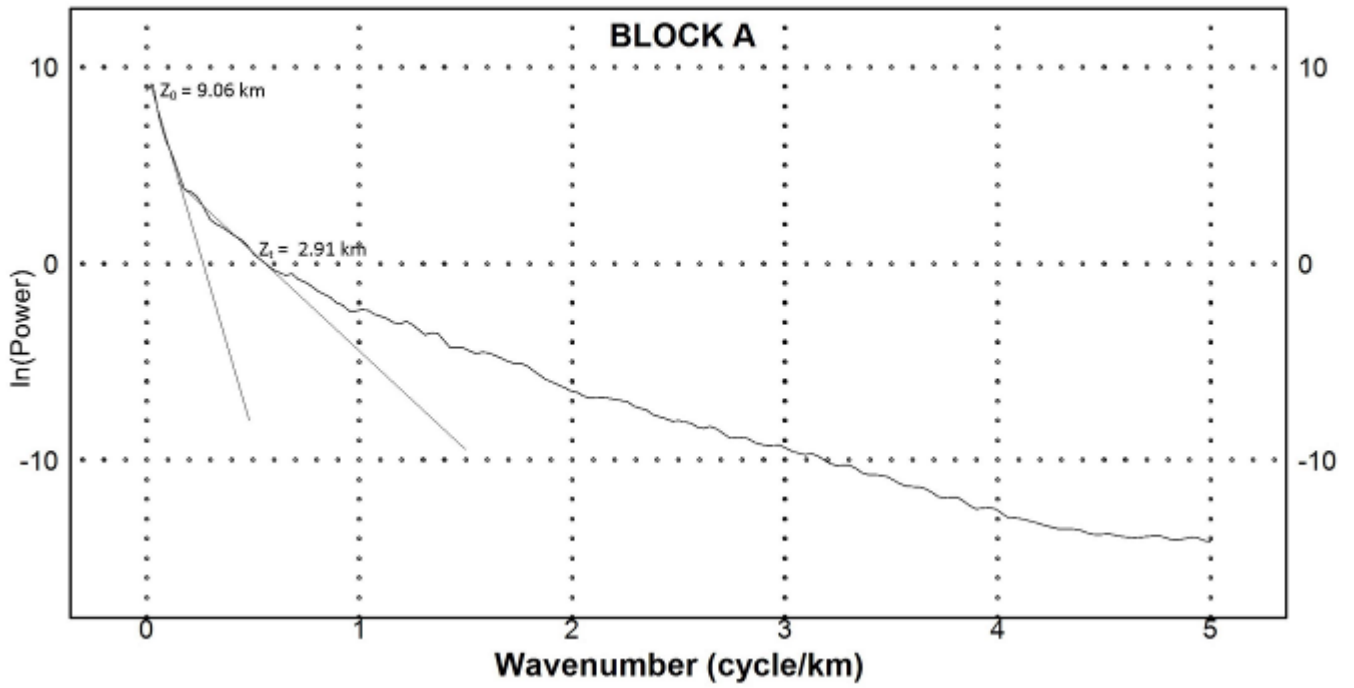


Fig 9.11 Plots of spectrum energy against wave number (spectral block H Sheet 227A)

RADIALLY AVERAGED POWER SPECTRUM

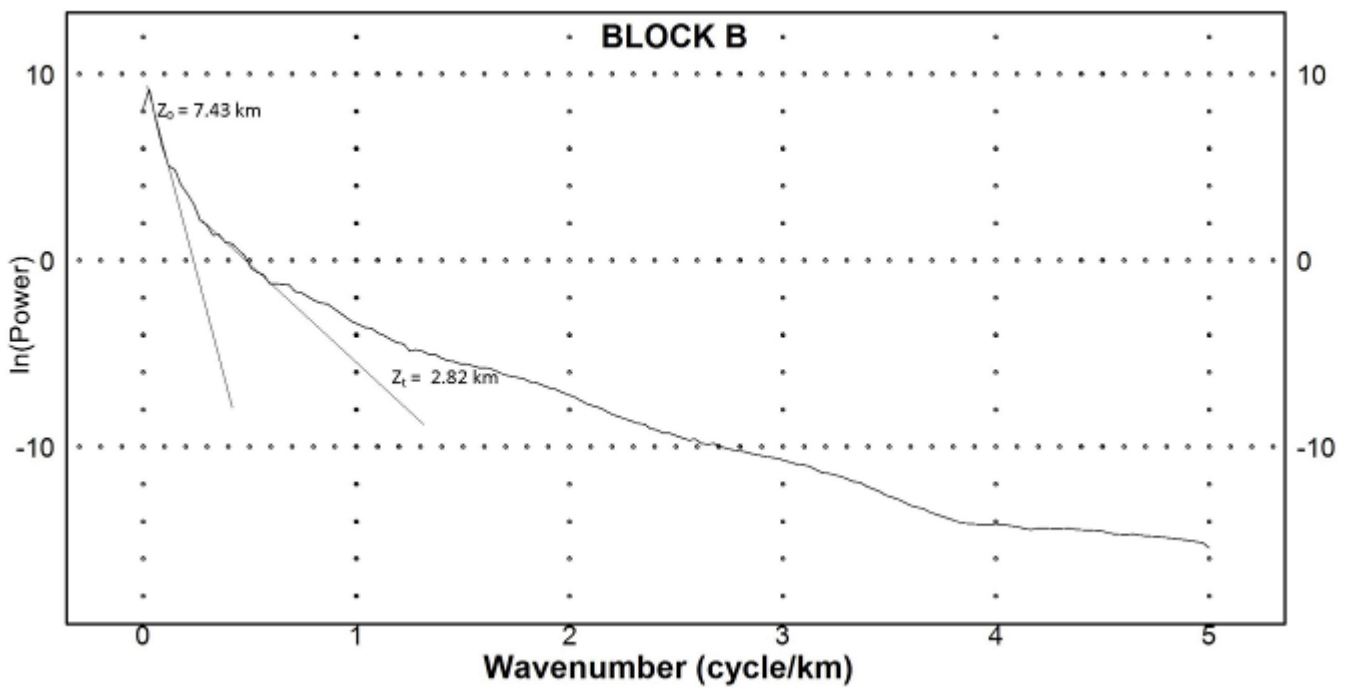


Fig 9.1m Plots of spectrum energy against wave number (spectral block H Sheet 227B)

RADIALLY AVERAGED POWER SPECTRUM

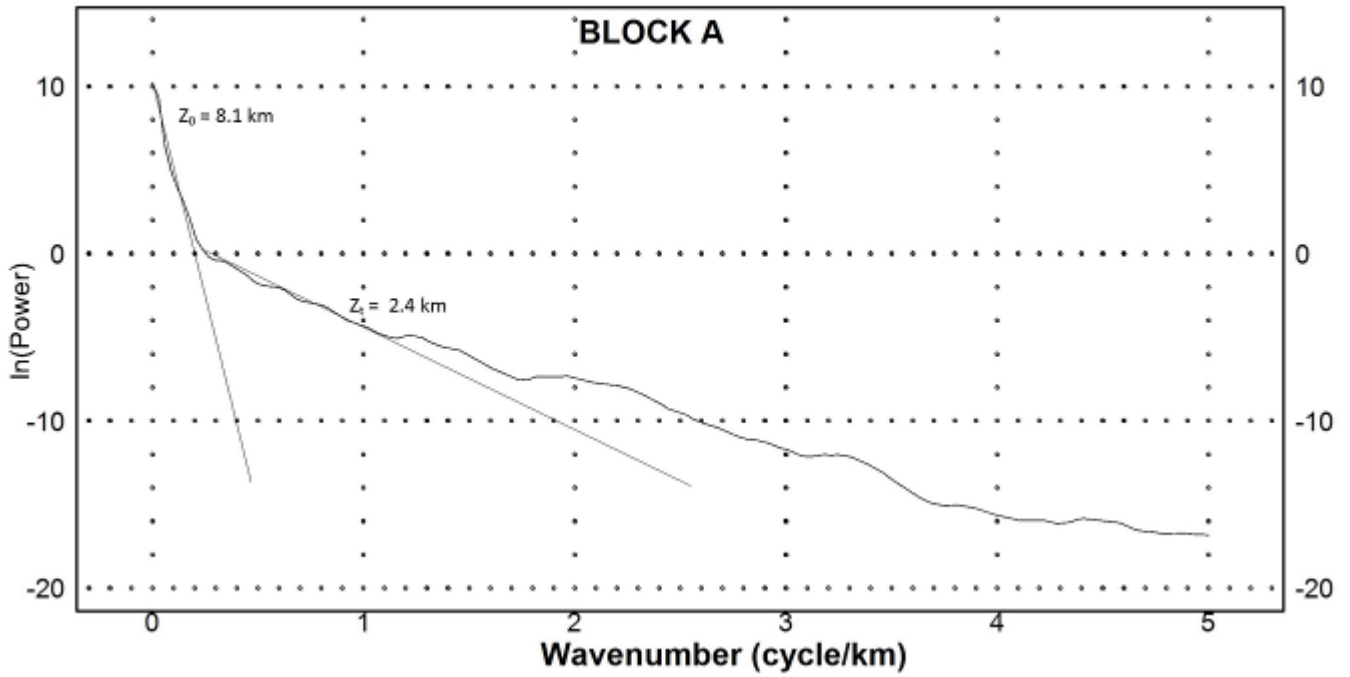


Fig 9.1n Plots of spectrum energy against wave number (spectral block H Sheet 232A)

RADIALLY AVERAGED POWER SPECTRUM

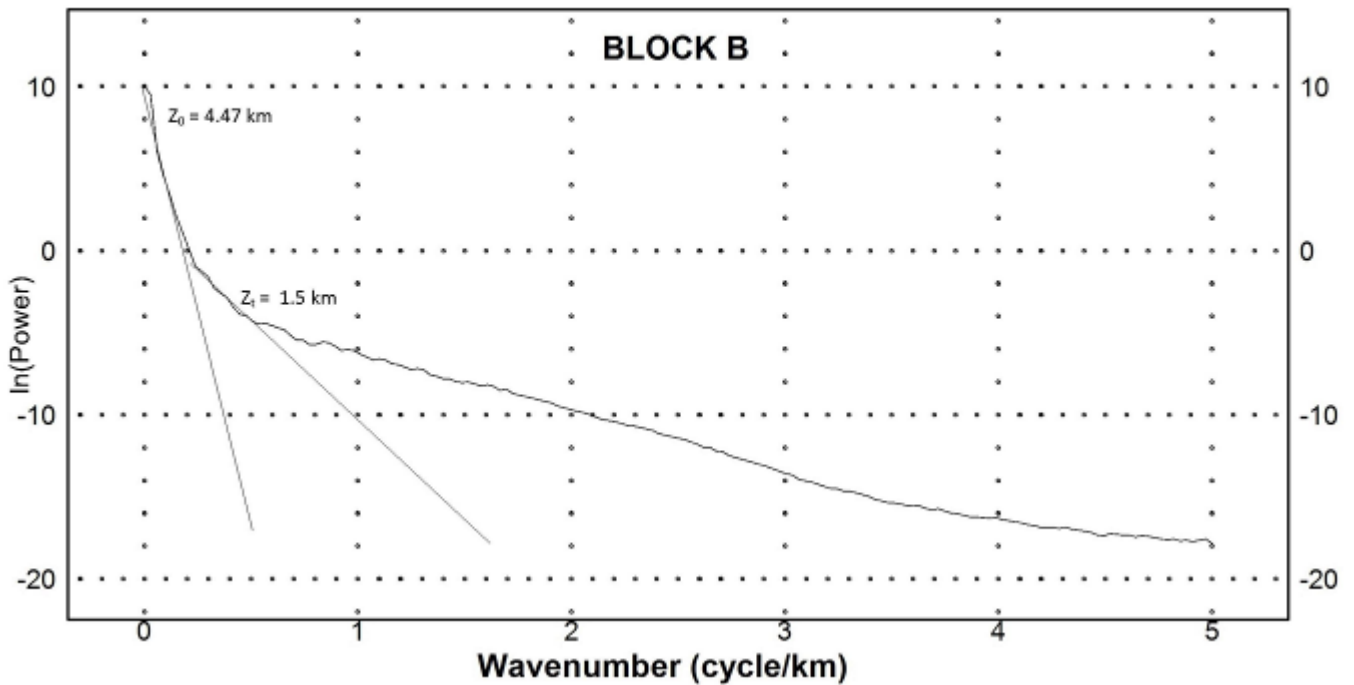


Fig 9.1o Plots of spectrum energy against wave number (spectral block H Sheet 232B)

RADIALLY AVERAGED POWER SPECTRUM

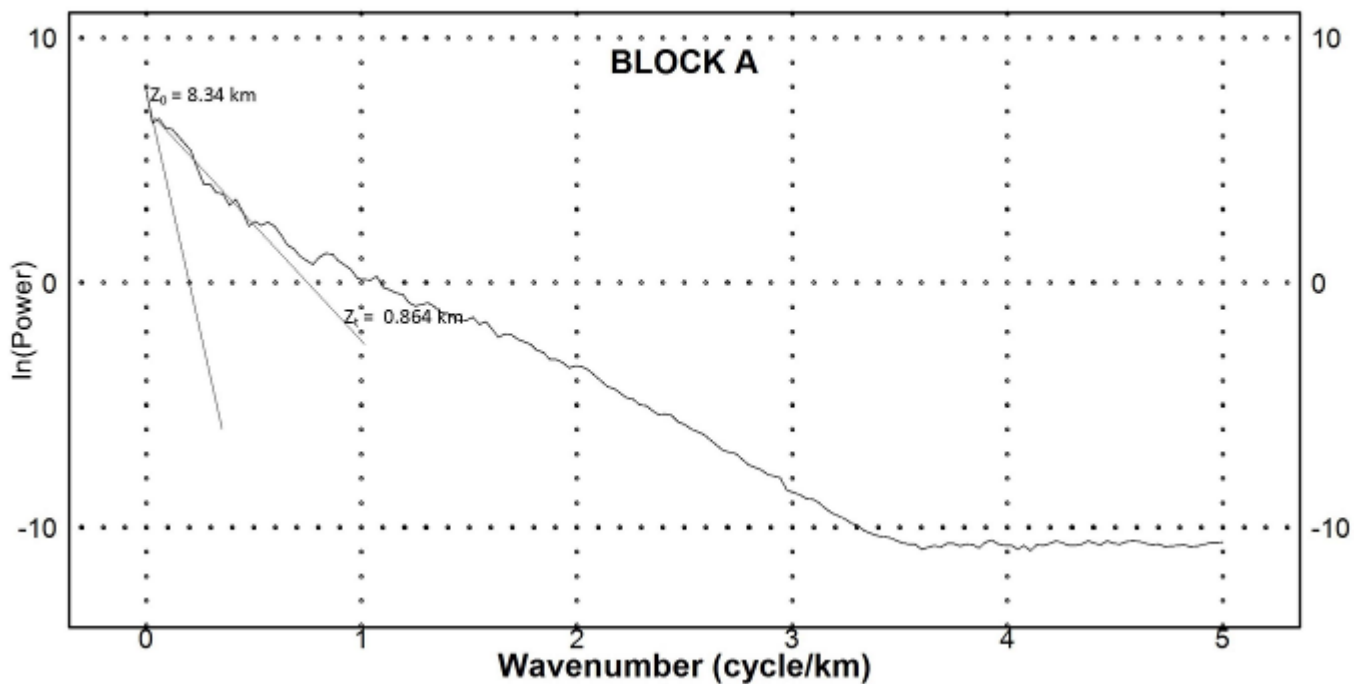


Fig 9.1p Plots of spectrum energy against wave number (spectral block H Sheet 243A)

RADIALLY AVERAGED POWER SPECTRUM

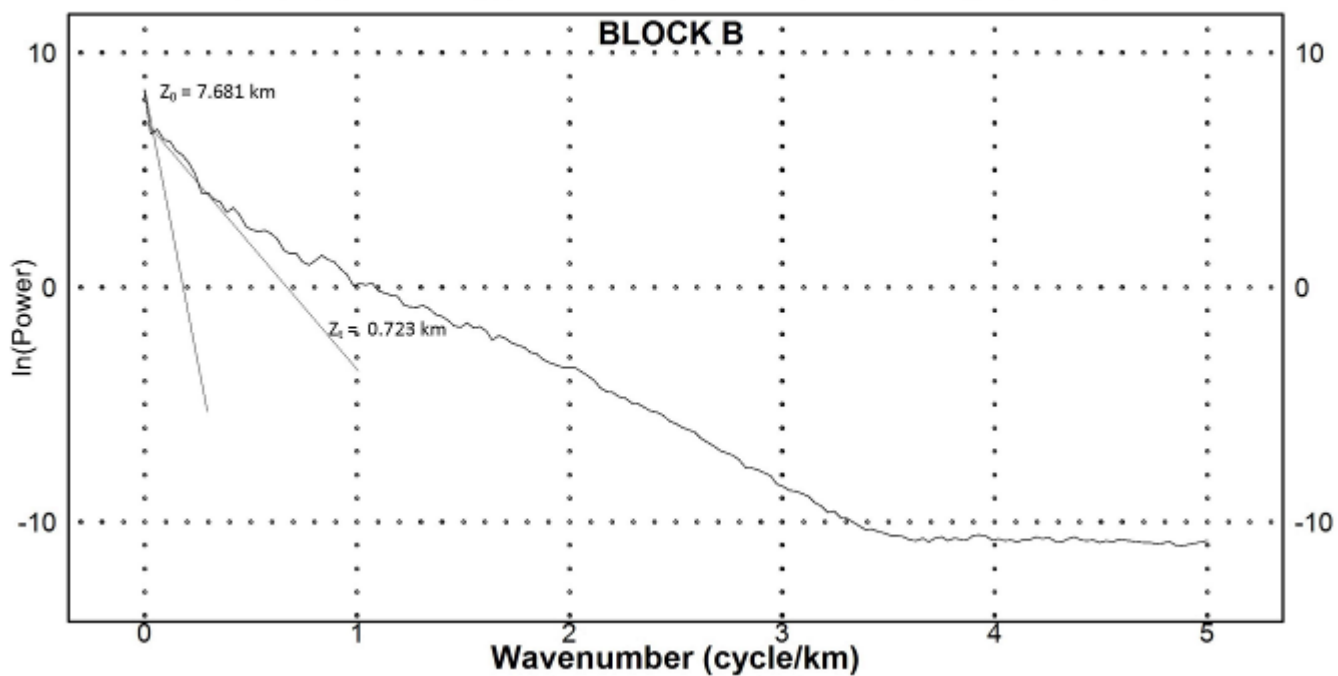


Fig 9.1q Plots of spectrum energy against wave number (spectral block H Sheet 243B)

RADIALLY AVERAGED POWER SPECTRUM

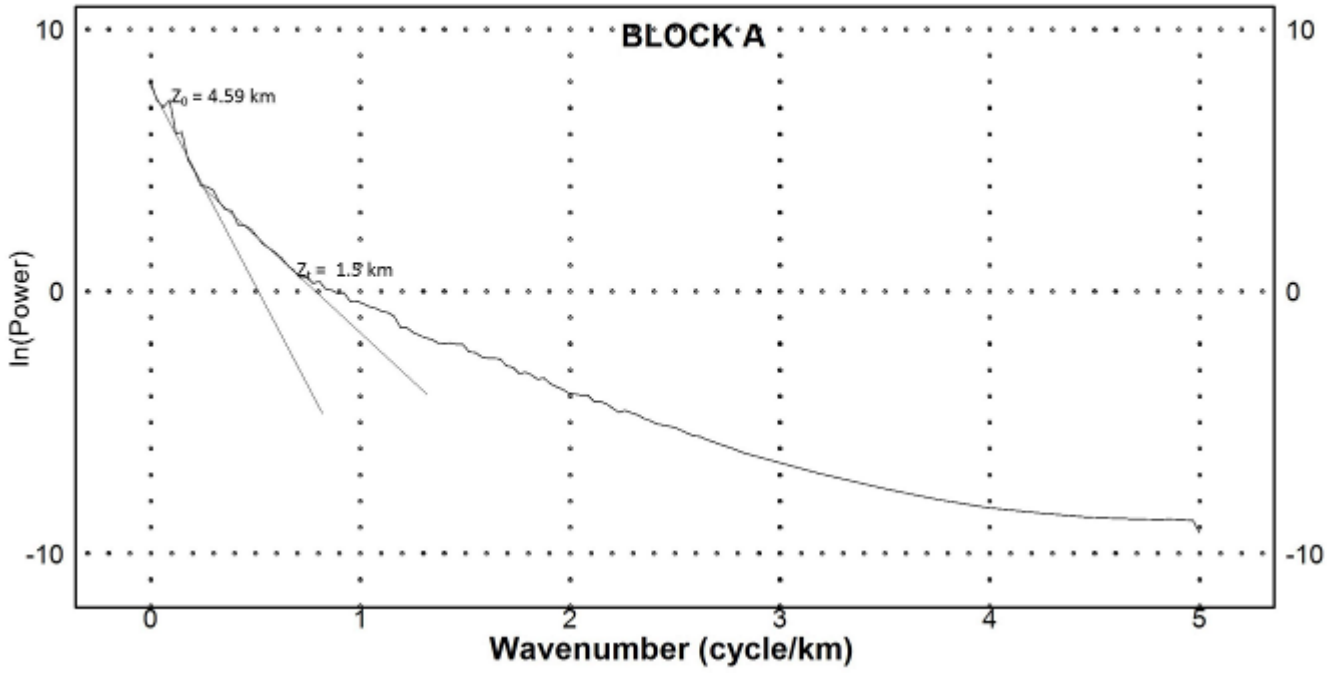


Fig 9.1r Plots of spectrum energy against wave number (spectral block H Sheet 244A)

RADIALLY AVERAGED POWER SPECTRUM

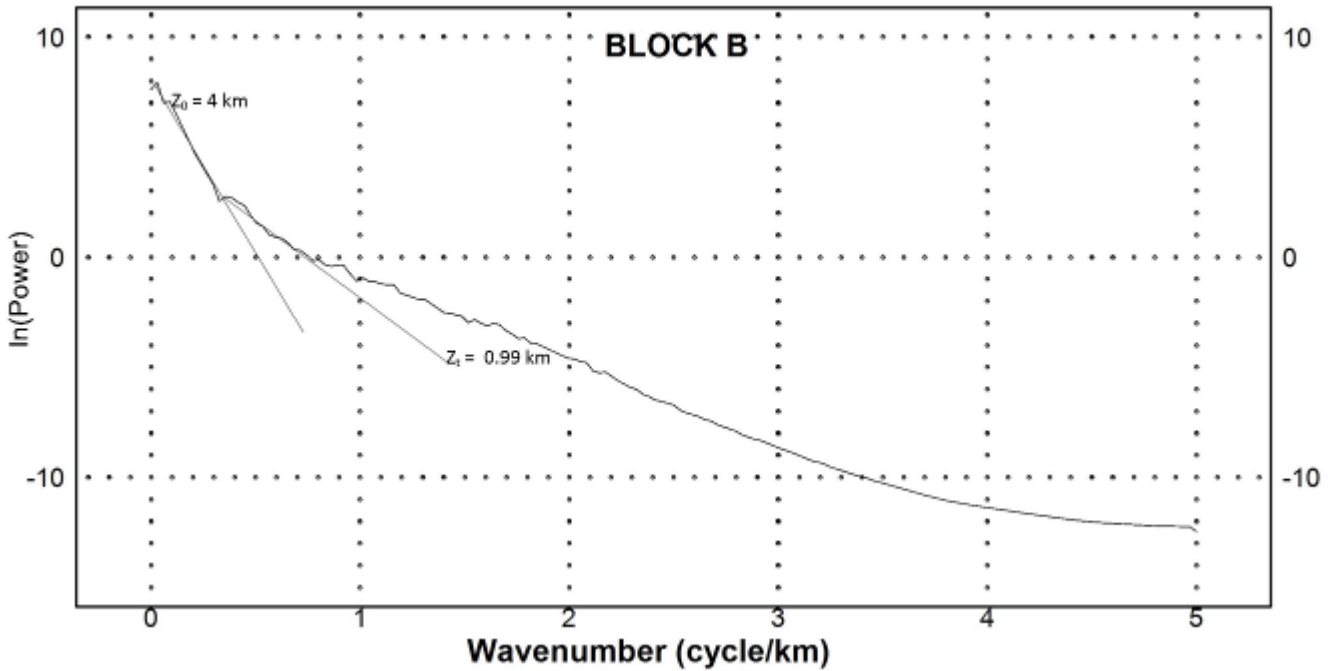


Fig 9.1s Plots of spectrum energy against wave number (spectral block H Sheet 244B)

RADIALLY AVERAGED POWER SPECTRUM

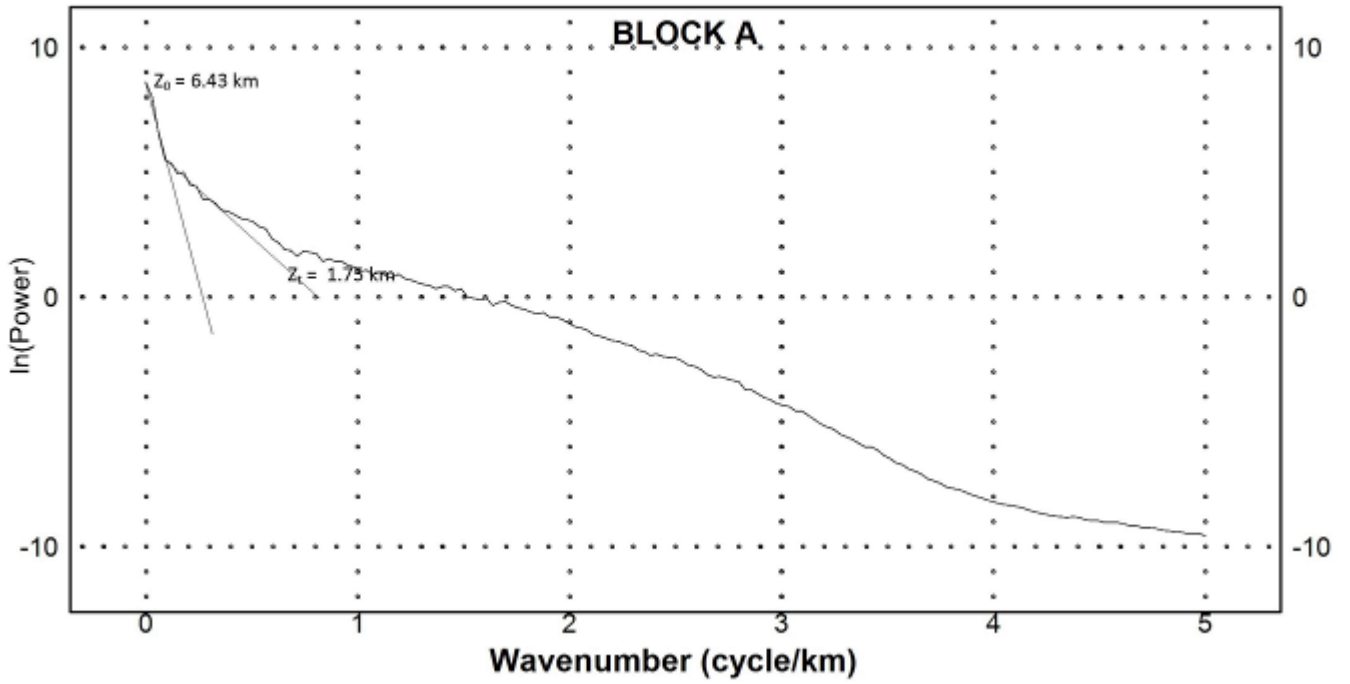


Fig 9.1t Plots of spectrum energy against wave number (spectral block H Sheet 247A)

RADIALLY AVERAGED POWER SPECTRUM

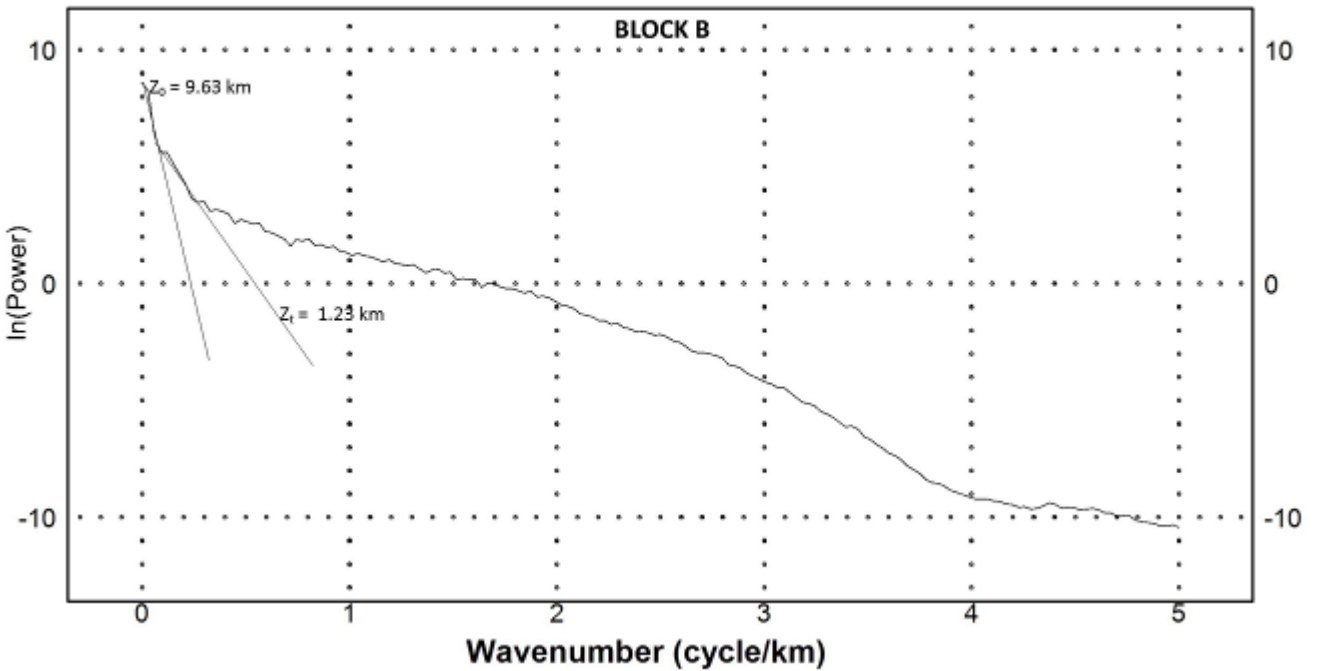


Fig 9.1u Plots of spectrum energy against wave number (spectral block H Sheet 247B)

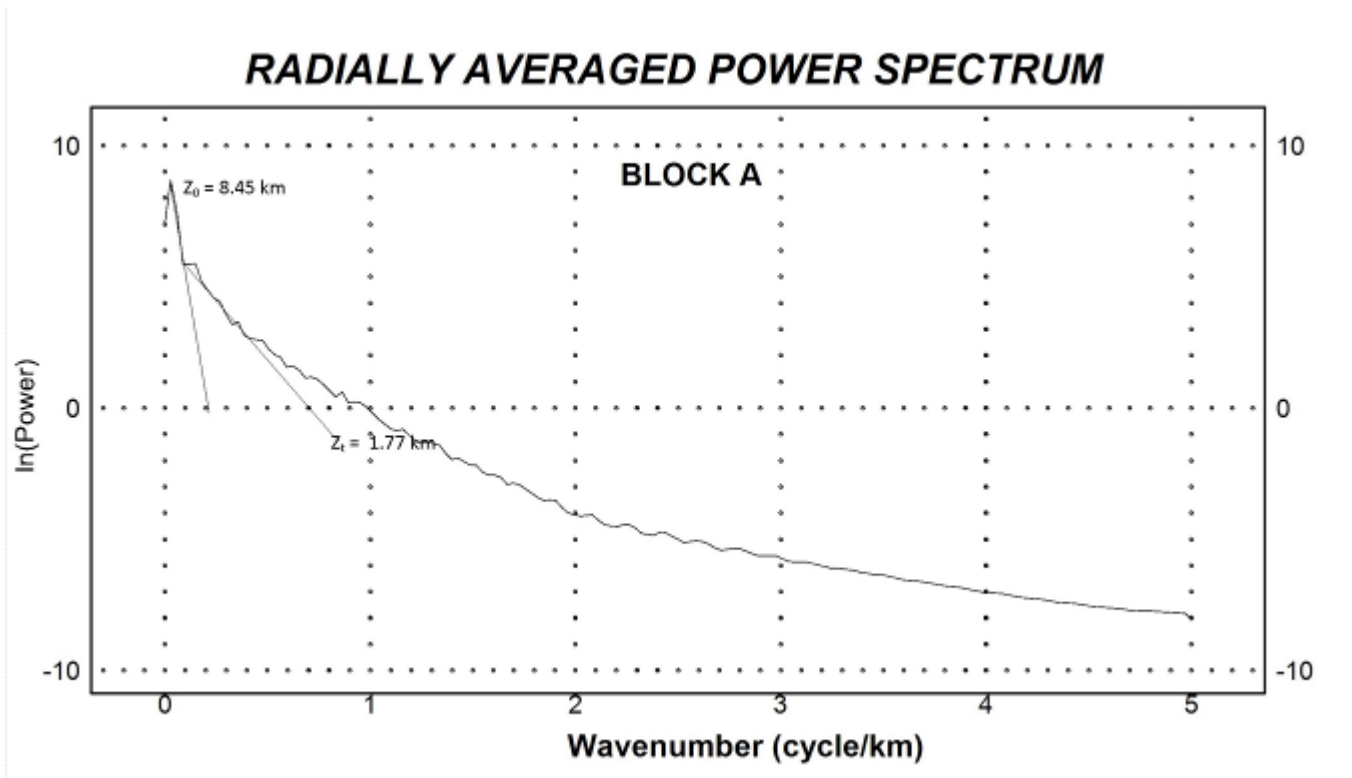


Fig 9.1v Plots of spectrum energy against wave number (spectral block H **Sheet 266A**)

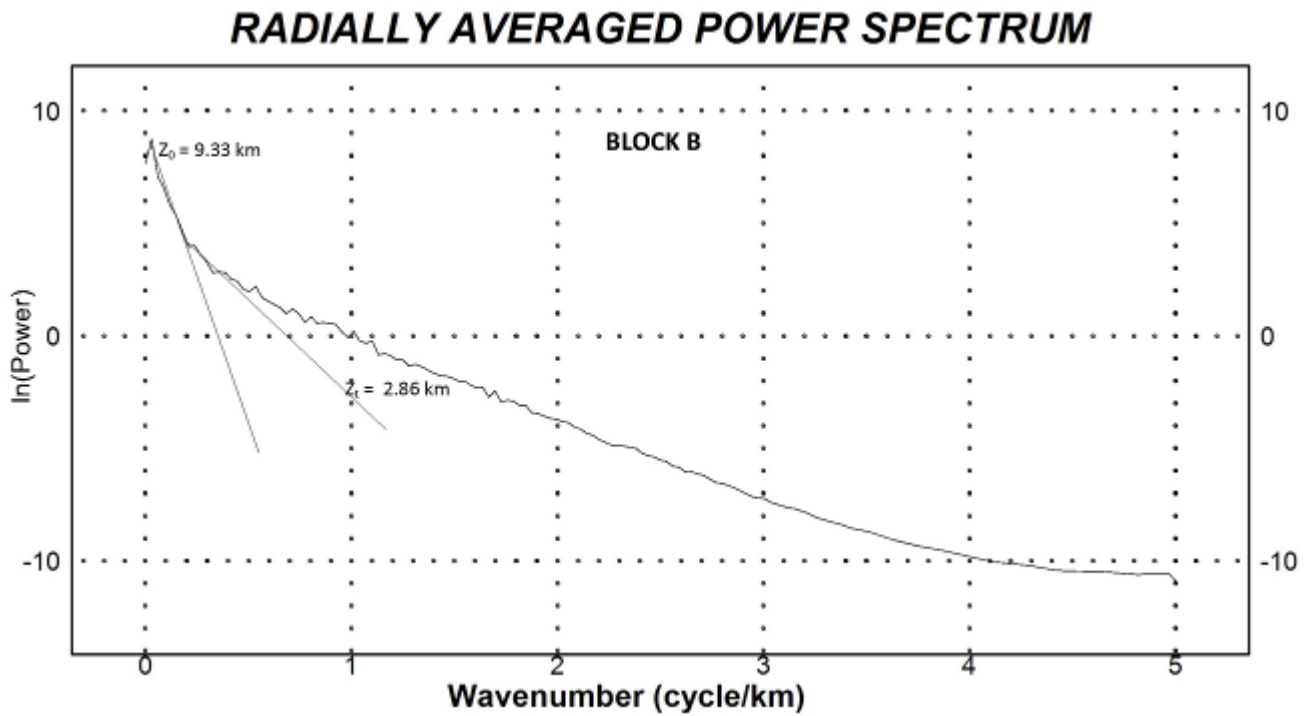


Fig 9.1w Plots of spectrum energy against wave number (spectral block H **Sheet 266B**)

RADIALLY AVERAGED POWER SPECTRUM

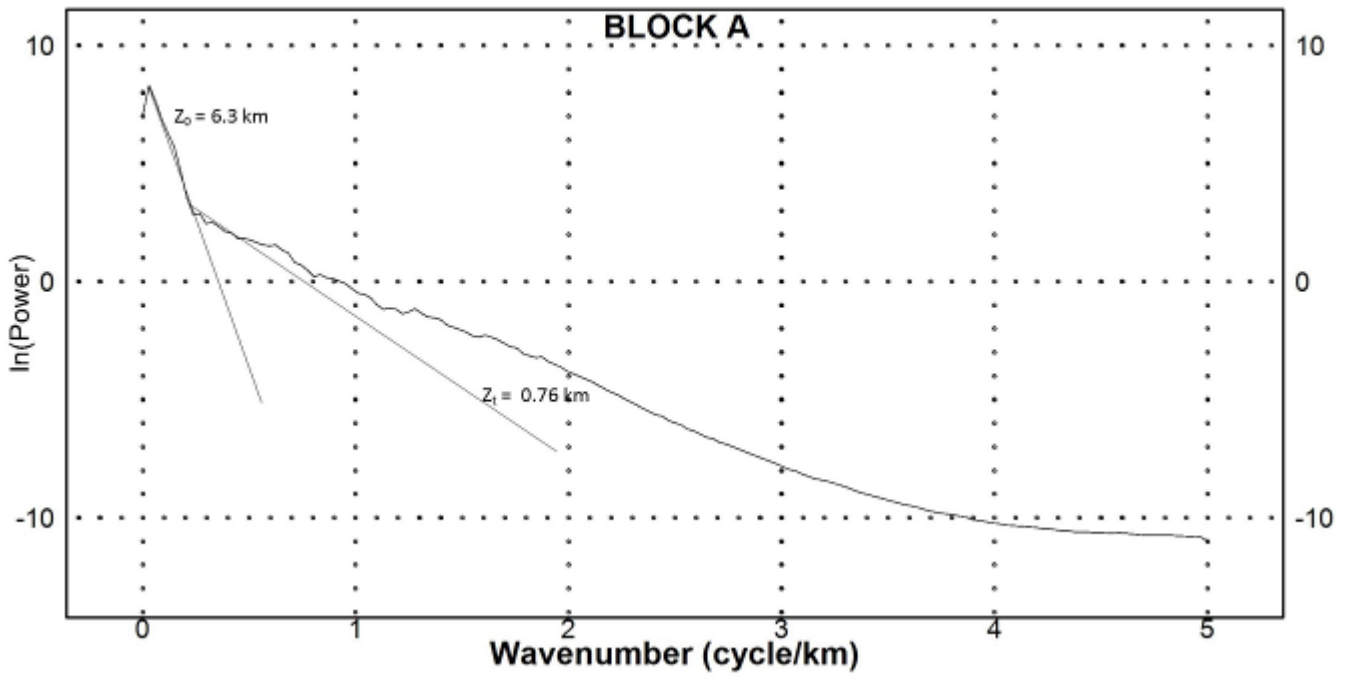


Fig 9.1x Plots of spectrum energy against wave number (spectral block H Sheet 280A)

RADIALLY AVERAGED POWER SPECTRUM

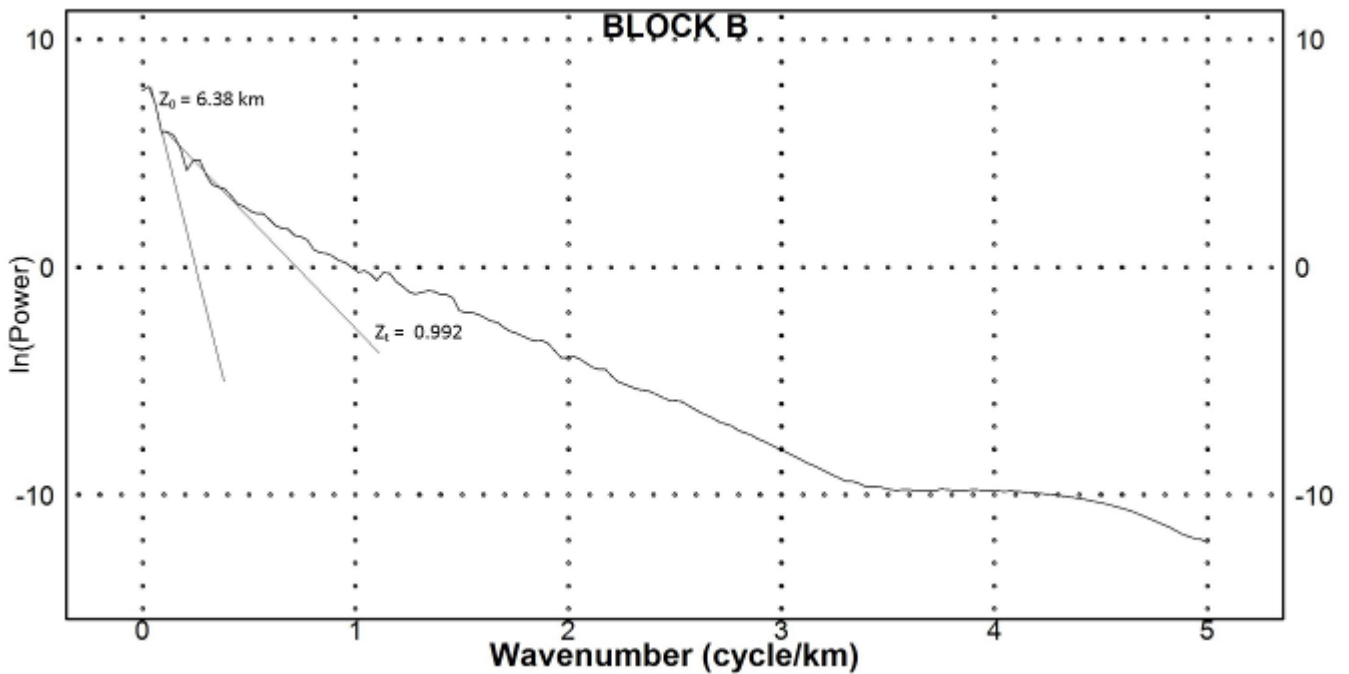


Fig 9.1y Plots of spectrum energy against wave number (spectral block H Sheet 280B)

RADIALLY AVERAGED POWER SPECTRUM

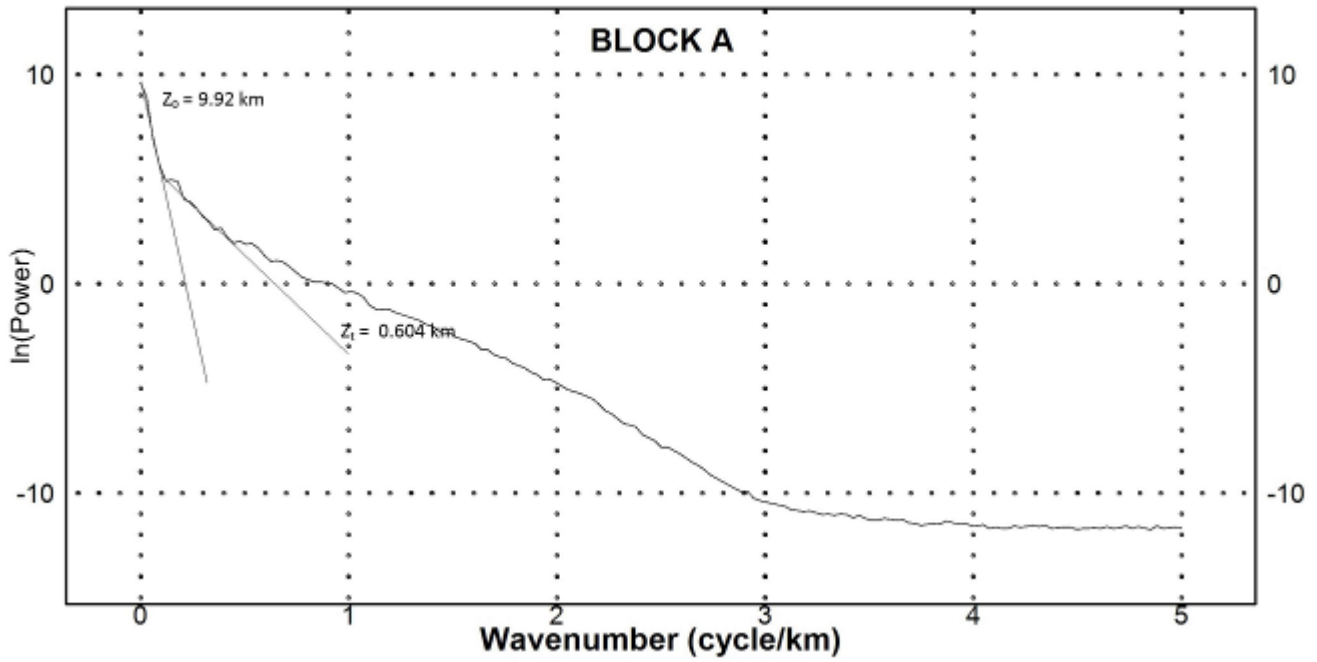


Fig 9.1z Plots of spectrum energy against wave number (spectral block H Sheet 281A)

RADIALLY AVERAGED POWER SPECTRUM

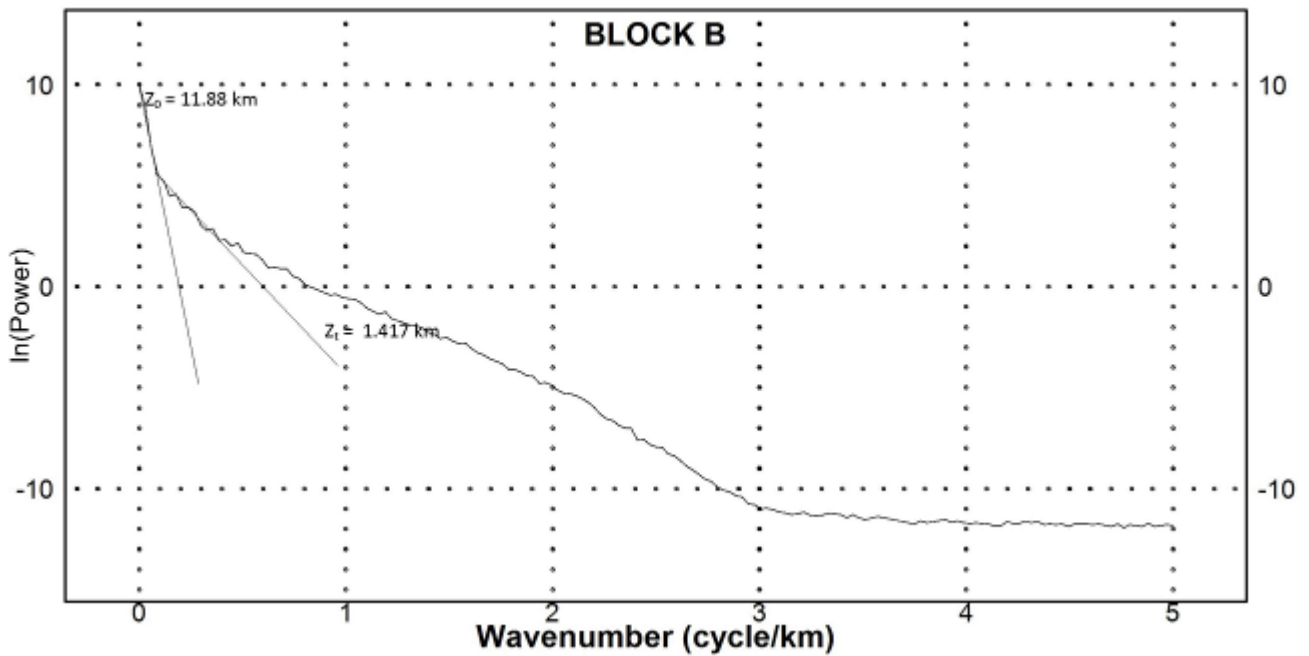


Fig 9.1Za Plots of spectrum energy against wave number (spectral block H Sheet 281B)

RADIALLY AVERAGED POWER SPECTRUM

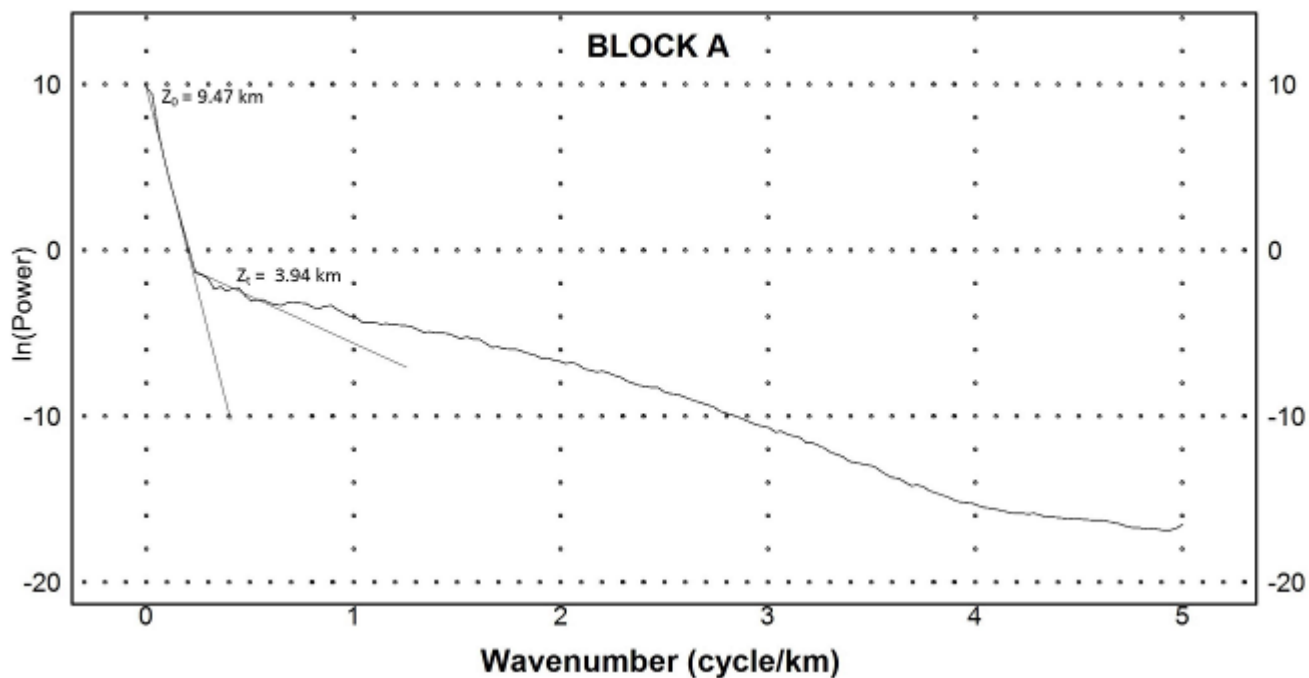


Fig 9.1Zb Plots of spectrum energy against wave number (spectral block H Sheet 287A)

RADIALLY AVERAGED POWER SPECTRUM

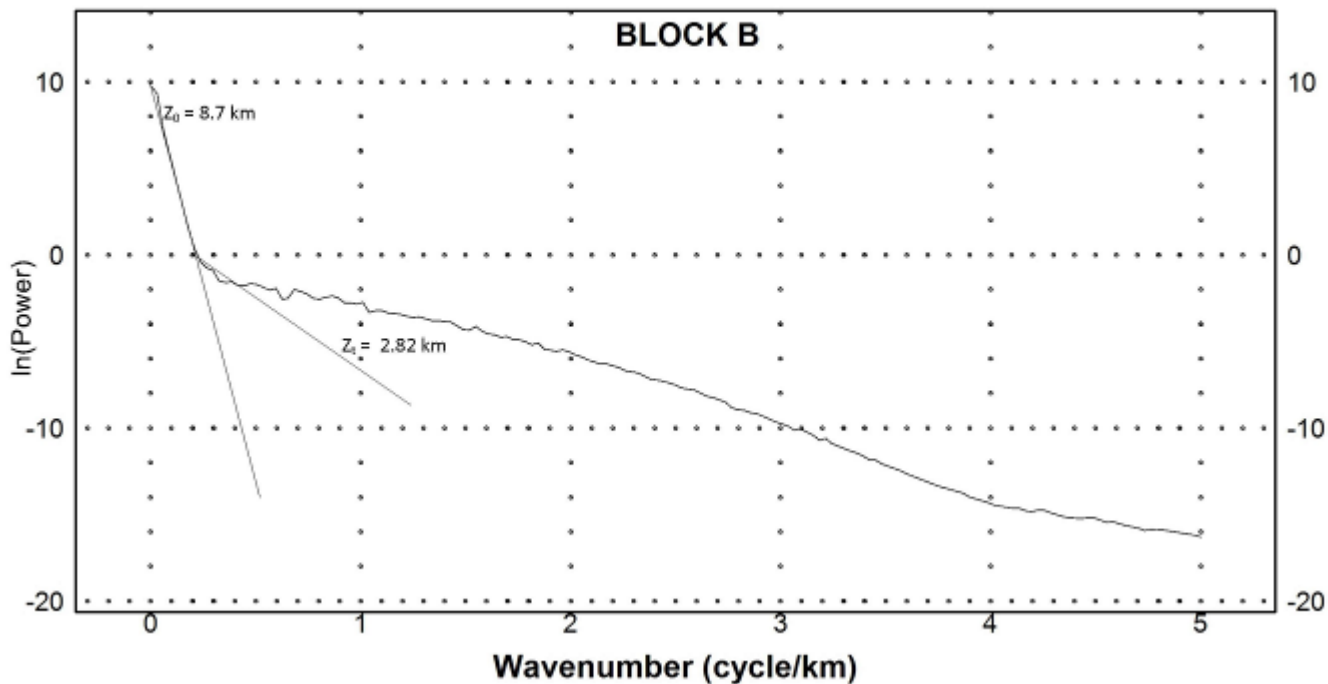


Fig 9.1Zc Plots of spectrum energy against wave number (spectral block H Sheet 287B)

RADIALLY AVERAGED POWER SPECTRUM

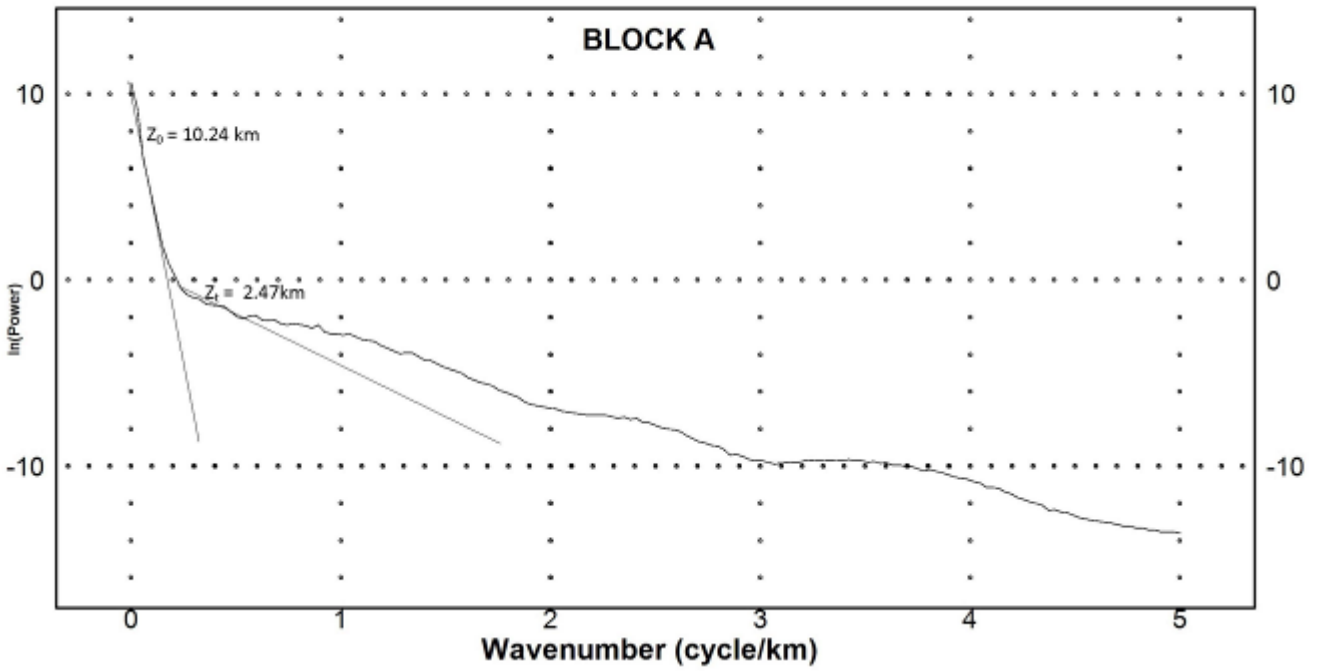


Fig 9.1Zd Plots of spectrum energy against wave number (spectral block H Sheet 300A)

RADIALLY AVERAGED POWER SPECTRUM

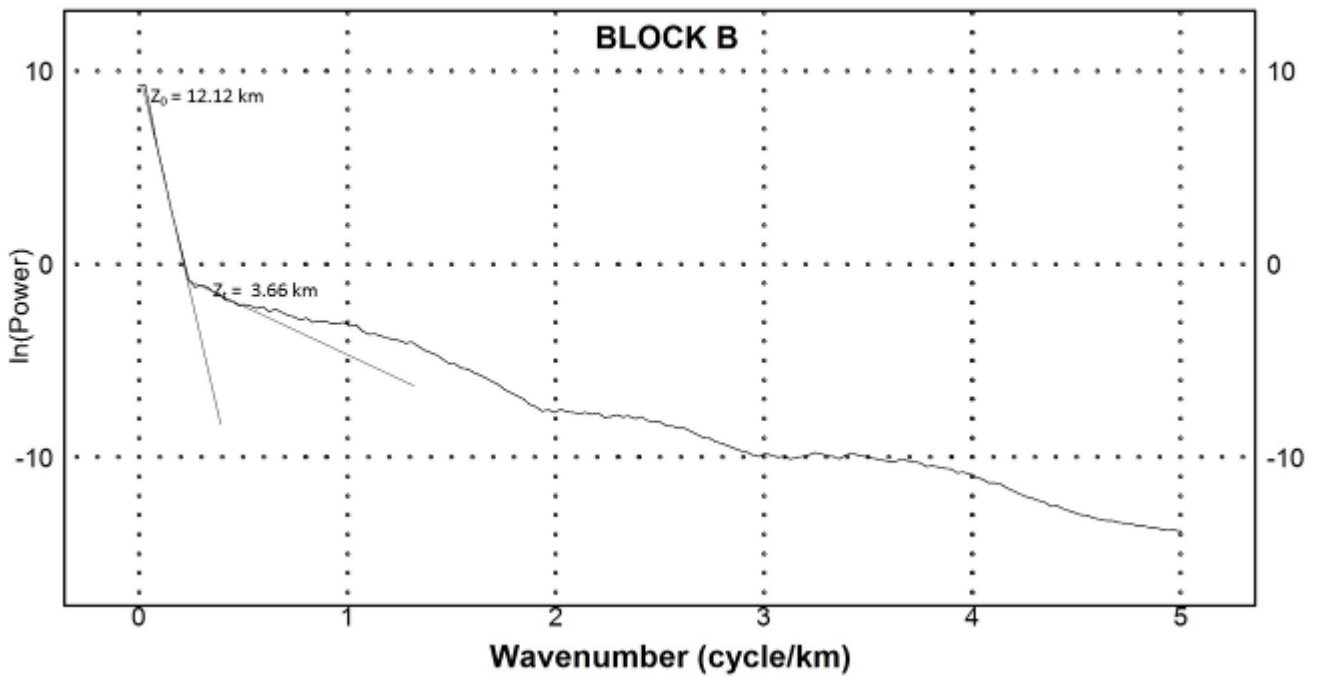


Fig 9.1Ze Plots of spectrum energy against wave number (spectral block H Sheet 300B)

RADIALLY AVERAGED POWER SPECTRUM

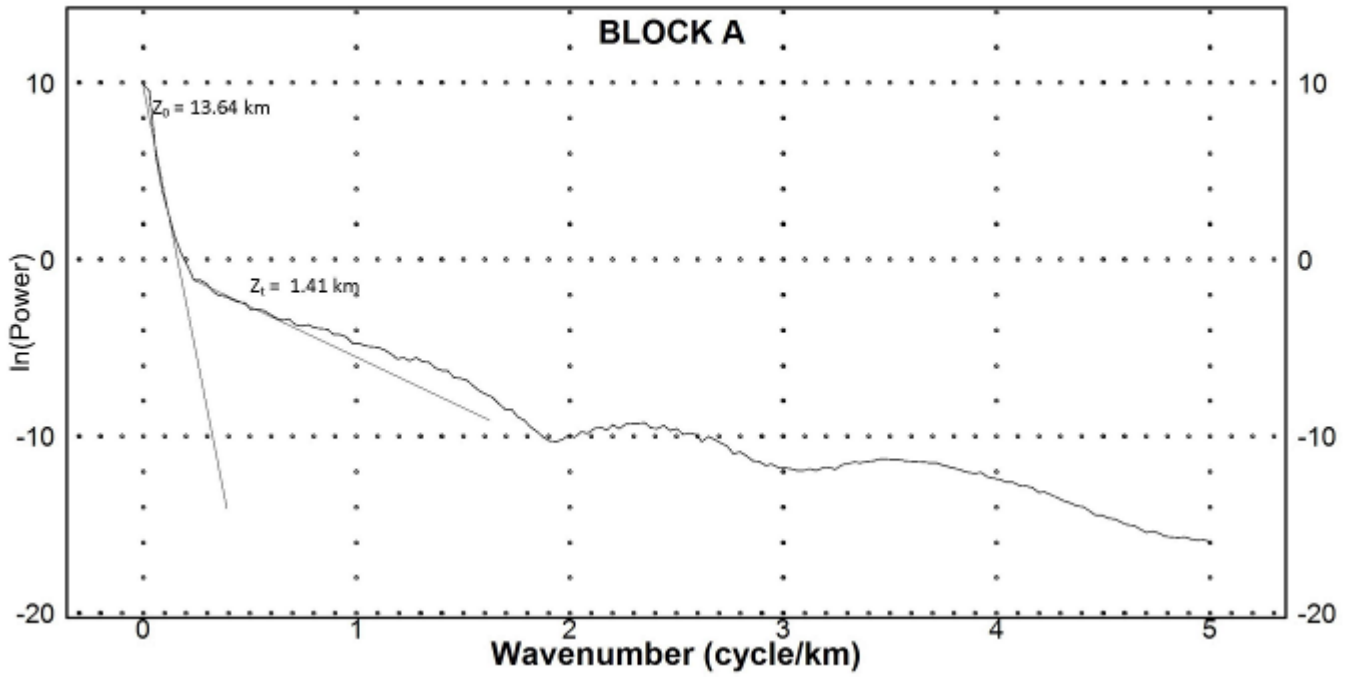


Fig 9.1Zf Plots of spectrum energy against wave number (spectral block H Sheet 311A)

RADIALLY AVERAGED POWER SPECTRUM

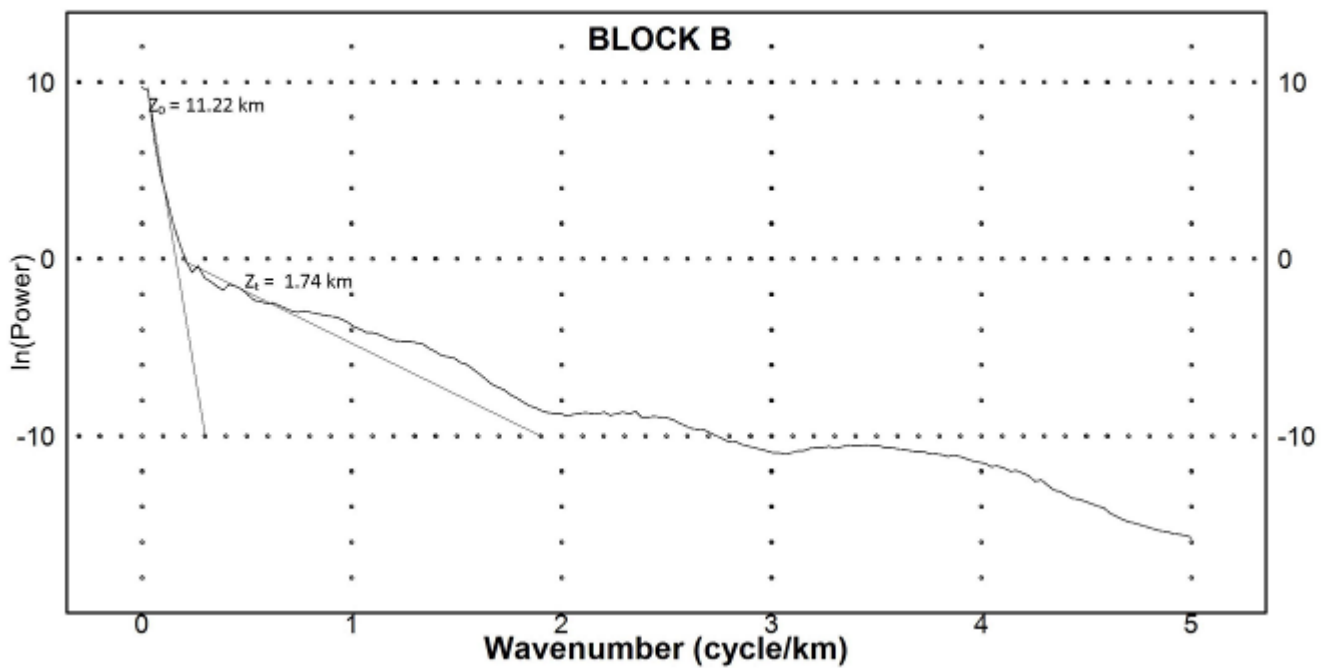


Fig 9.1Zg Plots of spectrum energy against wave number (spectral block H Sheet 311B)

APPENDIX 2:

Geological and Hydrogeological images across Nigeria



Geothermal exploration along Lokoja-Abuja Road with undergraduate students



The lead researcher on geological and hydrogeological studies in Egenja Kogi State



Lead researcher and one of the team member taking attitude of quartz schist at Ikogosi in Ekiti State



The lead researcher on geological and hydrogeological studies in Egeneja, Kogi State



Lead researcher and one of the team members taking dip of quartz schist at Ikogosi in Ekiti State



Research team with taking a group photograph in Ugep Cross River State



Photograph section of Olumirin water fall in Erin Ijesa, Osun State



The research team with the Postgraduate students taking ground magnetic data in Ikogosi, Ekiti State



The research team with the Postgraduate students taking ground magnetic data in Ishiagu, Ebonyi State



The research team with the Postgraduate students taking ground magnetic data in A, Ekiti State



The research team with the Postgraduate students taking ground magnetic data in Igbonla, Kwara State.



The research team with the Postgraduate student taking ground magnetic data in Azukala, Edo State



The research team taking ground magnetic data in Okigwe, Imo State



The research team taking ground magnetic data in Ruwan Zafi, Nasarawa State



The research team with the Postgraduate students taking ground magnetic data in Keana, Nasarawa State



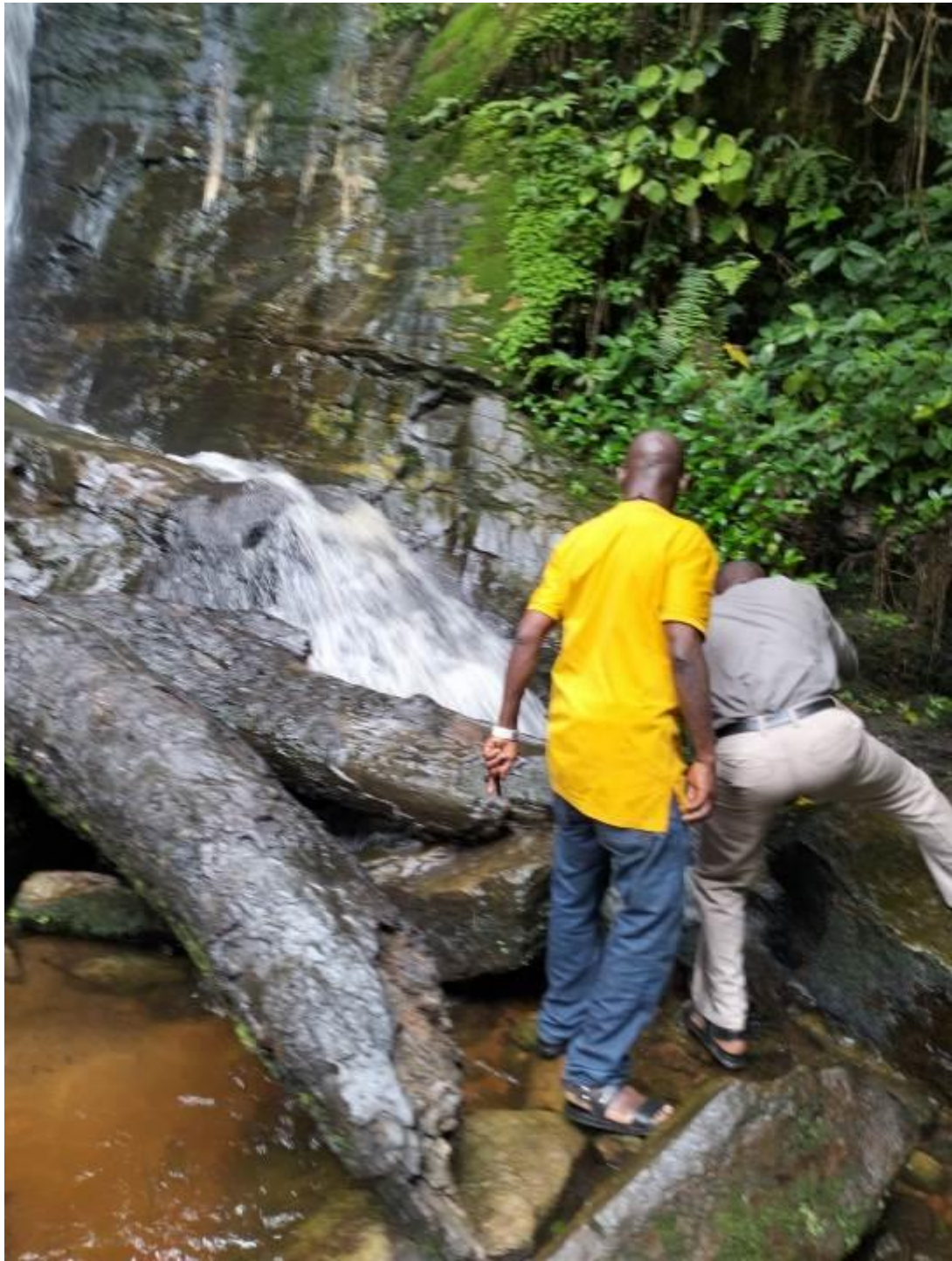
Lead research taking spring surface temperature in Olumirin Ijesa, Osun State



Photograph Section of Ribi spring in Nasarawa State



Lead research making an observation in Olumirin water fall, Osun State



Lead research taking surface temperature of Olumiri water fall in Erin, Osun State



Lead research with the postgraduate student and team member in Erin, Osun State



Lead research making an observation in Olumirin (Erin), Osun State



Lead research and team member making an observation in Wikki, Upper Benue Trough



Lead research making and team member of the research preparing to acquire geophysical data in Ikogosi, Ekiti State



Research team with postgraduate student acquiring geophysical data in Erin, Osun State



Lead research making an observation in Ikogosi, Ekiti State





Research team preparing for data acquisition in Nsukka, Enugu State



The research team with undergraduate group photograph in Wikki, Bauchi State.

Innovative Geothermal Energy Assessment of Akiri and Environs for Clean Energy generation Nigeria



Aigbedion Isaac*, **Aikhuele Daniel O**, **Salufu Samuel O** and **Aigbedion**

Elijah O *Geophysics/Physics Department, Ambrose Alli University, University of Port Harcourt, Ekpoma, Edo State, Nigeria* **Submission:** August 30, 2022;

Published: September 20, 2022

***Corresponding author:** Aigbedion Isaac, Geophysics Department, Ambrose Alli University,

Abstract

Innovative geothermal energy source of clean energy: the need of Nigerian Telecommunications Industry for Efficient Communication delivery study focused on investigating the geothermal resource potential in Akiri and environs was carried out using geological, hydrological studies and high-resolution aeromagnetic data. From the geological and hydrogeological studies, the temperature of the warm Akiri spring at the time of measurement was 54°C. Awe spring 2 has temperature of 39.2°C. Awe spring 3 releases water with temperature 32.7°C. The Keana temperature of the spring was measured to be 34°C. Ribí Thermal Spring temperature was measured as 33.9°C. Kanje temperature was measured to be 34°C and the temperature of Azara spring water was measured as 32.7°C.

The aeromagnetic data of Akiri_ (Sheet 232) was subjected to spectral analysis with the aim of accessing the geothermal potential of the study area and environs. The Curie point depth values range from (7.44- 20.81) km, the geothermal gradient values range from (27.87- 77.95) °C/km and the heat flow values range from (69.68- 194.87) mW/m². The NE edge covering Jangwa, Azara, Akiri, and Ribí hosts the anomalous heat flow and geothermal gradient with corresponding shallowest values of curie point depth. Other regions like Kumar, Jutu, Kanje, Adawa, Atatakoro, and Kaza also show good geothermal manifestations, except few areas in SW covering Tunga with low heat flow below the recommended threshold value of 80mW/m². It can therefore be deduced from this study that regions that fall within the range of 80 to 100mWm⁻² and warm springs with thermal and hypothermal are good spots for geothermal energy resources.

Keywords: Geothermal Energy Resources; Clean Energy; Earth's surface; Volcanic Materials; Energy Exploration; Bedrock Valleys; Mud Rock

Introduction

Geothermal energy is heat derived within the sub-surface of the earth. Water and/or steam carry the geothermal energy to the Earth's surface. Depending on its characteristics, geothermal energy can be used for heating and cooling purposes or be harnessed to generate clean electricity. However, for electricity, generation high or medium temperature resources are needed, which are usually located close to tectonically active regions through geophysical study.

Geothermal energy originates from the formation of the earth and from decay of long-lived isotopes of uranium, thorium, and potassium found within the Precambrian basement rocks

[1].The uprising of magma to the surface during the rifting often results in different geodynamic activities such as the surface expressions of tectonic lineaments and manifestation of geothermal resources

[2].These lineaments such as faults and fractures play major roles in the study of the evolution and dynamism of the rift zones. Investigations into the tectonic lineaments and surface thermal structures are very crucial to the understanding of the geothermal activities and processes associated with the region. Continuous accumulation of tectonic strain helps to maintain faults and fractures as conduits for fluids flow thereby sustaining the geothermal systems

In geothermal energy exploration, the potential fields of gravity and magnetic have been used to delineate bedrock valleys concealed by sediments or volcanic materials and mapping of permeable fractures during the early stages of investigation of Olkaria and Meningai fields, Kenya [3].This measurement can significantly reduce the number of wells needed to characterize a prospect while improving the confidence of interpretations. There is need for renewable geothermal energy resources in developing countries, as a way to dependable economic growth and power supply. To reduce the global environment impact on fossil fuel, geothermal energy can also be used as an alternative to fossil fuel. In Nigeria, the much dependence on oil and gas as the main source of energy has virtually collapsed her economy. It therefore becomes pertinent to find an alternative source of energy. So, the exploitation of possible geothermal resource areas in Nigeria could be a vital alternative to an industrializing nation like Nigeria [4].Nigeria is recognized as one of the African countries with potential for geothermal energy [5]. Surface manifestations of subsurface

heat as springs and lava flow have been reported in both the sedimentary and the Precambrian Basement Complex areas of Nigeria [6-11]. Geophysical investigation involves direct and indirect methods that measure both chemical and physical parameters. The direct approach involves temperature, fluid content, and resistivity/conductivity that are directly influenced by geothermal activity such as the thermal, electrical resistivity, and magneto telluric approaches, while indirect methods that investigate the physical parameters of the host rock such magnetic property, density, seismic velocity that allow the mapping of subsurface geological properties [8,12]. Hot springs waters may be classified as cold (<20°C), hypothermal (20-30°C), thermal (>30- 40°C) or hyperthermal (>40°C). Based on this classification, we were able to classify the few springs we study across the Akiri and environs in this research work. Regional aeromagnetic data are used to delineate the bottom of the magnetic source of the crust, map the Curie isotherm surface, High heat flow, and geothermal gradients which are good constituent of geothermal energy reserves. The regional distribution of thermal anomalies in the crust is controlled by regional tectonic patterns.

The Nigerian Geological Survey Agency provided the aeromagnetic data (Sheet 232) used for this research. The data was obtained as part of the NGSA-sponsored nationwide aeromagnetic survey in 2009 and the data were collected along a series of 200-meter-spaced NE SW flight lines with an average flight elevation of about 80 meters, with tie lines every 500 meters. Using the International Geomagnetic Reference Field (IGRF), 2005, the geomagnetic gradient was removed from the data. Also, the data was made available in the form of grids with a scale of 1:100,000. The total area covered in this study is approximately 55 by 55 km², extending from Latitude 7° N to 7° 30' N and Longitude 6° E to 6° 30' E. This study evaluates the potential of geothermal energy in the study area using anomalous heat flow and geothermal gradients by engaging high resolution aeromagnetic data and Temperature measurement.

Geology of Azara, Akiri, Awe, Kanje, Keana and Ribi

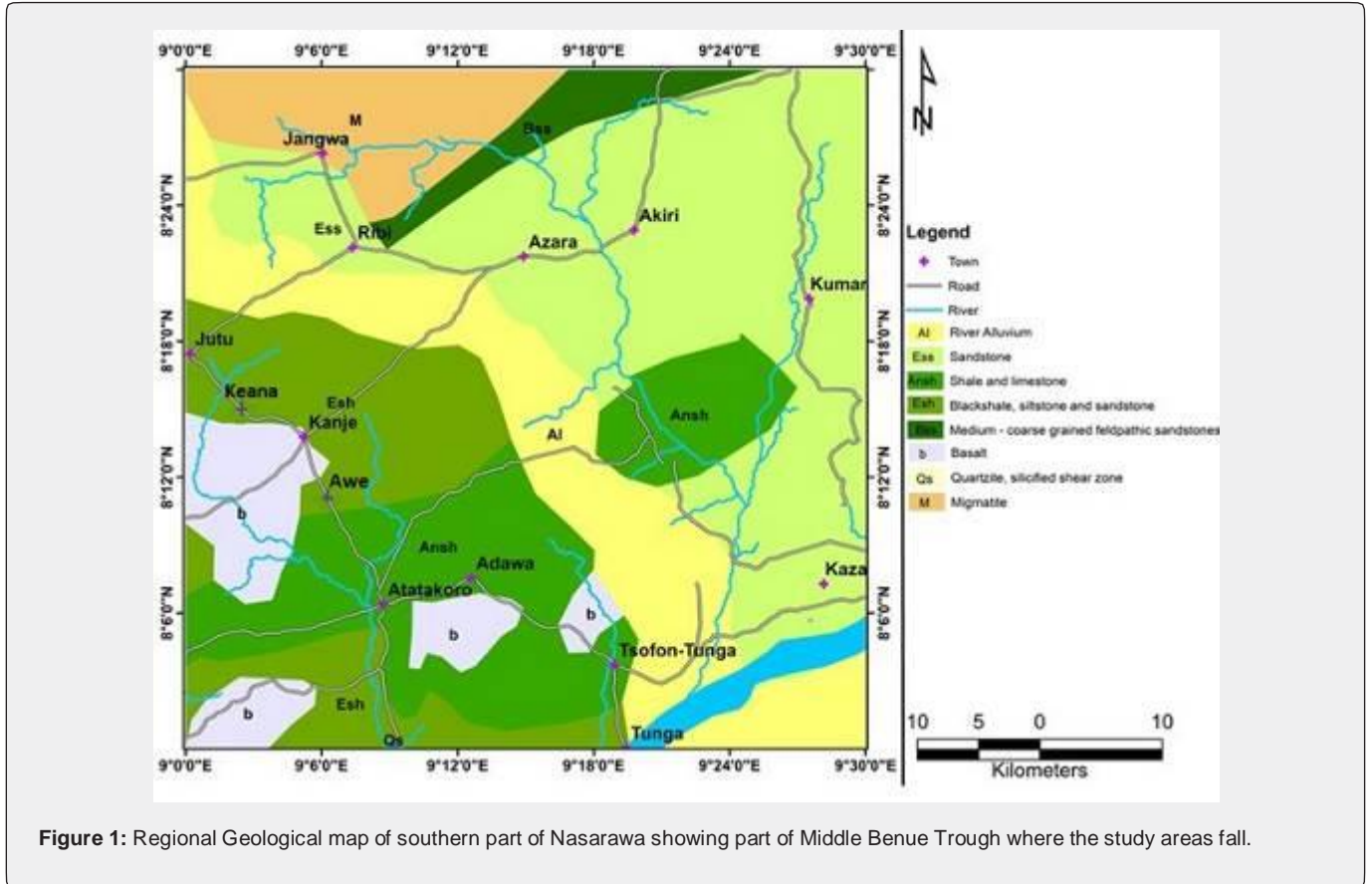


Figure 1: Regional Geological map of southern part of Nasarawa showing part of Middle Benue Trough where the study areas fall.

Azara, Akiri, Awe, Keana and Ribí are located in the southern parts of Nasarawa State, Nigeria. The southern part of Nasarawa is covered by sedimentary rocks. The sedimentary rocks belong to Middle Benue Trough which is the part of the sedimentary basin that extends from the Gulf of Guinea and stretches to the part of northeast of Nigeria. The regional geology of the area is being controlled structurally by two troughs: Middle and Lower Benue Troughs. Keana, Awe and Kanje are bounded from the north to the east by alluvia deposits, at the southwest of the area, they are bounded by Basalt intrusions while the southwest is shale and limestone (figure 1).

Azara, Akiri and Ribí are covered towards the southwest by alluvia deposits, at the southeast is shale and limestone boundary them and at the north is feldspathic sandstone, poorly sorted medium-coarse grained sandstone except for Ribí that is only bounded from the north to the southeast by a migmatites. The formations in these areas are Eze-Aku Formation, Keana, Awe, and Asu River. The stratigraphic order of the areas is in the order of the Latest Cenomanian-Turonian succession in the central and southern Benue Trough.

The local Geology of Keana Awe and Kanje is siltstone that graded upward to fissile black shale. The black shale (figure 2a) transits upward into a micaceousarkosic, poorly sorted sandstone bed (figure 2b), with occasionally interbedded mud rock, planar cross-bedded, characterizes this formation. The partial anticline like feature around Awe town indicated that the formation has relatively high dips of 17-32° towards the north and south parts, while towards the northeast, the dip becomes lower in the range of 3-9° in that direction. Longitudinal strike-slip faults parallel to the major fold axis, dominate the area. This observation shows that the area has experienced series of crustal plate movement and the structure is an anticline that has been faulted. Azara, Akiri and Ribí are underlain micaceous, poorly sorted cemented sandstone. The sandstone unit is cut across by close conjugate fractures (Joint) with infill of silica material.



Figure 2: (a) The lead researcher taking the temperature of Akiri Spring with thermometer with the assistant of the member of the team
(b) The lead researcher taking the temperature of Awe Spring with thermometer at Awe 1thermal spring in Awe, Nasarawa State, Nigeria
(c) The lead researcher taking the temperature of Azara Spring with thermometer.

Hydrogeology of Azara, Akiri, Awe, Kanje, Keana and Ribi

Akiri Thermal Spring is located in Akiri, about 4 kilometers north of Azara and less than 3 kilometers west of River Ankwe. It is covered by alluvial deposits of sand. The spring discharges from these sediments (figure 2c). Pool of the spring serves as a source of water for bathing and livestock and local source for salt. The temperature of the spring at the time of measurement was 54°C (table 1). The area is famous for barite mining and traditional salt production based on salty sediments. Awe Thermal Springs is located in Awe. It drains Awe Formation. It comprises three thermal springs. Awe spring 1 is the most visible among the three springs. It is 67km away from Lafia town. The area of the spring Awe 1 is about 500m in diameter. It is a low circular depression of seeps warm spring with temperature of 41.5°C. Awe spring 2 has temperature of 39.2°C. Awe spring 3 releases water with temperature 32.7°C (table 1).

The Keana thermal spring is located in an open slope valley at south Keana in Nasarawa State, about two kilometers east of the town. The valley and the slope bordering it are underlain by sandstone and clayey silt deposits. The sandstone is exposed in the sides of the depression which is about 2m deep. The temperature of the spring was measured to be 34°C. Ribi Thermal Spring is located at Rimi village. It is about 20-kilometer NNE from the Kanje Town. The thermal spring temperature was 33.9°C. Kanje Thermal Spring is located at Kanje town drains alluvia deposits of sandstone and clayey siltstone. The temperature was measured as 34°C close to the source of the spring and still remains 34°C, 10 away from the major source (table 1). Azara Thermal Spring is located at Azara village. The spring form offset a stream that drains the underlying sandstone rock units in the area. The temperature of the spring water was measured as 32.7°C (table 1).

Materials and Methods

Air temperatures at borehole sites and temperature of water at the bottom of borehole, were measured in situ with mercury maximum-minimum thermometer in Akiri and environs. The spectral analysis was carried out on the high-resolution aeromagnetic data of the study areas Akiri (Sheet 232). This study's procedures include creating a Total Magnetic Intensity (TMI) map with Geosoft Oasis montaj software, separating regional and residual anomalies, dividing the residual map into eight overlapping blocks, performing spectral analysis on each block, evaluating the depth to the magnetic source with spectral analysis, and estimating the geothermal gradient and heat flow. The spectral analysis by FFT was performed on each overlapping blocks and the plots of the logarithm of spectral energy $\ln(E)$ against the wave number (cycle/km) was carried out using a Matlab program specifically designed to obtain the gradients for deepest depth (centroid depth) and depth to top of magnetic source (table 2, figure 2d).

S/N	Geothermal Site	Point along the spring	Rock units	Temperature (°C)	Thermal Resources
1	Akiri	Closest to the source	Sandstone	54	hyperthermal
2	Akiri	10m away from source	Sandstone	54	hyperthermal
3	Awe 1	Closest to the source	Sandstone /shale	41.5	hyperthermal
4	Awe 2	Closest to the source	Sandstone /shale	39.2	Thermal
5	Awe 3	Closest to the source	Sandstone /shale	32.7	Thermal
6	Ribi	Closest to the source	Sandstone	33.9	Thermal
7	Ribi	10m away from the source	Sandstone	33.5	Thermal
8	Kanje	Closest to the source	Sandstone /Silt	34	Thermal
9	Kanje	10m away from the source	Sandstone /Silt	34	Thermal
10	Keana	Closest to the source	Sandstone /Silt	34	Thermal
11	Keana	10m away from the source	Sandstone /Silt	34	Thermal
12	Azara	Closest to the source	Sandstone	32.7	Thermal
13	Azara	10m away from the source	Sandstone	32.6	Thermal

Table 1: Point of water collection, conditions, and rock unit and water temperature along the thermal springs flow in Akiri and environs, Nasarawa State, Nigeria.

*The geothermal site here (Akiri - Azara), hyper thermal/thermal might be prospective for geothermal energy utilization. The geothermal and hydro geological conditions here are favourable for geothermal exploration and development

Table 2: Summary of the results of the centroid depth, depth to basement, curie depth, geothermal gradient, and the heat flow.

Blocks	X	Y	Centroid	Depth to Basement	Curie Depth	Geothermal Gradient	Heat Flow (mWm ⁻²)
A	9.125	8.375	8.1	2.4	13.8	42.0 2	105.05
B	9.207	8.375	4.47	1.5	7.44	77.9 5	194.87
C	9.29	8.37	4.65	1.34	7.96	72.8 6	182.15
D	9.124	8.38	4.98	1.49	8.47	68.4 7	171.17
E	9.125	8.125	11.4	2.56	20.81	27.8 7	69.68
F	9.207	8.125	8.24	1.52	14.96	38.7 7	96.92
G	9.207	8.125	9.12	2.54	15.7	36.9 4	92.35
H	9.38	8.125	11.2	2.7	19.7	29.4 4	73.6

Each sub-sheet was further subjected to Fast Fourier Transform, a process that decomposes the gravity data into its energy spectrum and wave number components. The location was labelled A-H (Sheet 232). The energy spectrum was plotted against wave number components using MatLab software (figure 2d). This process deduced gradients in the form of depth to the top (Z_T) and centroid (Z_0) of sources. The depth to top of basement and centroid were used to evaluate Curie point depth (Z_b) and thereafter estimate the geothermal gradient and heat flow of study area. Curie point depths varies with geological situations [13].

Tanaka et al. [14] established that CPD ranging below 10km are attributable to volcanic and geothermal regions, 10km to 15km are attributable to Island arch and ridges, 20km and above are attributable to Plateaus and 30km and above are attributable to trenches. The heat flow value between

80mWm⁻² and 100mWm⁻² has been established to indicate geothermal anomalous conditions in an area for geothermal prospecting [15]. It can therefore be deduced from this study that regions that fall within the range of 80 to 100 mWm⁻² are good spots for geothermal energy resources.

Results and Discussion

From the geological and hydrogeological studies, the temperature of the warm spring at the time of measurement was 54°C. Awe spring 2 has temperature of 39.2°C. Awe spring 3 releases water with temperature 32.7°C. The Keana temperature of the spring was measured to be 34°C. Ribí Thermal Spring temperature was measured as 33.9°C. Kanje temperature was measured to be 34°C and the temperature of Azara spring water was measured as 32.7°C (table 1). These temperature manifestations results collaborated the Spectral analysis of the aeromagnetic data.

Results of the aeromagnetic data of the study area using **Akiri_ (Sheet 232)** with the aim of accessing the geothermal potential of the study area and environs revealed the occurrence of geothermal parameters: The Curie point depth values range from (7.44-20.81) km, the geothermal gradient values range from (27.87-77.95) °C/km and the heat flow values ranges from (69.68-194.87) mW/m² (table 2). The NE edge covering Jangwa, Azara, Akiri, and Ribí hosts the anomalous heat flow and geothermal gradient with corresponding shallowest values of Curie point depth (figures 3-5). Other regions like Kumar, Jutu, Kanje, Adawa, Atatakoro, and Kaza also show good geothermal manifestations, except few areas in SW covering Tunga with low heat flow below the recommended threshold value of 80 mW/m².

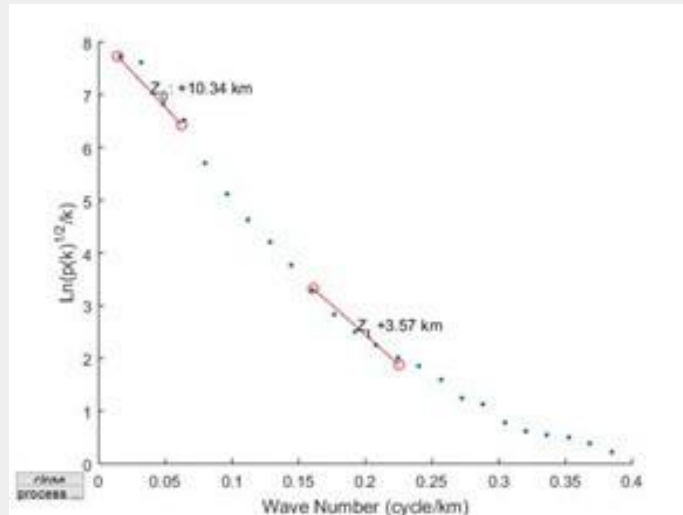


Figure 2d: Plot of spectrum energy against wave number spectral block.

The shallow curie depths with corresponding heat flow are observed around the Akiri and Awe hot springs. The observed anomalies geothermal conditions can be attributed to the intense Cenozoic magmatic activities with numerous volcanic intrusions within the Benue trough. Generally, for a viable geothermal reservoir, a heat flow range of (80-100) mW/m² is recommended, hence it can be inferred that every other region on the study area could be considered as having good prospect in the study area with high heat flow above 80-100 mWm⁻² (figure 5).

Conclusion

From the geological and hydrogeological studies, the temperature of the warm spring at the time of measurement was 54°C. Awe spring 2 has temperature of 39.2°C. Awe spring 3 releases water with temperature 32.7°C. The Keana temperature of the spring was measured to be 34°C. Ribi Thermal Spring temperature was measured as 33.9°C. Kanje temperature was measured to be 34°C and the temperature of Azara spring water was measured as 32.7°C (table 1).

Results of the aeromagnetic data of the study area using **Akiri_ (Sheet 232)** with the aim of accessing the geothermal potential of the study area and environs revealed the occurrence of geothermal parameters: The Curie point depth values range from (7.44-20.81) km, the geothermal gradient values range from (27.87- 77.95) °C/km and the heat flow values ranges from (69.68- 194.87) mW/m² (table 2). The NE edge covering Jangwa, Azara, Akiri, and Ribi hosts the anomalous heat flow and geothermal gradient with corresponding shallowest values of Curie point depth (figures 3-5). Other regions like Kumar, Jutu, Kanje, Adawa, Atatakoro, and Kaza also show good geothermal manifestations, except few areas in SW covering Tunga with low heat flow below the recommended threshold value of (80-100) mW/m².

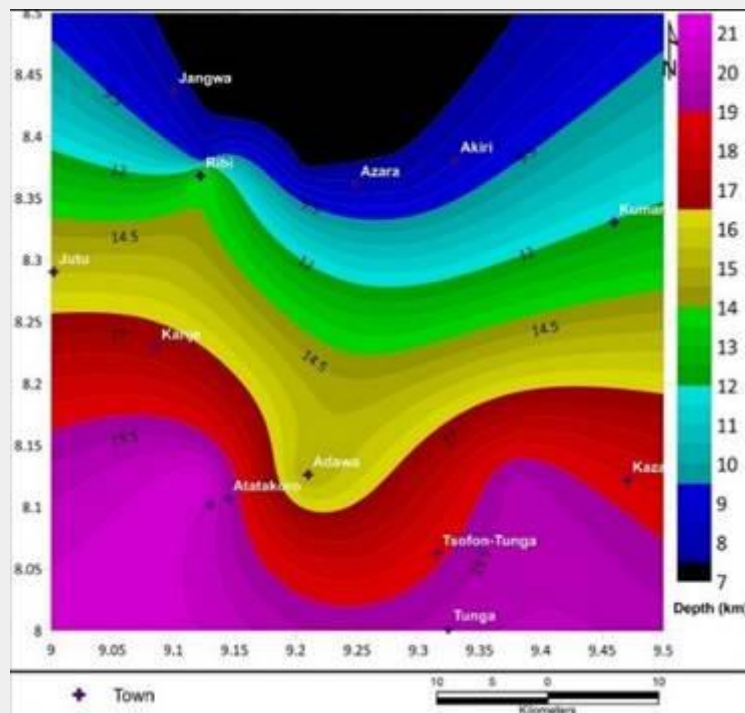


Figure 3: CPD contour map of Sheet 232 corresponding to Akiri.

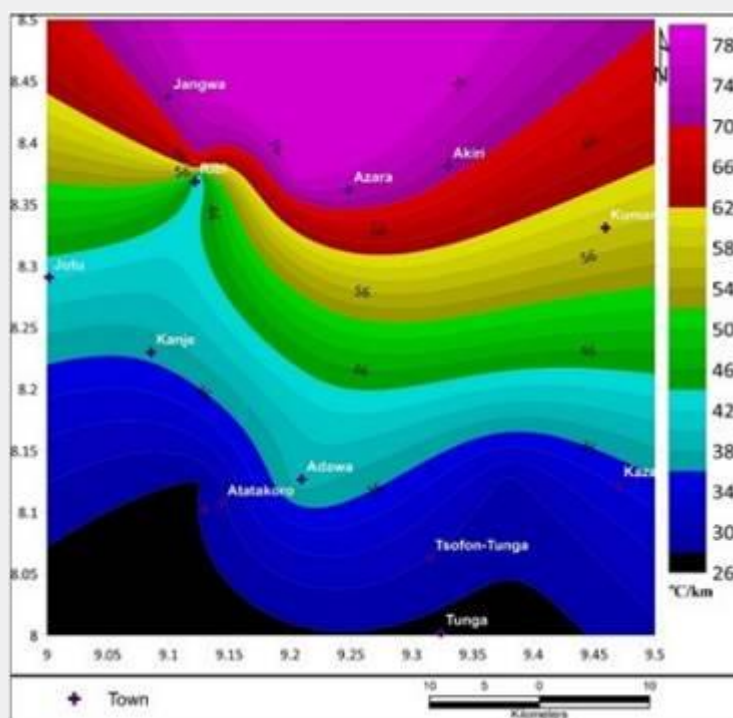


Figure 4: Geothermal Gradient contour map of Sheet 232 corresponding to Akiri.

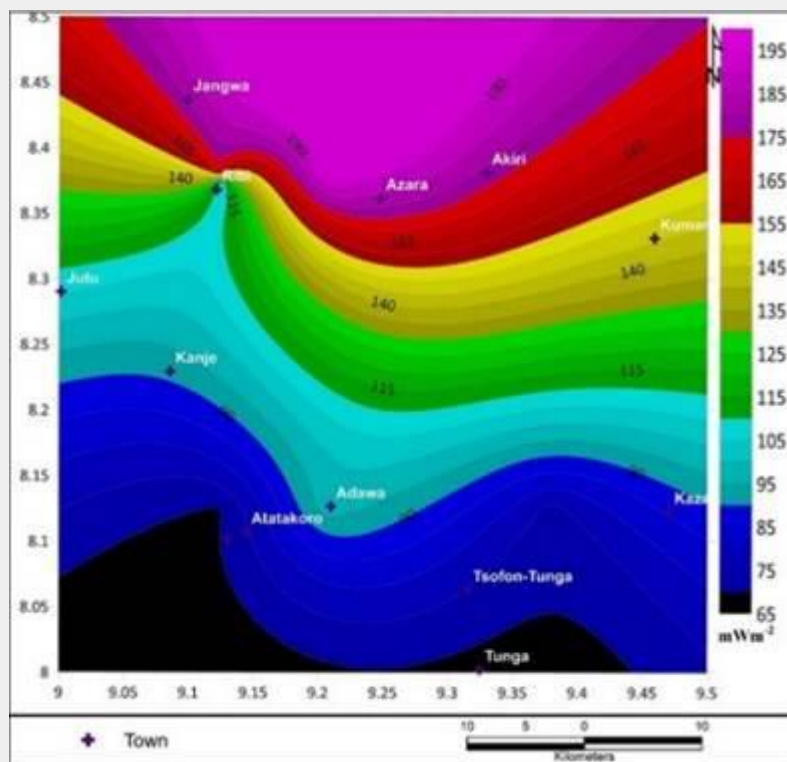


Figure 5: Heat flow contour map of Sheet 232 corresponding to Akiri.

The shallow curie depths with corresponding heat flow are observed around the Akiri and Awe hot springs. The integration of the hot spring results with of the aeromagnetic studies revealed that Akiri can be used for clean electricity generation in Nigeria. It can therefore be deduced from this study that regions that fall within the range of 80 to 100 mWm^{-2} are good spots for geothermal energy resources within the study area.

Acknowledgments:

The researchers would like to thank the Nigeria Telecommunications commission (NCC) for sponsoring this laudable project.

REFERENCES

1. Downing RA, Gray DA (1986) Geothermal energy - the potential in the United Kingdom. British Geological Survey report p. 3-7.
2. Komolafe AA (2010) Investigations into the tectonic lineaments and thermal Structure of Lake Madadi, southern Kenya rift using integrated geophysical methods. M.Sc unpublished thesis, International Institute for geo-information Science and Earth observation, Enschede, The Netherlands 60.
3. Mariita NO (2013) Applications of potential field methods for geothermal exploration - A case for Olkaria and Menengai geothermal fields, Kenya. Short Course VIII on Exploration for Geothermal Resources.
4. Obande EG, Lawal KM, Ahmed AL (2013) Geothermal characterization using spectral analysis and apparent magnetization of Wikki warm spring, northern Nigeria. *Journal of Mining and Geology* 49(1): 53-63.
4. International Geothermal Association (IGA) (2020) Geothermal outlook in East Africa: Perspective for Geothermal Development. (Presentation by P. Omenda, Director IGA; Consultant).
5. El-Qady G (2006) Exploration of a geothermal reservoir using geoelectrical resistivity inversion: case study of Hammam Mousa, Sinai, Egypt. *J Geophysics Eng* 3(2): 114-121.
6. Kana JD, Djongyang N, Raidandi D, Nouck PN, Daje A (2015) A review of geophysical methods for geothermal exploration. *Renewable and Sustainable Energy Reviews* 44: 87-95.
7. Shah M, Sircar A, Vaidya D, Sahajpal S, Chaudhary A, et al. (2015) Overview of Geothermal Surface Exploration Methods. *IJARIEE* 1(4): 55-64.
8. Chabaane A, Redhaounia B, Gabtni H (2017) Combined application of vertical electrical sounding and 2D electrical resistivity imaging for geothermal groundwater characterisation: Hammam Sayala Hot Spring case study (NW Tunisia). *Journal of African Earth Sciences* 134: 292-298.
9. Azaiez H, Gabtni H, Chabaane A, Sayem G, Bedri M (2020) Geophysical study of Hanmam Sidi Maamar geothermal site in Central Tunisia for sustainable development. *Journal of African Earth Sciences* 170: 103897.
10. Okiyi IM, Ibeneme SI, Obiora EY, Onyekuru SO, Selema AI, etl al. (2021) Evaluation of

- Geothermal Energy Resources in Parts of Southeastern Sedimentary Basin, NIGERIA. *Ife Journal of Science*: 23(1): 195-211.
11. Georgsson LS (2013) Geophysical methods used in geothermal exploration. Paper presented at Short Course VIII on Exploration for Geothermal Resource, Organised by (UNU – GTP, GDC and KenGen, at Lake Bogoria and Lake Naivasha, Kenya. Oct 31-Nov 22.
 12. Ross HE, Blakely RJ, Zoback MD (2006) Testing the use of aeromagnetic data for the determination of Curie depth in California. *Geophysics* 71(5): L51-L59.
 13. Tanaka A, Okubo Y, Matsubayashi O (1999) Curie point depth based on spectrum analysis of magnetic anomaly data in East and Southeast Asia. *Tectonophysics* 306(3-4): 461-470.
 14. Jessop AM, Lewis TJ, Judge AS, Taylor AE, Drury MJ (1984) Terrestrial heat flow in Canada. *Tectonophysics* 103(1-4): 239-261.



This work is licensed
under Creative
Commons
Attribution 4.0
License DOI:
[10.19080/IMST.2022
.03.555615](https://doi.org/10.19080/IMST.2022.03.555615)

Your next submission with Juniper Publishers

will reach you the below assets

- Quality Editorial service
- Swift Peer Review
- Reprints availability
- E-prints Service
- Manuscript Podcast for convenient understanding
- Global attainment for your research
- Manuscript accessibility in different formats
(Pdf, E-pub, Full Text, Audio)
- Unceasing customer service

Innovative Geothermal Assessment of Akiri – Azara and Environs for Power Generation as a source of Clean Energy in Nigeria

*Aigbedion I, Salufu S.O , Aikhuele D.O and Aigbedion Elijah Osemudiamen
Ambrose Alli University, Ekpoma¹*

University of Port Harcourt, Rivers State¹.

Abstract

Geological and hydrological studies across *Akiri – Azara*, Nigeria was done to identify potential areas with viable thermal resources. The results of the study reveals that the warm springs, Akiri-Awe have their thermal resources as hyper thermal, and thermal, with no hypothermal evidence. Only warm springs with hyper thermal and thermal resources are viable for the electricity generation. The temperature of the springs at the time of measurement was found to ranged from (54-32.7)°C . The spectral analysis was carried out on the bouguer of the gravity anomaly data of the study areas. Results of spectral analysis for study revealed the occurrence of geothermal parameters: Curie point depth varied between 7.39 to 20.71 km, geothermal gradient varied between 28.01 to 78.48 °C/km and heat flow values varied between 70.29 to 197.99 mW/m².

A recommended threshold value of heat flow for a good source of geothermal energy is set at 80 to 100 mW/m². These ranges of values can be observed between the light blue colours depicted within southern regions of the heat flow contour map. Values of heat flow above the stated range is considered as excess, however, the entire study area with exception of the extreme Southern parts can be considered in locating potential geothermal reservoirs. The shallow curie depths with corresponding heat flow are observed around the Akiri and Awe hot springs. The observed anomalies geothermal conditions can be attributed to the intense Cenozoic magmatic activities with numerous volcanic intrusions within the Benue trough.

Introduction

Geothermal study is made through exploration, evaluation, and exploitation of this type of energy. This type of energy manifests on the surface in the form of volcanoes, geysers, fumaroles, hot springs, etc. Geothermal power plants have very low gaseous emissions to the air when compared with all other power generation technologies that emit carbon dioxide (CO₂) as a normal part of the operation.

Geothermal energy is mainly one of the important energy sources ascribing substantially to the global sustainable energy supply drive. Geothermal energy sources are used as a means of electricity in many parts of the world (Guo and Wang, 2012, Baioumy *et al.*, 2015). The generation

of electricity using geothermal energy could not neglected from the use and need for a world shift from environmentally harmful “fossil fuel” means of energy generation to more clean and renewable sources of energy. Nigeria has not been able to produce enough energy for many decades to meet the needs of people demand both domestic and industrial. The capacity of Nigeria’s current electricity generation installed is approximately 6000 MW (NCN, 2014), with maximum output of 4000 MW which is basically produced from two major primary sources such as hydro (36%) and gas-fired (fossil fuel) sources with 64% contribution (NCN, 2014). The currently energy generation from fossil fuel has been impacting the safety of this part of the world negatively. The air pollution, gas emission, and oil spillage problems are the major negative impacts. However, there is need to look into another means or sources of energy that can be generated without causing no damage or harm to the surrounding (NCN, 2014, Abraham and Edet, 2017). To add to the country quantum of energy, there is need to investigate other healthier and renewable sources of energy for its sustainable development and growth (NCN, 2014, Abraham and Edet, 2017). The high-temperature gradients, shallow Curie point depths, low regional gravity anomalies, the presence of structural lineaments, high heat production, the outcropping of younger volcanic or granitic rocks, and hot or warm spring locations are the major parameters that needs to be considered for reasonable accumulation of geothermal resources. The pattern subsurface geological fissures such as fault and fracture zones enhance the permeability of rocks, which allow easy flowing of hot fluid from the Earth’s interior to the surface (Wibowo 2006, Kiavarz *et al.*, 2013). The major occurrence of geothermal energy resources within the Earth is indicated by hot/warm springs. In some major geothermal areas, volcanic rocks occurrence serve as cap rocks. The volcanic rock that occur within the subsurface exhibits low gravity anomaly, while the high-temperature gradients and shallow Curie Point Depth show the high possibility of geothermal resources ((Wibowo 2006). Volcanic rock outcrops, mud volcanoes, fracture distributions, hot springs, hydrothermal alterations, and faults was used to first discovered the majority of the global geothermal energy fields. Geothermal investigation is normally carried out in different phases. The first stage (phase) is by viewing the regions of the major geothermal occurrence involving integration of several data sources in a regional extent, following by identifying the proximity area and further investigation of the regions of high proximity indicated from the results of first phase (Kiavarz *et al.*, 2013). Other studies used subsurface geological properties such as rock distributions, hot/warm springs, structural distributions, and mud pods that

revealed geothermal indicators (Kurowska and Schoeneich, 2010, Abdullahi *et al.*, 2014, Musa *et al.*, 2016). The major objective of this research is to use efficient approach to delineate the properties controlling the geothermal energy prospects, identify, and map prospective geothermal zones, and finally construct a geothermal prospectivity map of the study area.

Geology of the Study Area

Akiri -Azara, and other springs like Awe, Keana and Ribi are located in the southern parts of Nasarawa State, Nigeria. The southern part of Nasarawa is covered by sedimentary rocks. The sedimentary rocks belong to Middle Benue Trough which is the part of the sedimentary basin that extends from the Gulf of Guinea and stretches to the part of northeast of Nigeria. The regional geology of the area is being controlled structurally by two troughs; Middle and Lower Benue Troughs. Keana, Awe and Kanje are bounded from the north to the east by alluvia deposits, at the southwest of the area, they are bounded by Bauchi intrusions while the southwest is shale and limestone (Fig. 1.1b). Azara, Akiri and Ribi are covered toward the southwest by alluvia deposits, at the southeast is shale and limestone boundary them and at the north is feldspathic sandstone, poorly sorted medium-coarse grained sandstone except for Ribi that is only bounded from the north to the southeast by a migmatites. The formations in these areas are Eze-Aku Formation, Keana, Awe, and Asu River. The stratigraphic order of the areas is in the order of the Latest Cenomanian-Turonian succession in the central and southern Benue Trough.

The local Geology of Keana Awe and Kanje is siltstone that graded upward to fissile black shale. The black shale (Fig. 1.2a) transits upward into a micaceousarkosic, poorly sorted sandstone bed (Fig. 1.2b.6b), with occasionally interbedded mudrock, planar cross-bedded, characterizes this formation. The partial anticlinelike feature around Awe town indicated that the formation has relatively high dips of 17–32° towards the north and south parts, while towards the northeast, the dip becomes lower in the range of 3–9° in that direction. Longitudinal strike-slip faults parallel to the major fold axis, dominate the area. This observation shows that the area has experienced series of crustal plate movement and the structure is an anticline that has been faulted. Azara, Akiri and Ribi are underlain micacious, poorly sorted cemented sandstone. The sandstone unit is cut across by close conjugate fractures (Joint) with infill of silica material.

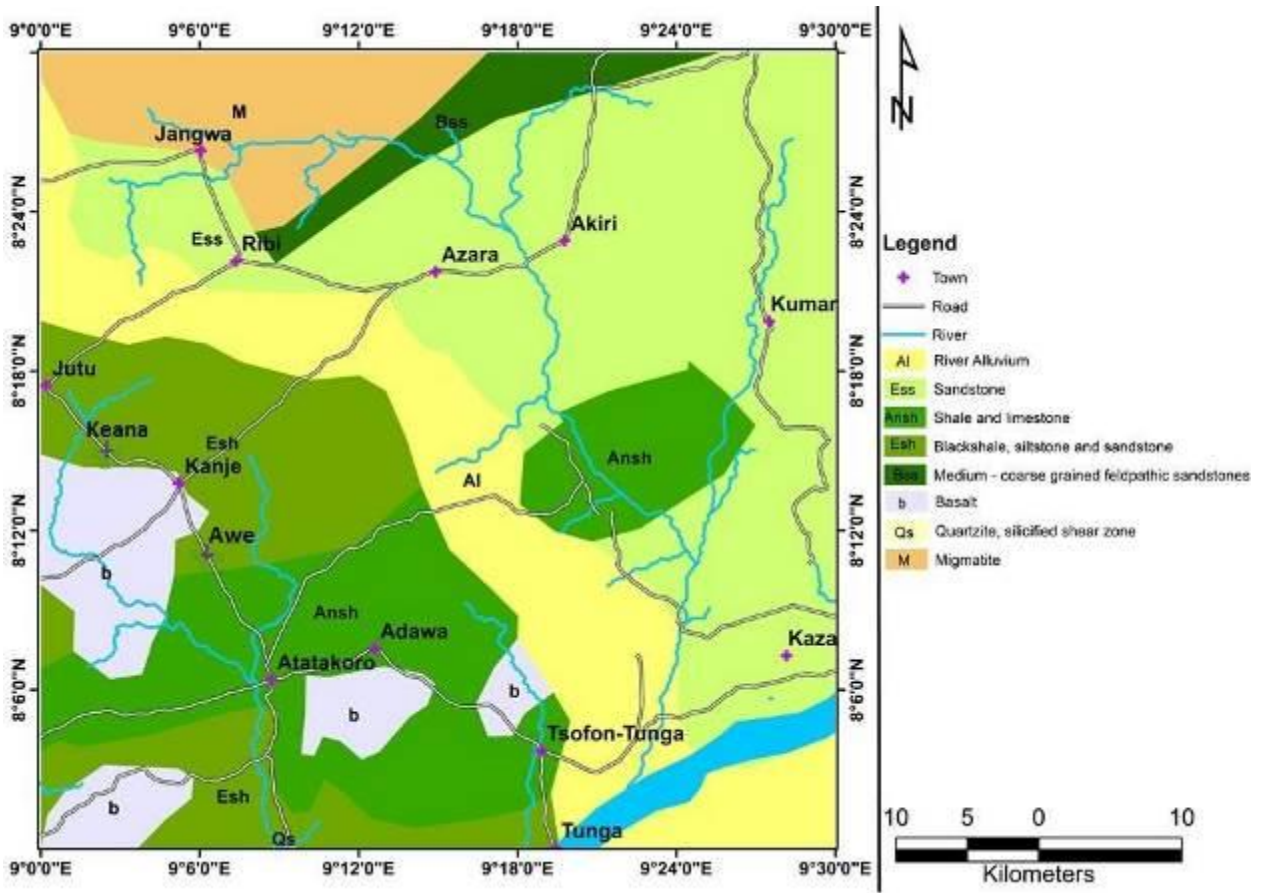


Fig. 1.1: Regional Geological map of southern part of Nasarawa showing part of Middle Benue Trough where the study areas



Fig. 1.2: (a) Keana Formation in Nasarawa showing black shale, siltstone and sandstone lithology units (b) Awe Formation in Nasarawa showing outcrop exposure of black shale

Hydrogeology of Azara, Akiri, Awe, Kanje, Keana and Ribi

Akiri Thermal Spring is located in Akiri, about 4 kilometers north of Azara and less than 3 kilometers west of River Ankwe. It is covered by alluvial deposits of sand. The spring discharges from these sediments. Pool of the spring serves as a source of water for bathing and livestock and local source for salt. The temperature of the spring at the time of measurement was 54° C. The area is famous for barite mining and traditional salt production based on salty sediments. Awe spring 1 is the most visible among the three springs. It is 67 km away from Lafia town. The area of the spring Awe 1 is about 500m in diameter. It is a low circular depression of seeps warm spring with temperature of 41.5°C. Awe spring 2 has temperature of 39.2°C. Awe spring 3 releases water with temperature 32.7°C. The Keana thermal spring is located in an open slope valley at south Keana in Nasarawa State, about two kilometers east of the town. The valley and the slope bordering it are underlain by sandstone and clayey silt deposits. The sandstone is exposed in the sides of the depression which is about 2m deep. The temperature of the spring was measured to be 34°C. Ribi Thermal Spring is located at Rimi village. It is about 20 kilometer NNE from the Kanje Town. The thermal spring temperature was 33.9°C. Kanje Thermal Spring is located at Kanje town drains alluvial deposits of sandstone and clay siltstone. The temperature was measured as 34°C close to the source of the spring and still remains 34° 10m away from the major source. Azara Thermal Spring is located at Azara village. The spring forms a stream that drains the underlying sandstone rock units in the area. The temperature of the spring water was measured as 32.7°C

Materials and Methods

The resources (materials) used for this study include; The global positioning system (GPS), Thermometer, clinometer, Geosoft oasis montaj, surfur, Arc Gis and mat lab software's, airborne gravity data, and geological maps. The geothermal potential of the study area from geological and hydrogeological point of view was determined as the first principle objective of the research using the thermometer, clinometer and GPS. Aeromagnetic data was also applied to generate the geological maps using Oasis Montaj, Malab program, surfur and Arc GIS software's for the geology and Hydrogeology of the study area. The spectral analysis was carried out on the bouguer

of the gravity anomaly data of the study area, using Akiri (Sheet 232). Each sub-sheet was further subjected to Fast Fourier Transform, a process that decomposes the gravity data into its energy spectrum and wave number components. The location was labelled A-L (Sheet 232). The energy spectrum was plotted against wave number components using MatLab software (Fig1.3b.). This process deduced gradients in the form of depth to the top (ZT) and centroid (Z0) of sources. The depth to top of basement and centroid were used to evaluate Curie point depth (Zb) and thereafter estimate the geothermal gradient and heat flow of study area. Curie point depths varies with geological situations (Ross *et al.*, 2006). Tanaka *et al.* (1999) established that CPD ranging below 10 km are attributable to volcanic and geothermal regions, 10 km to 15 km are attributable to Island arch and ridges, 20 km and above are attributable to Plateaus and 30 km and above are attributable to trenches. The heat flow value between 80mWm^{-2} and 100mWm^{-2} has been established to indicate geothermal anomalous conditions in an area for geothermal prospecting (Jessop *et al.*, 1976). It can therefore be deduced from this study that regions that fall within the range of 80 to 100mWm^{-2} are good spots for geothermal energy resources.

IJSER

Results and Discussion

The temperature of the Akiri spring at the time of measurement was 54°C , while the temperature of the Azara spring water was measured as 32.7°C .

Results of spectral analysis for study area revealed the occurrence of geothermal parameters: Curie point depth varied between 7.39 to 20.71 km, geothermal gradient varied between 28.01 to 78.48°C/km and heat flow values varied between 70.29 to 197.99mW/m^2 . Table 1 presents the summary of the results of the centroid depth, depth to basement, curie depth, geothermal gradient and the heat flow A general trend of low to peak geothermal gradient and heat flow values is observed from the southern to northern region of study area respectively (Fig.1. 3a). An inverse trend is observed for curie point depth. A recommended threshold value of heat flow for a good source of geothermal energy is set at 80 to 100mW/m^2 . These ranges of values can be observed between the light blue colours depicted within southern regions of the heat flow contour map. Values of heat flow above the stated range is considered as excess, however, the entire study area with exception of the extreme Southern parts can be considered in locating potential geothermal reservoirs. Only heat flow results in excess of 80mW/m^2 indicating anomalous geothermal

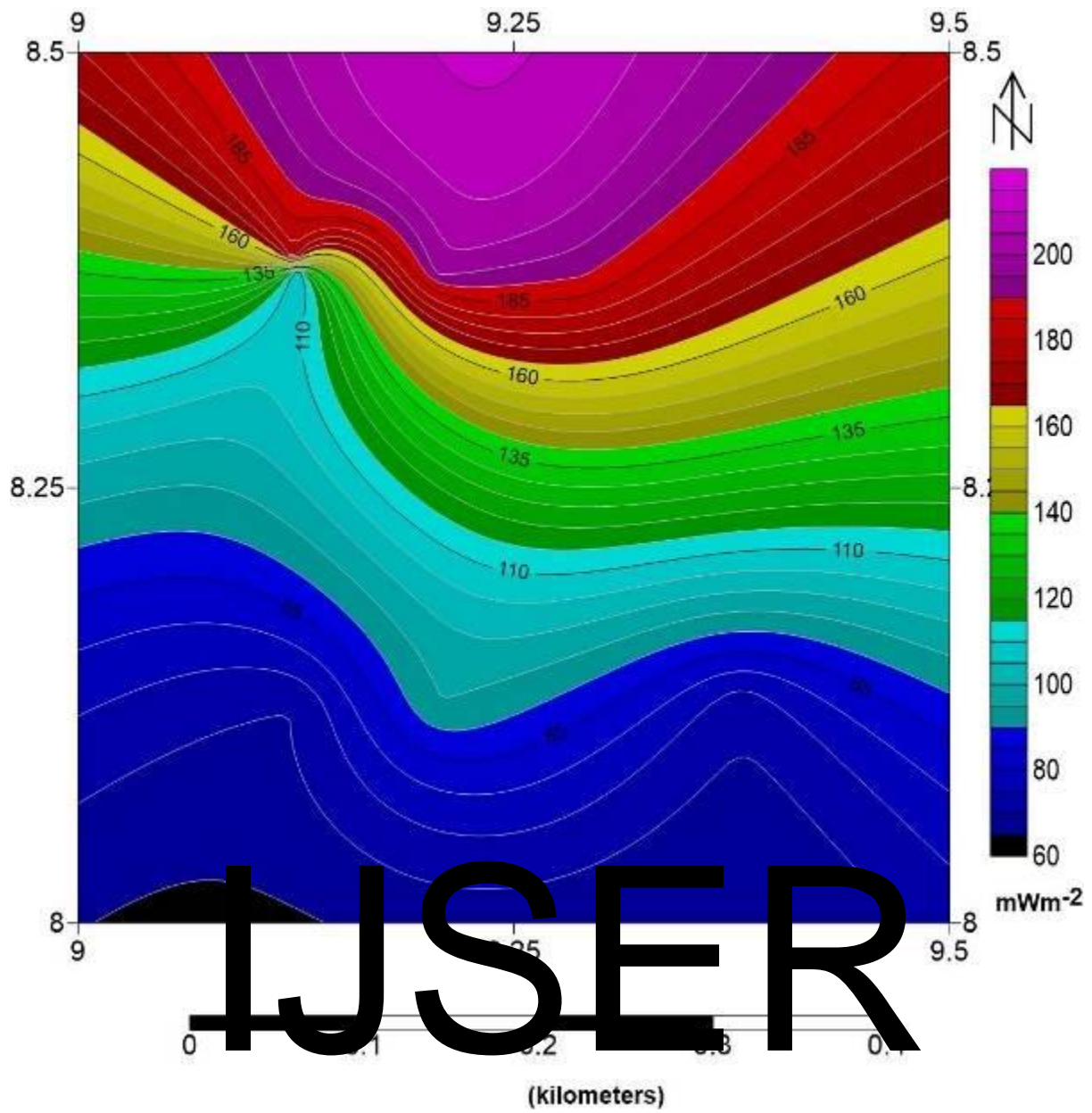


Fig.1.3a Heat flow contour map of sheet 232 corresponding to Akiri

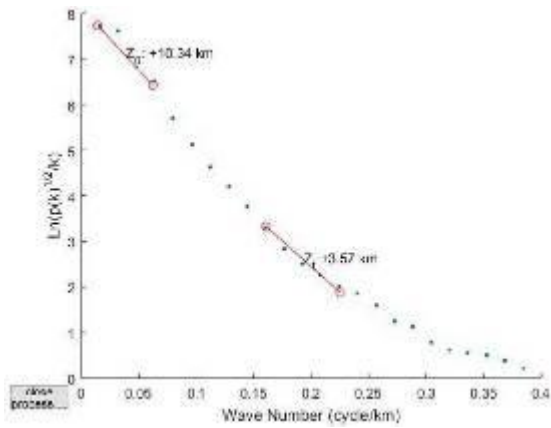


Fig 1.3b: Plots of spectrum energy against wave number (a) spectral block A1.

Conclusion

The results of the Geological and hydrological studies across Akiri-Azara to identify potential areas with viable thermal resources reveals that the warm springs in the areas, have thermal resources as hyper thermal (surface manifestations). The temperature of the Akiri spring at the time of measurement was 54° C, while the temperature of the Azara spring water was measured as 32.7°C.

Results of spectral analysis for study area revealed the occurrence of geothermal parameters: Curie point depth varied between 7.39 to 20.71 km, geothermal gradient varied between 28.01 to 78.48 °C/km and heat flow values varied between 70.29 to 197.99 mW/m². A recommended threshold value of heat flow for a good source of geothermal energy is set at 80 to 100 mW/m². These ranges of values can be observed between the light blue colours depicted within southern regions of the heat flow contour map. Values of heat flow above the stated range is considered as excess, however, the entire study area with exception of the extreme Southern parts can be considered in locating potential geothermal reservoirs. Only heat flow results in excess of 80 mW/m² indicating anomalous geothermal conditions can be utilized in geothermal clean electricity generation.

Acknowledgments:

The authors are sincerely grateful to the Nigeria Telecommunications commission (NCC) for sponsoring this research work.

References

- Abdullahi, B.U., Rai, J.K., Olaitan, O.M. and Musa, Y.A. (2014). A Review of the Correlation between Geology and Geothermal Energy in North-Eastern Nigeria. *IOSR J. Appl. Geol. Geophys.* 2, 74–83.
- Abraham, E.M. and Edet, E. (2017). Review of Geothermal Energy Research in Nigeria: The Geoscience Front. *J. Earth Sci. Geophys.* 3, 1–10.
- Baioumy, H., Nawawi, M., Wagner, K. and Arifin, M.H. (2015). Geochemistry and geothermometry of non-volcanic hot springs in West Malaysia. *J. Volcanol. Geotherm.* 12–22.
- Energy Commission of Nigeria, Federal Republic of Nigeria (2014). National Energy Masterplan; Energy Commission of Nigeria: Abuja, Nigeria. Res. 290,
- Guo, Q. and Wang, Y. (2011). Geochemistry of hot springs in the Tengchong hydrothermal areas, Southwestern China. *J. Volcanol. Geotherm. Res.*, 215–216, 61–73.
- Jessop, A. M., Lewis, T. J., Judge, A. S., Taylor, A. E., & Drury, M. J. (1984). Terrestrial heat flow in Canada. *Tectonophysics*, 103(1-4), 239-261.
- Kiavarz, M., Noorollahi, Y., Samadzadegan, F., Ali, M. and Itoi, R. (2013). Spatial data analysis for exploration of regional scale geothermal resources. *J. Volcanol. Geotherm. Res.* 266, 69-83.
- Kurowska, E. and Schoeneich, K. (2010). Geothermal Exploration in Nigeria. In Proceedings of the World Geothermal Congress, Bali, Indonesia, 25–29 April, pp. 25–29.
- Musa, O.K., Kurowska, E.E., Schoeneich, K., Alagbe, S.A. and Ayok, J. (2016). Tectonic control on the distribution of onshore mud volcanoes in parts of the Upper Benue Trough, northeastern Nigeria. *Contemp. Trends Geosci.* 5, 28–45.
- Ross, H. E., Blakely, R. J., & Zoback, M. D. (2006). Testing the use of aeromagnetic data for the determination of Curie depth in California. *Geophysics*, 71(5), L51-

L59.

Tanaka A, Okubo Y, Matsubayashi O (1999) Curie point depth based on spectrum analysis of magnetic anomaly data in East and Southeast Asia. *Tectonophysics* 306:461–470.

Wibowo, H. (2006). Spatial Data Analysis and Integration for Regional-Scale Geothermal Prospectivity Mapping, West Java, Indonesia. Master's Thesis, International Institute for Geo- Information Science and Earth Observation, Enschede, The Netherlands.

IJSER



Annual
International
Conference
& Exhibition

**NAPE
2022**

Nov 13 - 17, 2022 Eko Hotel & Suites, Lagos, Nigeria

**NIGERIAN ASSOCIATION OF
PETROLEUM EXPLORATIONISTS**
An International Geoscience Organisation



BOOK OF ABSTRACTS & CONFERENCE PROCEEDINGS

Theme

**Global Energy Transition and the Future of the
Oil and Gas Industry:
Evolving Regulations, Emerging Concepts & Opportunities**

Sponsor



GREEN ENERGY
INTERNATIONAL LIMITED



Lithofacies Discrimination using Model Based Post Stack Seismic Inversion in 'STD' Field, Niger Delta Okiemute Enaugh and Difference Ogagarue

Centre of Excellence in Geosciences and Petroleum Engineering, University of Benin

Abstract

Lithofacies discrimination is very important for improved reservoir development and reduction in uncertainties associated with hydrocarbon reservoir characterization. In this study, a model driven post stack acoustic impedance inversion was carried out by integrating well logs comprising GR, density and compressional sonic log, and a near offset 3D post stack seismic data obtained from "STD" field in the Niger Delta. The aim was to delineate lateral variations in subsurface rock properties, especially lithology. The forward model involved the convolution of source wavelet derived from a combination of the seismic and well data, with the earth reflectivity function to derive a low frequency model which was thereafter inverted to obtain variations in earth properties away from well control. The inversion results revealed three distinct lithofacies (sand, sandy shale and shale) based on acoustic impedance variations. Low acoustic impedance values of 10388 (ft/s) (g/cc) to 11963 (ft/s) (g/cc) in the time slice of 1650ms to 1700ms, was indicative of a prospective gas filled sand facies. The results are helpful for improved structural and stratigraphic interpretation to reduce drilling risk and make informed economic decisions.

Keywords: Acoustic impedance, Model-based Inversion, Lithofacies

Innovative Geothermal Technology as a Source of Clean Energy in Nigeria.

Aigbedion, I and Salufu.O

Geophysics Department, Ambrose Alli University, Ekpoma.

Abstract

The nations in the world have a common goal of making the world a global village, and the world a clean and safe place. Electricity generation is based on three major categories of energy, namely nuclear energy, fossil fuels and renewable energy sources (non fossil fuel). Most electricity is generated with steam turbines using fossil fuels, nuclear, biomass, geothermal and solar thermal energy. Other major electricity generation technologies include gas, hydro and wind turbines and solar photovoltaics. In Nigeria the primary sources of energy for the production of electricity are water, oil, gas and coal. However, epileptic supply of energy to run every day to day activities in the industries and our homes has caused serious setback in Nigeria, to meet up with the goal of the nations of the world. As a result, the industries and homes in Nigeria had to adopt alternative source of energy to meet up by self-generation of power, using diesel/fuel generators. This method of generating energy is inefficient, costly, and inadequate to support regular supply. There is the emission of carbon iv-oxide, (CO₂) and greenhouse gases being associated with this alternative source of energy generation. These emissions constitutes serious environmental challenges thus, makes heat to be trapped in the atmosphere and the CO₂ depleting ozone layer. Then we need a better source of energy that will guarantee regular and efficient supply of power that will be cleaner and safer than the existing ones. The answer to this is geothermal energy. Geothermal energy has been known to be the safest and the cleanest source of energy. It occurs within the earth. Locating it is a major problem. However, geophysical methods with geological information from detail geological mapping across Nigeria to track geothermal field and geothermal reservoir across Nigeria for onward utilization as source of power generation to run our industries and homes exist. The fact is that, geothermal energy does not deplete, there is no epileptic associated with it. It is steady and regular. The Nigerian Telecommunication industry is already looking towards this direction of Geothermal as a source of clean Energy for efficient power delivery. Bottom Hole Temperature logs (BHT data) results from oil wells reveals that geothermal gradient in Niger Delta ranges from (1.1 - 4.8°C) /100m and in Anambra Basin it can reach 5.7°C/100m. Exploration for Geothermal energy in northern Nigeria based on shallow water wells (down to 500 m deep) was carried out over 22 years ago. Research on geothermal energy in Northern Nigeria was done mainly on geothermal conditions within Sokoto and Nigerian part of Chad sedimentary basins, where relatively high Geothermal gradients were found: (7.5° - 5.8°C)/100m. In Most areas of our study it was observed that geothermal gradient was influenced by sedimentation and the lithology of the area. Geothermal gradients evaluation indicate that steam would be encountered at a depth of about 1,767m in the Lagos and Auchí-Agbede areas of Edo State, and at about 1,280 m in the Abakaliki area. The other aspect of geothermal exploration in Nigeria is investigating of the thermal springs and seepages, which occur mainly within sediments of the Middle and Upper Benue Trough. The water of the warmest springs in that area: Akiri and Ruwan Zafi have the temperature about 54°C and it suggests the occurrence of some geothermal anomalies. Similarly, the water from Ikogosi warm spring is 40°C which also suggest the occurrence of some geothermal anomalies in South-Western part of the country, in Ekiti state.

BOOK OF ABSTRACTS & CONFERENCE PROCEEDINGS



Chronicles of Fluid Prediction Techniques-Merits, Pitfalls and Application in the Niger Delta: A Quantitative Interpretation Perspective.

Obinna Chudi and Uche Johnbosco
Shell Petroleum Development Company (SPDC)

Abstract

There exists a catalogue of seismic quantitative Interpretation technique (QI) that has frequently been deployed for lithology and fluid prediction. However, the key challenge that the interpreter is often faced with is understanding the optimal technique that would yield the desired outcome within a limited time frame whilst still achieving top quartile business impact centered on detecting commercial hydrocarbon accumulations, delineating their lateral extent, and ultimately calculating volumes. It is therefore advised that prior to embarking on a QI journey, feasibility study particularly deploying log-based rock physics analysis be adequately done to confirm if the expected result would be achieved for a given QI technique. This typical involves using well log data to predict how seismic response will change with different reservoir fluid fill (gas, oil or brine), with changing reservoir properties such as porosity. This paper showcases how the integration of rock physics and some DHI techniques such as post-stack amplitude analysis (bright-spot, flat spot), offset-dependent amplitude analysis (AVO analysis), acoustic impedance inversion and spectral decomposition have been deployed in differentiating fluid types whilst understanding their advantages and pitfalls. This would be illustrated with some examples across the Niger Delta – from onshore to deep-water.

Geothermal Electricity Generation Opportunities in Ikogosi Warm Spring and Environs, Southern Nigeria

*

Aigbedion Isaac, Akhuele.D and Salufu.S.O.

Ambrose Alli University, Ekpoma

Abstract

The spectral analysis was carried out on the bouguer of the gravity anomaly data of the study areas, Ado (Sheet 244). The gravity data set of Ikogosi and Environs were analysed using Geosoft Oasis montaj software. The bouguer map was divided into eight overlapping sub-sheets of 27.5 X 27.5 km sizes. The spectral analysis by FFT was performed on each overlapping blocks and the plots of the logarithm of spectral energy $\ln(E)$ against the wavenumber (cycle/km) was produced using a Matlab program specifically designed to obtain the gradients for deepest depth (centroid depth) and depth to top of magnetic source. The curie point depth values ranges from 7.0 to 14.92 km, geothermal gradient values ranges from 39.90 to 82.85 °C/km and heat flow values ranges from 97.63 to 207.97 mW/m². Heat flow values from 95 to 110 mW/m² is seen in black to light blue colours within the SE regions while values from 120 and above 200 mW/m² is observed largely in NW regions and partly in the SW regions depicted in green to purple colours. The entire study area could be said to be prospective for geothermal energy exploration since no value of heat flow falls below the recommended range of 80 to 100 mW/m² for a good source of geothermal energy.

Origin and Timing of Calcite Cementation in Shallow Marginal Marine Sandstone: A Case Study from the Thistle field, Brent Group, North Sea

Auwalu Y. Lawan^{a,*}, Richard H. Worden^{a,*}, James E.P. Utley^a, Stephen F. Crowley^a

^aDepartment of Earth, Ocean and Ecological Sciences, University of Liverpool, Liverpool, L69 3GP, UK

^bDepartment of Geology, Bayero University, Kano State, Nigeria

Abstract

Pervasive calcite cementation in the Rannoch Formation of the Thistle Field is a major diagenetic event, characterised by five cemented intervals (doggers) interbedded with non calcite cemented sandstone. The calcite-cemented intervals have thicknesses ranging from 1.95 ft (0.6 m) to 12.1 ft (3.7 m) and mainly occur as stratabound horizons. The total cored thickness of the Rannoch Formation is 237 ft (72.2 m), while the cumulative thickness of the calcite-cemented intervals are 31.4 ft (9.6 m), which corresponds to 13.3 % of the total thickness of the Rannoch Formation. To understand the origin and timing of calcite cementation and temporal and spatial variability of the cemented interval, 52 samples were collected from the five calcite-cemented intervals and analysed by XRD, total carbon (weight fraction) and carbon and oxygen stable isotope. 29 samples were subsequently made into thin section and analysed for quantitative SEM-EDS and for light optical and BSEM petrography.



NIGERIAN ASSOCIATION OF PETROLEUM EXPLORATIONISTS

BLOCK 47A, FEMI OKUNNU HOUSING ESTATE, LEKKI/EPE
EXPRESS WAY, LEKKI PENINSULA, LAGOS P. M. B. 12598,
MARINA, LAGOS, NIGERIA. TEL: (234)-1-3429082, 234-
9092143198

E-mail: info@nape.org.ng Website: www.nape.org.ng

Date: 22nd

August 2022.

Attention:

Aigbedion

Isaac,

ACCEPTANCE OF ABSTRACT FOR POSTER PRESENTATION

**AT THE 40TH NAPE ANNUAL INTERNATIONAL CONFERENCE AND EXHIBITION,
2022**

Congratulations on the acceptance of your abstract for **POSTER PRESENTATION** at the 40th NAPE Annual International Conference and Exhibition holding from November 13 - 17, 2022 at Eko Hotel and Suites, Lagos Nigeria. NAPE AICE 2022 is an in-person (physical) event.

Your poster presentation information is as follows:-

2203-EPAE-11: Geothermal Electricity Generation Opportunities in Ikogosi Warm Spring and Environs, Southern Nigeria

This letter has been addressed to you as the Lead Author of this poster. Kindly inform your co-authors (where applicable) of the acceptance of this abstract for presentation.

Kindly confirm your availability to present this poster at the conference not later than September 09, 2022. It is important to note that ‘**no show**’ situation will attract a suspension from participation in any NAPE-organized technical event for a period of not less than one year for erring authors. However, if the lead author will be unavoidably absent, one of the co-authors should be available for the poster presentation.

Please note that it is mandatory for all presenters to submit a **FULL PAPER** to the Editor-in-Chief through the following e-mail: - editorinchief@nape.org.ng and copy:chrisjackconsult4all@yahoo.co.uk ; victoria.nneka.okorie@gmail.com ; tunde.a@nape.org.ng on or before **September 30, 2022** as this is one of the key criteria in the selection process for the conference Best Poster Award and subsequent publication in the NAPE Bulletin.

In addition, **your poster and brief self-introduction of Lead Author** (not more than 250 words) should be sent to the N A P E Editor-in-Chief not later than **October 30, 2022** for upload on the poster presentation software; **as no poster shall be accepted during the conference.** It is also mandatory for all prospective presenters to register for the conference as *no registration, no presentation* policy applies.

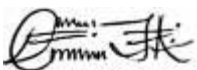
ADVERTISING AND SALES PROMOTION IN ANY FORM ARE STRICTLY PROHIBITED during all presentations.

Further details regarding the poster template, dimension, schedule, etc shall be sent to you in our subsequent email.

We thank you for your contributions to NAPE Conference and anticipate a successful and enriching event for all participants across the globe.

Once again, congratulations!

Yours Faithfully,



For: **NIGERIAN ASSOCIATION OF PETROLEUM EXPLORATIONISTS**

Dr. Christopher Asuquo Jackson

(NAPE Editor-in-Chief &

Chairman, Editorial Board/Technical Programme Subcommittee)

From: FAPSCON 2022 Technical / Publications Subcommittee

Sent: 01/09/2022

Subject: Letter of Acceptance

*4th INTERNATIONAL CONFERENCE OF SCIENCE, TECHNOLOGY,
INNOVATION AND ENTREPRENEURSHIP FACULTY OF PHYSICAL
SCIENCES, CHUKWUEMEKA ODUMEGWU OJUKWU UNIVERSITY,
ULI CAMPUS, ANAMBRA STATE*

*IN ASSOCIATION WITH ANAMBRA STATE MINISTRY OF
PETROLEUM AND MINERAL RESOURCES, AWKA*

Paper Title: Innovative Geothermal Energy Assessment of Akiri for Power Generation

Author (s): Aigbedion.I , Akhuele.D and Salufu.S.O

Abstract ID: FAPSCON22/GEO/003

Dear Sir/Madam,

**ACCEPTANCE OF ABSTRACT FOR PRESENTATION AT FAPSCON
2022: SCIENCE, TECHNOLOGY, INNOVATION AND
ENTREPRENEURSHIP CONFERENCE**

On behalf of the Local Organising Committee (LOC) of FAPSCON 2022, I am pleased to inform you that the Abstract of your paper has been accepted for Oral Presentation during the conference which holds from 18 – 22 October, 2022 at TETFund Engineering Auditorium, Uli Campus of Chukwuemeka Odumegwu Ojukwu University, Anambra State. Your presentation shall be for a maximum of ten (10) minutes including question time and shall be supported by projector facilities. Your oral presentation should be in MS-PowerPoint and you are requested to come with your presentation in USB Flashdrive.

To ensure that your accepted abstract gets published in the Conference Book of Abstracts, you are required to register for the conference by paying the discounted Conference Fee of Fifteen Thousand (N15,000.00) Naira per accepted abstract into the Faculty of Physical Science Conference account (ECOBANK ACCOUNT NUMBER: 4390033399) on or before 1st October, 2022 and transmit evidence of payment to the LOC via fpsconference@coou.edu.ng and copied to kk.nwozor@coou.edu.ng stating clearly your full name and unique identity number assigned to your accepted abstract. Note that the Full conference fee of Twenty Thousand (N20,000) Naira applies for registration after 1st October, 2022. Undergraduate students are required to pay Three Thousand (N3,000) Naira per accepted abstract into the above-stated account.

Further to this, feel free to submit FULL PAPERS of your accepted abstracts to the Technical / Publications Subcommittee not later than 30th November, 2022 for peer review and consideration for publication in the Special Conference Edition of COOU Journal of Physical Sciences.

Please, accept our hearty congratulations as the Local Organising Committee looks forward to welcoming you to FAPSCON 2022.

Yours Sincerely



Professor Ike Mgbeafulike

Chairman, Technical / Publications Subcommittee, FAPSCON 2022

+234 803 551 2511

Dean / Convener: Professor K.K. Nwozor

Chairman: Professor Osita Chiaghanam

Technical / Publications Chair: Professor Ike Mgbeafulike

Information & Strategy: Dr Oge Onyemesili

I



Event Link: <https://sairap.org/conf/index.php?id=1687128>

Paper Id: SAIRAP_73946

Paper Title: Assessment of Geothermal Energy Potential of Farin Ruwa and Environs, Nasarawa State-Northern Nigeria Using Airborne gravity Data

Authors Name: Aigbedion Isaac, Salufu S.O , Akhuele D

Dear Authors,

With heartiest congratulations I am pleased to inform you that based on the recommendations of the reviewers and the Technical Program Committees, your paper identified above has been accepted for publication and oral presentation by **INTERNATIONAL CONFERENCE ON APPLIED SCIENCE, MATHEMATICS AND STATISTICS ICASMS-22**

(**ICASMS-22**) conference received over 80 submissions from countries and regions, reviewed by international experts and your paper cleared all the criteria, got accepted for the conference. Your paper will be published in the conference proceeding after registration.

Sincerely,

Dr. Joe

For registration: <https://sairap.org/conf/registration.php?id=1687128>

Herewith, the conference committee sincerely invites you to come to present your paper at ICASMS-22 to be held on 07TH SEP 2022, ABUJA,



REFERENCES

- Abraham EM, Lawal KM, Ekwe AC, Alile O, Murana KA, (2014) Spectral analysis of aeromagnetic data for geothermal energy investigation of Ikogosi Warm Spring – Ekiti State, southwestern Nigeria. *Geothermal Energy* 2: 1-21.
- Abraham, E.M. and Nkitnam, E.E. (2017): Review of Geothermal Energy Research in Nigeria: The Geo-Science Front. *International Journal of Earth Science and Geophysics*, 3, 15. <https://doi.org/10.35840/2631-5033/1815>
- Akinnubi and Adetona, (2018) Investigation Of The Geothermal Potential Within Benue State, Central Nigeria, From Radiometric And High-Resolution Aeromagnetic Data, *NJP futminna.edu.ng:8080/jspui/handle/123456789/6466*.
- Akpabio I., Ejedawe J., and Ebeniro J. (2013): Thermal State of the Niger Delta Basin. Thirty Eighth Work. *Geotherm. Reserv. Eng.*,
- Akuru U. B, Okoro O. I: (2014): Renewable Energy Investment in Nigeria: A review of the Renewable Energy Master Plan, volume 25, p. 34 – 39
- Akuru, U.B. and Okoro, O.I. (2009): Sustainable application of solar energy as SMEs in a developing nation, *African Journal of Physics* Vol. 2, pp. 184-209, ISSN: 1948-0229 CD ROM: 1948-0245 ONLINE: 1948-0237
- Alimonti C, Soldo E (2014): Study of geothermal power generation from a very deep oil well with a wellbore heat exchanger. *Renewable energy* 86:292–301
- Aliu, J. and Mazian, H. (2018) Evaluation and Detection of Geothermal Potential Zones in Yankari Park, South- Central Part of Bauchi State, North-Eastern Nigeria *Journal of Applied Sciences and Environmental Management* 22(9):1381 DOI:10.4314/jasem.v22i9.03
- Anyadiegwu F,C and Aigbogun C.O(2021) Estimation of the Curie Point Depth, Heat Flow and Geothermal Gradient Determined from Analysis of Aeromagnetic Data over parts of the Lower Benue Trough and Anambra Basin, Nigeria ,*AJOL*, vol25 No10.
- ARCGIS: (1999): (Aeronautical Reconnaissance Coverage Geographic Information System)
- Atlas Wireline services, (1985), Schlumberger Publications.
- Ayuba, M.G and Lawal, M.K (2019) Investigating Geothermal Energy Resource Potential In Parts Of South Western Nigeria Using Aeromagnetic Data, *Science World Journal* Vol. 14(No 3) .
- Baker and Huges (2023) Personal communication at Nigerian Association of Petroleum Exploratonist Conference.

- Beckers, Timothy .J. Reber, Jefferson .W. Tester 2013 :The Transformative Potential of Geothermal Heating in the U.S energy market: a Regional Study of New York and Pennsylvania.
- Blakely R.J (1988): Curie temperature analysis and tectonic implications of aeromagnetic data from Nevada. *J Geophys Res* 93(B10):11817–11832.
- Bloomquist , R,Culver.G, Ellis .P.F, Higbee .C 1989 Geothermal Direct used Engineering and Design Guidebook
- Brimmo, A. T., Sodiq, A., Sofela S. and Kolo, I., (2017): Sustainable energy development in Nigeria: Wind, hydropower, geothermal and nuclear. *Renewable and Sustainable Energy Reviews*. 74: 474 – 490.
- Chukwu, C.G; Udensi, E.E; Abraham, E.M; Ekwe, A.C; Selemo, A.O (2017): Geothermal energy potential from analysis of aeromagnetic data of part of the Niger-delta basin, southern Nigeria. *Energy* (143):846 853.
- DiPippo R; (2012). *Geothermal Power Plants: Principles, Applications, Case Studies and Environmental Impact*. 3rd ed. Waltham, MA. USA: Butterworth-Heinemann, Elsevier Ltd.
- ECN, (2013) Electricity Corporation of Nigeria, Nigeria Energy situation ,*Energypedia*.
- Eko,G.E , Ismail, B.Y.Nornel H.I and RaJ,K,2022. Geothermal Energy Assesment through CPD, geothermal and Heat flow around the Akiri Hot spring, environmental Earth science Jornal, Elsevier.
- Emujakporue ,O and Ekine, A (2014):Determination of Geothermal Gradient in the Eastern Niger Delta Sedimentary Basin from Bottom Hole Temperatures 2014; *Journal of Earth Sciences and Geotechnical Engineering*, vol. 4, no. 3, 2014, 109-114 ISSN: 1792-9040 (print), 1792-96
- Fawale. O and Nwankwo, L.I,(2019) Evaluation Of Subsurface Heat Flow Of Ikogosi- Ekiti Warm Spring Using High Resolution Aeromagnetic Data. *Journal of Ghana Science Association*, Vol. 18, No. 2. 43-53.
- Geosoft Oasis Montaj (2015) *Data Processing and Analysis Systems for Earth Science Applications* (Ver. 8.3.3). Geosoft Inc., Toronto.
- Gul, S. and Aslanoglu, V. (2018) *Drilling and Well Completion Cost Analysis of Geothermal Wells in Turkey*”, *Proceeding, 43rd Workshop on Geothermal Reservoir Engineering*, Stanford, California, USA.

- Hammons, T.J. (2007) Geothermal Power Generation: Global Perspectives; U.S.A, and Iceland; Technology, Direct Uses, Plants and Drilling. (203) International Journal of Power and Energy Systems – 2007.ss
- Jessop, A. M., Habart, M. A. and Sclater, J. G. (1976). The world heat flow data collection 1975. Geothermal Services of Canada, 50:55–77.
- Jessop, A. M., Lewis, T. J., Judge, A. S., Taylor, A. E., & Drury, M. J. (1984). Terrestrial heat flow in Canada. *Tectonophysics*, 103(1-4), 239-261.
- Jitong, J.S (2019): Assessment of Geothermal Resources in the Nigerian Sector of the Chad Basin, Ne-Nigeria.
- Johnson,P.E,(2010) Oil Production Waste Stream, A Source Of Electrical Power, PROCEEDINGS, Thirty-Fifth Workshop on Geothermal Reservoir Engineering Stanford University, Stanford, California, February 1-3, 2010 ,SGP-TR-18.
- Kasidi, S. and Nur, A. (2012) Curie Depth Isotherm Deduced from Spectral Analysis of Magnetic Data over Sarti and Environs of North-Eastern Nigeria. School Journal of Biotechnology, 1, 49-56.
- MATLAB & Simulink –(MathWorks, 1984).
- Mayhew, M.A: Curie isotherm surfaces inferred from high altitude magnetic anomaly data. *J Geophys. Res.* 1985, **90**(B3):2647–2654. 10.1029/JB090iB03p02647.
- Mohammed ,Y. K, Ewa ,K Timothy, B (2019) Geothermal exploration in Nigeria. SCIENCE FORUM (JOURNAL OF PURE AND APPLIED SCIENCES) 18 67 – 75.
- Newsom, C. (2012). Renewable Energy Potential in Nigeria: Low-Carbon Approaches to Tackling Nigeria’s Energy Poverty. International Institute for Environmental Development, 2(3), 45-52.
- Nwachukwu, S.O., (1976). Approximate Geothermal Gradients in Niger Delta Sedimentary Basin, American Association of Petroleum Geologists Bulletin. 60, (No.7), pp. 1073- 1077
- Nwankwo, C.N; Ekine, A.S; Nwosu, L.I (2009). Estimation of the Heat Flow Variation in the Chad Basin, Nigeria. *J. Appl. Sci. Environ. Manage.* (13):73–80
- Nwankwo, L.I; Shehu, A.T (2015). Evaluation of Curie- point depths, geothermal gradients and near-surface heat flow from high-resolution aeromagnetic (HRAM) data of the entire Sokoto Basin, Nigeria. *J. of Volcanology and Geothermal Res.* 305 45 – 55.

- Nwankwo, L.I (2015). Estimation of depths to the bottom of magnetic sources and ensuing geothermal parameters from aeromagnetic data of Upper Sokoto Basin, Nigeria. *Geothermics* 54: 76 – 81.
- Nwankwo, C.N. and Ekine, A.S. (2009) Geothermal Gradient in the Chad Basin, Nigeria, from Bottom Hole Temperature Logs. *International Journal of Physical Sciences*, 4, 777-783.
- Obande, G.E, Lawal, K.M, Ahmed ,L.A (2014) Spectral analysis aeromagnetic data for geothermal investigation of Wikki warm spring, north-east Nigeria. *Geothermics* 50: 85-90.
- Odumodu, C.F.R and Mode, A.W. (2016) Geothermal gradients and heat flow variations in parts of the eastern Niger delta, Nigeria. *Journal of Geological Society of India* volume 88, pages 107–118
- Ojoawo,A.I and Sedara, S.O (2016) Magnetic data analysis for potential geothermal energy development: Case of Ikogosi warm spring, Ekiti, Southwestern Nigeria, *Elixir, Earth Science Journal*.
- Okubo Y, Matsunaga T (1994) Curie point depth in northeast Japan and its correlation with regional thermal structure and seismicity. *J Geophysical Research* 99(B11):22363–22371
- Olaoye, T, Ajilore ,T, Akinluwade K, Omole F, Adetunji A (2016) Energy crisis in Nigeria: Need for renewable energy mix. *American Journal of Electrical and Electronic Engineering*4: 1-8.
- Olorunfemi, M.O, Adepelumi AA, Falebita DE, Alao OA (2011) Crustal thermal regime of Ikogosi warm spring, Nigeria inferred from aeromagnetic data. *Arabian J Geosciences*.
- Onyejiuwaka, I. S. and Iduma, U. K. (2020). Assessment of Geothermal Energy Potential of Ruwan Zafi, Adamawa State and Environs, Northeastern Nigeria, using High Resolution Airborne Magnetic Data. *Current Research in Geoscience*, 10(1), 1-15. <https://doi.org/10.3844/ajgsp.2020.1.15>
- Oyedepo ,S.O (2012) Energy and sustainable development in Nigeria: The way forward. *Energy, Sustainability and Society* 2: 15.
- Ross, H. E., Blakely, R. J., & Zoback, M. D. (2006). Testing the use of aeromagnetic data for the determination of Curie depth in California. *Geophysics*, 71(5), L51-L59.
- Sambo, A. S., (2015), the way forward for electricity supply in Nigeria. Ideas and Insights from Explorers, National Geographic. October 20. Assessed from www.voices.nationalgeographic.com/2015/10/20/the-way-forward-for-electricity-supply-in-Nigeria/

- Schlumberger, (1989) Well logs applications and interpretation, Schlumberger publications.
- Stampolidis A, Tsokas G (2002) Curie point depths of Macedonia and Thrace, N. Greece. *Pure and Applied Geophysics* 159:1–13
- Surfer Version 15 software's
- Tanaka A, Okubo Y, Matsubayashi O (1999) Curie point depth based on spectrum analysis of magnetic anomaly data in East and Southeast Asia. *Tectonophysics* 306:461–470.
- Tochukwu, N. Mukhophadiyay, M. Ampana, S. (2022) Reconnaissance investigation of geothermal resources in parts of the Middle Benue Trough, Nigeria using remote sensing and geophysical methods
- Tselentis, G.A (1991). An attempt to define Curie depth in Greece from Aeromagnetic and heat Flow data. *PAGEOPH*, 136(1):87-101. Spector, A, Grant, FS (1970). Statistical models for interpreting aeromagnetic data, *Geophysics*. 35:293- 302.
- Tsokas, G.N., Hansen, R.O., and Fytikas, M., 1998. Curie point depth of the island of Crete (Greece). *Pure and App. Geophy.*, 152, pp. 747-757.
- Zhu L, Huo S, Qin L (2015). A microalgae-based biodiesel refinery: sustainability concerns and challenges. *International Journal of Green Energy*, 2015, 12(6): 595–602



Prof. Aigbedion Isaac, FIMC, AAPG, SEG, NAPE, NMGS, GSH, AGU,

(Lead Researcher)

08037192278.